Theoretical Investigations of Waves and Instabilities in Dusty and Strongly Coupled Dusty Plasmas

THESIS SUBMITTED TO
DELHI TECHNOLOGICAL UNIVERSITY
For the Award of the Degree of

DOCTOR OF PHILOSOPHY

By

Ms. Kavita Rani
(2K14/PhD/AP/05)

Under the supervision of
PROF. (DR.) SURESH C. SHARMA

Department of Applied Physics
DELHI TECHNOLOGICAL UNIVERSITY
Delhi-110042, India
(September, 2018)

Dedicated

To

My Son-Urav

Delhi Technological University

(Govt. of National Capital Territory of Delhi)

Shahbad Daulatpur, Bawana Road, Delhi-110042

CERTIFICATE

This is to certify that the thesis entitled ***"Theoretical Investigations of Waves and Instabilities in Dusty and Strongly Coupled Dusty Plasmas"*** submitted by **Ms. Kavita Rani (2K14/PhD/AP/05)** to Delhi Technological University (DTU), Delhi, India for the degree of Doctor of Philosophy, is a bonafide record of the research work carried out by her under my supervision and guidance. The work embodied in this thesis has been carried out in the Plasma & Nano Simulation Lab, Department of Applied Physics, Delhi Technological University (DTU), Delhi, India. The work of this thesis is original and has not been submitted in parts or fully to any other Institute or University for the award of any other degree or diploma.

_____

Prof. (Dr.) Suresh C. Sharma
Supervisor
Head, Department of Applied Physics
Delhi Technological University
Shahbad Daulatpur, Bawana Road
Delhi-110042, India

Delhi Technological University

(Govt. of National Capital Territory of Delhi)

Shahbad Daulatpur, Bawana Road, Delhi-110042

CANDIDATE'S DECLARATION

I, herby certify that the thesis titled ***"Theoretical Investigations of Waves and Instabilities in Dusty and Strongly Coupled Dusty Plasmas"*** submitted in the fulfilment of the requirements for the award of the degree of Doctor of Philosophy is an authentic record of my research work carried out under the supervision of **Prof. (Dr.) Suresh C. Sharma**. Any material borrowed or referred to is duly acknowledged.

_____

Kavita Rani
(2K14/PhD/AP/05)
Delhi Technological University
Shahbad Daulatpur, Bawana Road
Delhi-110042, India

ACKNOWLEDGEMENTS

It gives me immense pleasure to acknowledge my obligations, sincere thanks and sense of gratitude to those without support of whom this thesis would not have been possible.

The completion of this thesis required a lot of guidance, assistance and encouragement from numerous people including my university, supervisor, my employer, colleagues, friends, and my family. I am extremely privileged to thank all who in one or another way supported me during the course of time.

First and Foremost, it gives me profound pleasure to express my deep sense of thanks and utmost gratitude to my esteemed supervisor, ***Prof. Suresh C. Sharma****, Head of Department, Applied Physics, Delhi Technological University, Delhi, India for not only guiding me with his profound knowledge and experience but also providing me a flexible and serene environment to carry out research. I am highly indebted to him for his valuable suggestions, healthy criticism, unending patience and consistent encouragement throughout the journey of my Ph.D. research work. I owe him special thanks for promoting me to enter into the art of research under his scholarly guidance. I have been extremely lucky to have a caring and supporting supervisor like him.*

I take the opportunity to express my profound respect to ***Hon'ble Prof. Yogesh Singh****, Vice Chancellor, DTU and officials of DTU for their precious support and providing ample research facilities to conduct this research. I would also like to acknowledge their financial support to attend the "****8th International Conference on Physics of Dusty Plasmas****" held in Prague, Czech Republic (May 2017). I would also like to thank library staff members of DTU as well.*

I would like to thank ***Prof. Rinku Sharma*** *and all other faculty and staff members of Department of Applied Physics, DTU for their help and cooperation throughout my study period.*

I would also like to express huge and warm thanks to my other fellow mates in Plasma & Nano-Simulation Research Laboratory: ***Ms. Neha Gupta, Mr. Ravi Gupta, Ms. Pratibha Malik, Ms. Jyotsna Panwar, Ms. Umang Sharma, Ms. Monika Yadav, Ms. Ruchi Sharma, Ms. Renu Kumari, Ms. Anshu Dahiya, Ms. Suman Dahiya and Ms. Aarti Tewari,*** *for the stimulating discussions, selfless support, and for all the fun during the research period.*

I express my sincere gratitude to the management of "Bhagwan Parshuram Institute of Technology" Delhi for providing me an atmosphere to carry out research. I also explicitly thank ***Prof. Payal Pahwa*** *(principal),* ***Prof. Abhijit Nayak*** *(Dean& HOD, Dept. of Applied Physics, Bhagwan Parshuram Institute of Technology,) for all their selfless support. I am also thankful to my colleagues,* ***Dr. Nidhi Sharma, Deepika Sandil,*** *and* ***Priya Sinha*** *for supporting me in one or the another way in my research.*

I am indebted to some of my dear friends cum colleagues, ***Sugandha Gupta, Muskan Kapoor,*** *and* ***Lata*** *for influencing me in a positive way and for their moral support and motivation, which drives me to give my best.*

I would like to acknowledge all my teachers since my childhood as I would not have been here without their guidance, blessings and support.

I do not have enough words to honour my parents ***(Ms. Asha Rani and Mr. Ramesh Kumar)*** *for their blessings, encouragement and moral support without which it would not have been possible to carry out this research work.*

I feel a deep sense of love and gratitude towards my son ***(URAV)*** *who constantly motivated me for doing well in my research work, giving the time that he deserved from me.*

I would like to pay high regards to my mother in law ***(Ms. Urmila Segwal)****, to my father in law* ***(Mr. Sarvan Kumar)****, sister-in-law* ***(Renuka Segwal Gupta)****, for motivating and supporting me throughout my life in general. I*

*also thank my brothers **(Rahul and Lalit)** and my sister **(Ritu)** for consistently encouraging me to follow my research route.*

*Last but not the least; I am highly indebted to my husband **(Mr. Tilak Raj Segwal)** who has been by my side in every difficult situation. His cooperation, understanding, and sincere encouragement were the sustaining factors in accomplishing this thesis successfully.*

*Above all, I owe my reverence to the Almighty and **Guruji** by grace of whom it has been possible to complete my research work completely. I thank **Guruji** for giving me the strength & patience and irradiating all the stones coming in my path.*

(Kavita Rani)

ABSTRACT

Dusty plasmas are characterized by the presence of micron to sub-micron sized dust particles immersed in partially or fully ionized plasma. It can be produced by dispersing dust grains into a plasma (Q-machine) or by growing dust in the plasma of certain chemically reactive gases like Silane (SiH_4) and Oxygen (O_2). Various processes like interaction of dust grains with gaseous plasma particles, energetic particles (electrons and ions), photons, secondary electron emission, thermionic emission, and photoelectric emission are responsible for charging of dust grains in a plasma. These dust grains in plasmas acquire a high negative charge and the presence of these highly charged dust particles in a plasma can have significant influence on the collective properties of the plasma.

Dusty plasmas are widespread in astrophysical situations like planetary rings, comet tails, and interstellar clouds. In plasma processing reactors, dust particles grow from gaseous molecules to nano-meter sized particles. The removal of these plasma-grown dust particles is a crucial problem in computer chip manufacturing industry. In contrast, novel materials, such as solar cells with highly improved efficiency, can be manufactured from thin films by incorporating the dust particles. An interesting property of dusty plasmas is that the dust particles can arrange themselves into ordered structures, so-called plasma crystals which are a consequence of strong coupling among dust grains. The study of strongly coupled plasmas also has great potential due to their vast applications in astrophysical plasmas such as interplanetary medium, white dwarf matter etc. and laboratory plasmas such as laser produced plasmas, and plasma crystals. Moreover, strongly coupled dusty plasmas have received profound attention because of (i) their ability to form "Coulomb Crystals" and (ii) the excitation of the dust acoustic (DA) and dust lattice (DL) waves.

The studies of waves and instabilities in dusty as well as strongly coupled dusty plasmas have also received great attention in past few years. Moreover, it is a well known fact that the waves and instabilities can be excited either by the free sources of energy such as plasma currents produced by the electrostatic and electromagnetic fields present within the plasma or by external beam sources propagating inside it. Hence, we aim at the theoretical investigations of waves and instabilities in dusty plasmas.

Moreover, we extend our investigations to observe the low frequency modes in strongly coupled dusty plasmas as well.

A theoretical model to elucidate the excitation of an ion beam driven ion acoustic waves (IAWs) in a plasma cylinder having negatively charged dust grains have been developed. The first order perturbation technique has been used to evaluate the growth rate of instability. The destabilizing effect of relative concentration of negatively charged dust on the frequency and the growth rate, and phase velocity of ion beam driven ion acoustic instability has been observed. It has been found that electrostatic ion-acoustic waves are driven unstable in a magnetized dusty plasma cylinder through an ion beam via Cerenkov interaction. Moreover, the beam parameters such as density and energy play a significant role in enhancing the real frequency and the growth rate of the IAW modes.

It has also been observed that the dust charge fluctuations play an important role in suppression of the current driven electrostatic ion-cyclotron waves in a magnetized collisional dusty plasma.

Kelvin Helmholtz instability in a magnetized dusty plasma can be driven by an ion beam via Cerenkov interaction. Unstable KHI modes frequencies and axial wave vectors increase with the relative density of negatively charged dust grains δ in the presence of beam. The KHI mode frequency is enhanced in the presence of dust charge fluctuations while dust charge fluctuations play a significant role in damping of the KH- instability modes. A comparison of frequency and the growth rate for finite and infinite geometry of plasma waveguide shows a reduction in both frequency and the growth rate for finite geometry. Moreover, the radial boundaries also affect the dispersion properties of the KHI modes.

The Kelvin Helmholtz instability in a magnetized plasma having negative ions can also be driven by an ion beam via a Cerenkov interaction. The KHI mode frequencies and axial wave numbers of the both positive ions and negative ions increase with the relative density of negative ions ε in the presence of beam. The presence of beam and its various parameters significantly modify the growth rate of both the KHI ion modes. Moreover, the stabilizing effect of relative mass of positive and negative ions has also been observed. It has been observed that the presence of

negative ions destabilizes the KHI modes which can find applications in surface plasma technologies.

Low frequency longitudinal and transverse modes driven by magnetic field aligned current drifts in a magnetized strongly coupled collisional dusty plasma have been theoretically investigated. Longitudinal modes contain ion dust hybrid modes while transverse mode is similar to an elastic wave. The theoretical models which are based on generalized hydrodynamic approach have been developed for hydrodynamic and strongly coupled kinetic regime for the local and nonlocal plasmas, respectively. The strong correlation parameter is found to have a stabilizing effect on current driven longitudinal modes due to increase in viscous damping while for transverse modes the effect of viscous damping is weak due to restoring force provided by elastic effects.

The present research work can be extended to study waves and instabilities in non-linear regimes of plasmas and findings of the present research work may be useful in investigating astrophysical situations, near earth environment, and fusion plasma devices, etc.

LIST OF PUBLICATIONS

International Journals

1. **Kavita Rani** Segwal and Suresh C. Sharma, "Theoretical modelling of an ion beam driven Kelvin Helmholtz instability in a plasma cylinder having negatively charged dust grains" ***IEEE Transactions on plasma science*** **46,** 775 (2018).

2. **Kavita Rani** Segwal and Suresh C. Sharma, "Current driven Low frequency electrostatic waves in a collisional strongly coupled magnetized dusty plasma" ***IEEE Transactions on plasma science*** **46**, 797 (2018).

3. **Kavita Rani** and Suresh C. Sharma, "Theoretical Modelling of Kelvin Helmholtz Instability driven by ion beam in a Negative ion plasma" ***Progress in Electromagnetics Research B*** **71**, 167 (2016).

4. **Kavita Rani** and Suresh C. Sharma, "Excitation of Kelvin Helmholtz Instability by an ion beam in a plasma with negatively charged dust grains," ***Physics of Plasmas*** **22**, 023708 (2015).

5. Suresh C. Sharma, **Kavita Sharma** and Ajay Gahlot, "Effect of dust charge fluctuations on current-driven electrostatic ion-cyclotron instability in a collisional magnetized plasma", ***Physics of Plasmas*** **20**, 053704 (2013).

6. Suresh C. Sharma, **Kavita Sharma** and Ritu Walia, "Ion beam driven ion-acoustic waves in a plasma cylinder with negatively charged dust grains," ***Physics of Plasmas*** **19**, 073706 (2012).

Communicated paper in International Journal

7. **Kavita Rani** Segwal and Suresh C. Sharma, "A non-local theory of current driven low frequency modes in a magnetized strongly coupled collisional dusty plasma" ***IEEE Transactions on plasma science,*** **2018** (communicated).

International /National Conference Presentations

1. **Kavita Rani** Segwal and Suresh C. Sharma, "Current driven Low frequency electrostatic waves in a collisional strongly coupled magnetized dusty plasma" presented at ***"8TH International conference on physics of Dusty Plasmas"*** held at Prague, Czech Republic, pp. 88, (May 20-25, 2017). **ISBN 978-80-7378-339-6.**

2. **Kavita Rani** Segwal and Suresh C. Sharma, "*Theoretical modeling of an ion beam driven Kelvin Helmholtz instability in a plasma cylinder having Negatively charged dust grains"* presented at ***"8TH International conference on physics of Dusty Plasmas"*** held at Prague, Czech Republic, pp. 158, (May 20-25, 2017). **ISBN 978-80-7378-339-6**.

3. **Kavita Rani** and Suresh C. Sharma, "Theoretical Modelling of KH Instability driven by an Ion Beam in a magnetized plasma cylinder having negative Dust grains" presented at ***"International symposium on non linear waves in fluids and plasmas-BUTIFEST"*** held at IIT, Delhi (March 1-2, 2017).

4. **Kavita Sharma,** Ajay Gahlot and Suresh C. Sharma "*"Effect of dust charge fluctuations on current-driven electrostatic ion-cyclotron instability in collisional magnetized plasma"* presented in **"National conference on advanced materials and devices"** at Hindu college, Sonepat, Haryana (Feb 27-28, 2013).

CONTENTS

Chapter 2: Ion Beam driven Electrostatic Ion-Acoustic Waves

List of Figures

Chapter: 5

Chapter :6

LIST OF TABLES

CHAPTER 1

INTRODUCTION

1.1 BACKGROUND

It has often been said that 99% of the known matter in the universe is in the plasma state. W. Crookes [1] firstly named the ionized medium inside a gas discharge tube as the 'fourth State of matter'. Tonk and Langmuir [2] in 1929 named this fourth state of matter-"plasma" while observing the oscillations in an electric discharge tube. In general, plasma is an ionized state of matter which results due to continuous heating of a solid matter that undergoes phase transitions until an ionized gaseous state result. It is a quasineutral gas of charged and neutral particles which exhibit collective behaviour [3]. The many particles interacting charged system exert electromagnetic forces on each other resulting into currents and magnetic fields. These fields play an important role in dynamics of plasmas with introduction of a range of phenomena (waves and oscillations) of startling complexity and of great practical utility. Plasmas occur pervasively in nature as solar wind, interstellar mediums, planetary rings, Earth's magnetosphere, and ionosphere etc. It can be produced in laboratories through DC and RF discharges, in material processing reactors, and in thermonuclear fusion devices. The plasmas mostly coexist with a ubiquitous ingredient known as 'Dust'. These dust particulates may be as large as a micron, and charged positively or negatively depending on the plasma environment in which they enter. An admixture of such micron or submicron charged dust particles, electrons, ions and neutrals forms a so called "DUSTY PLASMA" [4].

The history of dusty plasmas started from the observation of dusty plasma by Langmuir in 1924 in a tungsten arc discharge where he imputed the unusual effects of charging of tungsten vapors through attachment of electrons on its surface and then

moving under the effect of electric fields. The charging of dust grains through the photoelectric emission by Ultraviolet (UV) radiations in interstellar medium was firstly discussed by Spitzer [5] in 1941. He also pointed the collection of charged particles from the ionized plasma gas even though the system was quasineutral. The origin of planets, and comets by coagulation of dust particles in Solar Nebulae was pointed by Laureate Hannes Alfven in 1954 as mentioned in the review article by Merlino and Goree [6]. Two unique discoveries that provided great impetus to the field of dusty plasma were the images of dynamic radial spokes in Saturn's B Rings taken from Voyager 2 space craft at intervals of ten minutes [7] and source of dust contamination in the semiconductor industry [8]. The first one suggested that the rings were composed of fine dust particulates which are affected by the electromagnetic fields. Moreover, the images of spokes in Saturnian rings taken by Cassini spacecraft in 2005 showed that the sporadic charging events charge and lift the boulders off the rings planes. The second serendipitous discovery made by Selwyn *et al.* [8] after Roth *et al.* [9], during the semiconductor processing while they were measuring the concentration of reactive gases using laser induced fluorescence in a plasma processing device suggested that the dust particles actually form and grow inside the plasma processing reactors itself at the moment when RF power switches off. These dust particulates reduce the efficiency of silicon wafers by contaminating them.

Whereas the field of dusty plasma was of great endurance to astronomers, the semiconductor manufacturers were facing an inevitable problem of dust contamination. The two communities, astrophysics and semiconductor industry then found a common platform to study charging and transport phenomena associated with the dust grains. After several attempts experimentalists found a way to levitate the dust sufficiently high above the silicon wafer using RF power. Sideways, the observation of noctilucent clouds, polar mesospheric echoes, Comet tails [10] - [13] etc. tends to flourish the field of cosmic dusty plasmas. Moreover, in fusion devices, the "dust" arises a result of the strong interaction between the material walls and energetic plasma which causes flaking, blistering, arching and erosion of the carbon limiters or beryllium surfaces [14] and hence poses a serious contamination problem as it can be transported deep into the plasma. Then an important feature of the dusty plasma was observed i.e., a transition from the fluid state to crystalline state or a plasma crystal [15]-[20]. In addition, the observations of rocket exhausts, thermonuclear fireballs, various linear and non-linear

wave phenomenon, and magneto-hydrodynamic fluid instabilities provide a sufficient background to study dusty plasmas. There have been a number of theories that led to various experimental researches and vice versa which provided great impetus for studying the field of dusty plasmas.

1.2 DUSTY PLASMAS

Dusty plasmas are partially or fully ionized low temperature electrically conducting gases having electrons, ions, neutral atoms and charged dust grains (either dielectric or conducting). Dust grains are massive with a mass ~ 10^{12} times the mass of proton and size ranging from nm to mm. What makes the field interesting and technologically important is the fact that the dust grains acquire a charge & mostly become negatively charged because of their frequent encounter with the highly mobile electrons than with the clumsy ions of the plasma. The magnitude of this charge is of the order of 10^3e -10^4e for 1μm sized particles, where e is the elementary charge. Dust grains are said to be 'isolated' if dust grain radius $a \ll \lambda_D < a_d$, and non isolated if $a \ll a_d < \lambda_D$, where λ_D is the plasma Debye length and a_d be the average intergrain distance. The presence of the isolated dust grains has little influence on the properties of plasma while the presence of non isolated charged dust grains introduces collective phenomena in a plasma. The presence of charged dust grains does not only modify the existing wave modes (e.g., ion–acoustic waves (IAW), electrostatic ion cyclotron waves (EICW), lower hybrid waves (LHW) etc), but also introduces new kind of dust wave modes (e.g., dust-acoustic waves (DAW), dust ion-acoustic waves (DIAW), etc) and the plasma instabilities like ion streaming, Kelvin Helmholtz (KH), Rayleigh-Taylor (RT), etc [4]. To understand these collective wave phenomena introduced as a result of dust particle dynamics, one should firstly go through its characteristics, production, and dust charging processes.

1.2.1 Characteristics

The dust grains entered into the plasma modifies the usual properties of the plasma as given below:

1.2.1.1 Quasi-Neutrality

In the absence of external forces, the dusty plasmas like a normal plasma is macroscopically neutral. So in equilibrium the charge neutrality condition reads

$$en_{i0} - en_{e0} + Q_d n_{d0} \approx 0, \tag{1.1}$$

where n_{i0}, n_{e0} and n_{d0} are the equilibrium densities of ions, electrons, and dust grains, e be the electronic charge and $Q_d = \pm Z_d e$ be the dust charge for positively/ negatively charged dust grains (here, Z_d be the dust charge state ~ 10^3-10^4). However, in many space and experimental plasmas, charging of dust grains may lead to nearly complete depletion of electron number density.

1.2.1.2 Debye Shielding

One of the fundamental characteristic of a plasma is its ability to shield out the electric potentials applied to it by creating a Debye sphere called Debye shielding (Fig. 1.1). The radius of Debye sphere is known as Debye length over which the electric field of any charged particle influences the other charged particle inside a plasma [3]. A positive potential applied to the dusty plasma would be surrounded by a cloud of electrons and negatively charged dust grains and a negative potential would surrounds a cloud of ions and positively charged dust grains if any. In perfect shielding case, there is no agitation of charges on the cloud i.e., a cold plasma. However, for finite temperatures, the charged particles tend to escape from the edge of the clouds and a potential of order $k_B T/e$ can leak into the plasma resulting into a finite electric potential and incomplete shielding. The approximate thickness for such a charged cloud or sheath is also known as Debye length. The mathematical relation for Debye length as discussed by Shukla and Mamun [4] is

$$\lambda_D = \frac{\lambda_{De}\lambda_{Di}}{\sqrt{\lambda_{De}^2 + \lambda_{Di}^2}}, \tag{1.2}$$

where $\lambda_{De} = \left(T_e / 4\pi n_{e0} e^2\right)^{1/2}$ and $\lambda_{Di} = \left(T_i / 4\pi n_{i0} e^2\right)^{1/2}$ are electron and ion Debye lengths, respectively.

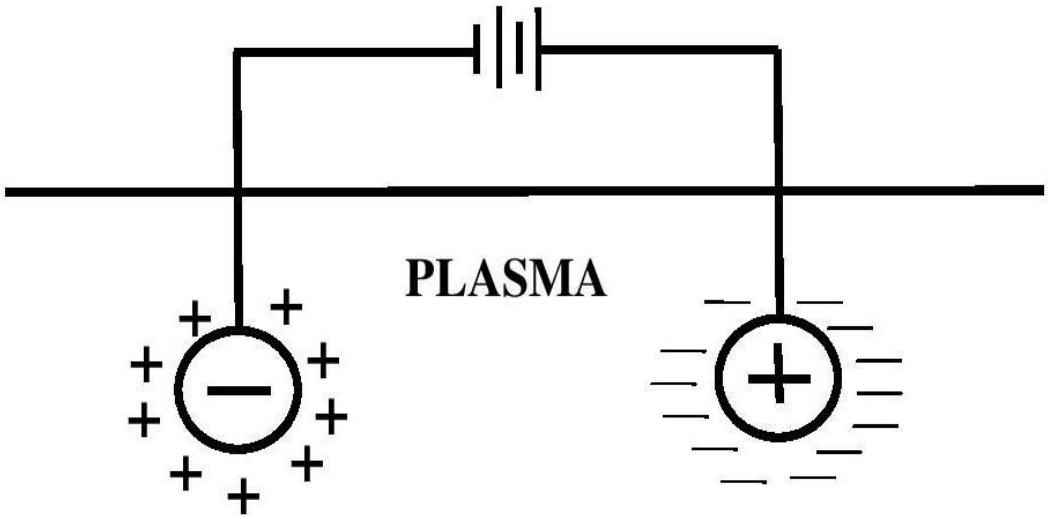

Fig. 1.1 Debye Shielding [3]

1.2.1.3 Weak vs. Strong Coupling

The important aspect of many particles interacting system is the Coulomb coupling parameter Γ which is defined as the ratio of coulomb interaction energy of the particles to their thermal energy

$$\Gamma = \frac{Q_d^2}{a_d T_d} exp\left(-\frac{a_d}{\lambda_D}\right), \tag{1.3}$$

where $\left|Q_d\right| = +Z_d e$ is the dust charge, Z_d is dust charge state, $a_d = \left(4\pi n_{d0}/3\right)^{-1/3}$ is intergrain spacing, n_{d0} is dust density, $a_d/\lambda_D = \kappa$ is the screening of dust charge over plasma Debye length λ_D. A dusty plasma with Γ <<1 is defined as a weakly coupled plasma while a dusty plasmas with Γ>>1 is characterized as a strongly coupled plasma. The dust grains in most of the laboratory plasmas are strongly coupled because of low temperature and high charge on the dust grains [4]. Moreover, they can easily be cooled down to room temperature through neutral collisions. The parameter plays a decisive role in deciding the state of dusty plasma whether liquid, solid or a gas. The

plasma behaves as a gas for Γ <<1, liquid when 170> Γ>1, where Γ =170 is the crystallization limit, i.e. beyond this the phase transition takes place leading to the plasma crystals (a solid state) [15] but in one of the dusty plasma experiment [DPX], dust is observed in the fluid state upto Γ =300 [21].

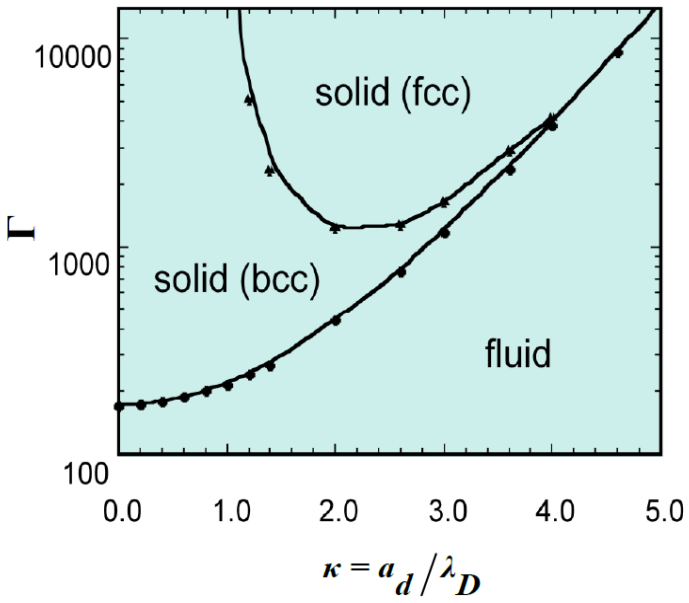

Fig. 1.2 Phase diagram of a Yukawa system [22]

The strongly coupled dust system are more often called as Yukawa system [22] as their dynamics can be modelled using Yukawa potential $\phi = \frac{1}{r} exp\left(-\frac{r}{\lambda_D}\right)$. Hamaguchi *et al.* [22] studied the transition temperatures at the fluid-solid & solid-solid phase boundaries as functions of the screening parameter $\kappa\left(= a_d / \lambda_D\right)$ in a Yukawa system. Fig. 1.2 shows the triple point of a Yukawa system. The figure shows that an increase in strong coupling and screening parameter changes the state of dusty plasma into an ordered lattice.

1.2.2 Methods of Production

As the micron sized massive dust particles simply fall to the bottom of a plasma under the effect of gravity unless an external electrostatic or electromagnetic field is applied to levitate and confine the dust grains [23]. However, in most of the laboratory

plasmas this problem is not of great concern as the typical micro particles relaxation time is much longer than the charging time. Thus, it became possible to produce a dusty plasma by just sprinkling dust into the plasma. A number of techniques have been devised till date to produce a dusty plasma depending on the applications. A dusty plasmas can be produced by dispersing dust grains into a plasma in a Q- Machine [24, 25] or by growing dust in plasma produced from certain chemically reactive gases like Silane (SiH_4) and Oxygen (O_2) [26] or by suspending 40 μm diameter Silica (SiO_2, which is negatively charged) particles in an argon glow discharge [27].

Recently, a magnetized dusty plasma experiment (MDPX) has been devised to study the dynamics of fully magnetized dusty plasmas [28] in more relevance to the astrophysical and fusion plasmas. We will have a brief overview of few techniques devised to study laboratory dusty plasmas.

1.2.2.1 Dusty Plasma Device (Q-Machine)

A dusty plasma device (DPD) is a single ended Q-machine modified to disperse dust into the plasma column [24]. The schematic of a Q- machine is shown in Fig. 1.3 in which a fully ionized potassium plasma column of diameter ~ 4 cm and length ~80 cm is produced by surface ionization of potassium atoms from an atomic beam oven on a hot Tantalum Plate (~ 2500K). The plasma column is radially confined by applying a longitudinal magnetic field $B_S \leq 4000$ Gauss. The plasma densities range from 10^5-10^{10} cm^{-3} with electrons and K^+ ions at equal temperatures ~ 0.2 eV. The neutral gas pressure is kept low ~ 10^{-6} Torr so that the mean free path of electron-neutral and ion-neutral collisions are larger than the dimensions of machine. A portion of plasma column is surrounded over by a rotating dust dispenser consisting of a rotating metal cylinder and a stationary screen. The dust particles are initially loaded into bottom and then carried to top of rotating cylinder and fall on the screen. A series of stiff metal bristles attached inside cylinder scrapes across the outer surface of screen during rotation of cylinder to evenly disperse dust into plasma column. The dust grains collected at the bottom are then recycled. A continuous dust recycling occurs to maintain a sufficient dust density in the plasma column. .

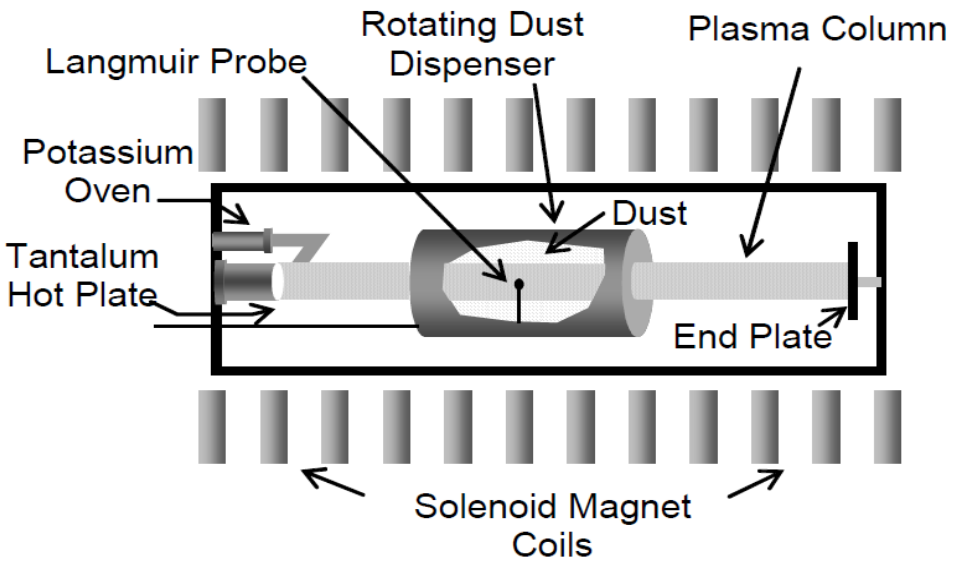

Fig. 1.3 Schematic of a Q-machine consisting of a rotating dust dispenser and a movable Langmuir probe [25]

The dust grains used are usually Alumina (Al_2O_3) and hydrated aluminum silicate (Kaolin), $Al_2Si_2O_7\ nH_2O$ of different sizes and shapes. An electron microscope is used to analyze the sample. The main diagnostic tool is a movable Langmuir probe oriented normally to the magnetic field which moves along the axis of plasma column and measures the electron current & charge on the floating grains.

The studies of waves and instabilities in a dusty plasma can be done using the Q-machines.

1.2.2.2 RF Glow Discharge Device

Chu and I [26] in 1994 confine the RF plasma in a cylindrically symmetric system and observe the dust crystals at low RF power. The Schematic of the experimental set up is shown in Fig. 1.4. The device consists of a hollow outer electrode capacitively coupled to a 14 MHz RF power amplifier working at 30 W RF power, a grounded centre electrode with a ring shaped groove on the top for particle trapping and a glass window on the top for observation. A CCD video camera is used to monitor particle images illuminated by a laser. The device is pumped through a diffusion pump. Silane (SiH_4) and Oxygen (O_2) gases are introduced with background argon pressure of 10 mTorr. The partial pressures of Silane and oxygen are kept below 10 mTorr. An axial magnetic field between 50-100 Gauss is applied to enhance particle

production efficiency. The particle size and density increase with rate of flow and pressure of the reactive gases. After formation of micron sized dust grains, the reactive gases flow and magnetic field is turned off to trap them into toroidal groove [4]. Under gravity the particle diameter slowly increases with decreasing height. The size of particle is limited to 3mm along vertical direction. An increase in RF power tends to melt the Coulomb crystals.

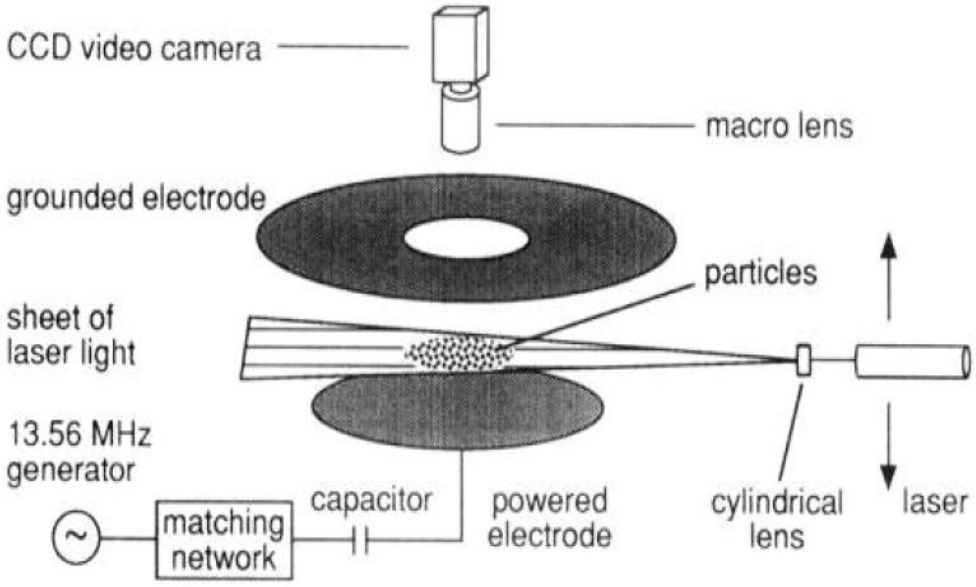

Fig. 1.4 Schematic of an RF discharge system which shows Coulomb crystal for low RF power [26]

Plasma processing reactors generally employ RF discharge devices for processing of silicon wafers. Plasma assisted chemical reactions lead to formation of unwanted negatively charged dust particles (SiO_2) at the bottom of plasma [6].

Many other devices have been devised for producing a DC glow discharge devices [29] to observe ordered structures of micron sized dust particles and to trap dust particles for investigating the dispersion properties of DAWs [30]-[31]. A typical salt shaker kind of device [25] can be used to measure charge on the individual grains [32], effects of dust on plasma waves [33]-[35], neutral and ion drag forces on the dust grains [36].

1.2.3 CHARGING OF THE DUST GRAINS

In 1941 Spitzer was first to describes the processes involving charging of dust grains in the interstellar medium [5]. Charging of dust grains basically involves three processes [4]:

- Interaction of dust grains with plasma constituents
- Interaction of dust grains with energetic particles such as electrons and ions
- Interaction of dust particles with photons

The dust grains immersed in a plasma get charged due to collection of electrons and ions from the plasma, photoelectron emission by UV radiations, thermionic emission, secondary electron emission and ion sputtering etc [37]. The dust grains act as probe and float to a potential so that at equilibrium, the net current (due to electrons I_e, ions I_i, secondary emission I_{SE}, and photoemission I_{PE}) flowing on the surface of dust grains becomes zero

$$\sum I = I_e + I_i + I_{SE} + I_{PE} \approx 0. \tag{1.4}$$

In typical laboratory plasma, where currents due to photoemission and secondary electron emission are nil, the grains charged to a negative potential $\phi_S \left(= V_S - V_p\right)$ with respect to plasma, due to high mobility of electrons until the electron current becomes equal to ion current. Here, V_S is the grain surface potential and V_p is the plasma potential.

Moreover, incidence of energetic particles (electrons or ions) on the grain surface excites electrons to escape from the grain surface. These secondary electrons released from the grain surface make the surface potential positive. Photoemission of electrons from the grain surface also tends to make it positively charged.

1.2.3.1 Mechanism

To explain the charging mechanism including all the processes discussed above altogether is a tedious task. Hence, the main focus lies on the laboratory dusty plasmas in which we considered two cases: (i) isolated dust grains (ii) non isolated dust grains.

1.2.3.1.1 Isolated Dust Grains

In low temperature laboratory plasmas, where charging of dust grains dominate through collection of ions and electrons, the currents due to secondary emission and photoemission are nil. As electrons transit faster than ions so dust grains charged to a negative potential through collection of electrons and hence repel further electrons moving towards the grains which enhances the collection of positive ions until the electrons current becomes equal to ions current, i.e., a balance is achieved. Then, for the spherical isolated grains of radius $a \ll \lambda_D$ plasma Debye length, where intergrain distance $a_d \gg \lambda_D$, the grain floats to a potential that net current becomes zero. If V_S be the surface potential and I_e and I_i be the magnitudes of electron and ion currents to the dust grain then at equilibrium, the condition

$$\left(I_i - I_e\right)_{V=V_S} = 0 \tag{1.5}$$

is satisfied. The orbital motion limited (OML) electrons and ions currents [38]-[40] in Maxwellian plasmas are given by

$$I_e = -en_{e0}\sqrt{\frac{k_B T_e}{2\pi m_e}}\exp\left(\frac{e\phi_S}{k_B T_e}\right)4\pi a^2 \tag{1.6}$$

and

$$I_i = en_{i0}\sqrt{\frac{k_B T_i}{2\pi m_i}}\left(1-\frac{e\phi_S}{k_B T_i}\right)4\pi a^2. \tag{1.7}$$

Here n_{e0} & n_{i0} are electrons and ion plasma equilibrium densities, T_e & T_i are electron and ion temperatures, and m_e & m_i the masses of electrons and ions. The above equations are valid till the particles streaming speed is less than their thermal speeds. The balance of electrons and ion currents yields

$$\exp\left(\frac{e\phi_S}{k_B T_e}\right) = \sqrt{\frac{m_e T_i}{m_i T_e}}\left(1-\frac{e\phi_S}{k_B T_i}\right). \tag{1.8}$$

For a Hydrogen plasma, $\phi_S\left(=-2.5k_B T_e/e\right)$ while for a singly charged Argon plasma

$\phi_s \left(= -4.0 k_B T_e / e\right)$ [25, 37]. The dust grain charge Q_d is given by $Q_d = C\phi_s$, where $C\left(= 4\pi\varepsilon_0 a\right)$ is the grain capacitance. Fig. 1.5 shows a plot between normalized relative dust surface potential as a function of temperature ratio of electrons to ion as shown by Merlino [25] which shows that the surface potential of dust grains is more negative for the Argon plasma. Hence, the dust will be more negatively charged for a plasma having massive ions leading to a relative increase in electron attachment to the dust particles. Now, if secondary emission currents are significant then an additional term containing currents due to secondary electron emission will be considered for the calculations of dust surface potential as given by Chow *et al.* [41]. The energies required to support the secondary emission in a dusty plasma should exceed 10 eV for electrons and 1keV for ions impinging on the dust grains which for the laboratory plasmas is rarely possible so the these currents can be neglected.

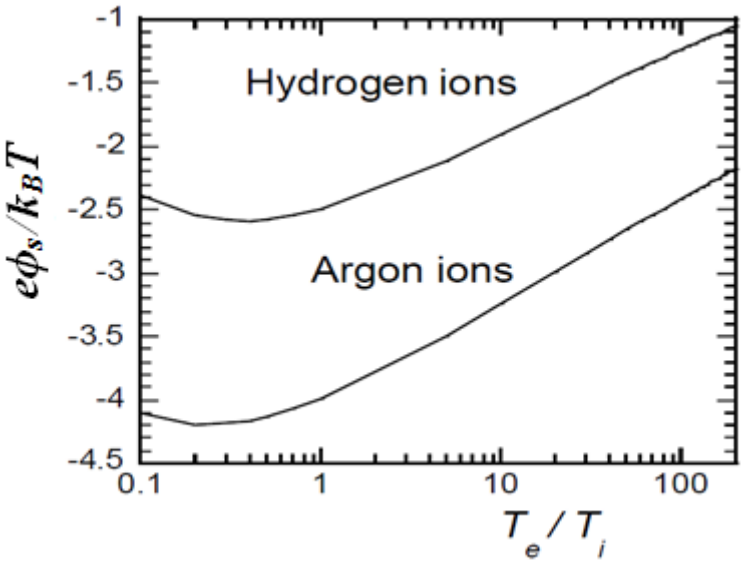

Fig. 1.5 The normalized relative dust surface potential as a function of temperature ratio of electron to ion for Hydrogen and Argon ion plasmas [25]

Moreover, charging of dust through the emission of photoelectrons from the grain surface depends on (i) wavelength of incident photons (ii) nature of the dust material, and (iii) surface area of the dust grains. This phenomenon is of great importance when the dust grains are exposed to UV radiations. As the work function of some metals like Ag, Cu, Al, Ca, Cs etc. required for the photoemission is less than 5 eV so release of photoelectrons become easy. The charging of dust through

photoemission is a dominant phenomenon in mostly astrophysical plasmas and near earth environments (less dense) than laboratory plasmas (more dense). The phenomenon yields a positively charged dust. The photoemission current is estimated by Rosenberg *et al.* [42] as

$$I_{PE} = e\, J_P\, Q_A\, Y_{PE}\, exp\left(-\frac{e\phi_S}{k_B T}\right)\pi a^2, \tag{1.9}$$

where J_P is the photon flux, Q_A is efficiency of photon absorption, Y_{PE} is yield of photoemission, T be average temperature of photoelectrons.

A number of other charging mechanisms like, thermionic emission, field emission, radioactive emission, impact ionization have been known but depends on the specific applications of a dusty plasma.

1.2.3.1.2 Non Isolated Dust Grains

For the case of densely packed non isolated dust grains, where the intergrain spacing $a_d \le \lambda_D$ plasma Debye length, an increase in number density of the dust grains tend to reduce the concentration of electrons available per dust grain. Hence, the grain surface potential relative to plasma $\phi_S \left(= V_S - V_p\right)$ will have a small magnitude than the case of isolated grains and consequently the average dust charge will decrease. Then, the average dust charge can be determined by charge neutrality condition [43] $en_{i0} = en_{e0} - Z_d en_{d0}$. The electron and ion currents for the negatively charged dust grains are similar to Eqs. (1.6 & 1.7)

The balance of two currents yields [43]

$$1 - Z_d \frac{n_{d0}}{n_{i0}} = \sqrt{\frac{m_e T_i}{m_i T_e}}\left(1 - \frac{e\phi_S}{k_B T_i}\right)\exp\left(-\frac{e\phi_S}{k_B T_e}\right). \tag{1.10}$$

For isolated grains, the parameter $Z_d\, n_{d0}/n_{i0} \ll 1$, so the relative dust surface potential ϕ_S and dust charged state Z_d depend only on dust grain radius while for non

isolated dust grains, $Z_d n_{d0}/n_{i0} \sim 1$, so dust potential and charge depend also on its density. Now if $T_i = T_e = T$, the following equation is obtained

$$\sqrt{\frac{m_i}{m_e}}\left(1+\frac{4\pi\varepsilon_0}{e}P\frac{e\phi_S}{k_BT}\right)\exp\left(\frac{e\phi_S}{k_BT}\right)+\frac{e\phi_S}{k_BT}-1=0, \qquad (1.11)$$

where $P\left(=\frac{ak_BT}{e}\frac{n_{d0}}{n_{i0}}\right)$ is called Havnes Parameter. The above equation shows the variation of dust potential, hence the dust density with Havnes parameter P. The solution of above equation for a potassium K^+ plasma as a universal plot of grain potential $\left(e\phi_S/k_BT\right)$ vs. *log P* is given in Fig. (1.6).

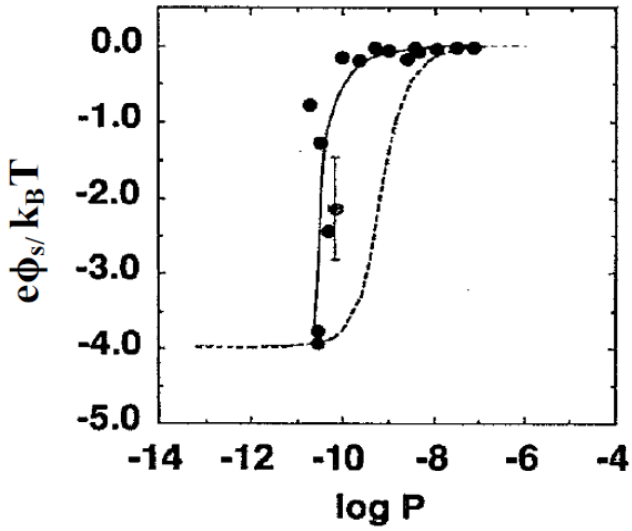

Fig. 1.6 The variation of relative grain potential $\left(e\phi_S/k_BT\right)$ vs. *log P* (The dashed line shows theoretical curve obtained from Eq. (1.11)) [38]

It is obvious from Fig. 1.6 that a gradual increase in dust density decreases the intergrain spacing and hence, the average dust grain charge or the potential also decreases. As the plasma density relative to dust density is increased (for small P) the grain potential approaches the isolated grain potential $\phi_S\left(=-4.0k_BT_e/e\right)$. Furthermore by plotting variation of Havnes parameter P with dust grain radius a one can obtain the critical value of n_{d0}/n_{i0} for which the dust charge reduces. One can see from it that

for grains of larger radii accumulates more charge than smaller sized grains. This may be significant in transition from strongly coupled dusty plasma to weakly coupled dusty plasma as the coulomb coupling parameter increases significantly with charge on dust grains.

1.2.3.2 Measurement Of Dust Charge

Few methods have been devised to measure dust charge in the laboratories for isolated or non isolated grains.

1.2.3.2.1 Isolated Grains

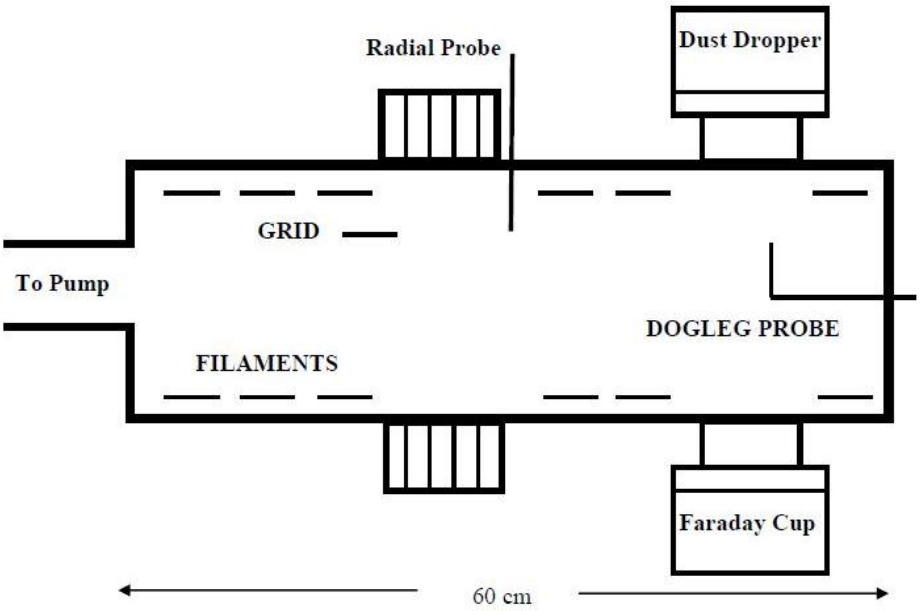

Fig. 1.7 The schematic of double plasma (DP) device containing Langmuir probe, Dust Dropper and Faraday Cup for determination of dust charge [4, 44]

The Schematic of set up used to measure dust charge on the isolated grain is shown in Fig. 1.7 [4, 44]. The experiment devised to measure charge on isolated dust grains (Walch *et al.* [44]) consists of double plasma (DP) machine having two identical aluminum cylinders (30 cm diameter and 30 cm long) joined end to end, dust dropper, Faraday cup and an electrometer. A diffusion pump of 15 cm diameter with a base pressure 0.6 μTorr is used to create vacuum. Three strings of 0.1 mm Tungsten wire

having 10 filaments (operating at 17 A and 45 V with a positive end biasing up to -125 V) are inserted inside each cylinder.

Single dust grains (SiC) are dropped from the top by agitating a thin metallic disc using an electromagnet cemented to it. Relatively large grains about 25-150 μm sizes are used to detect large signal to noise ratio. The dust charge is detected and measured by a sensitive electrometer attached to a Faraday cup (made of Copper and 8 cm in diameter) on the bottom. The charge falling into the cup is transferred to a feedback capacitor (200 pF) by an OP-AMP to generate a step wise increment in voltage and which returned to ground by feedback resistor (200 MΩ) with a decay constant of 40 ms. Experiments [33] with electrons from the emissive filaments but without plasma indicates that the grains charged to approximately the filament potential and are nearly independent of filament emission currents up to 2 A. The charge on the dust grains is of order 10^6e for SiC grains. At higher bias voltage the charge reduces as secondary emission becomes important. The charge on grains increases with grain size. The grains charge both positively and negatively. The plasma parameters can be determined from the Langmuir probe.

1.2.3.2.2 Non Isolated Dust Grains

An experimental set up used to investigate charging of the micron sized non isolated dust grains was described by Barkan *et al.* [37]. The experiment utilizes a Q-machine [45], [46] similar to [24]-[25] as shown in Fig. 1.3 in which a fully ionized, magnetized ($B_S \leq 4000$ Gauss) potassium plasma column of diameter ~ 4 cm, and ~80 cm length is produced by surface ionization of potassium atoms from an atomic beam oven on a hot Tantalum Plate (~ 2500K). The plasma densities range from 10^5-10^{10} cm^{-3} with electrons and K^+ ions at equal temperatures ~ 0.2 eV. The Plasma column is surrounded by rotating dust dispenser to evenly disperse dust in to it through rotation. The dust grains were hydrated aluminum silicate (Kaolin) with size limited up to 100 μm by the screen of dispenser. The photographs taken from electron microscope shows an average grain size ~ 5 μm and grain density ~ 6 x 10^4 cm^{-3}.

The main diagnostic tool was the movable Langmuir probe of a tantalum disk ~ 5 mm in diameter, oriented normally to the magnetic field and capable of motion along the axis of plasma column. The Langmuir probe measures the electron currents and

determines how the negative charge is distributed among free electrons and negatively charged dust grains. Fig. 1.8 shows the Langmuir characteristics under similar conditions for two cases (i) absence of dust grains (dust off) (ii) presence of dust grains (dust on). When the dust is turned on, the electron saturation current I_e collected at the positive biased probe reduces from the electron current I_{e0} in the absence of dust grains. It is due to the fact that the electron concentration available as free electrons reduces in the presence of dust as they get collected by the dust grains making them negatively charged.

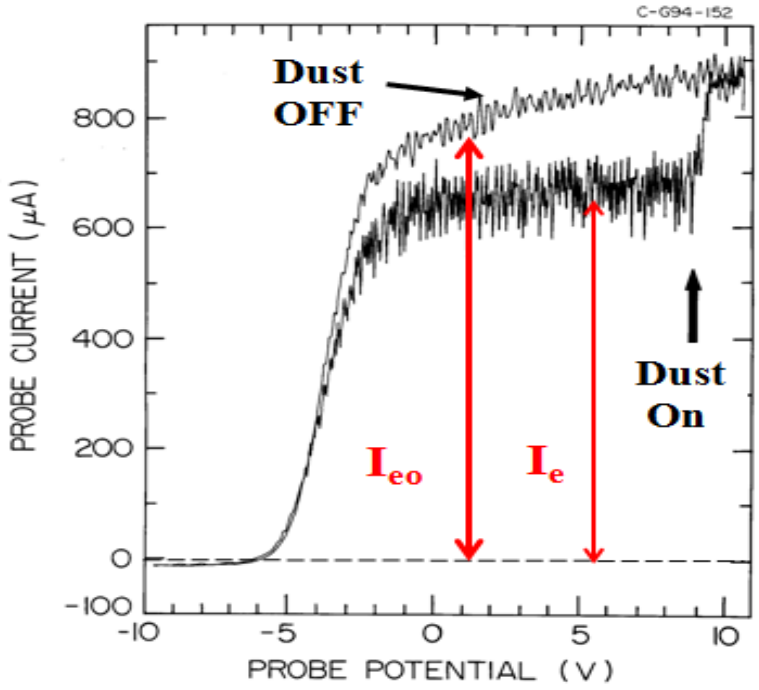

Fig. 1.8 Langmuir probe characteristics [37]

The Langmuir probe characteristic ratio is given by $\eta = \left(I_e / I_{e0} \Big/ I_i / I_{i0} \right)$ which is a measure of fraction of negative charge present as free in a plasma. Since the saturation currents are proportional to the respective densities, and densities of electrons and ions in the absence of dust are same $n_{e0} = n_{i0}$, so $\eta = n_e / n_i$, where $n_e \,\&\, n_i$ are electrons and ion densities in presence of dust, respectively and the ratio I_i / I_{i0} is a measure of attenuation of plasma in the presence of dust cloud. The plasma density $n_0 = n_{e0}$ can be computed using relation $I_{e0} = e n_{e0} v_{te} A$, where v_{te} is the

electron thermal velocity and A is the area of collecting probe. The quantity $Z_d n_d$ is estimated by measuring the reduction in the electron probe current $Z_d n_d = n_0\left(1-\left(I_e / I_{e0}\right)\right)$ and the charge neutrality condition $n_i = n_e + Z_d n_d$, where Z_d & n_d be dust charged state and dust density, respectively. On keeping the parameters n_d, T and a fixed one can measure η as a function of plasma density n_0. It is also observed from the experiment that at a constant dust density, a decrease in plasma density leads to a change in dust charge due to the dust charge fluctuations [38] and when the intergrain spacing nearly equals plasma Debye length. The results obtained through experiments well matches the theoretical predictions for non isolated grains.

1.2.3.3 Dust Charge Fluctuations

It is clear that any perturbations in plasma currents may lead to the fluctuations in dust charge which further introduces collective effects [37]. Now the dust charge fluctuations are given by

$$\frac{d}{dt}Q_{d1} = \frac{I_{e1}}{I_{e0}} + \frac{I_{i1}}{I_{i0}}, \tag{1.12}$$

where $Q_{d1}\left(=Q_d - Q_{d0}\right)$ is the perturbed dust charge, I_{e1} & I_{i1} be perturbed plasma currents. The size of dust particles is considered much smaller than the wavelength of perturbations as well as the Debye length of plasma so as to participate collectively.

The dust charge fluctuations and dynamics are then governed by

$$\frac{dQ_{d1}}{dt} + \eta Q_{d1} = -\left|I_{e0}\right|\left(\frac{n_{i1}}{n_{i0}} - \frac{n_{e1}}{n_{e0}}\right), \tag{1.13}$$

where n_{e1} & n_{i1} be the electron and ion perturbed densities and $\eta = \frac{\left|I_{e0}\right|e}{C_g}\left[\frac{1}{T_e} + \frac{1}{T_i - e\phi_{s0}}\right]$ is the dust charging rate. Here, $C_g = \left[a\left(1 + a/\lambda_{De}\right)\right]$ is dust capacitance and ϕ_{s0} be equilibrium floating potential of dust grains. λ_{De} is the

electron plasma Debye length. It is obvious from Eq. (1.13) that the dust charge fluctuations are determined by the electron and ion density perturbations in a plasma and natural decay rate η. Physically the charge fluctuations decay because any deviation in grain potential from equilibrium floating potential is opposed by the plasma currents [38].

1.3 WAVES AND INSTABILITIES IN DUSTY PLASMAS

We have already discussed in the previous sections that the presence of dust grains in a plasma modifies the existing wave modes and introduce new ones along with certain instabilities due to fluctuation of dust charge and dynamics of dust grains under the effect of various forces and external perturbations. It is well known that an electron- ion plasma support both longitudinal as well as transverse wave modes [4]. In ideal unmagnetized plasma only longitudinal modes can sustain as a result of density and potential fluctuations while in a magnetized plasma, both longitudinal and transverse wave modes can be excited. Moreover, the strong coupling among dust grains also affects the behaviour of wave modes. In this section, we will discuss a few waves and instabilities in the weakly coupled dusty plasmas and strongly coupled dusty plasmas.

1.3.1 Waves in Weakly Coupled Dusty Plasmas

As already discussed in previous section (1.2.1.3) that the coulomb coupling parameter $\Gamma<<1$ for a weakly coupled dusty plasma. Moreover, for weakly coupled dusty plasmas the dust grain radius a and average intergrain distance a_d is much smaller than the plasma Debye length λ_D and a sufficient dust density is maintained to observe the collective wave modes and instabilities..

1.3.1.1 Acoustic Wave Modes

In unmagnetized collisionless dusty plasma, two basic wave modes exist - dust acoustic waves (DAWs) and dust ion acoustic waves (DIAWs). These are similar to longitudinal sound waves which travel in form of compression and rarefaction. These

modes found applications in radio frequency generation and transmission through wave guides.

DAWs were theoretically predicted by Rao *et al.* [31] in the multi-component collisionless plasma, assuming the wave phase velocity to be much smaller than the electron and ion thermal speed. In the limit of low phase velocity, the inertia less electrons and ions provide the restoring force while the dynamic dust grains provide inertia. In these modes, the pressure gradient force is balanced by the electric force leading to a change in density perturbations which can be obtained using continuity

$$\frac{\partial n_j}{\partial t} + \nabla.\left(n_j \ \vec{v_j}\right) = 0 \tag{1.23}$$

and momentum equation,

$$\frac{\partial \vec{v}_j}{\partial t} + \vec{v}_j.\left(\nabla v_j\right) = \frac{q_j \vec{E}}{m_j} - \frac{T_j \nabla n_j}{m_j n_j}. \tag{1.24}$$

Here, $j = e$ or i or d for electrons, ions and dust, respectively and n_j, v_j, q_j, m_j, and T_j represents the density, velocity, charge, mass and temperature of the plasma constituents. A dispersion relation for DAWs has been obtained using the Poisson equation $-\nabla^2\phi = 4\pi\left(-en_{e1} - Z_d en_{d1} + en_{i1}\right)$, where dust charge fluctuations have been neglected which is

$$\omega^2 = 3k^2 v_{td}^2 + k^2 C_d^2 \Big/ \left(1 + k^2 \lambda_{Dd}^2\right). \tag{1.25}$$

Here v_{td}, λ_{Dd} & $C_d \left(= v_{td}^2 + \varepsilon Z_d^2 \frac{T_i}{m_d} \frac{1}{1 + \left(T_i/T_e\right)\left(1 - \varepsilon Z_d\right)} \right)$ are dust thermal speed, dust Debye length and dust acoustic speed, respectively. As the DAW phase velocity is much smaller than thermal speed so Eq. (1.25) reduces to

$$\omega^2 = k^2 C_d^2 \Big/ \left(1 + k^2 \lambda_{Dd}^2\right). \tag{1.26}$$

The effect of dust charge fluctuations have been considered by Melandsø *et al.* [47] and Varma *et al.* [48]. DAWs were observed in a number of laboratory

experiments [30], [49]-[53] in the weakly coupled unmagnetized plasma. Till now a number of theories and experiments have been performed to study the excitation and dispersion properties of DAWs [54].

DIAWs are the dust ion acoustic waves modified in the presence of immobile massive dust grains [31]. The influence of dust lies in the reduction of density of electrons due to attachment at the dust grains. The dust does not take part in dynamics. The inertia less electrons provides restoring force while ions provide inertia to the DIAWs. The DIAWs were firstly reported by Shukla and Silin [55]. The phase velocity of the waves is much larger than the ion and dust thermal speeds and the wave frequency is of the order of the ion plasma frequency $\omega_{pi} = \left(4\pi n_{i0} e^2 / m_i\right)^{1/2}$. The dispersion relation for DIAWs in the absence of dust density and charge fluctuations is given by

$$\omega^2 = k^2 c_s^2 \Big/ \left(1 + k^2 \lambda_{De}^2\right), \tag{1.27}$$

which in the long wavelength limit $k\lambda_{De} << 1$ reduces to $\omega = kc_S$, where $c_S = \sqrt{\frac{T_i}{m_i} + \frac{T_e}{m_i\left(1-\varepsilon Z_d\right)}}$ is dust modified ion acoustic speed, ε is relative dust concentration [56] and $\lambda_{De}\left[= T_e \Big/ 4\pi n_{e0} e^2\right]^{1/2}$ is electron Debye length. The relation shows an increase in phase velocity ω/k of the DIAWs with increasing relative density of dust grains which is responsible with the depletion of electron concentration and appearance of stronger space charge electric field in the presence of dust grains. The DIAWs reported in the experimental investigations [57] & [33] confirms the theoretical predictions of DIAWs.

1.3.1.1.1 Presence of Magnetic Field

As most of the space and laboratory dusty plasmas are confined in an external magnetic field so it is of great interest to observe the properties of dusty magneto-plasma. It has been observed that the presence of an external magnetic field B modifies the dispersion properties of different dusty plasma wave modes [55], [56],

[58]-[62]. In the limit of frequency $\omega \ll \omega_{ci}\left(=eB/m_i c\right)$ the ion cyclotron frequency, $k_z/k \gg \omega_{pd}/\omega_{pi}$ and $k_\perp \rho_i \gg k\lambda_{De}$, the modified frequency of DIAWs [4] in an external magnetic field applied along z-direction is given as

$$\omega^2 = k_z^2 c_s^2 \Big/ \left(1 + k_\perp^2 \rho_i^2\right). \tag{1.28}$$

Here, $\rho_i\left(=c_s/\omega_{ci}\right)$ is the ion gyro-radius, and $\omega_{pd}\left[=\left(4\pi n_{d0} Z_d^2 e^2/m_d\right)^{1/2}\right]$ is dust plasma frequency. Whereas in the limit $k_z/k \ll \omega_{pd}/\omega_{pi}$, the frequency corresponds to a modified DAW as shown in Eq. (1.29)

$$\omega^2 = k^2 \lambda_{De}^2 \omega_{pd}^2 \Big/ \left(1 + k^2 \lambda_{De}^2 + k_\perp^2 \rho_i^2\right) \tag{1.29}$$

The dust charge fluctuations have been neglected here for the sake of simple picture of the model but the effect of dust charge fluctuations on DIAWs have been examined by Shukla [58]. These waves propagate parallel to the direction of applied external magnetic field.

1.3.1.1.2 Finite Geometry effects

It has also been reported by Shukla and Rosenberg [61] that the presence of finite boundaries and collisions significantly modify the dispersion properties of DAWs and DIAWs. The LHS of Poisson equation $-\nabla^2\phi = 4\pi\left(-en_{e1} - Z_d en_{d1} + en_{i1}\right)$ used to find dispersion of wave modes in the finite geometry case can be written for cylindrical coordinates (r, θ, z) as

$$\nabla^2\phi = \nabla_\perp^2\phi + \frac{\partial^2\phi}{\partial z^2} = \frac{1}{r}\frac{\partial}{\partial r}\left(r\frac{\partial\phi}{\partial r}\right) + \frac{1}{r^2}\frac{\partial^2\phi}{\partial\theta^2} + \frac{\partial^2\phi}{\partial z^2}. \tag{1.31}$$

Then assuming perturbed potential $\sim \exp\left(ikz - \omega t\right)$, the Poisson equation for axially and azimuthally symmetric case can be written as

$$\frac{1}{r}\frac{\partial}{\partial r}\left(r\frac{\partial\phi}{\partial r}\right) + p_m^2\phi = 0, \tag{1.32}$$

where, $p_m^2 = -k_z^2 + \dfrac{\omega\left(\omega + i\nu\right)}{\lambda_{De}^2\left(\omega_{pi}^2 - \omega\left(\omega + i\nu\right)\right)}$.

Eq. (1.32) is the Bessel equation of zero order, the solution of which is $\phi(r) = \phi_0 J_0(p_m r)$, where, $J_0(p_m r)$ is the Bessel function of zero order with argument $p_m r$. On the surface of the cylindrical waveguide of radius R, the potential must vanish so one must have $J_0(p_m R) = 0$. Thus if x_n be the root of Bessel function, $p_m R = x_n$ be the zeros of Bessel function. For dominant mode, one must have m= n. First few zeros of Bessel functions are $x_1 = 2.404$, $x_2 = 5.5$, and $x_3 = 8.7$.

The modified dispersion relation for DIAWs in the bounded collisional dusty plasma can be given as

$$\frac{\omega(\omega + i\nu)}{\left(\omega_{pi}^2 - \omega(\omega + i\nu)\right)} = \left(k_z^2 + p_m^2\right)\lambda_{De}^2 . \tag{1.33}$$

The finite cylindrical boundary leads to an effective wave number which is given by $\left(k_z^2 + p_m^2\right)^{1/2}$, where radial wave number $k_\perp \approx p_m = \frac{x_n}{R}$ is quantized [4] for fixed plasma cylinder radius R. It is observed that the frequency of DIAWs is finite even in the absence of collisions for $k_z = 0$ due to a minimum effective radial wave number. Moreover, the collisional effects cause damping of DIAWs and DAWs as well.

1.3.1.2 Electrostatic Cyclotron Wave Modes

It has already been discussed that the presence of magnetic field modifies the electrostatic and electromagnetic wave modes in the weakly coupled dusty plasmas. In the presence of a static magnetic field (say along z direction), the cyclotron motions of electrons, ions and dust introduce the wave modes that propagate nearly perpendicular to the direction of magnetic field with a finite parallel wave number $k_z \ll k_\perp$, the perpendicular wave number are called electrostatic cyclotron waves. There can be two wave modes: electrostatic dust ion cyclotron waves (EDICWs) and electrostatic dust cyclotron waves (EDCWs). These wave modes are of great importance in particle accelerators, earth's ionosphere, and nuclear fusion technologies.

EDICWs are dust modified electrostatic ion cyclotron waves which are excited due to magnetic field aligned electron drifts. In these modes dust is treated as an

immobile charged neutralizing background. The frequency of these modes is just above the ion cyclotron frequency ω_{ci} and increases with increase in relative dust concentration ε [35].

In the limit, ω_{cd}, kv_{td}, $kv_{ti} \ll \omega \ll k_z v_{te}$, ω_{ce}, $k\lambda_{De} << 1$ and $Z_d m_i \ll m_d$, the dispersion relation can be written as

$$\omega^2 = \omega_{ci}^2 + k_\perp^2 c_s^2 \tag{1.34}$$

where, $c_s = \sqrt{\frac{T_i}{m_i} + \frac{T_e}{m_i\left(1-\varepsilon Z_d\right)}}$ is dust modified ion acoustic speed and ε is the relative dust concentration. The critical drift required to excite the EDICW modes decreases with an increase in dust concentration as well.

In EDCWs are low frequency waves in which the dynamics of magnetized dust play an important role while ions remain in Boltzmann equilibrium along magnetic field. These modes are hard to excite as a strong magnetic field is required to magnetize the massive dust particles. The dispersion relation in the long wavelength limit is given by

$$\omega^2 \approx \omega_{cd}^2 + k_\perp^2 C_d^2, \tag{1.35}$$

where, $\omega_{cd}\left(=\frac{Z_d eB}{m_d c}\right)$ is the dust cyclotron frequency and C_d is the modified dust acoustic speed (as discussed in sec. 1.3.1.1).

Shukla and Rahman [60], and Shukla and Mamun [63] have also discussed the possibility of mixed modes in the magnetized bounded plasmas, where dust dynamics play an important role. For the wave propagation exactly along the direction of magnetic field (parallel propagation), a coupled dust cyclotron and dust Alfven modes have been studied [4]. In the limit of frequency $\omega \ll \omega_{cd}$ dust cyclotron frequency, the dispersive dust Alfven modes have been discussed while in the opposite limit, modes frequency is dust whistler wave frequency. On the other hand, for oblique propagation with $k_z \ll k_\perp$, a coupled dust cyclotron and modified dust acoustic mode can exist [4]

& [63]. The finite geometry effects on the cyclotron modes are similar to acoustic modes which provide a finite perpendicular quantized wave number for fixed plasma radius.

1.3.2 Instabilities in Dusty Plasmas

Most of the space and laboratory dusty plasmas are far from the thermodynamic equilibrium. The non-equilibrium in the plasma produces collective modes whose amplitude grow exponentially or is damped due to collisions or collisionless phenomenon (Landau damping or dust charge fluctuations). Dusty plasmas can be driven unstable when the sources of free energy are available in the system. The flows driven by external fields, pressure gradients, dust charge fluctuations, and electron or ion beams propagating inside the plasma couple with the normal modes and made them unstable. Besides all above, the usual hydrodynamic instabilities: Kelvin Helmholtz, Rayleigh Taylor and parametric instabilities also arise in the dusty plasmas. The dust plasma instabilities received much attention due to their possible applications in study of earth's ionosphere, earth's magnetopause, fluid dynamics, solar wind etc. The studies of instabilities are of great importance for understanding the origin of growth or damping of wave amplitudes, and voids (nonlinear microgravity phenomenon) in the space and laboratory plasmas [4]. The dispersion relation consists of the two parts (i) real ω_r and (ii) imaginary ω_i. For the weak damping $\left|\omega_i\right| \ll \omega_r$, the frequency and growth rate of the instabilities can be found using the relations: $\mathrm{Re}\,\varepsilon\left(\omega_r, k\right) = 0$ and $\omega_i = -\dfrac{\mathrm{Im}\ \varepsilon\left(\omega,k\right)}{\partial\,\mathrm{Re}\,\varepsilon\left(\omega,k\right)}\Bigg|_{\omega=\omega_r}$, respectively [64].

1.3.2.1 Current Driven Instability

The major mechanism related to instabilities of various electrostatic waves is associated with the equilibrium drift of electrons relative to ions in the plasma [35], [57] & [65] the so called current driven instability which is well known for ion acoustic waves as well as electrostatic ion cyclotron waves. The instability overcomes the collisionless Landau damping due to resonant energy exchange as a result of electron-

wave interaction. In an ordinary electro–ion plasma Landau damping makes the excitation of ion acoustic waves difficult but the presence of negatively charged dust grains reduces the Landau damping and corresponding spatial damping thereby enhancing the growth rate of current driven instabilities. It also shows that the critical drift required for exciting instabilities decreases in the presence of negatively charged dust grains and reduces the cyclotron damping of ions also.

1.3.2.2 Ion Dust Streaming Instability

In ion dust streaming instability the dust modes couple with the ions currents triggered due to externally applied static electric and magnetic fields. These ion dust streaming instabilities of DAWs are identical to current driven instability of DIAWs. It has been observed in the RF discharge plasmas [49] and has been theoretically studied by Rosenberg [42], [63] & [66]-[67]. The presence of the ion flux modifies the dispersion properties of DAWs.

1.3.2.3 Velocity Shear Instability

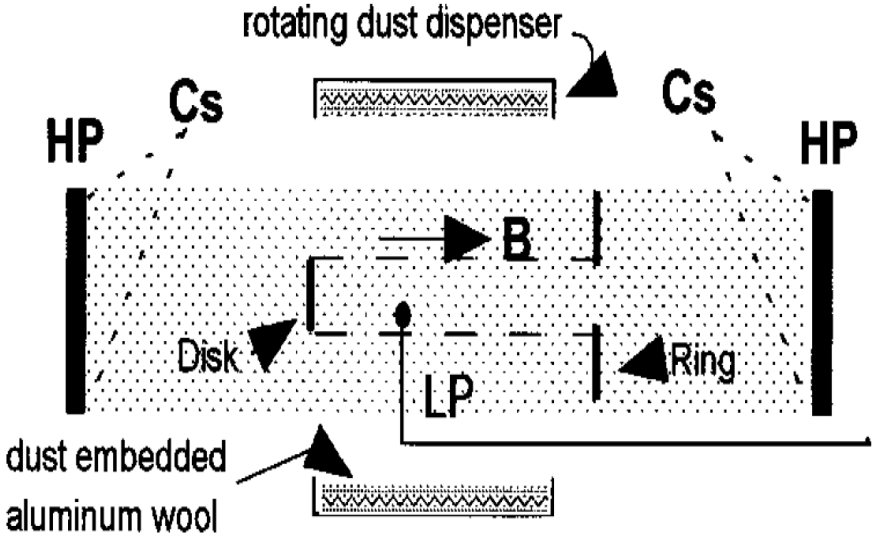

Fig. 1.9 The experimental set up used to produce magnetized plasma with sheared ion flow [71]

This is the parallel velocity shear instability (PVSI) which produces in the non-uniform magnetized plasmas. It is a fluid instability that occurs in the plasma in which ion flows along the direction of applied magnetic field with a velocity which varies in the direction of transverse density gradient i.e., perpendicular to magnetic field. This instability is also known as Kelvin Helmholtz instability (KHI) [68]. This instability was firstly observed by D'Angelo [69] for electron-ion plasma. The presence of negatively charged dust modifies the growth rate of PVSI of low frequency electrostatic waves [70]-[71]. The growth rate of the instability increases with the relative shear in ion flows. The instability feeds on the mean energy of ion flow. It can be produced by inserting a disk and ring arrangement in a dusty plasma [71] as shown in Fig. 1.9.

1.3.3 Waves in Strongly Coupled Dusty Plasmas

Dusty plasmas observed in laboratory or space environments like white dwarfs, supernovas, plasma produced by laser compression of matter etc. mostly have dust grains in the strongly coupled liquid or crystalline states as already discussed in previous section (1.2.1.3). The uncorrelated weakly coupled dusty plasma are due to a strong influx of energy in to the gaseous sub system of dust grains which cause an increase in temperature of the dust grains and hence, decrease in coupling parameter. This heating can be due to spatial or temporal charge variation or due to dust wave instabilities induced in the dusty plasmas [72]. The dispersion properties of strongly coupled plasmas significantly deviate from the ideal weakly coupled dusty plasmas.

The waves in strongly coupled dusty plasmas have been studied using different theoretical approaches e.g., Quasi-localized charge approximation (QLCA) [73]–[75], generalized hydrodynamic (GH) Model [76]–[78], and multi-component kinetic theory [79]. One numerical simulation technique known as Molecular Dynamic (MD) simulation technique has also been evolved to study the dispersion properties of strongly coupled dusty plasmas in a broad range of Coulomb coupling parameter Γ, from gaseous to strongly coupled liquid and then crystalline state [80]-[81]. The results obtained from MD simulations are found in good agreement with the results given by above theories.

The simple physical picture of the viscoelastic effects due to strong correlations among dust grains can be described by GH model [76]. This phenomenological model is generally valid over a large range of strong correlation parameter, $1 \le \Gamma \ll 200$ i.e., from weakly coupled gas phase to strongly coupled liquid phase. The linearized GH momentum equation for dust grains is given by [76]

$$\left(1+\tau_m \frac{\partial}{\partial t}\right)\left[m_d n_{d0} \frac{\partial}{\partial t}\delta\vec{u_d} + \nabla \delta P + Z_d e n_{d0} \delta\vec{E}\right] = \eta \nabla.\nabla \delta u_d + \left(\zeta + \frac{\eta}{3}\right)\nabla\left(\nabla.\delta\vec{u_d}\right), \tag{1.36}$$

where δu_d is the perturbed velocity of dust, δP is pressure, η and ζ are shear and bulk viscosity coefficients, respectively and τ_m is the relaxation time. The compressibility and relaxation time of dust fluid is given as

$$\mu_d = 1 + \frac{1}{3}u(\Gamma) + \frac{1}{9}\frac{\partial u(\Gamma)}{\partial \Gamma}, \tag{1.37}$$

and

$$\tau_m = \left(\zeta + \frac{4}{3}\eta\right) \Big/ \left(n_{d0} T_d \left(1 - \gamma_d \mu_d + {}^{4u(\Gamma)}\!/_{15}\right)\right). \tag{1.38}$$

Here $u(\Gamma)$ is a measure of excess internal energy. In the range, $1 \le \Gamma \le 200$ Slattery *et al.* [82] have given the relation $u(\Gamma) = -0.89\Gamma + 0.95\Gamma^{1/4} + 0.19\Gamma^{-1/4} - 0.82.$ Transport coefficients have been given by Ichimaru *et al.* [83]. In the strongly coupled liquid dust regime basically two wave modes have been observed: (i) Longitudinal waves (ii) Transverse waves. The modes can be studied in the two regimes: hydrodynamic regime $\omega\tau_m \ll 1$ and strongly coupled regime $\omega\tau_m \gg 1$.

1.3.3.1 Longitudinal Waves

In these wave modes dust provide inertia while electrons and ions provide thermal effects. The low frequency longitudinal modes are similar to the dust acoustic waves modified due to strong correlations among dust grains. The dispersion relation in the hydrodynamic regime $\omega\tau_m \ll 1$ using GH model is given by Kaw and Sen [76] as

$$\omega\left(\omega+i\left(\nu_d+\eta^* k^2\right)\right)\simeq k^2\left[v_{td}^2\gamma_d\mu_d+\frac{C_d^2}{\left(1+k^2\lambda_{De}^2+k^2\lambda_{Di}^2\right)}\right], \qquad (1.39)$$

where ν_d is the dust neutral collisional frequency, and $\eta^*=\frac{\left(\zeta+\frac{4}{3}\eta\right)}{m_d n_{d0}\omega_{pd}a_d^2}$. Here a_d is the intergrain distance. In hydrodynamic regime the longitudinal modes are similar to dust acoustic modes whose phase velocity is modified due to compressibility and shear viscosity of the strongly correlated dust system. The phase velocity increases with wave number k but showed a decrease for large k values (see Fig. 1.10). The modified dust acoustic waves suffers viscous damping along with collisional damping with the damping rate proportional to $\eta^* k^2$.

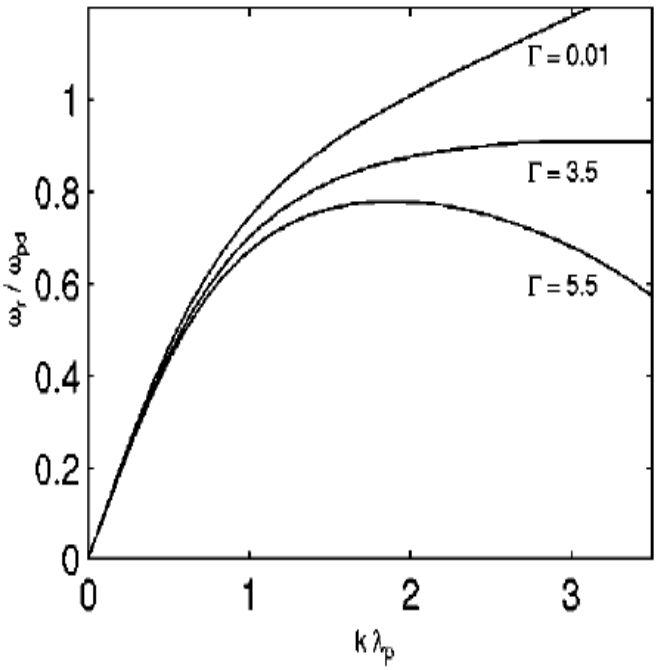

FIG. 1.10 Dust acoustic mode dispersion relation at different values of strong coupling Parameter Γ [76]

Moreover, in the strongly correlated regime, $\omega\tau_m \gg 1$, one have the dispersion relation [76]

$$\omega(\omega+i\nu_d) \simeq k^2\left[v_{td}^2\gamma_d\mu_d+\frac{C_d^2}{\left(1+k^2\lambda_{De}^2+k^2\lambda_{Di}^2\right)}+\frac{\eta^*}{\tau_m}\right]. \qquad (1.40)$$

Equation (1.40) is also the modified dust acoustic wave. The longitudinal waves in strongly coupled dusty plasmas are also subjected to ion dust streaming instabilities that may be a reason of deviation of theoretical and experimental results for dust acoustic type longitudinal modes.

1.3.3.2 Transverse Waves

The GH model describe that a dusty plasma having strong correlations among dust grains acquires significant ‘‘rigidity’’ to transverse wave motion and may therefore be able to support ‘‘shear’’ wave modes with $\vec{k}\bullet\overrightarrow{\delta u_d}=0,$ or $\vec{k}\times\overrightarrow{\delta u_d}\neq 0$. The dispersion relation for transverse modes can be obtained by eliminating longitudinal component form GH momentum equation. The dispersion relation obtained by Kaw and Sen [76] is

$$\omega=-i\frac{\eta^*k^2}{\left(1-i\tau_m\omega\right)}, \qquad (1.41)$$

which in the hydrodynamic limit yields a purely damped mode, $\omega=-i\eta^*k^2,$ while in the strong coupling regime, yields a propagating elastic wave, $\omega^2=\frac{\eta^*k^2}{\tau_m}$. The transverse shear modes are also significantly affected by the neutral collisions. These modes in strongly coupled liquids have been experimentally observed by Pramanik *et al.* [84], and Kaw [77] but a different approach is required to observe transverse waves in plasma crystals called dust lattice waves.

At large strong correlation parameter Γ, there is a need to introduce the effect of screening parameter κ because the viscoelastic coefficients vary with the screening of the dust grains as the strong coupling parameter decreases with increasing screening parameter. But the one component plasma (OCP) results of GH model are fairly valid for $\kappa \leq 1$ [85].

1.4 NEGATIVE ION PLASMA

The negative ion plasmas consist of electrons, positive ions and negative ions instead of dust grains. They are produced by introducing electronegative gas such as sulfur hexafluoride (SF_6**)** and chlorofluorocarbon etc. into vacuum system at a pressure ~10^5 Torr. These SF_6 ions have strong affinity for low energy electrons so a fraction of electrons gets attached to make them negatively charged SF_6^- ions and hence the negative ion plasmas. These are characterized by the parameter $\varepsilon = n_{-0}/n_{+0}$, the relative concentration of negative ions in a plasma. These occur naturally in space and astrophysical environments, neutral beam sources, photosphere of sun, earth's ionosphere, plasma processing reactors etc. They found great applications in surface plasma technologies, chemical vapour deposition techniques, ultra large scale integration (ULSI) fabrications etc. The behaviour of negative ions in a plasma is similar to the negatively charged dust grains present in plasma. The basic difference between negative ion plasma and dusty plasma is the charge and size of the dust grains varies and this variation in negative charge, and size of the dust grains also introduces collective phenomenon while the negative ions behave as the counterpart of positive ions in an electron– ion plasma as well as a background massive species providing the inertia.

1.5 PLASMA RADIATIONS

The plasma absorbs or emits radiations through two basic mechanisms: (i) radiations from emitting atoms (ii) radiations from accelerated charges. These emitted or absorbed radiations are used to observe various properties of confined plasmas such as in thermonuclear fusion reactors. The radiations emitted through a plasma is a distinctive characteristics of state of plasma particles and have great dependence on the collective properties of plasma. The radiations passing through a plasma are generally absorbed or damped so the intensity of radiations get reduced. According to test charge theory of plasma radiations [64] three basic radiations occurring in the plasma are:

- **Bremsstrahlung radiations** due to deflection of one charged particle from another charged particle

- **Cyclotron or Synchrotron radiations** from a charged particle gyrating in a magnetic field at cyclotron frequency
- **Cerenkov radiations** from charged particles moving faster than the phase speed of characteristic waves inside a plasma

The radiations emitted from the plasma are generally Blackbody radiations (temperature dependent according to Stefan's law) or Bremsstrahlung radiations (due to encounter of one particle with the other). In contrast to Bremsstrahlung, the energy loss through blackbody radiations exceeds the energy generated within the confined plasmas. The blackbody radiations are irrelevant for laboratory plasmas as it require a large plasma size. The atoms or ions in excited states in the partially ionized plasma also radiate energy known as impurity radiations. This energy loss can be controlled by improved vacuum technologies.

The charged particles moving in the magnetically confined plasmas also radiate energy at cyclotron frequency called cyclotron radiations. The electrons inside the magnetically confined plasmas usually in controlled nuclear fusions are mildly relativistic hence radiate energy which exceeds the energy generated in the reactions. For relativistic electrons, the radiations emitted are of high energy and called Synchrotron radiations. For the plasmas having electrons and ions at same temperature this problem is of great concern. These radiations dominate in the solar radio burts, radiations from Jupiter and crab nebulae etc

The third process by which the plasma absorbs energy is the Cerenkov radiation in which a beam of charged particle propagates at a speed greater than the phase velocity of plasma or electromagnetic waves inside the plasma. It loses its energy to the plasma thereby exciting the plasma waves or electromagnetic waves inside the plasma medium.

1.6 OBJECTIVES & THESIS LAYOUT

The present research work aims on the investigation of electrostatic waves and instabilities in magnetized dusty plasmas in weak coupling or strong coupling among dust grains. Main focus of the research work is to investigate the dispersion properties

and role of dust particle dynamics on different electrostatic waves and instabilities in a plasma having weakly or strongly coupled dust grains. Theoretical model to study excitation of waves and instabilities in dusty plasmas have been developed and calculations of the mode frequencies and growth rate at different experimental parameters have been done. The theoretical results have been compared with experiments and their possible applications in various dusty plasma fields have been discussed. Moreover, most of the investigations have been performed in presence of variable charge dust grains. In addition, since dusty plasma experimental devices are bounded and hence the effect of finite boundaries in investigation of electrostatic waves and instabilities has been considered.

The present research work is based on the following major objectives which are outlined below:

1. Ion beam driven ion-acoustic waves in a plasma cylinder with negatively charged dust grains.

2. Effect of dust charge fluctuations on current-driven electrostatic ion-cyclotron instability in a collisional magnetized plasma.

3. Excitation of Kelvin Helmholtz instability by an ion beam in a plasma with negatively charged dust grains.

4. Theoretical modelling of an ion beam driven Kelvin Helmholtz instability in a plasma cylinder having negatively charged dust grains.

5. Theoretical modelling of Kelvin Helmholtz instability driven by ion beam in a negative ion plasma.

6. Current driven low frequency electrostatic waves in a collisional strongly coupled magnetized dusty plasma.

7. A nonlocal theory of current driven low frequency modes in a magnetized strongly coupled collisional dusty plasma.

THESIS LAYOUT

The entire research work divides the thesis into seven chapters which are as discussed below:

Chapter 1: Chapter 1 deals with the introduction to dusty plasmas, production, and charging mechanisms of the dust grains. Moreover, background of the ion acoustic waves (IAWs), electrostatic ion cyclotron waves (EICWs), Kelvin Helmholtz instability (KHI) in weakly coupled regime and collective wave modes in strongly correlated regime of dust grains in laboratory and space plasmas have been discussed.

Chapter 2: This chapter contains the theoretical model to elucidate the excitation of an ion beam driven ion acoustic waves (IAWs) in a plasma cylinder having negatively charged dust grains. Fluid treatment is employed to study the plasma and beam response. The growth rate of the instability has been obtained using first order perturbation techniques. The theoretical results are simplified using experimental plasma parameters to study the effect of relative concentration of negatively charged dust grains on the growth rate, mode frequency and phase velocity of ion beam driven ion acoustic instability. The applicability of orbital motion limited (OML) theory [38] to IAW propagating in a magnetized dusty plasmas has been discussed in which size and shape effects of dust grains have been neglected.

Chapter 3: In this chapter, a theoretical model based on fluid treatment has been developed to excite the current driven electrostatic ion cyclotron instability in a collisional magnetized dusty plasmas, taking into account the dust dynamics and dust charge fluctuations. A model of dust charge fluctuations given by Whipple *et al.* [38] and Jana et al. [39] is incorporated to evaluate the growth rate of the instability under the assumption of small growth rate as compared to mode frequency. The effect of dust dynamics and dust charge fluctuations on the wave frequency and the growth rate of EICWs have been discussed.

Chapter 4: An analytical model based on the local and nonlocal fluid treatment on plasmas species and ion beam have been developed to study the excitation of Kelvin Helmholtz instability (KHI) by an ion beam in a magnetized dusty plasmas. Theories have been simplified to elucidate the effect of negatively charged dust grains on the frequency and growth rate of KHI. The effect of velocity shear as well as the ion beam has been analyzed in detail. This chapter also aims to develop a theoretical model to study the effect of negatively charged dust grains on the Kelvin Helmholtz instability

driven by an ion beam in a magnetized plasma having cylindrical geometry. The effect of radial boundaries has been elucidated through radial density and potential profiles of dusty plasma. The effect of relative concentration of dust grains, shear parameters and beam parameters have been analyzed in detail and their possible applications to laboratory plasmas also been enumerated.

Chapter 5: In this chapter, theoretical model for Kelvin Helmholtz instability driven by an ion beam containing two kind of ions-positive and negative in a magnetized plasma having a finite cylindrical geometry and infinite geometry has been developed. A comparison of mode frequency and growth rate of KHI for both the positive and negative ion modes has been done for finite geometry and infinite geometry of plasma. The effect of presence of beam and various parameters of beam on the growth rate of KHI for both the ion modes has also been studied for both the geometries of plasmas. Moreover, the effect of relative mass of positive and negative ions has been discussed in detail.

Chapter 6: This chapter deals with the theoretical model based on generalized hydrodynamic approach [76] to study the excitation of low frequency electrostatic wave modes in a collisional strongly coupled magnetized dusty plasma. The longitudinal and transverse modes have been studied under the effect of magnetic field aligned ion currents. The effect of strong correlation parameters, drift velocity of ions on the dispersion properties of longitudinal and transverse wave modes have been discussed in the hydrodynamic regime. The chapter also includes the investigation of low frequency longitudinal and transverse shear modes driven by magnetic field aligned ion and dust currents in a collisional strongly coupled dusty plasmas having a cylindrical geometry. The generalized hydrodynamic model using one component plasma (OCP) theory has been employed to develop the theoretical model for axially and azimuthally symmetric case of plasma cylinder. The dispersion properties have been studied under the effect of magnetic field aligned plasma drifts and collisions in the kinetic regime (frequency much higher than the dust particle relaxation time). The effect of magnetic field and finite boundaries has also been investigated.

Chapter 7: The major findings of different investigations and their significance have been summarized in this chapter. Moreover, the future prospective has also been highlighted.

REFRENCES

[1] W. Crookes, *Phil. Trans. R. Soc. Lond.* **170**, 135 (1879).

[2] L. Tonk and I. Langmuir, *Phy. Rev.* **33**, 195 (1929).

[3] F. F. Chen, "*Introduction to Plasma Physics and Controlled Fusion"* Second edition, Vol. **1 (**1974): Plasma Physics, Los Angeles.

[4] P. K. Shukla and A. A. Mamun, "*Series in Plasma Physics: Introduction to Dusty Plasma Physics"* Institute of Physics Publishing Ltd., Bristol and Philadelphia (2002), Chapter I.

[5] L. Spitzer, "*Physical Processes in the Interstellar Medium,*" (1978) John Wiley, New York.

[6] R. Merlino, and J. Goree, *Phys. Today* **57**, 32 (2004).

[7] B. A. Smith et al., *Science* **212**, 163 (1981); *Science* **215**, 504 (1982).

[8] G.S. Selwyn, J. Singh and R. S. Bennet, *J. Vac. Sci. Technol. A* **7**, 2758 (1989).

[9] R. M. Roth, K.G. Spears, and G. Wong, *Appl. Phys. Lett.* **46**, 253 (1985).

[10] J. Y. N. Cho, and M. C. Kelley, *Rev. Geophys.* **31**, 243 (1993).

[11] O. Havnes, J. Trøim, T. Blix, W. Mortensen, L. I. Naeshim, E. Thrane and Tønnesen, *J. Geophys. Res.* **101,** 10829 (1996).

[12] J. Glanz, *Science* **264**, 28 (1994).

[13] G.A. Wurden, A. J. Wurden, and I. M. Glasdstone, *IEEE Trans. Plasma Sci.* **27**, 142 (1999).

[14] J. Winter, *Plasma Phys. Control. Fusion*. **40**, 1201 (1998); *Phys. Plasmas* **7**, 3862 (2000); *Plasma Phys. Control. Fusion* **46**, B583 (2004).

[15] S. Ichimaru, *Rev. Mod. Phys.* **54**, 1017 (1982).

[16] H. Ikezi, *Phys. Fluids* **29**, 1764 (1986).

[17] J. H. Chu, J. B. Du, and I. Lin, *J. Phys. D: Appl. Phys.* **27**, 296 (1994).

[18] H. Thomas , G. E. Morfill, V. Demmel, J. Goree, B. Feuerbacher, and D. Möhalmann, *Phys. Rev. Lett.* **73**, 652 (1994).

[19] H. Hayashi, and K. Tachibana, *Japan J. Appl. Phys.* **33**, 804 (1994).

[20] A. Melzer, T. Trottenberg, and A. Piel, *Phys. Lett. A* **191,** 301 (1994).

[21] E. Thomas Jr., R. Fisher, and R.L. Merlino, *Phys Plasmas* **14**, 123701 (2007).

[22] S. Hamaguchi, R. T. Farouki, and D. H. E. Dubin, *Phys. Rev.* E **56,** 4671 (1997).

[23] L. Boufendi, A. Bouchoule, *Plasma Sources Sci. Tech.* **3,** 262 (1994).

[24] W. Xu, B. Song, R. L. Merlino, and N. D'Angelo, *Rev. Sci. Instrum.* **63**, 5266 (1992).

[25] R. L. Merlino, "*Plasma Physics Applied" Transworld research network, India,* Chapter-V (2006), 73-110.

[26] J. H. Chu and I. Lin, *Phys. Rev. Lett.* **72,** 4009 (1994).

[27] E. Thomas Jr., *Phys. Plasmas* **7**, 3194 (2000).

[28] E. Thomas Jr., U. Konopka, D. Artis, B. Lynch, s. Leblane, S. Adams, R. L. Merlino, and M. Rosenberg, *J. Plasma Phys.* **81**, 345810206 (2015).

[29] V. E. Fortov, A. P. Nefedov, V. M. Torchinsky, V. I. Molokov, O. F. Petrov, A. A. Samarian, A. M. Lipaev, and A. G. Kharpak , *Phys. Lett. A* **229,** 317 (1997).

[30] C. Thompson, A. Barkan, N. D'Angelo, and R. L. Merlino, *Phys. Plasmas* **4**, 2331 (1997).

[31] N. N. Rao, P. K. Shukla, and M. Y. Yu, *Planet. Space Sci.* **38**, 543 (1990).

[32] B. Walch, M. Horányi, and S. Robertson, *Phys. Rev. Lett.* **75**, 838 (1995).

[33] Y. Nakamura, and H. Bailung, *Rev. Sci. Instrum.* **70**, 2345 (1999).

[34] N. D'Angelo, *Planet. Space Sci.* **38**, 1143 (1990).

[35] R. L. Merlino, A. Barkan, C. Thompson, and N. D'Angelo, *Phys. Plasmas* **5**, 1607 (1998).

[36] M. Hirt, D. Block, and A. Piel, *Phys. Plasmas* **11**, 5690 (2004).

[37] A. Barkan, N. D'Angelo, and R. L. Merlino, *Phys. Rev. Lett.* **73,** 3093 (1994).

[38] E.C. Whipple, T.G. Northdrop and D.A. Mendis, *J. Geophys. Res.* **90**, 7405 (1985).

[39] M. R. Jana, A. Sen, and P. K. Kaw, *Phys. Rev. E* **48**, 3930 (1993).

[40] M.S. Barnes, J. K. Keller, J. C. Forster, J. A.O'Neill, and D. K.Coultas, *Phys. Rev. Lett.* **68**, 313 (1992).

[41] V. W. Chow, D. A. Mendis, and M. Rosenberg, *J. Geophys. Res.* **98**, 19065 (1993).

[42] M. Rosenberg, *J. Vac. Sci. Tech. A* **14**, 631 (1996).

[43] O. Havnes, C. K. Geortz, G. E. Morfill, E. Grün, W. Ip, *J. Geophys. Res.* **92**, 2281 (1987).

[44] B. Walch, M. Horányi, and S. Robertson, *IEEE Trans. Plasma Sci.* **22**, 97 (1994).

[45] R. W. Motley, *Q-Machines* (Academic Press, San Diego, CA, 1975).

[46] A. Barkan, N. D'Angelo and R.L. Merlino, *Planet. Space Sci.* **44**, 239 (1996).

[47] F. Melandsø, T. K. Aslaksen, and O. Havnes, *J. Geophys. Res.* **98**, 13315 (1993a); *Planet. Space Sci.* **41**, 321 (1993b).

[48] R. K. Varma, P. K. Shukla, and V. Krishan, *Phys. Rev. E* **47**, 3612. 1993.

[49] A. Barkan, R. L. Merlino, and N. D'Angelo, *Phys. Plasmas* **2**, 3563 (1995).

[50] J. B. Pieper and J. Goree, *Phys. Rev. Lett.* **77**, 3137 (1996).

[51] H. Prabhakara and V. Tanna, *Phys. Plasmas* **3**, 3176 (1996).

[52] V. I. Molotkov, A. P. Nefedov, V. M. Torchinskii, V. E. Fortov, and A. G. Khrapak, *JETP* **89**, 477 (1999).

[53] E. Thomas Jr., and R. L. Merlino, *IEEE Trans. Plasma Sci.* **29**, 152 (2001).

[54] R. L. Merlino, *J. Plasma Phys.* Doi: 10.1017/S0022377814000312 (2014).

[55] P. K. Shukla and V. P. Silin, *Phys. Scr.* 45, 508 (1992).

[56] V. W. Chow and M. Rosenberg, *Planet. Space Sci.* **43**, 613 (1995).

[57] A. Barkan, N. D'Angelo, and R. L. Merlino, *Planet Space Sci.* **44**, 239 (1996).

[58] P. K. Shukla, *"Waves in dusty Plasmas: in Physics of Dusty Plasmas"* Singapore, (1996), pp. 107-121.

[59] R. Bharuthram and T. Pather, *Planet. Space Sci.* **44**, 137 (1996).

[60] P. K. Shukla and H. U. Rahman, *Planet. Space Sci*. **46**, 541 (1998).

[61] P. K. Shukla and M. Rosenberg, *Phys. Plasmas* **6**, 1038 (1999).

[62] P. K. Shukla, *Astrophys. Space Sci*. **264**, 235 (1999).

[63] P. K. Shukla and A. A. Mamun, *J. Plasma Phys.* **65**, 97 (2001).

[64] N. A. Krall, and A. W. Trivelpiece, "*Principles of Plasma Physics",* (1973), McGraw-Hill, USA, Chapter I & XI.

[65] R. L. Merlino, *IEEE Trans. Plasma Sci.* **25,** 60 (1997).

[66] P.K. Kaw and R. Singh, *Phys. Rev. Lett.* **79**, 423 (1997).

[67] R. L. Merlino, *Phys. Plasmas* **12**, 124501 (2009).

[68] S. Chandrasekhar, "*Hydrodynamic and Hydromagnetic Stability*" (Oxford University Press, Oxford, 1961), Chap. XI.

[69] N. D' Angelo, *Phys. Fluids* **8**, 1748 (1965).

[70] N. D' Angelo, and B. Song, *Planet. Space Sci.* **38**, 1577 (1990).

[71] Q. Z. Luo, N. D' Angelo, and R. L. Merlino, Phys. Plasmas **8**, 31 (2001).

[72] V. E. Fortov, G. E. Morfill, "*Series in Plasma Physics: Complex and Dusty Plasmas-From Laboratory to Space"* CRC Press Taylor & Francis Group, FL, (2010), Chapter II.

[73] G. Kalman and K. I. Golden, *Phys. Rev. A* **41**, 5516 (1990).

[74] M. Rosenberg and G. Kalman, *Phys. Rev. E* **56,** 7166 (1997).

[75] G. Kalman, M. Rosenberg, and H. E. DeWitt, *Phys. Rev. Lett.* **84**, 6030 (2000).

[76] P. K. Kaw and A. Sen, *Phys. Plasmas* ***5,*** 3552 (1998).

[77] P. K. Kaw, *Phys. Plasmas* **8**, 1870 (2001).

[78] B. S. Xie, Y. P. Chen and M. Y. Yu, *IEEE Trans. Plasma Sci.* **29**, 226 (2001).

[79] M. S. Murillo, *Phys. Plasmas* **7**, 33 (2000a); *Phys. Rev. Lett.* **85**, 2514 (2000b).

[80] D. Winske, and M. S. Murillo, *Phys. Review E* **59**, 2263 (1999).

[81] H. Ohta and S. Hamaguchi, *Phys. Rev. Lett.* **84**, 6026 (2000).

[82] W. L. Slattery, G. D. Doolen, and H. E. DeWitt, *Phys. Rev. A* **21**, 2087 (1980); *Phys. Rev. A* **26**, 2255 (1982).

[83] S. Ichimaru, H. Iyetomi, and S. Tanaka, *Phys. Rep.* **149**, 91 (1987).

[84] J. Pramanik, G. Prasad, A. Sen, and P. K. Kaw, *Phys. Rev. Lett.* **88**, 175001 (2002).

[85] R. T. Farouki and S. Hamaguchi, *J. Chem. Phys.* **101**, 9885 (1994).

CHAPTER 2

Ion Beam Driven Ion-Acoustic Waves in a Plasma Cylinder with Negatively Charged Dust Grains

This chapter describes the excitation of an ion beam driven ion acoustic waves (IAWs) in a plasma cylinder having negatively charged dust grains. A theoretical model based on fluid treatment is employed to study the plasma and beam responses. The growth rate of ion-acoustic instability has been obtained using first order perturbation technique. The effect of relative concentration of negatively charged dust grains on the growth rate, mode frequency and phase velocity of ion beam driven ion acoustic instability has been elucidated. Size and shape effects of dust grains have been neglected to discuss the applicability of orbital motion limited (OML) theory.

2.1 INTRODUCTION

The study of electrostatic ion acoustic (EIA) waves in multi-component plasmas [1]-[14] has been a great topic of interest in past few decades. Low frequency electrostatic ion acoustic and ion-cyclotron waves have been investigated by D'Angelo [1] in magnetized dusty plasma. The mode frequencies were found to increase with increasing the ratio of density of negatively charged dust grains to density of ions. Barkan *et al.* [2] have reported ion acoustic waves in magnetized dusty plasmas and found that an increase in relative density of negatively charged dust grains $\delta\left(=n_{i0}/n_{e0}\right.$, where n_{i0} is the ion plasma density and n_{e0} is the electron plasma

density, respectively) increases the phase velocity of the ion acoustic waves and at the same time reduces the collisionless (Landau) damping. Song *et al.* [3] have reported in their experimental results that the phase velocity of a fast ion acoustic mode increases with the relative density of negative ions ε ($= n_{SF_6^-}/n_{K^+}$, where $n_{SF_6^-}$ and n_{K^+} are the equilibrium densities of sulfur hexafluoride and potassium ions, respectively). In addition, the damping of wave decreases with increasing ε. Song *et al.* [4] have reported potential relaxation instability and ion acoustic waves in a single-ended Q-machine plasma having negative ions and found that the frequency of the IAWs increases and the critical electric drift velocity required for wave excitation decreases as the negative ion concentration is increased.

Rao *et al.* [5] have studied the linear and nonlinear dispersion properties of dust acoustic waves (DAW). Shukla and Silin [6] have studied low frequency electrostatic DIAWs in collisionless unmagnetized dusty plasma. It was observed that the dust ion acoustic modes can exist even for same electron and ion temperatures $T_e \sim T_i$ (T_e and T_i are the electron and ion temperatures, respectively) as long as the density ratio of ions to electrons is much greater than unity. Rosenberg [7] has studied dust ion acoustic and dust acoustic instabilities in an unmagnetized dusty plasma using Vlasov theory. Tystovich and Havnes [8] demonstrate the damping effect of charge fluctuations on ion-acoustic waves. They found that the damping due to charge fluctuations is more than the collisionless Landau damping. N. D'Angelo [9] has studied ion acoustic waves in unmagnetized dusty plasmas using fluid theory and showed that the IA modes damp at the frequency of injection of ions inside the plasma. Ma and Yu [10] have developed self consistent theory of ion acoustic waves in unmagnetized dusty plasma. Pandey and Kumar [11] developed a self consistent kinetic theory of ion acoustic waves in a dusty plasma and found that the attachment of ions to the grains leads to damping of ion-acoustic wave modes. Merlino *et al.* [12] have presented theoretical and experimental results on low frequency electrostatic waves in plasma containing negatively charged dust grains. It has been investigated that the dispersion properties of electrostatic ion acoustic waves gets modified through the quasi-neutrality condition in the presence of negatively charged dust grains even when the dust grains do not participate in the wave dynamics.

Vladimirov *et al.* [13] have investigated the ion acoustic wave modes in dust contaminated plasmas and later on developed a self-consistent theory of linear ion-acoustic waves in complex laboratory plasmas having both dust grains and negative ions [14]. Charging and trapping of macro particles in near electrode regions of fluorocarbon plasmas with negative ions has been studied by Ostrikov *et al.* [15].

Sharma and Gahlot [16] have developed a theoretical model on ion-beam driven ion-acoustic waves in a plasma cylinder having negative ions and found that the phase velocity of sound waves is enhanced with increase in relative density of negative ions. Background of all the studies provided great impetus to study the ion acoustic wave instability driven by an ion beam in a magnetized plasma cylinder with negatively charged dust grains.

2.2 INSTABILITY ANALYSIS

We consider a cylindrical dusty plasma column of radius a_1 with equilibrium electron, ion and dust particle densities being given as n_{eo}, n_{io}, and n_{d0} immersed in a static magnetic field B_S in the z direction i.e., $\vec{B}_s \| \hat{Z}$. The charge, mass and temperatures of three species are denoted by $(-e, m_e, T_e)$, (e, m_i, T_i) and $(-Q_{d0}, m_d, T_d)$, respectively. An ion beam with velocity $\vec{v}_{b0} \| \hat{z}$, mass m_b, density n_{bo}, and radius $r_0 (\equiv a_1)$ propagates through the plasma with negatively charged dust grains along the direction of magnetic field (cf. Fig. 2.1). The beam plasma system prior to the perturbation is quasineutral, such that $en_{e0} - en_{i0} - en_{bo} + Q_{d0} n_{d0} \approx 0$.

The equilibrium is perturbed by an electrostatic perturbation to the potential

$$\phi_1 = \phi_1(r)\ e^{-i(\omega t - \vec{k}.\vec{r})}. \tag{2.1}$$

Now using the mass conservation

$$\frac{\partial n_j}{\partial t} + \nabla.(n_j\ \vec{v_j}) = 0, \tag{2.2}$$

and momentum equation for plasma species as

$$\frac{\partial \vec{v}_j}{\partial t} + \vec{v}_j \bullet \left(\nabla \vec{v}_j\right) = \frac{q_j \vec{E}}{m_j} - \frac{T_j \nabla n_j}{m_j n_j} - \frac{q_j}{m_j c} \vec{v}_j \times \overrightarrow{B_S}, \tag{2.3}$$

where $j = e$ or i or d for electrons, ions and dust, respectively and n_j, v_j, q_j, m_j, and T_j represents the density, velocity, charge, mass and temperature of the plasma constituents, we obtain the perturbed densities of plasma constituents.

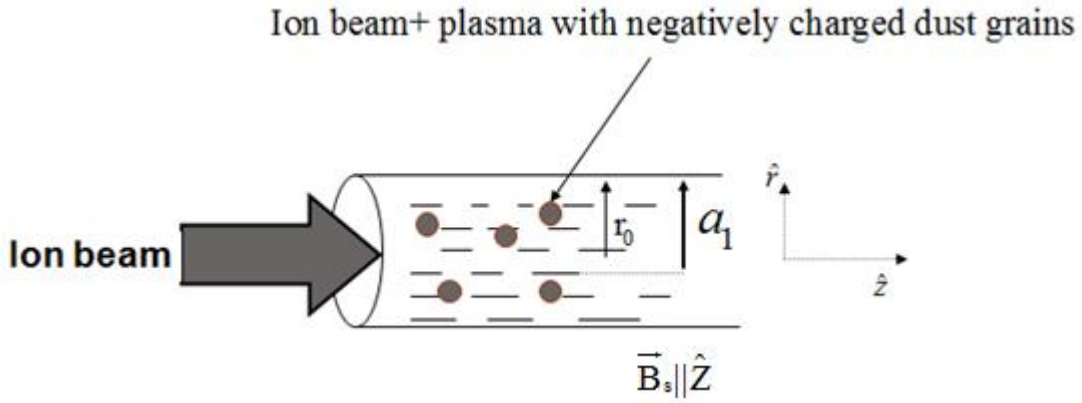

Fig. 2.1 Schematic of ion beam and plasma cylinder with negatively charged dust grains

The perturbed electron density is given by

$$n_{e1} = n_{e0} \frac{e\phi_1}{T_e}. \tag{2.4}$$

The response of ions is given by

$$\left(1 - \frac{c_s^2 k_z^2}{\omega^2}\right) n_{i1} + \frac{c_s^2 \nabla_\perp^2 n_{i1}}{(\omega^2 - \omega_{ci}^2)} = -\frac{e\ n_{i0}}{m_i} \left[\frac{\nabla_\perp^2 \phi_1}{\omega^2 - \omega_{ci}^2} - \frac{k_z^2 \phi_1}{\omega^2}\right], \tag{2.5}$$

where $c_S = \left(T_e / m_i\right)^{1/2}$ is the ion sound velocity and $\omega_{ci}\left(= eB_S / m_i c\right)$ is the ion cyclotron frequency, respectively.

In the limit $\omega < \omega_{ci},\ k_{\perp} c_s < \omega_{ci}\left(\frac{k_{\perp} c_s}{\omega - \omega_{ci}} << 1 \text{ or } \left|k_{\perp}\rho_i\right| << 1\right)$, (where $\rho_i \left(=c_s/\omega_{ci}\right)$ is the ion gyro-radius) of strongly magnetized plasma, Eq. (2.5) gives the perturbed density for ions.

$$n_{i1} = \frac{e\ n_{i0}}{m_i}\left[\frac{\nabla_{\perp}^2\phi_1}{\omega_{ci}^2} + \frac{k_z^2\phi_1}{\omega^2}\right]. \tag{2.6}$$

Similarly the perturbed density for negatively charged dust grains is given by

$$n_{d1} = \frac{Q_{d0} n_{d0}}{m_d}\frac{\nabla_{\perp}^2\phi_1}{\omega^2}. \tag{2.7}$$

Here dust is treated as unmagnetized because $\omega_{pi} \sim \omega >> \omega_{cd}$ with $\omega_{cd}\left(=Q_{d0}B_s/m_d c\right)$ be the dust gyro-frequency.

Following the analysis of Sharma and Srivastava [17], the beam density perturbations is given by

$$n_{b1} = \frac{n_{b0} e k_z^2\ \phi_1}{m_b(\omega - k_z v_{b0})^2}. \tag{2.8}$$

2.2.1 Determination of Dust Charge Fluctuations

Applying probe theory to a dust grain as already discussed in previous chapter 1 section (1.2.3.1.2 & 1.2.3.3), the charge on a dust grain Q_d is known to be balanced with the plasma currents on the grain surface [18]- [19] as

$$-\frac{dQ_d}{dt} = I_e + I_i \tag{2.9}$$

Electron and ion currents on the grain surface are given by

$$I_e = -\pi a^2 e\left(\frac{8T_e}{\pi m_e}\right)^{1/2} n_e \exp\left[\frac{e\left(\phi_g - V\right)}{T_e}\right]$$

and

$$I_i = \pi a^2 e\left(\frac{8T_i}{\pi m_i}\right)^{1/2} n_i\left[1-\frac{e\left(\phi_g - V\right)}{T_i}\right],$$

where a is the dust grain sphere radius, n_e and n_i are the electron and ion densities in the absence of dust grains, $\left(\phi_g - V\right)$ is the difference between the grain surface potential and plasma potential. In equilibrium, the electron and ion grain currents are equal, i.e., $\left|I_{e0}\right| = \left|I_{i0}\right|$, where I_{e0} and I_{i0} denote the equilibrium electron and ion currents on the grain surface. For example, we may write

$$\left|I_{e0}\right| = \pi a^2 e\left(\frac{8T_e}{\pi m_e}\right)^{1/2} n_{e0}\exp\left[\frac{e\phi_{g0}}{T_e}\right].$$

Then the dust charge fluctuations are governed by the equation

$$\frac{dQ_{d1}}{dt} + \eta Q_{d1} = -\left|I_{e0}\right|\left(\frac{n_{i1}}{n_{i0}} - \frac{n_{e1}}{n_{e0}}\right), \tag{2.10}$$

where $\eta = \frac{\left|I_{e0}\right|e}{C_g}\left[\frac{1}{T_e} + \frac{1}{T_i - e\phi_{g0}}\right]$ and $Q_{d1}\left(= Q_d - Q_{d0}\right)$ is the perturbed dust grain charge, $C_g = \left[a\left(1 + a/\lambda_{De}\right)\right]$ is the capacitance of dust grain [20], λ_{De} is the electron Debye length. Substituting $\frac{d}{dt} = -i\omega$ in Eq. (2.10), we obtain the dust charge fluctuations as

$$Q_{d1} = \frac{\left|I_{e0}\right|}{i(\omega + i\eta)}\left(\frac{n_{i1}}{n_{i0}} - \frac{n_{e1}}{n_{e0}}\right). \tag{2.11}$$

On substituting the values of n_{e1} and n_{i1} from Eqs (2.4) & (2.6) in Eq. (2.11), we get

$$Q_{d1} = \frac{e\left|I_{e0}\right|}{i(\omega + i\eta)}\left[\frac{\nabla_\perp^2\phi_1}{m_i\omega_{ci}^2} + \frac{k_z^2\phi_1}{m_i\omega^2} - \frac{\phi_1}{T_e}\right]. \tag{2.12}$$

2.2.2 Finite Geometry Analysis

Using Eqs.(2.4), (2.6), (2.7) and (2.8) and (2.12) in the Poisson equation, $\nabla^2\phi_1 = 4\pi\ (n_{e1}e - n_{i1}e\ - n_{b1}e + n_{d0}Q_{d1} + Q_{d0}n_{d1})$, we obtain a second order differential equation in ϕ_1, which can be rewritten for axially symmetric cylindrical geometry case similar to as discussed earlier in chapter 1,

$$\frac{\partial^2\phi_1}{\partial r^2} + \frac{1}{r}\frac{\partial\phi_1}{\partial r} + p_1^2\phi_1 = -\frac{\omega_{pb}^2 k_z^2\ \ \phi_1}{(\omega - k_z v_{b0})^2\left[1 + \frac{4\pi\delta n_{eo}e^2}{m_i\ \ \omega_{ci}^2} + \frac{i\beta}{\omega + i\eta}\ \ \frac{4\pi\ \ n_{eo}e^2}{m_i\ \ \omega_{ci}^2\delta} - \frac{\omega_{pd}^2}{\omega^2}\right]}, \quad (2.13)$$

where

$$p_1^2 = \frac{-\frac{4\pi n_{e0}e^2}{T_e} + \frac{4\pi n_{i0}e^2}{m_i}\frac{k_z^2}{\omega^2} + \frac{i\beta}{\omega + i\eta}\frac{4\pi n_{e0}e^2}{m_i}\frac{k_z^2}{\omega^2} - k_z^2}{1 + \frac{4\pi\delta n_{e0}e^2}{m_i\omega_{ci}^2} - \frac{\omega_{pd}^2}{\omega^2} + \frac{i\beta}{\omega + i\eta}\frac{4\pi n_{e0}e^2}{m_i\omega_{ci}^2}}, \quad (2.14)$$

$\omega_{pb}^2 = \frac{4\pi n_{b0}e^2}{m_b}$, $\omega_{pd}^2 = \frac{4\pi n_{d0}Q_{d0}^2}{m_d}$, $\beta = \frac{|I_{e0}|}{e}\frac{n_{d0}}{n_{e0}}$, and $\delta = {}^{n_{i0}}\!/_{n_{e0}}$.

In the absence of the beam, the solution of Eq. (2.13) is given by

$$\phi_1 = AJ_0(p_{n_1}r) + BY_0(p_{n_1}r), \quad (2.15)$$

where A and B are constants, and the functions $J_o\left(p_{n_1}r\right)$ and $Y_0(p_{n_1}r)$ are called the zeroth-order Bessel functions of the first and second kind. At r = 0, $Y_0\left(p_{n_1}r\right)$ does not exist and, hence B = 0, this implies that $\phi_1 = AJ_o(p_{n1}r)$, and $p_1 = p_{n1}$.

At $r = a_1$, ϕ_1 must vanish, hence, $J_o(p_{n1}a_1) = 0$, i.e., $p_{n1} = \frac{x_n}{a_1}$ (n=1, 2, …..), x_n are the zeros of the Bessel function $J_o(x)$. In the presence of the beam, the

solution of wave function ϕ_1 can be expressed as a series of orthogonal sets of wave functions:

$$\phi_1 = \sum_m A_m J_o (p_{m_1} r). \tag{2.16}$$

Now substituting the value of Eq. (2.16) in Eq. (2.13), we multiply both sides of Eq. (2.13) by $rJ_o (p_{n_1} r)$ and integrating over r from 0 to a_1 (where a_1 is the plasma radius), we get

$$p_1^2 - p_{n1}^2 = -\frac{\omega_{pb}^2 k_z^2 \beta_1}{(\omega - k_z v_{b0})^2 \left[1 + \frac{4\pi\delta n_{eo} e^2}{m_i \omega_{ci}^2} + \frac{i\beta}{\omega + i\eta}\frac{4\pi n_{eo} e^2}{m_i \omega_{ci}^2} - \frac{\omega_{pd}^2}{\omega^2}\right]}, \tag{2.17}$$

where $\beta_1 = \dfrac{\int_0^{r_0} rJ_0(p_{m_1} r) J_0(p_{n_1} r) dr}{\int_0^{a_1} r \; J_0(p_{m_1} r) J_0(p_{n_1} r) dr} = 1 \; if \; r_0 = a_1$, and

$$p_1^2 - p_{n1}^2 = -\frac{\omega_{pb}^2 k_z^2}{(\omega - k_z v_{b0})^2 \left[1 + \frac{4\pi n_{eo} e^2 \delta}{m_i \omega_{ci}^2} + \frac{i\beta}{\omega + i\eta}\frac{4\pi n_{eo} e^2}{m_i \omega_{ci}^2} - \frac{\omega_{pd}^2}{\omega^2}\right]}. \tag{2.18}$$

On substituting the value of p_1^2 from Eq. (2.14), Eq. (2.18) can be rewritten as

$$1 + \frac{\omega_{pe}^2}{v_{te}^2 k^2} - \frac{\omega_{pi}^2}{\omega^2}\frac{k_z^2}{k^2} + \frac{\omega_{pi}^2}{\omega_{ci}^2}\frac{p_n^2}{k^2} + \frac{i\beta}{\omega + i\eta}\frac{\omega_{pi}^2}{\omega_{ci}^2 \delta}\frac{p_n^2}{k^2} - \frac{i\beta}{\omega + i\eta}\frac{\omega_{pi}^2}{\omega^2 \delta}\frac{k_z^2}{k^2}$$

$$- \frac{\omega_{pd}^2}{\omega^2}\frac{p_n^2}{k^2} = \frac{\omega_{pb}^2}{(\omega - k_z v_{b0})^2}\frac{k_z^2}{k^2}, \tag{2.19}$$

where $\omega_{pe}^2 = \dfrac{4\pi n_{eo} e^2}{m_e}$, $\omega_{pi}^2 = \dfrac{4\pi n_{eo} e^2 \delta}{m_i}$, $\omega_{pd}^2 = \dfrac{4\pi n_{d0} Q_{d0}^2}{m_d}$, and $v_{te}^2 = \dfrac{T_e}{m_e}$.

Multiplying both sides of Eq. (2.19) by k^2 / p_n^2, we get

$$1-\frac{\omega_{pi}^2}{\omega^2}\frac{k_z^2}{p_n^2\alpha_1}+\frac{\omega_{pi}^2}{\omega_{ci}^2\alpha_1}+\frac{i\beta}{\omega+i\eta}\frac{\omega_{pi}^2}{\omega_{ci}^2\delta}\frac{1}{\alpha_1}-\frac{i\beta}{\omega+i\eta}\frac{\omega_{pi}^2}{\omega^2\delta}\frac{k_z^2}{p_n^2\alpha_1}-\frac{\omega_{pd}^2}{\omega^2\alpha_1}$$

$$=\frac{\omega_{pb}^2}{(\omega-k_z v_{bo})^2}\frac{k_z^2}{p_n^2\alpha_1}, \qquad (2.20)$$

where $\alpha_1 = \frac{k^2}{p_n^2}+\frac{\omega_{pe}^2}{v_{te}^2 p_n^2}\approx\frac{4\pi n_{eo}e^2}{m_e v_{te}^2 p_n^2}\approx\frac{\omega_{pe}^2}{v_{te}^2 p_n^2}$.

Equation (2.20) can be rewritten as

$$\omega^2\alpha_2-\omega_{pi}^2\frac{k_z^2}{p_n^2\alpha_1}-\frac{\omega_{pd}^2}{\alpha_1}-\frac{i\beta}{\omega+i\eta}\frac{\omega_{pi}^2}{\delta p_n^2}\frac{k_z^2}{\alpha_1}=\frac{\omega^2\omega_{pb}^2k_z^2}{(\omega-k_z v_{bo})^2\alpha_1 p_n^2}. \qquad (2.21)$$

Equation (2.21) further can be rewritten as

$$(\omega^2-b_1^2)(\omega-k_z v_{bo})^2 = \frac{\omega_{pb}^2k_z^2\omega^2}{\alpha_1\alpha_2 p_n^2}, \qquad (2.22)$$

where $b_1^2=\frac{k_z^2}{k^2}\frac{\omega_{pi}^2}{\alpha_1\alpha_2}-\frac{\omega_{pd}^2}{\alpha_1\alpha_2}-\frac{i\beta}{\omega+i\eta}\frac{\omega_{pi}^2}{\delta\alpha_1\alpha_2}\frac{k_z^2}{p_n^2}$, $\alpha_2=1+\frac{\omega_{pi}^2}{\alpha_1\omega_{ci}^2}+\frac{i\beta}{\omega+i\eta}\frac{\omega_{pi}^2}{\alpha_1\omega_{ci}^2\delta}$,

and $k^2 = {p_n}^2+{k_z}^2$, ${p_n}^2>{k_z}^2$ or

$$b_1^2=\frac{k^2c_s^2\delta}{\left(1+k^2c_s^2\frac{\delta}{\omega_{pi}^2}\right)\alpha_2}-\frac{\omega_{pd}^2}{\left(1+\frac{\omega_{pi}^2}{k^2c_s^2\ \delta}\right)\alpha_2}-\frac{i\beta}{\omega+i\eta}\frac{k^2c_s^2\delta}{\left(1+k^2c_s^2\frac{\delta}{\omega_{pi}^2}\right)\alpha_2}. \qquad (2.23)$$

Equation (2.22) is the dispersion relation of ion beam driven IAWs in a magnetized plasma cylinder having negatively charged dust grains.

In the absence of dust charge fluctuations ($\eta \to \infty$) and dust dynamics (i.e., $\omega_{pd} = 0$ when $m_d \sim \infty$), Eq. (2.23) can be rewritten as

$$b_1^2 = \frac{k^2 c_s^2 \delta}{\left(1 + k^2 c_s^2 \frac{\delta}{\omega_{pi}^2}\right)\alpha_3}, \tag{2.24}$$

where $\alpha_3 = 1 + \frac{\omega_{pi}^2}{\omega_{ci}^2 \alpha_1}$. For infinite geometry, ω_{ci} & $\omega_{pi} \to \infty$, so Eq.(2.24) gives

$$b_1^2 = k^2 c_s^2 \delta . \tag{2.25}$$

Equation (2.25) is similar to the dispersion relation of usual ion-acoustic wave given by Shukla and Silin [6] for the long wavelength limit (cf. Eq. (4)).

2.2.3 Dispersion Properties of DIAWs

Here $\omega \approx b_1$, corresponds to the ion acoustic mode and $\omega \approx k_z v_{b0}$ corresponds to the beam mode. We look for the solutions when $b_1 \approx k_z v_{b0}$, i.e., when the beam is in Cerenkov resonance with the ion acoustic mode. In this case, the two factors on the left-hand side of Eq. (2.22) are simultaneously zero in the absence of beam.

In the presence of beam, we expand ω as $\omega = b_1 + \delta_1 = k_z v_{b0} + \delta_1$, where δ_1 is the small frequency mismatch due to the finite right-hand side of Eq. (2.22). Then Eq. (2.22) gives the **growth rate** of the unstable mode

$$\gamma = I_m \delta_1 = \left[\frac{b_1}{2}\frac{\omega_{pb}^2 k^2}{\alpha_1 \alpha_2 p_n^2}\right]^{1/3} \frac{\sqrt{3}}{2}. \tag{2.26}$$

It can be seen that the growth rate of DIAWs scales as one third power of beam density n_{b0}.

The **real frequency** of unstable mode in terms of beam energy is given by

$$\omega_r = k_z \left(\frac{2eV_b}{m_b} \right)^{1/2} - \frac{1}{2} \left[\frac{b_1}{2} \frac{\omega_{pb}^2 k^2}{\alpha_1 \alpha_2 p_n^2} \right]^{1/3}, \qquad (2.27)$$

where eV_b is the beam energy. The mode frequency depends on square root of beam energy eV_b and one third power of beam density. The relative density of negatively charged dust grains can be characterized by $\delta\left(=\left(n_{i0}/n_{e0}\right) > 1\right)$. In the absence of dust, i.e., $\delta = 1$, Eq. (2.24) can be rewritten to obtain phase velocity of ion beam driven dust ion acoustic waves in the magnetized plasma cylinder as

$$v_{ph}(\delta) = b_1/k = \frac{c_s \delta^{1/2}}{\left(1 + \frac{k^2 c_s^2 \delta}{\omega_{pi}^2}\right)^{1/2} \left(\alpha_3\right)^{1/2}}, \qquad (2.28)$$

where $v_{ph}(\delta)$ is the **phase velocity** of sound wave in presence of negatively charged dust grains. The coupling parameter β can be rewritten after using the charge neutrality condition and the value of equilibrium electron current [21] as,

$$\beta = 0.397 \left(1 - \frac{1}{\delta}\right) \left(\frac{a}{v_{te}}\right) \omega_{pi}^2 \left(\frac{m_i}{m_e}\right), \qquad (2.29)$$

where $\delta = n_{io}/n_{eo}$.

The charging rate η can also be rewritten for Q-Machine plasmas [21], in the limit $T_e \cong T_i$ i.e., electron temperature is equal to the ion temperature as

$$\eta = 0.79a \left(\frac{\omega_{pi}}{\lambda_{Di}}\right) \left(\frac{1}{\delta}\right) \left(\frac{m_i}{m_e} \frac{T_i}{T_e}\right)^{\frac{1}{2}}. \qquad (2.30)$$

2.3 RESULTS AND DISCUSSION

To analyze the dispersion properties of ion beam driven IAWs in the presence of negatively charged dust grains, we use experimental plasma parameters of Barkan *et al.* [2] which are summarized in Table-2.1. Using Eq. (2.24), we have plotted in Fig. 2.2, the dispersion curves of ion-acoustic waves in the presence of negatively charged dust grains and the beam mode for potassium ion beam of energy E_b=10eV. The frequencies and the corresponding wave numbers of the unstable waves are obtained by the point of intersections between the plasma and the beam modes, and given as Table-2.2.

Table-2.1 The parameters used in the current model [2]

Parameter	Value
Plasma density n_{e0}	1x 10^9 cm^{-3}
Relative density of negatively charged dust grains $\delta = n_{i0}/n_{e0}$	1, 2, 4, 6
Electron Temperature T_e	2 eV
Ion Temperature T_i	2 eV
Plasma radius a_1	2 cm
Beam radius r_0	2 cm
Dust grain size a	0.5x10^{-4} cm
Guide magnetic field B_z	1x10^3 Gauss
Mode Number n	1
Ion Beam energy E_b	10 eV
Ion beam density n_{b0}	2.5x10^8 cm^{-3}

From Table-2.2, we can say that the unstable wave frequencies for IAW increases with the relative density of negatively charged dust grains δ. Using Eqs.(2.26) & (2.28), we have plotted the normalized phase velocity $[v_{ph}(\delta)/v_{ph}(1)]$ and the normalized growth rate γ/ω_{ci} as a function of relative density of negatively charged dust grains (cf. Fig. 2.3) for the same parameters as used

for plotting Fig. 2.2 plus the wave frequencies and wave vectors (cf. Table 2.2) in addition to ion beam density n_{b0} =2.5x10^{8} cm^{-3}. From Fig. 2.3 it can be seen that the $v_{ph}(\delta)/v_{ph}(1)$ increases by a factor ~2.0 when δ changes from 1.0 to 4.0. If we compare our Fig. 2.3 with Fig. 4 of Barkan *et al.* [2], we can say that the trend of our plot for negatively charged dust grains seems to be consistent with the experimental observations of Barkan *et al.* [2]. In addition, this phase velocity result is also consistent with the experimental observations of Merlino *et al.* [12] and Barkan *et al.* [22].

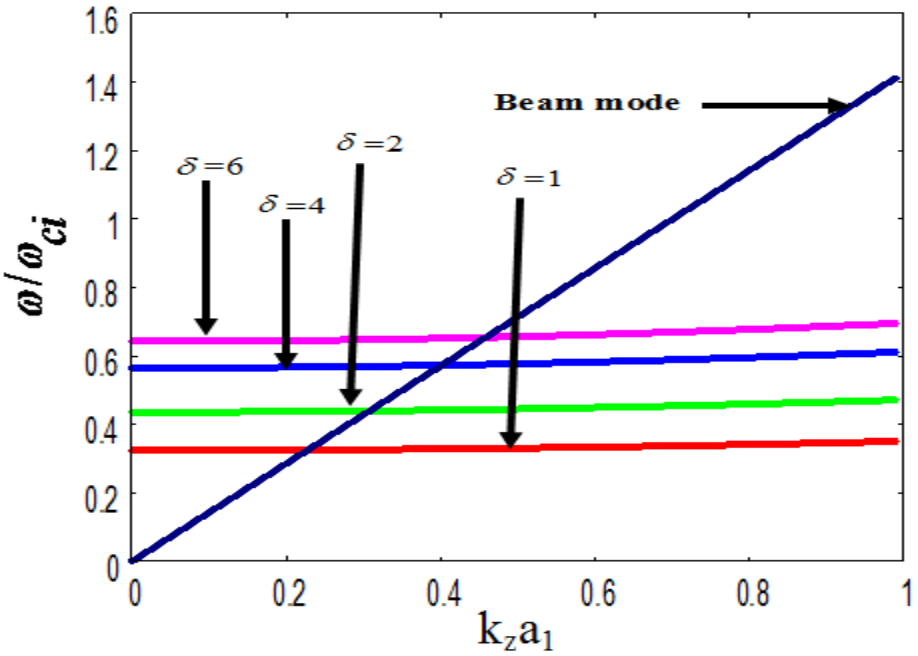

Fig. 2.2 Dispersion curves (ω/ω_{ci} vs. $k_z a_1$) of ion-acoustic waves with negatively charged dust grains and beam mode at different densities of dust grains δ. The parameters are given in the Table-2.1.

The experimental observations of Barkan *et al.* [2] showed that the wave damping decreases with δ which implies that the growth rate increases with δ. Our theoretical results are in compliance with the experimental observations of Barkan *et al.* [2]. Rosenberg [7] has also theoretically predicted the similar results obtained from kinetic treatment.

Table-2.2 The values of unstable wave frequencies ω (rad/s) and axial wave vectors k_z (cm^{-1}) for different values of δ obtained from Fig. 2.2.

δ	k_z (cm^{-1})	λ_z(cm)	ω (rad/s) x10^5
1.0	0.113731	55.218	0.803271
2.0	0.153909	40.803	1.083637
4.0	0.199807	31.430	1.410977
6.0	0.230237	27.276	1.616429

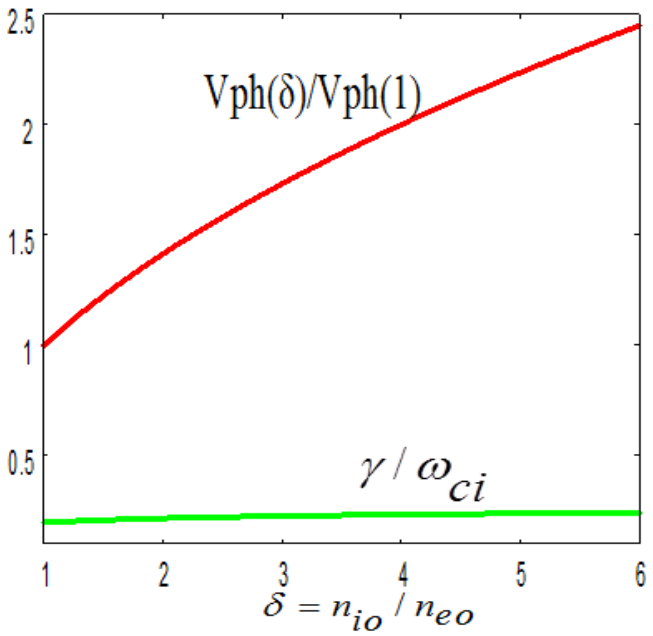

Fig. 2.3 Normalized phase velocity $v_{ph}(\delta)/v_{ph}(1)$ and normalized growth rate γ/ω_{ci} as a function of the relative density of negatively charged dust grains δ for the same parameters as Fig. 2.2 and for beam density n_{b0} =2.5x10^8 cm^{-3}.

The growth rate of unstable mode is enhanced with the increase in beam density and scales as the one-third power of the beam density [cf. Eq. (2.26)]. The real frequency of the unstable mode increases with an increase in the beam energy and scales as almost the one-half power of the beam energy [cf. Eqs. (2.27)].

The applicability of the electron and ion grain currents [cf. Eq.(2.9)] flowing on the grain surface is as follows: The orbital motion limited (OML) theory was initially derived for a Maxwellian plasma. It has been studied in detail in connection with electrostatic Langmuir probes which are usually stationary or quasi-stationary. The probe theory for magnetized plasma was not clear so far [23]-[24] so OML theory have limited applicability to dynamical systems in magnetized plasmas. To determine the electron and ion plasma currents entering into the probe, the fluctuating fields and the external magnetic fields are important as they can affect the plasma particle distribution and orbits. A complete dust charging OML theory is still an unknown fact for the magnetized plasmas [23]-[24].

Here, we have only discussed the applicability of the OML theory to magnetized dusty plasma in which an IAW propagates using a standard fluid model neglecting the dust size and shape effects. This model [25] is reasonably valid in the limit $a \ll \lambda_{De} \ll \lambda$, where a is dust grain size, λ_{De} is the electron Debye length, and λ is the fluctuation's wavelength provided the spread in Q_d / m_d (dust charge to mass ratio) for the dust particles may be neglected in equilibrium.

Moreover, Jana *et al*. [19] have given the limits of the OML theory for magnetized dusty plasma. According to Jana *et al*. the charging equation [cf. Eq. (2.9)] can be valid if $a \ll \rho_L$ [where $\rho_L = \left(v_{te} / \omega_{ce}\right)$ is the electron Larmor radius, a is the dust grain size, v_{te} is the electron thermal velocity, and ω_{ce} is the electron cyclotron frequency]. We have chosen parameters in such a way that the above mentioned condition is satisfied.

2.4 CONCLUSION

In conclusion, we may say that the electrostatic ion-acoustic waves are driven to instability in a magnetized dusty plasma cylinder by an ion beam via a Cerenkov interaction. The phase velocity increases with an increase in the relative density of negatively charged dust grains. This is in compliance with the experimental observations of Barkan *et al.* [2], Merlino *et al.* [12], and Barkan *et al.* [22]. Our

growth rate results are also qualitatively similar to the theoretical predictions of Rosenberg [7]. Barkan *et al.* [2] have not studied the effect of relative density of dust grains δ on the growth rate of the ion acoustic wave instability. The frequency of unstable mode increases with an increase in the relative density of negatively charged dust grains (cf. Table-2.2). The present model is based on a fluid treatment. However, kinetic theory would be more appropriate to study the conditions for excitation of unstable modes. As surface waves [26]-[27] may play a significant role in bounded plasmas hence care should be taken not to excite the surface waves, instead excite the propagating ion-acoustic waves only.

REFERENCES

[1] N. D'Angelo, *Planet. Space Sci.* **38**, 9, 1143 (1990).

[2] A. Barkan, N. D'Angelo and R. L. Merlino, *Planet Space Sci.* **44,** 239 (1996).

[3] B. Song, N. D'Angelo and R. L. Merlino, *Phys. Fluids* **B3 (2)**, 284 (1991).

[4] B. Song, R.L. Merlino and N. D'Angelo, *Phys. Lett. A* **153**, 233 (1991).

[5] N. N. Rao, P. K. Shukla, and M. Y. Yu, *Planet. Space Sci.* **38**, 543 (1990).

[6] P. K. Shukla and V. P. Silin, *Phys. Scripta* **45**, 508 (1992).

[7] M. Rosenberg, *Planet Space Sci.* **41**, 229 (1993).

[8] V. Tsytovich and O. Havnes, *Comm. Plasma Phys. Controlled Fusion* **15**, 267 (1993).

[9] N. D'Angelo, *Planet. Space Sci.* **42**, 507 (1994).

[10] J. X. Ma and M. Y. Yu, *Phys. Plasmas* **1**, 3520 (1994).

[11] B. P. Pandey and S. Kumar, *PRAMANA-J. Phys.* **45,** 561 (1995).

[12] R. L. Merlino, A. Barkan, C. Thomson, N. D'Angelo, *Phys. Plasmas* **5**, 1607 (1998).

[13] S. V. Vladimirov, K. N. Ostrikov and M. Y. Yu, *Phys. Rev. E.* **60,** 3257 (1999).

[14] S. V. Vladimirov, K. Ostrikov, M. Y. Yu, and G. E. Morfill, *Phys. Rev. E* **67**, 036406 (2003).

[15] K. N. Ostrikov, S. Kumar and H. Sugai, *Phys. Plasmas* **7**, 3490 (2001).

[16] S. C. Sharma and A. Gahlot, *Phys. Plasmas* **15**, 073705 (2008).

[17] S. C. Sharma and M. P. Srivastava, *Phys. Plasmas* **8,** 679 (2001).

[18] E.C. Whipple, T.G. Northdrop and D.A. Mendis, *J. Geophys. Res.* **90**, 7405 (1985).

[19] M. R. Jana, A. Sen, and P. K. Kaw, *Phys. Rev. E* **48**, 3930 (1993).

[20] M. S. Barnes, J. K. Keller, J. C. Forster, J. A. O'Neill, and D. K. Coultas, *Phys. Rev. Lett.* **68**, 313 (1992).

[21] S. C. Sharma and A. Gahlot, *Phys. Plasmas* **16**, 123708 (2009).

[22] A. Barkan, N. D'Angelo, and R. L. Merlino, *Phys. Lett. A* **222**, 329 (1996).

[23] F. F. Chen, "*Plasma Diagnostic Techniques"*, edited by R. H. Huddlestone and S. L. Leonard, Academic, New York (1965), Chap. IV.

[24] F. F. Chen, "*Introduction to Plasma Physics"*, Academic (1965), New York.

[25] J. Goree, *Phys. Rev. Lett.* **69**, 277 (1992).

[26] K. N. Ostrikov, M. Y. Yu, and N. A. Azarenkov, *J. Appl. Phys.* **84**, 4176 (1998).

[27] N. A. Azarenkov, I. B. Denysenko, and K. N. Ostrikov, *J. Phys. D: Appl. Phys.* **28**, 2465 (1995).

CHAPTER 3

Effect of Dust Charge Fluctuations on Current Driven Electrostatic Ion-Cyclotron Instability in a Collisional Magnetized Plasma

The chapter describes the excitation of the electrostatic ion cyclotron instability in a collisional magnetized dusty plasma through plasma currents, taking into account the dust dynamics and dust charge fluctuations. A theoretical model based on fluid treatment has been developed which incorporates the effect of dust charge fluctuations using probe theory. The prime focus of the chapter lies in the investigations of the effect of dust dynamics and dust charge fluctuations on the frequency and the growth rate of EICWs.

3.1 INTRODUCTION

Electrostatic ion-cyclotron (EIC) waves have been observed in a widely in laboratory experiments [1]–[2] and space plasmas [3]-[4]. Electrostatic plasma oscillations near ion cyclotron frequency have been firstly reported by D'Angelo and Motley [1]. The observed oscillations were identified as the current-driven EIC instability, which had been theoretically predicted by Drummond and Rosenbluth [5]. Motley and D' Angelo [2] found that the ion cyclotron oscillations are excited if the electron drift velocity exceeds about ten times the ion thermal velocity. The current driven EIC instability is a low-frequency field-aligned instability, which has attracted much attention of the plasma physics community as it has one of the lowest threshold

electron drift velocities among all current-driven instabilities. The EIC wave propagates in the direction nearly perpendicular to the magnetic field and can be destabilized by an electron current (i.e., electron drift velocity) along the field lines [6]. Chaturvedi and Kaw [7] have studied current driven electrostatic and electromagnetic ion-cyclotron instabilities using fluid theory in a collisional plasma.

As already discussed in chapter-1, due to fluctuations of the dust grain charge [8]-[13], the studies of electrostatic and electromagnetic waves in the dusty plasmas received great attention.

Song *et al.* [14] have studied the current driven EIC instability in negative ion Q machine plasmas and found that the critical electron current (i.e., critical electron drift velocity) is decreased with an increase in the density ratio of negative to the positive ions. Later, Sharma and Srivastava [15] developed a model for ion-beam driven electrostatic ion cyclotron instability in a negative ion plasma cylinder and compared their theoretical predictions with the experimental observations of Song *et al.* [14] which has been found in good agreement. Chow and Rosenberg [16] investigated current driven EIC instability in a negative ion plasma and found that as the density ratio of heavy ions to the light ions is increased, the mode frequency is increased whereas the critical electron current is decreased. Moreover, the wavelength corresponding to the maximum growth rate shifts to a larger value with increase in the negative ion relative density ratio.

D'Angelo [17] derived the dispersion relations for low-frequency electrostatic waves (two electrostatic ion cyclotron and two ion acoustic modes) in the magnetized dusty plasma. In the presence of negatively charged dust grains, he found that the mode frequencies are increased as the density ratio of negatively charged dust grains to positive ions is increased. Experiments by Suszcynsky *et al.* [18] in a plasma with two positive ion species indicated that the critical electron current required for exciting EIC instability increases with the increase in relative density ratio of heavy ions to light ions.

Barkan *et al.* [19] reported experimentally that the presence of negatively charged dust grains enhances the growth rate of the current driven EIC instability in a plasma. The effect of charged dust on the collisionless EIC instability was investigated

by Chow *et al.* [20]-[21] using Vlasov theory, where the critical electron current (i.e., critical electron drift velocity) was evaluated in the presence of either positively or negatively charged dust grains. In the case of negatively charged dust, they found that the critical electron current gets decreased as the ratio of positive ion to electron density is increased. This showed that the mode gets more easily destabilized in the plasma containing negatively charged dust grains than the ordinary electron-positive ion plasma.

Merlino *et al.* [22] presented theoretical and experimental results on low frequency electrostatic waves in a plasma containing negatively charged dust grains. It has been observed that the presence of negatively charged dust modifies the dispersion properties of current driven EIC instability through the quasi-neutrality condition even though the dust grains do not participate in the wave dynamics. The current driven instabilities have been studied by various authors in collisional dusty plasmas [23]-[27]. Moreover, Sharma and Sharma [28] have studied the excitation of ion-cyclotron waves by an ion beam in two-ion component plasma. Sharma and Gahlot [29] have studied the excitation of an upper hybrid waves by a gyrating relativistic electron beam (REB) in a magnetized dusty plasma cylinder and found that the upper hybrid waves are more easily destabilized in the presence of dust grains. Sharma and Walia [30] have studied the excitation of lower hybrid waves by a spiraling ion beam in a magnetized dusty plasma cylinder. Sharma and Gahlot [31] have developed a theoretical model of ion-beam driven ion-acoustic waves in a plasma cylinder with negative ions and found that the phase velocity of sound waves in presence of positive and negative ions increases with increase in relative density of negative ions.

Current driven EIC waves in the presence of a transverse dc electric field in the collisional magnetized plasma without charged dust grains have been theoretically investigated earlier by various authors [32]-[34]. In the present work, we have developed a theoretical model of current-driven EIC instability in the presence of negatively charged dust grains in the collisional magnetized plasma, taking into account dust charge fluctuations using probe theory [8], [9], & [33] under the assumption of small growth rate as compared to frequency [35].

3.2 STABILITY ANALYSIS

We considered a homogeneous collisional dusty plasma immersed in a static magnetic field B in the z-direction with equilibrium electron, ion and dust particle densities being given as n_{eo}, n_{io}, and n_{d0}.The charge, mass, and temperature of the three species are denoted by $(-e, m_e, T_e)$, (e, m_i, T_i) and $(-Q_{d0}, m_d, T_d)$, respectively. The electron and ion neutral collisional frequencies are given by ν_e and ν_i. We assume that electrons have a drift velocity v_{de} along the magnetic field line (i.e., in the z-direction) and we look for the excitation of ion cyclotron waves in the perpendicular direction by this electron current. The electron temperature is assumed to be constant. In equilibrium, there is overall charge neutrality, i.e., $en_{i0} = en_{e0} + n_{d0}Q_{d0}$. Let a perturbation $\phi_1 = \phi_{k,\omega} \exp\left[-i(\omega t - \vec{k}.\vec{r})\right]$ is given to the electrostatic potential.

The response of plasma electrons to the perturbation may be derived from the momentum conservation equation, i.e.,

$$m_e \frac{d\vec{v}}{dt} = -e\vec{E} - \frac{e}{c}\vec{v}\times\vec{B} - \frac{\nabla(nT)}{n} - m_e\nu_e\vec{v}. \tag{3.1}$$

As we focus on low frequency EIC instability, so the inertia term for the electrons may be neglected in Eq. (3.1). On linearization Eq. (3.1) yields the perturbed velocity components, i.e.,

$$v_{x1} = \frac{e\omega_{ce}E_{y1}}{m_e\left(\nu_e^2+\omega_{ce}^2\right)} + i\frac{T_e}{m_e}\frac{\omega_{ce}k_y}{\left(\nu_e^2+\omega_{ce}^2\right)}\frac{n_{e1}}{n_{e0}}, \tag{3.2}$$

$$v_{y1} = -\frac{e\nu_e E_{y1}}{m_e\left(\nu_e^2+\omega_{ce}^2\right)} - i\frac{T_e}{m_e}\frac{\nu_e k_y}{\left(\nu_e^2+\omega_{ce}^2\right)}\frac{n_{e1}}{n_{e0}}, \tag{3.3}$$

$$v_{z1} = -\frac{eE_{z1}}{m_e\nu_e} - i\frac{T_e}{m_e}\frac{k_z}{\nu_e}\frac{n_{e1}}{n_{e0}}, \tag{3.4}$$

where $\omega_{ce}\left(=eB/m_e c\right)$ is the electron cyclotron frequency and subscript 1 refers to perturbed quantities. Substituting the perturbed velocities given by Eqs. (3.2) - (3.4) in the mass conservation equation, we obtain perturbed electron density as

$$\frac{n_{e1}}{n_{e0}}=\left(i\frac{e\,\nu_e k_\perp^2\phi_1}{m_e\omega_1(\nu_e^2+\omega_{ce}^2)}-i\frac{T_e}{m_e}\frac{\nu_e k_\perp^2}{\omega_1(\nu_e^2+\omega_{ce}^2)}\frac{n_{e1}}{n_{e0}}+i\frac{ek_z^2\phi_1}{\nu_e\omega_1 m_e}-i\frac{T_e}{m_e}\frac{k_z^2}{\nu_e\omega_1}\frac{n_{e1}}{n_{e0}}\right), \tag{3.5}$$

where, $\omega_1=\omega-k_z v_{de}$. Equation (3.5) can further be simplified in the limit, $\omega_{ce}^2\gg\nu_e^2$ and $(\rho_e^2/\rho_i^2)(k_\perp^2\rho_i^2)\ll 1$ with ρ_e and ρ_i being the electron and ion gyro radii and may be written by

$$\frac{n_{e1}}{n_{e0}}=\frac{e\phi_1}{T_e\left[1-i\nu_e\omega_1\Big/\left(k_z^2T_e/m_e\right)\right]}. \tag{3.6}$$

The response of plasma ions can be obtained from the momentum and mass conservation equations and the perturbed ion density may be given by

$$\frac{n_{i1}}{n_{i0}}=\left(\frac{ek_\perp^2\phi_1}{m_i(\omega^2-\omega_{ci}^2)}+\frac{T_i}{m_i}\frac{k_\perp^2}{(\omega^2-\omega_{ci}^2)}\frac{n_{i1}}{n_{i0}}+\frac{ek_z^2\phi_1}{m_i\omega^2}+\frac{T_i}{m_i}\frac{k_z^2}{\omega^2}\frac{n_{i1}}{n_{i0}}\right), \tag{3.7}$$

where $\omega_{ci}\left(=eB/m_i c\right)$ is the ion cyclotron frequency. In Eq. (3.7) we have neglected ion neutral collision frequency ν_i under the assumption that $\omega,\ \nu_e>>\nu_i$ (i.e., ion neutral collision frequency is much smaller than the unstable mode frequency and the electron neutral collision frequency). In addition, we have assumed that there is no ion drift velocity along the direction of the magnetic field.

Then, Eq. (3.7) may be rewritten as

$$\left(1-\frac{v_{ti}^2k_z^2}{\omega^2}-\frac{v_{ti}^2k_\perp^2}{\omega^2-\omega_{ci}^2}\right)\frac{n_{i1}}{n_{i0}}=c_s^2\left\{\frac{k_\perp^2}{\omega^2-\omega_{ci}^2}+\frac{k_z^2}{\omega^2}\right\}\frac{e\phi_1}{T_e}, \tag{3.8}$$

where, $v_{ti}\left[=(T_i/m_i)^{1/2}\right]$ is the thermal velocity of ions and $c_s\left[=\left(T_e/m_i\right)^{1/2}\right]$ is the ion sound speed. In the low ion temperature limit ω^2, $\left(\omega^2-\omega_{ci}^2\right)>>k_\perp^2 v_{ti}^2$, Eq. (3.8) may be further simplified as

$$\frac{n_{i1}}{n_{i0}}=c_s^2\left\{\frac{k_\perp^2}{\omega^2-\omega_{ci}^2}+\frac{k_z^2}{\omega^2}\right\}\frac{e\phi_1}{T_e}. \tag{3.9}$$

Similarly the dust density perturbations are given by

$$\frac{n_{d1}}{n_{d0}}=-\frac{k_\perp^2}{\omega^2}\frac{Q_{d0}\phi_1}{m_d}, \tag{3.10}$$

Here dust is treated as unmagnetized because $\omega\sim\omega_{ci}>>\omega_{cd}$ with $\omega_{cd}\left(=Q_{d0}B/m_d c\right)$ be the dust gyro frequency.

From probe theory (as discussed in previous chapter 2 sec. (2.2.1)) applied to a dust grain, the charge on a dust grain Q_d is known to be balanced with the plasma currents on the grain surface. Following the treatment of [8], [9], & [33], the dust charge fluctuations are governed by the equation

$$\frac{dQ_{d1}}{dt}+\eta Q_{d1}=-\left|I_{e0}\right|\left(\frac{n_{i1}}{n_{i0}}-\frac{n_{e1}}{n_{e0}}\right), \tag{3.11}$$

where

$$\eta=\frac{\left|I_{e0}\right|e}{C_g}\left[\frac{1}{T_e}+\frac{1}{T_i-e\phi_{g0}}\right],$$

and $Q_{d1}=Q_d-Q_{d0}$ is the perturbed dust grain charge, $C_g=\left[a\left(1+a/\lambda_{De}\right)\right]$ is the capacitance of dust grain [36], λ_{De} is the electron Debye length. Substituting $\frac{d}{dt}=-i\omega$ in Eq. (3.11), we obtain the dust charge fluctuations as

$$Q_{d1} = \frac{|I_{e0}|}{i(\omega + i\eta)}\left(\frac{n_{i1}}{n_{i0}} - \frac{n_{e1}}{n_{e0}}\right). \tag{3.12}$$

On substituting the values of n_{e1} and n_{i1} from Eqs (3.6) & (3.9) in Eq. (3.12), we get dust charge fluctuations as

$$Q_{d1} = \frac{|I_{e0}|}{i(\omega + i\eta)}\left(\left(\frac{k_\perp^2}{\omega^2 - \omega_{ci}^2} + \frac{k_z^2}{\omega^2}\right)c_s^2 - \frac{1}{\left(1 - \frac{i\nu_e\omega_1}{k_z^2 v_{te}^2}\right)}\right)\frac{e\phi_1}{T_e}, \tag{3.13}$$

where $v_{te}\left[=(T_e/m_e)^{1/2}\right]$ is the thermal velocity of electrons.

Now using Eqs.(3.6), (3.9), (3.10) and (3.13) in the Poisson equation, $\nabla^2\phi_1 = 4\pi(n_{e1}e - n_{i1}e + n_{d0}Q_{d1} + Q_{d0}n_{d1})$, and simplifying under assumption $k^2 \simeq k_\perp^2$ as $k_\perp^2 >> k_z^2$, we obtain

$$1 + \frac{\omega_{pe}^2}{k_\perp^2 v_{te}^2\left(1 - \frac{i\nu_e\omega_1}{k_z^2 v_{te}^2}\right)} - \frac{\omega_{pi}^2}{\left(\omega^2 - \omega_{ci}^2\right)} - \frac{\omega_{pi}^2}{\omega^2}\frac{k_z^2}{k_\perp^2} - \frac{i\beta}{(\omega + i\eta)}\frac{\omega_{pi}^2}{\left(\omega^2 - \omega_{ci}^2\right)}\frac{n_{e0}}{n_{i0}}$$

$$- \frac{i\beta}{(\omega + i\eta)}\frac{\omega_{pi}^2}{\omega^2}\frac{k_z^2}{k_\perp^2}\frac{n_{e0}}{n_{i0}} + \frac{i\beta}{(\omega + i\eta)}\frac{\omega_{pe}^2}{k_\perp^2 v_{te}^2\left(1 - \left(i\nu_e\omega_1/k_z^2 v_{te}^2\right)\right)} - \frac{\omega_{pd}^2}{\omega^2} = 0, \tag{3.14}$$

where $\omega_{pe}\left[=\left(4\pi n_{e0}e^2/m_e\right)^{1/2}\right]$, $\omega_{pi}\left[=\left(4\pi n_{i0}e^2/m_i\right)^{1/2}\right]$ and $\omega_{pd}\left[=\left(4\pi n_{d0}Q_{d0}^2/m_d\right)^{1/2}\right]$ are the electron, ion and dust plasma frequencies, respectively and $\beta = \frac{|I_{e0}|}{e}\left(\frac{n_{d0}}{n_{e0}}\right)$.

Equation (3.14) is the dispersion relation for current driven electrostatic ion cyclotron instability in a collisional magnetized dusty plasma in the presence of dust charge fluctuations and dust dynamics.

3.2.1 Dispersion Properties of Current Driven EICWs

To observe the effect of dust charge fluctuations on the frequency and the growth rate of current driven electrostatic ion cyclotron waves in the presence of dust dynamics, Eq. (3.14) can be rewritten in terms of real and imaginary part as

$$\varepsilon_r(\omega,k)+i\varepsilon_i(\omega,k)=0, \tag{3.15}$$

where $\varepsilon_r(\omega,k)=1+\frac{\omega_{pe}^2}{k_\perp^2 v_{te}^2}-\left(\frac{\omega_{pi}^2}{\omega^2-\omega_{ci}^2}+\frac{\omega_{pi}^2}{\omega^2}\frac{k_z^2}{k_\perp^2}\right)-\frac{\beta\eta}{\left(\omega^2+\eta^2\right)}\frac{n_{e0}}{n_{i0}}\left(\frac{\omega_{pi}^2}{\omega^2-\omega_{ci}^2}+\frac{\omega_{pi}^2}{\omega^2}\frac{k_z^2}{k_\perp^2}\right)$

$$-\frac{\beta}{\left(\omega^2+\eta^2\right)}\frac{\omega_{pe}^2}{k_\perp^2 v_{te}^2}\left(\omega\frac{\nu_e\omega_1}{k_z^2 v_{te}^2}-\eta\right)-\frac{\omega_{pd}^2}{\omega^2}, \tag{3.16}$$

$$\varepsilon_i(\omega,k)=\frac{\omega_{pe}^2\nu_e\omega_1}{k_\perp^2 k_z{}^2 v_{te}^4}\left(1+\frac{\beta\eta}{(\omega^2+\eta^2)}\right)-\frac{\beta\omega}{(\omega^2+\eta^2)}\frac{n_{e0}}{n_{i0}}\left(\frac{\omega_{pi}^2}{\omega^2-\omega_{ci}^2}+\frac{\omega_{pi}^2}{\omega^2}\frac{k_z{}^2}{k_\perp^2}\right)$$

$$+\frac{\beta\omega}{(\omega^2+\eta^2)}\frac{\omega_{pe}^2}{k_\perp^2 v_{te}^2}. \tag{3.17}$$

Let $\omega=\omega_r+i\gamma$ and assume a weakly damped or growing (i.e., $|\gamma|<<\omega_r$) mode. Then we can write

$$\varepsilon_r\left(\omega_r,k\right)=0, \tag{3.18}$$

to obtain the real frequency ω_r of current driven EICWs and the imaginary part of the frequency [35] is given by

$$\gamma=-\frac{\varepsilon_i(\omega_r,k)}{\partial\varepsilon_r(\omega_r,k)/\partial\omega_r}. \tag{3.19}$$

Now we will discuss the dispersion properties for three different cases.

CASE I: In the presence of dust charge fluctuations (i.e., dust charging rate η is finite) and dust dynamics (i.e., ω_{pd} is finite),

$$\varepsilon_r(\omega,k)=1+\frac{\omega_{pe}^2}{k_\perp^2 v_{te}^2}-\left(\frac{\omega_{pi}^2}{\omega^2-\omega_{ci}^2}+\frac{\omega_{pi}^2}{\omega^2}\frac{k_z^2}{k_\perp^2}\right)-\frac{\beta\eta}{\left(\omega^2+\eta^2\right)}\frac{n_{e0}}{n_{i0}}\left(\frac{\omega_{pi}^2}{\omega^2-\omega_{ci}^2}+\frac{\omega_{pi}^2}{\omega^2}\frac{k_z^2}{k_\perp^2}\right)$$

$$-\frac{\beta}{\left(\omega^2+\eta^2\right)}\frac{\omega_{pe}^2}{k_\perp^2 v_{te}^2}\left(\omega\frac{\nu_e\omega_1}{k_z^2 v_{te}^2}-\eta\right)-\frac{\omega_{pd}^2}{\omega^2}, \tag{3.20}$$

and

$$\varepsilon_i(\omega,k)=\frac{\omega_{pe}^2\nu_e\omega_1}{k_\perp^2 k_z{}^2 v_{te}^4}\left(1+\frac{\beta\eta}{(\omega^2+\eta^2)}\right)-\frac{\beta\omega}{(\omega^2+\eta^2)}\frac{n_{e0}}{n_{i0}}\left(\frac{\omega_{pi}^2}{\omega^2-\omega_{ci}^2}+\frac{\omega_{pi}^2}{\omega^2}\frac{k_z{}^2}{k_\perp^2}\right)$$

$$+\frac{\beta\omega}{(\omega^2+\eta^2)}\frac{\omega_{pe}^2}{k_\perp^2 v_{te}^2}. \tag{3.21}$$

Equations (3.18) and (3.20) yield

$$1+\frac{\omega_{pe}^2}{k_\perp^2 v_{te}^2}-\left(\frac{\omega_{pi}^2}{\omega_r^2-\omega_{ci}^2}+\frac{\omega_{pi}^2}{\omega_r^2}\frac{k_z^2}{k_\perp^2}\right)-\frac{\beta\eta}{\left(\omega_r^2+\eta^2\right)}\frac{n_{e0}}{n_{i0}}\left(\frac{\omega_{pi}^2}{\omega_r^2-\omega_{ci}^2}+\frac{\omega_{pi}^2}{\omega_r^2}\frac{k_z^2}{k_\perp^2}\right)$$

$$-\frac{\beta}{\left(\omega_r^2+\eta^2\right)}\frac{\omega_{pe}^2}{k_\perp^2 v_{te}^2}\left(\omega_r\frac{\nu_e\omega_{1r}}{k_z^2 v_{te}^2}-\eta\right)-\frac{\omega_{pd}^2}{\omega_r^2}=0, \tag{3.22}$$

where $\omega_{1r}=\omega_r-k_z v_{de}$.

CASE II: In the absence of dust charge fluctuations (i.e., $Q_{d1}\approx 0$, when dust charging rate $\eta\to\infty$) with dust dynamics (i.e., ω_{pd} is finite), Eqs. (3.16) & (3.17) can be rewritten as

$$\varepsilon_r(\omega,k)=1+\frac{\omega_{pe}^2}{k_\perp^2 v_{te}^2}-\left(\frac{\omega_{pi}^2}{\omega^2-\omega_{ci}^2}+\frac{\omega_{pi}^2}{\omega^2}\frac{k_z^2}{k_\perp^2}\right)-\frac{\omega_{pd}^2}{\omega^2}, \tag{3.23}$$

$$\varepsilon_i(\omega,k)=\frac{\omega_{pe}^2\nu_e\omega_1}{k_\perp^2 k_z{}^2 v_{te}^4} \tag{3.24}$$

Equations (3.18) and (3.23) yield

$$1+\frac{\omega_{pe}^2}{k_\perp^2 v_{te}^2}-\left(\frac{\omega_{pi}^2}{\omega_r^2-\omega_{ci}^2}+\frac{\omega_{pi}^2}{\omega_r^2}\frac{k_z^2}{k_\perp^2}\right)-\frac{\omega_{pd}^2}{\omega_r^2}=0. \tag{3.25}$$

CASE III: In the presence of dust charge fluctuations (i.e., dust charging rate η is finite) and absence of dust dynamics (i.e., $\omega_{pd}=0$ when dust grain mass $m_d\to\infty$),

$$\varepsilon_r(\omega,k)=1+\frac{\omega_{pe}^2}{k_\perp^2 v_{te}^2}-\left(\frac{\omega_{pi}^2}{\omega^2-\omega_{ci}^2}+\frac{\omega_{pi}^2}{\omega^2}\frac{k_z^2}{k_\perp^2}\right)-\frac{\beta\eta}{\left(\omega^2+\eta^2\right)}\frac{n_{e0}}{n_{i0}}\left(\frac{\omega_{pi}^2}{\omega^2-\omega_{ci}^2}+\frac{\omega_{pi}^2}{\omega^2}\frac{k_z^2}{k_\perp^2}\right)$$

$$-\frac{\beta}{\left(\omega^2+\eta^2\right)}\frac{\omega_{pe}^2}{k_\perp^2 v_{te}^2}\left(\omega\frac{\nu_e\omega_1}{k_z^2 v_{te}^2}-\eta\right), \tag{3.26}$$

and

$$\varepsilon_i(\omega,k)=\frac{\omega_{pe}^2\nu_e\omega_1}{k_\perp^2 k_z{}^2 v_{te}^4}\left(1+\frac{\beta\eta}{(\omega^2+\eta^2)}\right)-\frac{\beta\omega}{(\omega^2+\eta^2)}\frac{n_{e0}}{n_{i0}}\left(\frac{\omega_{pi}^2}{\omega^2-\omega_{ci}^2}+\frac{\omega_{pi}^2}{\omega^2}\frac{k_z{}^2}{k_\perp^2}\right)$$

$$+\frac{\beta\omega}{(\omega^2+\eta^2)}\frac{\omega_{pe}^2}{k_\perp^2 v_{te}^2}. \tag{3.27}$$

Equations (3.18) and (3.26) yield

$$1+\frac{\omega_{pe}^2}{k_\perp^2 v_{te}^2}-\left(\frac{\omega_{pi}^2}{\omega_r^2-\omega_{ci}^2}+\frac{\omega_{pi}^2}{\omega_r^2}\frac{k_z^2}{k_\perp^2}\right)-\frac{\beta\eta}{\left(\omega_r^2+\eta^2\right)}\frac{n_{e0}}{n_{i0}}\left(\frac{\omega_{pi}^2}{\omega_r^2-\omega_{ci}^2}+\frac{\omega_{pi}^2}{\omega_r^2}\frac{k_z^2}{k_\perp^2}\right)$$

$$-\frac{\beta}{\left(\omega_r^2+\eta^2\right)}\frac{\omega_{pe}^2}{k_\perp^2 v_{te}^2}\left(\omega_r\frac{\nu_e\omega_{1r}}{k_z^2 v_{te}^2}-\eta\right)=0. \qquad (3.28)$$

The coupling parameter β can be rewritten after using the charge neutrality condition and the value of equilibrium electron current [29] as,

$$\beta=0.397\left(1-\frac{1}{\delta}\right)\left(\frac{a}{v_{te}}\right)\omega_{pi}^2\left(\frac{m_i}{m_e}\right), \qquad (3.29)$$

where $\delta=n_{io}/n_{eo}$.

The charging rate η can also be rewritten for Q-Machine plasmas [29], in the limit $T_e\cong T_i$ i.e., electron temperature equals the ion temperature as

$$\eta=0.79a\left(\frac{\omega_{pi}}{\lambda_{Di}}\right)\left(\frac{1}{\delta}\right)\left(\frac{m_i}{m_e}\frac{T_i}{T_e}\right)^{\frac{1}{2}}. \qquad (3.30)$$

If n_{i0}/n_{e0} =1, i.e., $\beta\to 0$ (where β is the coupling parameter), we recover the expression for the growth rate (cf. Eq. (3.21) in the absence of a transverse dc electric field) of Sharma *et al.* [37]. Moreover, in the absence of parallel resistivity (i.e., $C_{er\|}$=1), we recover the growth rate expression [cf. second term of 6(b))] of Chaturvedi and Kaw [7].

3.3 RESULTS AND DISCUSSION

To estimate the numerical values of the real frequency and growth rate of the instability discussed above, we use typical physical parameters of dusty plasmas as shown in Table-3.1.

Table-3.1 The typical parameters of the collisional dusty plasma (Potassium)

Parameter	Value
Electron Plasma density n_{e0}	1.0 x 10^{10} -1.8 x 10^{10} cm^{-3}
Ion Plasma density n_{i0}	1.0 x 10^{10} - 9.0 x 10^{10} cm^{-3}
Relative density of negatively charged dust grains $\delta = n_{i0}/n_{e0}$	1- 5
Electron Temperature T_e	0.2 eV
Ion Temperature T_i	0.2 eV
Dust Density n_{d0}	5.0x10^4 cm^{-3}
Dust grain size a	1.0x10^{-4} cm
Guide magnetic field B	1x10^2 Gauss
Mass ratio , m_i/m_e	7.16x10^4
$k_z/k_\perp$	0.0306
Electron neutral collisional frequency, ν_{e0}	4.0x10^4 rad/sec

In the present model, we have considered the parameters that satisfy the applicability of the OML approximation to magnetized plasmas which support the propagation of low frequency EIC modes. The applicability of the OML theory to dynamical wave systems in magnetized plasmas is limited [38]-[39] as this model [40] is reasonably valid in the limit $a \ll \lambda_{De} \ll \lambda$, where a is grain size, λ_{De} is the electron Debye length, and λ is the wavelength of the fluctuating fields. The limits of the OML approximation for magnetized dusty plasma have been given by Jana *et al.* [9]. According to Jana *et al.* the charging equation [see Eq. (3.11), [9]] is valid only if dust size $a \ll \rho_L \left[= \left(v_{te} / \omega_{ce} \right) \right]$ the electron Larmor radius, where v_{te} and ω_{ce} are the thermal velocity and cyclotron frequency of electrons, respectively.

Fig. 3.1 illustrates the numerical solutions of Eqs. (3.22), (3.25) & (3.28) based on Laguerre's method for the above mentioned parameters in Table-3.1. We have plotted the normalized real frequency ω_r/ω_{ci} of the current-driven EIC instability in a collisional plasma as a function of the ratio of positive ion density to electron density $\delta = n_{i0}/n_{e0}$ in Fig. 3.1.

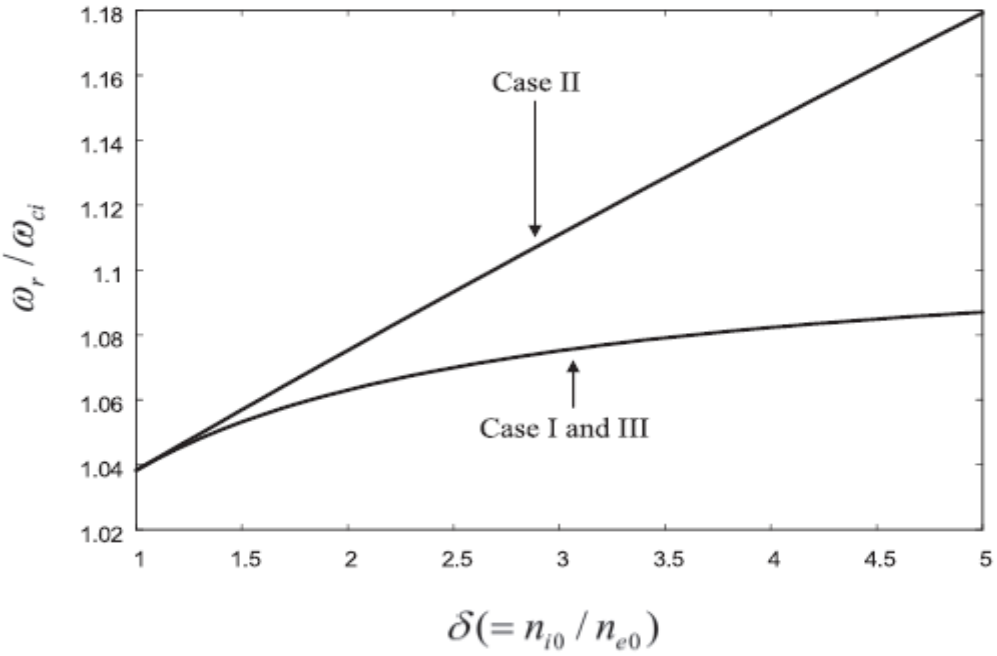

Fig. 3.1 Normalized real part of the frequency ω_r/ω_{ci} of the current driven EIC instability as a function of the relative density of negatively charged dust grains $\delta\left(= n_{i0}/n_{e0}\right)$ [with and without dust charge fluctuations in addition to dust dynamics for the cases I, II, & III as mentioned in sec. 3.2.1] at constant electron and ion temperatures $\left(T_e = T_i = 0.2 \text{ eV}\right)$ and electron-neutral collision frequency $\nu_e\left(= 4.0\times10^5\right)$ rad/sec.

From Fig. 3.1, it is observed that the normalized wave frequency ω_r/ω_{ci} increases 4.2% when δ changes from 1 to 4 for case I and case III, i.e., if dust charge fluctuations (with and without dust dynamics) are taken into account and 10.3% for case II, i.e., in the absence of dust charge fluctuations and with dust dynamics for the plasma parameters listed above. Unique curve has been obtained for case I and case III

due to insignificant contribution of the term containing dust dynamics effect, i.e., term containing ω_{pd} (due to dust grain mass) in comparison to other contributing terms.

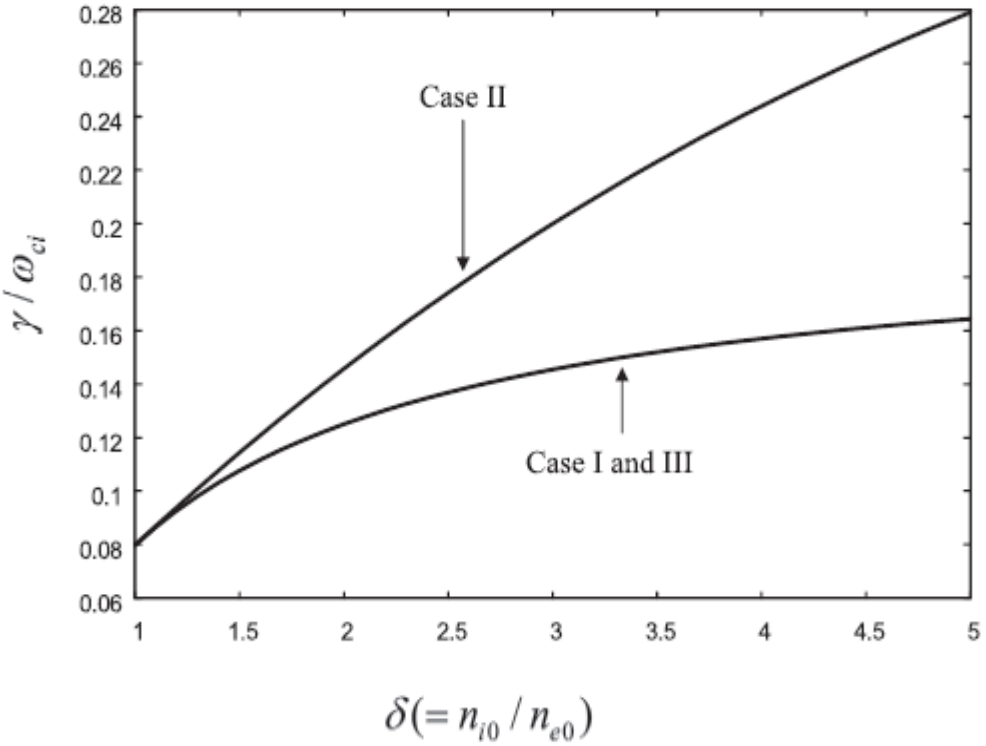

Fig. 3.2 Normalized growth rate γ/ω_{ci} of the current driven EIC instability as a function of the relative density of negatively charged dust grains $\delta\left(=n_{i0}/n_{e0}\right)$ [with and without dust charge fluctuations in addition to dust dynamics for three cases I, II, & III similar to Fig. 3.1] at constant electron and ion temperature $\left(T_e = T_i = 0.2 \text{ eV}\right)$ and electron-neutral collision frequency $\nu_e\left(=4.0\times10^5\right)$ rad/sec.

Barkan et al. [19] have found that presence of dust increases the wave frequency upto 10%–20% above the ion-cyclotron frequency. Chow and Rosenberg [20] have shown in their kinetic analysis on the effects of charged dust grains on the collisionless EIC instability that, the wave frequency ω_r/ω_{ci} increases about 11% when δ is changed from 1 to 4 under similar conditions. Moreover, the normalized wave frequency is not getting saturated at higher values of δ in the absence of dust charge fluctuations and with dust dynamics. In the present calculations, the unstable mode

frequency $\omega_r < \eta$ (where η is the dust charging rate) for all the calculations, where δ varies from 1 to 5.

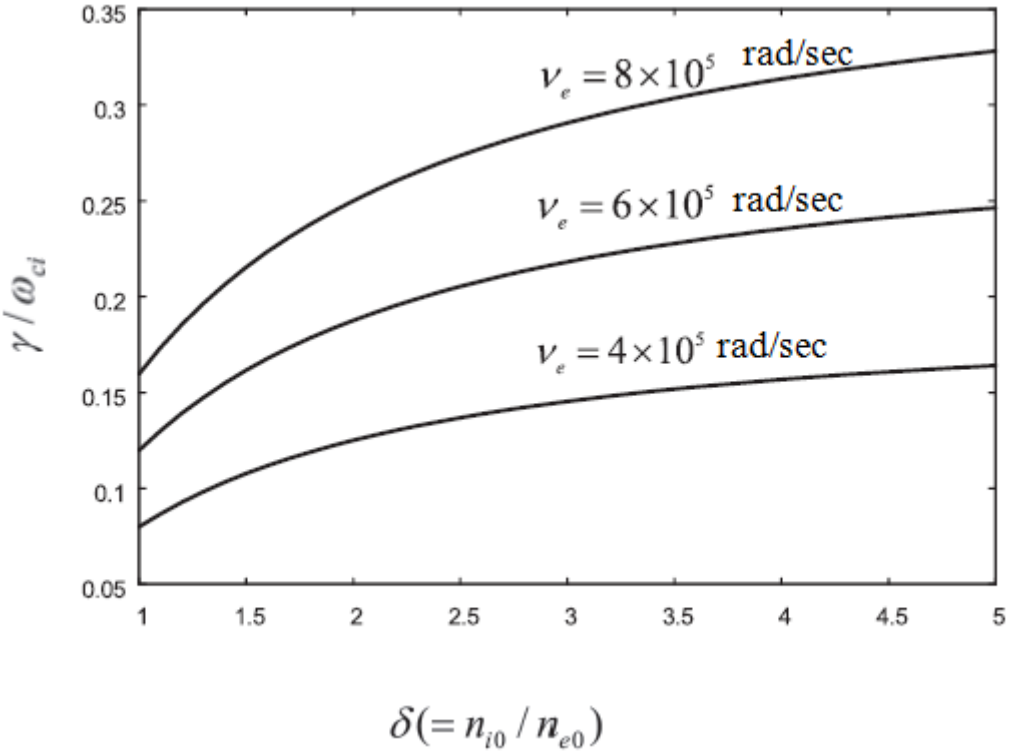

Fig. 3.3 Normalized growth rate γ/ω_{ci} of the current driven EIC instability as a function of the relative density of negatively charged dust grains $\delta\left(=n_{i0}/n_{e0}\right)$ for different electron neutral collisional frequencies (ν_e) at constant electron and ion temperature $\left(T_e = T_i = 0.2 \text{ eV}\right)$.

In Fig. 3.2 we have plotted the normalized growth rate γ/ω_{ci} using Eq. (3.19) for three cases as a function of δ for the same parameters as used in Fig. 3.1. From Fig. 3.2, it can be seen that the normalized growth rate γ/ω_{ci} increases by a factor 1.96 when δ changes from 1 to 4.0 for case I and case III and by a factor 3.06 for case II. Thus, the increase is more drastic in the absence of dust charge fluctuations. It shows that the dust charge fluctuations can play a significant role in suppression of EIC instability.

In the experimental observations by Barkan et al. [19] the EIC wave amplitude was also found to increase with increase in δ, the relative density of negatively charged dust grains. In the absence of dust grains, i.e., δ=1, the unstable mode frequency is $\omega_r = 2.55\times10^4$ rad/sec and the growth rate is $\gamma = 1.9\times10^3$ rad/sec for the parameters mentioned earlier.

It is also observed that the normalized real frequency ω_r/ω_{ci} remains unchanged with increase in electron neutral collision frequency ν_e , while Fig. 3.3 clearly shows that the normalized growth rate γ/ω_{ci} is increased linearly with the increase in electron neutral collision frequency ν_e. It is observed that the electron collisions destabilizes the current driven EIC instability which is in good agreement with the results shown by Chaturvedi and Kaw [7], Milic [41] and Satyanarayana *et al*. [42].

3.4 CONCLUSION

The conclusion represents that the stability of current-driven EIC waves in a collisional magnetized dusty plasma in the presence and absence of dust charge fluctuations in addition to dust dynamics have been examined. The growth rate and mode frequencies were evaluated based on existing dusty plasma parameters and it is found that the unstable mode frequency increases with δ in all the three cases. However, the increase in normalized unstable wave frequency ω_r/ω_{ci} with δ is more in the absence of dust charge fluctuations (cf. case II than the corresponding value of ω_r/ω_{ci} in the presence of dust charge fluctuations and with dust dynamics (cf. case I)). These results are found to be in good agreement with the results of EIC waves (in the absence of dust charge fluctuations) obtained by Barkan *et al.* [19], Chow and Rosenberg [20] & Merlino *et al.* [22]. Increase in electron-neutral collisional frequency ν_e increases the instability of EIC waves. This result is in compliance with Chaturvedi and Kaw [7], Milic [41] & Satyanarayana *et al.* [42].

From the results, we can also say that the term containing dust dynamics effect does not contribute significantly because of large dust grain mass. Hence due to insignificant contribution of the term containing dust dynamics in comparison to other contributing terms, the curves corresponding to case I and case III are overlapping in Figs. 3.1 and 3.2. These results may be useful in study of instabilities in earth's ionosphere [42] - [43] and fusion devices [44].

REFERENCES

[1]. N. D'Angelo and R. W. Motley, *Phys. Fluids* **5**, 633 (1962).

[2]. R. W. Motley and N. D'Angelo, *Phys. Fluids* **6**, 296 (1963).

[3]. N. D'Angelo, *J. Geophys. Res.* **78**, 3987 (1973).

[4]. R. Bergman, *J. Geophys. Res.* **89**, 953 (1984).

[5]. W. E. Drummond and M. N. Rosenbluth, *Phys. Fluids* **5**, 1507 (1962).

[6]. J. J. Rasmussen and R.W. Schrittwieser, *IEEE Trans. Plasma Sci.* **19**, 457 (1991).

[7]. P. K. Chaturvedi and P.K. Kaw, *Plasma Phys.* **17**, 447 (1975).

[8]. E. C. Whipple, T**.** G. Northdrop, and D. A. Mendis, *J. Geophys. Res.* **90**, 7405 (1985).

[9]. M. R. Jana, A. Sen, and P. K. Kaw, *Phys. Rev. E* **48**, 3930 (1993).

[10]. C. Cui and J. Goree, *IEEE Trans. Plasma Sci.* **22**, 151 (1994).

[11]. S. C. Sharma and M. Sugawa, *Phys. Plasmas* **6**, 444 (1999).

[12]. S. V. Vladimirov, K.N.Ostrikov, M.Y.Yu, and L. Stenflo, *Phys. Rev. E* **58**, 8046 (1998).

[13]. N. D' Angelo, *J. Phys. D: Appl. Phys.* **37**, 860 (2004).

[14]. B. Song, D. Suszcynsky, N. D'Angelo, and R. L. Merlino, *Phys. Fluids B* **1**, 2316 (1989).

[15]. S. C. Sharma and M. P. Srivastava, *Phys. Plasmas* **8**, 679 (2001).

[16]. V. W. Chow and M. Rosenberg, *Phys. Plasmas* **3**, 1202 (1996).

[17]. N. D'Angelo, *Planet. Space Sci.* **38**, 1143 (1990).

[18]. D. M. Suszcynsky, N. D'Angelo, and R. L. Merlino, *J. Geophys. Res.* **94**, 8966 (1989).

[19]. A. Barkan, N. D'Angelo, and R. L. Merlino, *Planet. Space Sci.* **43**, 905 (1995).

[20]. V. W. Chow and M. Rosenberg, *Planet. Space Sci.* **43**, 613 (1995).

[21]. V. W. Chow and M. Rosenberg, *Planet. Space Sci.* **44**, 465 (1996).

[22]. R. L. Merlino, A. Barkan, C. Thompson, and N. D' Angelo, *Phys. Plasmas* **5**, 1607 (1998).

[23]. R.L. Merlino, *IEEE Trans. Plasma Sci.* **25**, 60 (1997).

[24]. R. Annou, *Phys. Plasmas* **5**, 2813 (1998).

[25]. K. N. Ostrikov, M.Y.Yu, S. V. Vladimirov, and O. Ishihara, *Phys. Plasmas* **6**, 737 (1999).

[26]. M. Tribeche and T. H. Zerguini, *Phys. Plasmas* **8**, 394 (2001).

[27]. J. Vranjes, B.P. Pandey, and S. Poedts, *Phys. Rev. E* **64**, 66404 (2001).

[28]. J. Sharma and S. C. Sharma, *Phys. Plasmas* **17**, 123701(2010).

[29]. S. C. Sharma and A. Gahlot, *Phys. Plasmas* **16**, 123708 (2009).

[30]. S. C. Sharma and R. Walia, *Phys. Plasmas* **15**, 093703 (2008).

[31]. S. C. Sharma and A. Gahlot, *Phys. Plasmas* **15**, 073705 (2008).

[32]. B. Milic and D. Zyunder, *Sov. Phys. Tech. Phys.* **13**, 160 (1968).

[33]. R. K. Varma, P. K. Shukla, and V. Krishan, *Phys. Rev. E* **47**, 3612 (1993).

[34]. M. Rosenberg and V.W. Chow, *J. Plasma Phys.* **61**, 51 (1999).

[35]. N. A. Krall and A.W. Trivelpiece, *Principles of Plasma Physics*, McGraw-Hill, New York, (1973), 389, Chap. VIII.

[36]. M. S. Barnes, J. K. Keller, J.C. Forster, J.A. O' Neill, and D. K. Coultas, *Phys. Rev. Lett.* **68**, 313(1992).

[37]. S. C. Sharma, M. Sugawa, and V. K. Jain, *Phys. Plasmas* **7**, 457 (2000).

[38]. F. F. Chen, "*Plasma Diagnostic Techniques*", edited by R. H. Huddlestone and S. L. Leonard , Academic, New York, (1965), Chap. IV.

[39]. F. F. Chen, "*Introduction to Plasma Physics"*, Academic, New York, (1965).

[40]. J. Goree, *Phys. Rev. Lett.* **69**, 277 (1992).

[41]. B. Milic, *Phys. Fluids* **15**, 1630(1972).

[42]. P. Satyanarayana, P. K. Chaturvedi, M. J. Keskinen, J. D. Huba, and S. L. Ossakow, *J. Geophys. Res.* **90**, 1220 (1985).

[43]. A. A. Chernyshov, A. A. Ilyasov, M. M. Mogilevsky, I. V. Golovchanskaya, B. V. Kozelov, *Cosmic Res.* **54**, 52 (2016).

[44]. W. P. Hong and Y. D. Jung, *Phys. Lett. A* **380**, 1193 (2016)

CHAPTER 4

Excitation of Kelvin Helmholtz Instability by an Ion Beam in a Plasma having Negatively Charged Dust Grains

The chapter enlightens the fact that an ion beam propagating through a magnetized dusty plasma drives Kelvin Helmholtz Instability (KHI) via Cerenkov interaction. It consists of analytical models based on the local and non-local fluid treatment on plasmas species to study the excitation of Kelvin Helmholtz instability (KHI) by an ion beam in a magnetized dusty plasma. The local model elucidates the effect of negatively charged dust grains and relative velocity shear on the frequency and growth rate of ion beam driven KHI. A non-local theoretical model have also been developed to study the effect of negatively charged dust grains on the Kelvin Helmholtz instability driven by an ion beam in a magnetized plasma having cylindrical geometry. The effects of radial boundaries have been presented through radial density and potential profiles of dusty plasma. Moreover, the effects of relative concentration of dust grains, shear parameter and beam parameters have also been explicated.

4.1 INTRODUCTION

The study of Kelvin Helmholtz instability (KHI) has been a great deal of interest in planetary, space & geophysical sciences [1]–[9], astrophysical jets [10], solar wind [11], magnetospheric boundaries [12], and Tokomak environments [13] etc.

S. Chandrasekhar [14] has initially described the Kelvin Helmholtz instability (KHI) for a conductive, magnetized incompressible fluid. He stated that the KHI arises when different layers of a stratified heterogeneous fluid are in relative horizontal

motion. These small-scale electrostatic perturbations feed on the kinetic energy of mean flow. The KHI in a plasma arises when it flows in a direction parallel to the direction of applied magnetic field with a velocity that varies in the direction perpendicular to the magnetic field. The study on KHI was further extended for compressible fluids. D'Angelo [15] has found that the smaller relative speed of the order of ion acoustic speed between two adjacent layers is sufficient to produce the K-H instability. Moreover, a uniform magnetic field acting parallel to the direction of flow suppresses the KHI if relative speed does not exceed the root mean square Alfven speed between the different layers. Experimental observations of Q-machine [16] have also confirmed the above results.

D' Angelo and Song [17] found that the excitation of KHI in magnetized plasmas having positively charged dust grains is easier than for negatively charged dust grains as an increase in $Z\varepsilon$ reduces the critical shear for positive dust grains while the critical shear increases as the quantity $Z\varepsilon$ approaches unity for negatively charged dust, where ε is the relative density of negatively charged dust grains. Moreover, D'Angelo and Song [18] have examined the effect of negative to positive ion mass ratio on stability of KHI in a negative ion plasma. An *et al.* [19] have also investigated the destabilizing effect of negative ions on excitation of KHI in a magnetized potassium plasma.

Singh *et al.* [20] have studied the stabilizing effect of dust charge fluctuations on the growth of KHI in a dense plasma. Rao [21] has examined the effect of sheared flows on the excitation of electrostatic modes and the KHI in non-ideal dusty plasma. Luo *et al.* [22] have experimentally investigated the stabilizing effect of negatively charged dust grains on the growth rate of K-H instability in magnetized Cesium plasma. Wiechen [23] has developed the multi-fluid simulation theory of KHI in partially ionized dusty plasmas showing the stabilizing effect for massive dust grains and destabilizing effect for high charge numbers. The KHI has also been studied in presence of sheared magnetic field in dusty plasmas by Kumar *et al.* [24] showing the stabilizing effect of negatively charged dust grains.

It has been observed that the charged particles beam propagating through plasma have been a source of excitation of plasma oscillations, waves & instabilities [25]-[27] in gas discharge systems and ion beam plasma systems [28]-[30]. The effects of plasma boundaries on excitation of plasma instabilities is an important aspect of study as most of the laboratory plasma devices such as Q machines and gaseous discharge tubes are of finite geometry.

Thus, keeping in view the role of charged particle beams in excitation of plasma instabilities and finite geometry of plasma systems, we develop local and non-local (cylindrical geometry) theoretical model for an ion beam driven KHI in a plasma waveguide having negatively charged dust grains and explicate the effect of dust grains, plasma boundaries and ion beam parameters on the excitation of KHI.

4.2 LOCAL ANALYSIS

We considered the multi-species collisionless plasma (cf. Fig. 4.1) consisting of electrons, ions and dust particles immersed in a static magnetic field B which is in positive z-direction with equilibrium electron, ion and dust particle densities being given as n_{eo}, n_{io}, and n_{d0} and the charge, mass, and temperature of the three species are denoted by $(-e, m_e, T_e)$, (e, m_i, T_i) and $(-Q_{d0}, m_d, T_d)$, respectively. The equilibrium densities vary along negative x-direction as $n_0 = \overline{n_0} e^{-\lambda x}$, where $\overline{n_0}$(= constant) and λ is the inverse e-folding length of the density gradient [22]. The particles flow along the magnetic field B with velocity that depends only on the x-coordinate and the equilibrium velocity vectors being given by $v_0 = (0, v_{0y}, v_{0z}(x))$ with constant v_{0y}. An ion beam with velocity $v_{b0} \| \hat{z}$, mass m_b, density n_{b0}, and radius $r_0 (= a_1)$ propagates through plasma with negatively charged dust grains along the direction of magnetic field (cf. Fig. 4.1).

The beam plasma system prior to the perturbation is quasineutral, such that

$$en_{e0} - en_{i0} - en_{bo} + Q_{d0} n_{d0} \approx 0 .$$

The equilibrium is perturbed by an electrostatic perturbation to the potential.

$$\phi_1 = \phi_1(r) e^{-i(\omega t - \vec{k}.\vec{r})}. \qquad (4.1)$$

The first order quantities vary as $e^{-i(\omega t - k_y y - k_z z)}$.

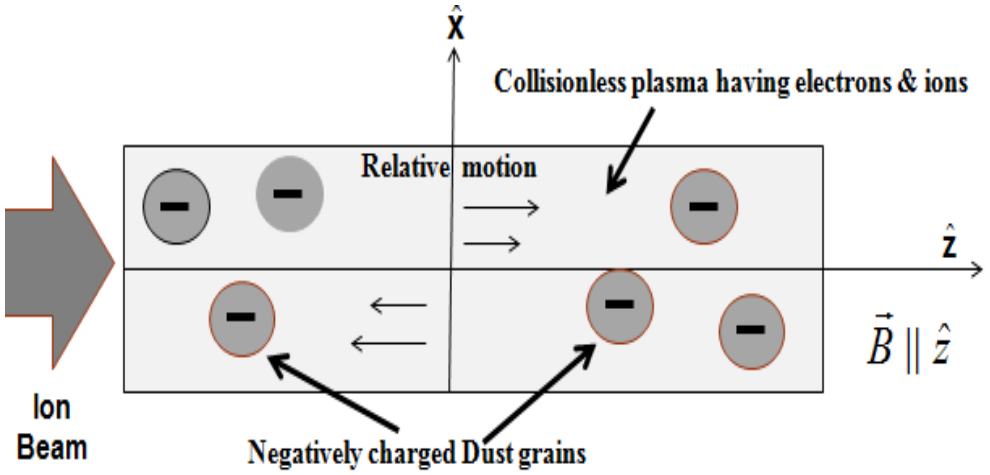

Fig. 4.1 Schematic showing relative motion in a plasma having negatively charged dust grains and an ion beam propagating through it.

The response of plasma electrons to the perturbation may be derived from the momentum conservation equation, i.e.,

$$m_e \frac{d\vec{v}}{dt} = -e\vec{E} - \frac{e}{c}\vec{v}\times\vec{B} - \frac{\nabla(nT)}{n}. \tag{4.2}$$

On linearization Eq. (4.2) yields the perturbed velocity components, i.e.,

$$v_{1x} = i\frac{\omega_{ce}k_y}{(\omega_{ce}^2-\omega_1^2)}\left[\frac{T_e}{m_e}\frac{n_{e1}}{n_{e0}} - \frac{e\phi_1}{m_e}\right], \tag{4.3}$$

$$v_{1y} = \frac{\omega_1 k_y}{(\omega_{ce}^2-\omega_1^2)}\left[\frac{e\phi_1}{m_e} - \frac{T_e}{m_e}\frac{n_{e1}}{n_{e0}}\right], \tag{4.4}$$

and

$$v_{1z} = -\frac{ek_z\phi_1}{m_e} + \frac{T_e}{m_e}\frac{n_{e1}}{n_{e0}}\frac{k_z}{\omega_1} + \frac{1}{i\omega_1}v_{1x}\frac{\partial v_{0z}}{\partial x}, \tag{4.5}$$

where $\omega_{ce}\left(=eB_s/m_ec\right)$ is the electron cyclotron frequency, $\omega_1 = (\omega - k_y v_{0y} - k_z v_{0z})$ and subscript "1" refers to perturbed quantities.

We obtain perturbed electron density on substituting the perturbed velocities from Eqs. (4.3)- (4.5) in the mass conservation equation, as

$$n_{e1} = n_{e0}\frac{e\phi_1}{T_e}. \tag{4.6}$$

The response of ions is given by

$$\left(1-\frac{v_{ti}^2 k_z^2}{\omega_1^2}\right)n_{i1}+\frac{v_{ti}^2\nabla_\perp^2 n_{i1}}{(\omega_1^2-\omega_{ci}^2)}=\frac{en_{i0}}{m_i}\left[\frac{-\nabla_\perp^2\phi_1}{\omega_1^2-\omega_{ci}^2}+\frac{k_z^2\phi_1}{\omega_1^2}+i\left(\frac{\lambda v_{1x}m_i}{e\,\omega_1}-\frac{k_z v_{1x}m_i}{e\,\omega_1^2}\frac{\partial v_{0z}}{\partial x}\right)\right], \tag{4.7}$$

where, $v_{ti}\left[=\left(T_i/m_i\right)^{1/2}\right]$ is the ion thermal velocity and $\omega_{ci}\left(=eB_s/m_ic\right)$ is the ion cyclotron frequency.

We assume $T_e \simeq T_i$ i.e., $\omega_1 < \omega_{ci}$, $k_\perp v_{ti} < \omega_{ci}\left(\frac{k_\perp v_{ti}}{\omega_1-\omega_{ci}} << 1\right)$, i.e., the case of a strongly magnetized plasma. Now using the value of v_{1x} for ions in Eq. (4.7), the perturbed density for ions is given as

$$n_{i1}=\frac{n_{i0}e\phi_1}{m_i}\frac{\left(\frac{\nabla_\perp^2}{\omega_{ci}^2}+\frac{k_z^2}{\omega_1^2}+\frac{\lambda k_y}{\omega_1\omega_{ci}}-\frac{k_y k_z}{\omega_1^2}\frac{1}{\omega_{ci}}\frac{\partial v_{0z}}{\partial x}\right)}{\left(1-\frac{k_z^2 v_{ti}^2}{\omega_1^2}-\frac{\lambda k_y v_{ti}^2}{\omega_1\omega_{ci}}+\frac{k_y k_z v_{ti}^2}{\omega_1^2}\frac{1}{\omega_{ci}}\frac{\partial v_{0z}}{\partial x}\right)}. \tag{4.8}$$

Similarly the dust density perturbations are given by

$$n_{d1}=\frac{Q_{d0}n_{d0}}{m_d}\frac{\nabla_\perp^2\phi_1}{\omega_1^2}. \tag{4.9}$$

Here dust is treated as unmagnetized because $\omega \sim \omega_{ci} >> \omega_{cd}$ with $\omega_{cd}\left(=Q_{d0}B/m_dc\right)$ be the dust gyro frequency.

From probe theory (as discussed in previous chapter 2 sec. (2.2.1)) applied to a dust grain [31]-[34], and Eqs. (4.6) and (4.8) we obtain perturbed dust charge as

$$Q_{d1}=\frac{e\left|I_{e0}\right|}{i(\omega+i\eta)}\left[\frac{\left(\frac{\nabla_{\perp}^{2}\phi_1}{m_i\omega_{ci}^{2}}+\frac{k_z^{2}\phi_1}{m_i\omega_1^{2}}+\frac{\lambda k_y\phi_1}{\omega_1\omega_{ci}}-\frac{k_yk_z\phi_1}{\omega_1^{2}}\frac{1}{\omega_{ci}}\frac{\partial v_{0z}}{\partial x}\right)}{\left(1-\frac{k_z^{2}v_{ti}^{2}}{\omega_1^{2}}-\frac{\lambda k_y v_{ti}^{2}}{\omega_1\omega_{ci}}+\frac{k_yk_zv_{ti}^{2}}{\omega_1^{2}}\frac{1}{\omega_{ci}}\frac{\partial v_{0z}}{\partial x}\right)}-\frac{\phi_1}{T_e}\right], \qquad (4.10)$$

where $\eta=0.79a\left(\frac{\omega_{pi}}{\lambda_{Di}}\right)\left(\frac{1}{\delta}\right)\left(\frac{m_i}{m_e}\frac{T_i}{T_e}\right)^{\frac{1}{2}}$ is the dust charging rate for Q-machine plasmas ($T_e = T_i$) as previously mentioned in chapter 2 sec. (2.2.3), $\delta\left[=n_{i0}/n_{e0}\right]$ and $\lambda_{Di}\left[=\left(T_i/4\pi n_{i0}e^{2}\right)^{1/2}\right]$ is the ion Debye length.

Following the analysis of Sharma and Srivastava [35], the ion beam density perturbations is given by

$$n_{b1}=\frac{n_{b0}e\left(k_y^{2}+k_z^{2}\right)\phi_1}{m_b(\omega_1-k_zv_{b0})^{2}}. \qquad (4.11)$$

Using Eqs. (4.6), (4.8)-(4.11) in the Poisson equation,

$$\nabla^{2}\phi_1=4\pi(n_{e1}e-n_{i1}e-n_{b1}e+n_{d0}Q_{d1}+Q_{d0}n_{d1}),$$

we obtain,

$$1-\frac{\omega_{pb}{}^{2}c_s^{2}\delta\left(k_y^{2}+k_z^{2}\right)}{\omega_{pi}^{2}\left(\omega_1-k_zv_{b0}\right)^{2}}-\frac{k_z{}^{2}}{\omega_1{}^{2}}\alpha_1^{2}-\frac{\lambda k_y}{\omega_1\omega_{ci}}\alpha_1^{2}+\frac{k_yk_z}{\omega_1{}^{2}}\frac{1}{\omega_{ci}}\frac{\partial v_{0z}}{\partial x}\alpha_1^{2}$$

$$-\frac{i\beta}{(\omega+i\eta)}\left(\frac{k_z{}^{2}c_s^{2}}{\omega_1{}^{2}}+\frac{\lambda k_yc_s^{2}}{\omega_1\omega_{ci}}-\frac{k_yk_zc_s^{2}}{\omega_1{}^{2}}\frac{1}{\omega_{ci}}\frac{\partial v_{0z}}{\partial x}\right)=0, \qquad (4.12)$$

where,

$$\alpha_1^2 = v_{ti}^2 + c_s^2\delta - \frac{\omega_{pb}^2}{\omega_{pi}^2}\frac{c_s^2 v_{ti}^2 \delta\left(k_y^2 + k_z^2\right)}{\left(\omega_1 - k_z v_{b0}\right)^2}, \tag{4.13}$$

and $\beta = \left(\left|I_{e0}\right|/e\right)\left(n_{d0}/n_{e0}\right) \approx 0.397\left(1-\frac{1}{\delta}\right)\left(\frac{a}{v_{te}}\right)\omega_{pi}^2\left(\frac{m_i}{m_e}\right)$. (as shown in chapter 2 sec (2.2.3)) Here, $\omega_{pb}\left[=\left(4\pi n_{b0}e^2/m_b\right)^{1/2}\right]$ and $\omega_{pi}\left[=\left(4\pi n_{i0}e^2/m_i\right)^{1/2}\right]$ are the beam and ion plasma frequencies, respectively. In Eq. (4.12), we have set $k^2 \simeq k_\perp^2 \cong k_y^2$ as $k_\perp^2 >> k_z^2$, $\omega_1^2 \ll \omega_{ci}^2$, and ignored ω_{pd}^2/ω_1^2 as $\omega_1^2 >> \omega_{pd}^2$ where, $\omega_{pd}\left[=\left(4\pi n_{d0}Q_{d0}^2/m_d\right)^{1/2}\right]$ is the dust plasma frequency.

Equation (4.12) can be rewritten as

$$\omega_1^2 - \frac{\lambda k_y \alpha_2^2}{\omega_{ci}}\omega_1 - k_z^2\alpha_2^2 + \frac{k_y k_z}{\omega_{ci}}\frac{\partial v_{0z}}{\partial x}\alpha_2^2 = \frac{\omega_{pb}^2 c_s^2 \delta\left(k_y^2 + k_z^2\right)\omega_1^2}{\omega_{pi}^2\left(\omega_1 - k_z v_{b0}\right)^2}, \tag{4.14}$$

which can be further simplified as

$$\left(\omega_1^2 - \frac{\lambda k_y \alpha_2^2}{\omega_{ci}}\omega_1 - k_z^2\alpha_2^2 + \frac{k_y k_z}{\omega_{ci}}\frac{\partial v_{0z}}{\partial x}\alpha_2^2\right)\left(\omega_1 - k_z v_{b0}\right)^2 = \frac{\omega_{pb}^2 c_s^2 \delta\left(k_y^2 + k_z^2\right)\omega_1^2}{\omega_{pi}^2}. \tag{4.15}$$

Here,

$$\alpha_2^2 = \alpha_1^2 + \frac{i\beta}{\omega + i\eta}c_s^2. \tag{4.16}$$

Now in the absence of beam density, i.e., $n_{b0} \to 0$, Eq. (4.15) gives

$$\left(\omega_1^2 - \frac{\lambda k_y \alpha_2^2}{\omega_{ci}}\omega_1 - k_z^2\alpha_2^2 + \frac{k_y k_z}{\omega_{ci}}\frac{\partial v_{0z}}{\partial x}\alpha_2^2\right)\left(\omega_1 - k_z v_{b0}\right)^2 = 0. \tag{4.17}$$

We look for solutions when the beam is in Cerenkov resonance with the KHI mode. In this case, the two factors on the left-hand side of Eq. (4.17) are simultaneously zero in the absence of beam density and give

$$\omega_1^2 - \frac{\lambda k_y \alpha_2^2}{\omega_{ci}} \omega_1 - k_z^2 \alpha_2^2 + \frac{k_y k_z}{\omega_{ci}} \frac{\partial v_{0z}}{\partial x} \alpha_2^2 = 0. \tag{4.18}$$

and

$$\omega_1 \cong k_z v_{b0}. \tag{4.19}$$

Here Eq. (4.18) corresponds to the KHI mode and Eq. (4.19) corresponds to the beam mode.

Equation (4.17) can further be simplified as

$$\omega_1^2 \left(1 - \frac{\omega_{pb}^2 c_s^2 \delta \left(k_y^2 + k_z^2 \right)}{\omega_{pi}^2 \left(\omega_1 - k_z v_{b0} \right)^2} \right) - \frac{\lambda k_y \alpha_2^2}{\omega_{ci}} \omega_1 - k_z^2 \alpha_2^2 + \frac{k_y k_z}{\omega_{ci}} \frac{\partial v_{0z}}{\partial x} \alpha_2^2 = 0. \tag{4.20}$$

Let us write $\omega_1 = \omega_r + i\omega_i$ and assume that the wave is either weakly damped or growing (i.e., $\left|\omega_i\right| << \omega_r$). We assume $\omega_1 / \omega_{ci} = \Omega$, $\rho_i^2 \left(= \alpha_2^2 / \omega_{ci}^2 \right)$, $\Lambda = \lambda \rho_i$, $\gamma = k_z \rho_i$, $\beta_1 = k_y \rho_i$, and the shear parameter $\mu \left(= \frac{1}{\omega_{ci}} \frac{\partial v_{0z}}{\partial x} \right)$. Also we assume that $\beta_1^2 \ll 1 (\text{i.e.}, k_y^2 \rho_i^2 \ll 1)$ i.e., ion Larmor radius is much smaller than the perpendicular wavelength and $\gamma^2 \ll 1 (\text{i.e.}, k_z^2 \rho_i^2 \ll 1)$ i.e., ion Larmor radius is much smaller than the parallel wavelength.

Let $q = \left(1 - \frac{\omega_{pb}^2 c_s^2 \delta \left(k_y^2 + k_z^2 \right)}{\omega_{pi}^2 \left(\omega_1 - k_z v_{b0} \right)^2} \right)$.

The Eq. (4.20) can further be simplified to yield the dispersion relation for beam driven Kelvin Helmholtz instability in a plasma as

$$\Omega^2 - \frac{\beta_1 \Lambda \Omega}{q} - \frac{\gamma\left(\gamma - \beta_1 \mu\right)}{q} = 0. \tag{4.21}$$

In the absence of beam (i.e., $\omega_{pb} \to 0$, q=1) and dust charge fluctuations (i.e., $\eta \to \infty$ and $Q_{d1} = 0$), we can recover the dispersion relation of Luo *et al.* [22] (cf. Eq.1) and D'Angelo & Song [17] (cf. Eq. 23).

From Eq. (4.21) the maximized Normalized growth rate $\Gamma\left(= \omega_i / \omega_{ci}\right)$ can be found as

$$\Gamma = \left[\frac{1}{4}\beta_1^2\left(\frac{\mu^2}{q} - \frac{\Lambda^2}{q^2}\right)\right]^{1/2}. \tag{4.22}$$

In the absence of beam and dust charge fluctuations, Eq. (4.22) reduces to the expression for growth rate as given by Luo *et al.* [22] (cf. Eq. 2).

4.2.1 Results and Discussion (Local Model)

In the calculations, we have used plasma parameters for the experiment of Luo *et al.* [22] as given in Table-4.1.

Using Eq. (4.18), Real part of KHI frequency $\Omega_r \left(= \omega_r / \omega_{ci}\right)$ as a function of normalized wave vector k_z / k_y have been plotted in Fig. 4.2, for different values of relative density of negatively charged dust grains neglecting the dust charge fluctuations (cf. Fig. 4.2) for the parameters of Cesium plasma (cf. Table-4.1). We have also plotted the beam mode using Eq. (4.19) for Cesium ions of energy E_b=10eV. The frequencies and the corresponding wave numbers of the unstable waves are obtained by the point of intersections between the beam mode and plasma modes and are given as Table-4.2. From Table 4.2, we can say that the unstable wave frequencies of the KHI increases with increase in the relative density of negatively charged dust grains δ. It can also be seen from the Table-4.2 that the axial wave vector k_z increases with increasing δ. This result is found to match the analytical results of Chow and

Rosenberg [36], where the an increase in k_z with increasing δ makes the wave unstable.

Table-4.1 The plasma parameters used in the present model.

Parameters	Value
Ion plasma density n_{i0}	5x 10^9 cm^{-3}
Relative density of negatively charged dust grains $\delta = n_{i0}/n_{e0}$	1 - 6
Electron Temperature T_e	0.2 eV
Ion Temperature T_i	0.2 eV
Plasma radius a_1	3 cm
Beam radius r_0	3 cm
Dust grain size a	0.4 x10^{-4} cm
Static magnetic field B_z	3x10^3 Gauss
Inverse density gradient length λ	2 cm^{-1}
Ion Beam energy E_b	10 eV
Ion beam density n_{b0}	2.5x10^8 cm^{-3}
Perpendicular wave number k_y	1.0 cm^{-1}
Parallel wave number k_z	0.0 - 2.0 cm^{-1}
Shear parameter μ	0.6-2.0

Using Eq. (4.21), we have plotted the normalized real part of the wave frequency as a function of relative density of negatively charged dust grains δ in presence as well as in absence of beam [cf. Figs. 4.3 (a) & (b)] (without and with dust charge fluctuations). From Figs. 4.3 (a) & (b), we can say that the wave frequencies for KHI slightly increases with an increase in the relative density of negatively charged dust grains δ in presence of beam for both the cases, without and with dust charge fluctuations. It has been studied that the presence of dust charge fluctuations stabilizes the K-H instability [20] with relative density of negatively charged dust grains δ. It is observed that the effect of beam is more prominently seen on the growth rate in the absence of dust charge fluctuations.

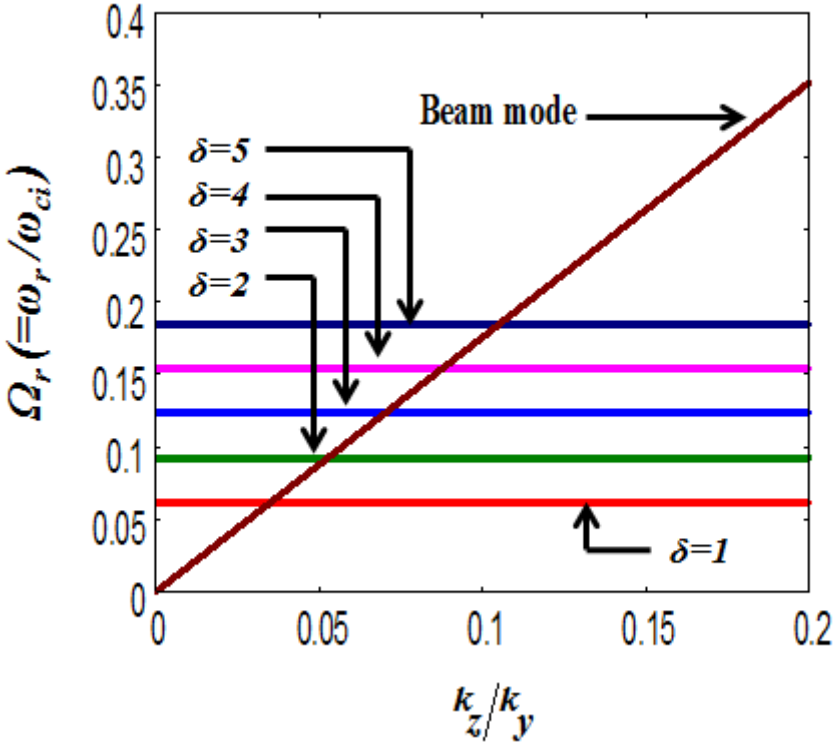

Fig. 4.2 Normalized real frequency $\Omega_r\left(=\omega_r/\omega_{ci}\right)$ of the KHI for different values of relative density of negatively charged dust grains $\delta(=1-5)$ as a function of normalized wave vector k_z/k_y [in the absence of dust charge fluctuations].The parameters are given in the text.

Table-4.2 The unstable wave frequencies ω_r (rad/s), normalized wave vector k_z/k_y, axial wave vectors k_z (cm^{-1}) and wavelength λ_z (cm) for different values of δ obtained from Fig. 4.2.

δ	k_z/k_y	k_z (cm^{-1})	λ_z(cm)	ω_r(rad/s) x10^4
1.0	0.035598	0.035598	17.641	1.29166
2.0	0.052628	0.052628	11.933	1.93696
3.0	0.070118	0.070118	8.956	2.58174
4.0	0.087833	0.087833	7.150	3.26556
5.0	0.105098	0.105098	5.975	3.89080

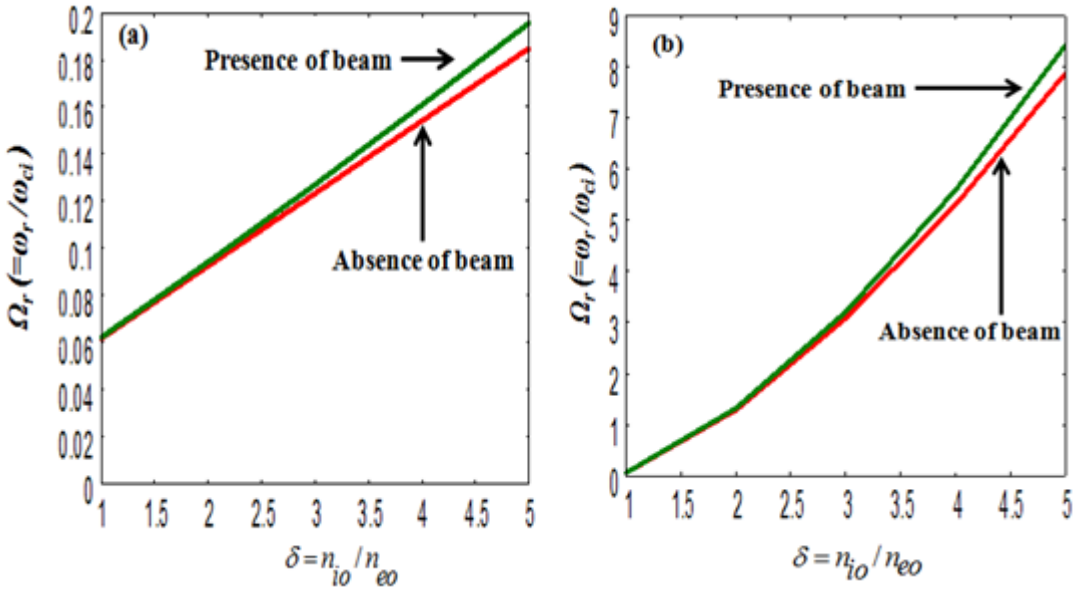

Fig. 4.3 Normalized real frequency $\Omega_r \left(=\omega_r/\omega_{ci}\right)$ of the KHI as a function of the relative density of negatively charged dust grains $\delta\left(=n_{io}/n_{eo}\right)$ **[a]**-without dust charge fluctuations **[b]**-with dust charge fluctuations in the absence and in the presence of beam for the same parameter as used in Fig. 4.2 except $k_y = 1.0\,\text{cm}^{-1}$ & $k_z = 0.2\,\text{cm}^{-1}$.

Hence, to see the significant effect of beam, we have plotted the normalized growth rate $\Gamma\left(=\omega_i/\omega_{ci}\right)$ with $\delta(=1-6)$ for different shear parameters in the absence of dust charge fluctuations and in presence as well as in absence of beam (cf. Fig 4.4) using the same parameters as given above and Eq. (4.22). From Fig. 4.4 we observe that the KHI is stabilized for low shear parameters while high value of shear parameters show the destabilizing effect at large values of δ (cf. Fig. 4.4). This result is in line with the experimental observations of Luo *et al.* [22].

It is observed that the growth rate of the KHI is more affected by beam at large values of shear parameters for large values of δ in the absence of dust charge fluctuations. We have chosen the dust grain size a such that $a << \rho_L$ [where $\rho_L = \left(v_{te}/\omega_{ce}\right)$ is the electron Larmor radius, v_{te} is the electron thermal velocity, and ω_{ce} is the electron cyclotron frequency] and $a << \lambda_{De}$ (where

$\lambda_{De}\left[=\left(T_e/4\pi n_{e0}e^2\right)^{1/2}\right]$ is the electron Debye length), for applicability of OML theory [32] are satisfied.

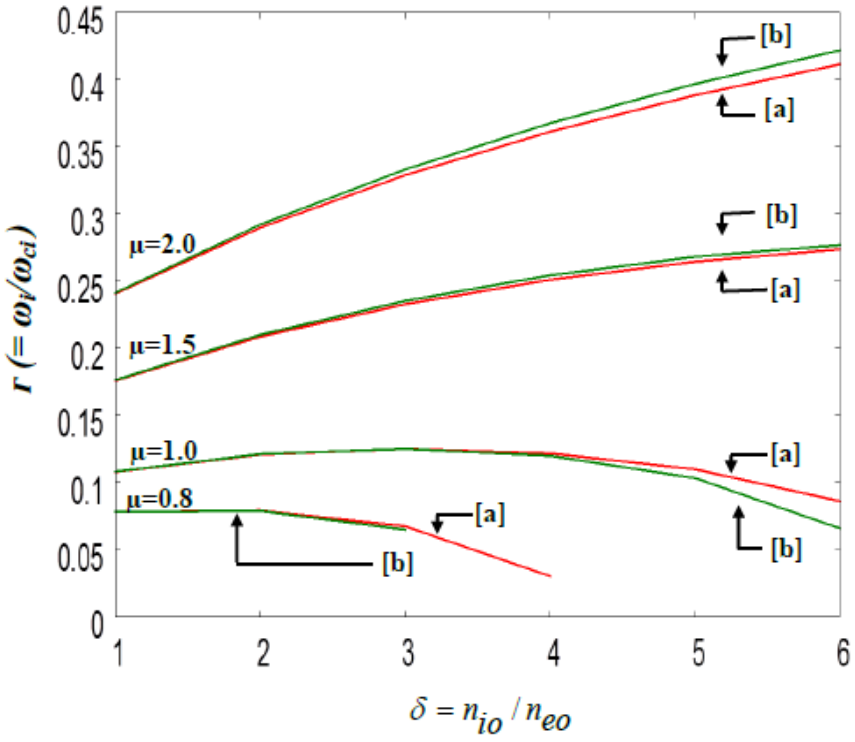

Fig. 4.4 Normalized growth rate $\Gamma\left(=\omega_i/\omega_{ci}\right)$ of the KHI as a function of the relative density of negatively charged dust grains $\delta\left(=n_{io}/n_{eo}\right)$ (without dust charge fluctuations) **[a]**-in the absence of beam **[b]**-in the presence of beam for the same parameters as Fig. 4.3, at different values of shear parameters $\mu = 0.8,\ 1.0,\ 1.5,\ 2.0$ and $\delta = 1-6$.

We can say that the Kelvin Helmholtz instability in a magnetized dusty plasma can be driven by an ion beam via a Cerenkov interaction. The effect of beam on the growth of Kelvin Helmholtz instability can be prominently seen in the absence of dust charge fluctuations. Our theoretical results are in good agreement with the experimental observations of Luo *et al.* [22].

4.3 NON-LOCAL ANALYSIS

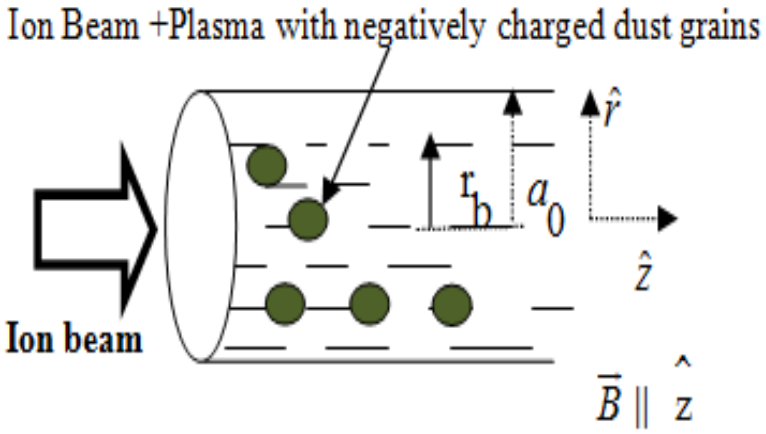

Fig. 4.5 Schematic of ion beam propagating in cylindrical plasma containing negatively charged dust grains

A multispecies collisionless magnetized plasma cylinder of radius a_0 consisting of electrons, ions and dust particles is studied as shown in Fig. 4.5, where magnetic field $\vec{B} \parallel \hat{z}$ and equilibrium densities varies radially as $n_0 = \overline{N} e^{-\lambda r}$, where $\overline{N}$(= constant) and λ is the inverse e-folding length [22]. Equilibrium densities of electron, ions and dust are given as n_{e0}, n_{i0} and n_{d0} and their charge, mass, temperatures are denoted by $\left(-e,\ m_e,\ T_e\right)$, $\left(e,\ m_i,\ T_i\right)$ and $\left(q_{d0},\ m_d,\ T_d\right)$, respectively. The particles flow along the magnetic field B with velocity v_{z0} that depends on the radial coordinates and the equilibrium velocity vectors being given by $v_0 = (0, v_{\phi 0}, v_{z0}(r))$ with constant $v_{\phi 0}$. The radial electric field which could excite transverse KHI due to shear in the perpendicular $\left(\vec{E} \times \vec{B}\right)$ velocity is kept constant and negligible to observe parallel shear effects [19]. An ion beam with mass m_b, homogenous density n_{b0}, radius $r_b < a_0$ and velocity $v_{b0} \parallel \hat{z}$, propagates along the direction of magnetic field through plasma cylinder (cf. Fig. 4.5).

Applying quasi-neutrality $en_{e0} - en_{i0} - en_{b0} + q_{d0}n_{d0} \approx 0$, and electrostatic perturbation $\phi_1 = \phi_1(r)e^{-i(\omega t - \vec{k}.\vec{r})}$, the response of plasma electrons to the perturbation may be derived from the momentum conservation Eq. (4.2).

On linearization Eq. (4.2) yields the transverse and parallel perturbed velocity components for electrons, i.e.,

$$\vec{v}_{\perp 1} = \frac{e}{m_e\left(\omega_1^2 - \omega_{ce}^2\right)}\left(i\omega_1\nabla_\perp\phi_1 + \nabla_\perp\phi_1 \times \vec{\omega}_{ce}\right) + \frac{T_e}{m_e\left(\omega_1^2 - \omega_{ce}^2\right)}\left(i\omega_1\nabla_\perp\frac{n_{e1}}{n_{e0}} + \nabla_\perp\frac{n_{e1}}{n_{e0}} \times \vec{\omega}_{ce}\right), \tag{4.23}$$

and

$$v_{z1} = -\frac{ek_z\phi_1}{m_e} + \frac{T_e}{m_e}\frac{n_{e1}}{n_{e0}}\frac{k_z}{\omega_1} + \frac{1}{i\omega_1}v_{1r}\frac{\partial v_{z0}}{\partial r}, \tag{4.24}$$

where $\omega_{ce}\left(= eB_S / m_e c\right)$ is the electron cyclotron frequency, v_{z0} is the equilibrium velocity along the direction of magnetic field and $\omega_1 = (\omega - \vec{k}\cdot\overrightarrow{v_0})$.

The perturbed electron density is obtained by substituting the perturbed velocities from Eqs. (4.23) & (4.24) in the mass conservation equation, in the short parallel wavelength limit $\omega \ll k_\perp v_{te}$ same as Eq. (4.6). For the case of a strongly magnetized plasma as discussed in the local analysis sec. 4.2, we obtain perturbed ion density as

$$n_{i1} = \frac{n_{i0}e\phi_1}{m_i}\frac{\left(\frac{\nabla_\perp^2}{\omega_{ci}^2} + \frac{k_z^2}{\omega_1^2} + \frac{\lambda k_\perp}{\omega_1\omega_{ci}} - \frac{k_\perp k_z}{\omega_1^2}\frac{1}{\omega_{ci}}\frac{\partial v_{z0}}{\partial x}\right)}{\left(1 - \frac{k_z^2 v_{ti}^2}{\omega_1^2} - \frac{\lambda k_\perp v_{ti}^2}{\omega_1\omega_{ci}} + \frac{k_\perp k_z v_{ti}^2}{\omega_1^2}\frac{1}{\omega_{ci}}\frac{\partial v_{z0}}{\partial x}\right)}. \tag{4.25}$$

Similarly the dust density perturbations are given by

$$n_{d1} = \frac{q_{d0}n_{d0}}{m_d}\frac{\nabla_\perp^2\phi_1}{\omega_1^2}. \tag{4.26}$$

Here dust is treated as unmagnetized i.e., $\omega \sim \omega_{ci} >> \omega_{cd}$.

From probe theory (as discussed in previous sec. (4.2)) applied to a dust grain [31]-[34], and Eqs. (4.6) and (4.25) we obtain perturbed dust charge as

$$q_{d1}=\frac{e\left|I_{e0}\right|}{i(\omega+i\eta)}\left[\frac{\left(\frac{\nabla_{\perp}^{2}\phi_1}{m_i\omega_{ci}^{2}}+\frac{k_z^{2}\phi_1}{m_i\omega_1^{2}}+\frac{\lambda k_{\perp}\phi_1}{\omega_1\omega_{ci}}-\frac{k_{\perp}k_z\phi_1}{\omega_1^{2}}\frac{1}{\omega_{ci}}\frac{\partial v_{z0}}{\partial x}\right)}{\left(1-\frac{k_z^{2}v_{ti}^{2}}{\omega_1^{2}}-\frac{\lambda k_{\perp}v_{ti}^{2}}{\omega_1\omega_{ci}}+\frac{k_{\perp}k_z v_{ti}^{2}}{\omega_1^{2}}\frac{1}{\omega_{ci}}\frac{\partial v_{z0}}{\partial x}\right)}-\frac{\phi_1}{T_e}\right], \quad (4.27)$$

where η is the dust charging rate as discussed in previous sec. 4.2.

Following the analysis of Sharma and Srivastava [35], the ion beam density perturbations in a cylindrical geometry is given by

$$n_{b1}=\frac{n_{b0}e\left(k_{\perp}^{2}+k_z^{2}\right)\phi_1}{m_b(\omega_1-k_z v_{b0})^{2}}. \quad (4.28)$$

Using perturbed densities of electrons, ions, dust grains and ion beam in the Poisson equation $\nabla^{2}\phi_1=4\pi(n_{e1}e-n_{i1}e-n_{b1}e+n_{d0}q_{d1}+q_{d0}n_{d1})$, and simplifying the above equation for axially and azimuthally symmetric case, we get

$$\frac{\partial^{2}\phi_1}{\partial r^{2}}+\frac{1}{r}\frac{\partial\phi_1}{\partial r}+A^{2}\phi_1=-\frac{\omega_{pb}^{2}\left(k_{\perp}^{2}+k_z^{2}\right)\phi_1}{(\omega-k_z v_{b0})^{2}}, \quad (4.29)$$

where

$$A^{2}=-k_z^{2}-\frac{\omega_{pe}^{2}}{v_{te}^{2}}+\left[\frac{\left(\frac{\omega_{pi}^{2}}{\omega_{ci}^{2}}k_{\perp}^{2}+\frac{\omega_{pi}^{2}}{\omega_1^{2}}k_z^{2}+\frac{\omega_{pi}^{2}}{\omega_1\omega_{ci}}\lambda k_{\perp}-k_{\perp}k_z\frac{\omega_{pi}^{2}}{\omega_{ci}^{2}}\frac{1}{\omega_{ci}}\frac{\partial v_{z0}}{\partial r}\right)}{\left(1-\frac{\lambda k_{\perp}}{\omega_1\omega_{ci}}v_{ti}^{2}+\frac{k_{\perp}k_z}{\omega_1^{2}}\frac{1}{\omega_{ci}}\frac{\partial v_{z0}}{\partial r}v_{ti}^{2}-\frac{k_z^{2}v_{ti}^{2}}{\omega_1^{2}}\right)}\right]$$

$$+\frac{i\beta}{(\omega+i\eta)}\left[\frac{\left(\frac{\omega_{pi}^{2}}{\omega_{ci}^{2}}k_{\perp}^{2}+\frac{\omega_{pi}^{2}}{\omega_1^{2}}k_z^{2}+\frac{\omega_{pi}^{2}}{\omega_1\omega_{ci}}\lambda k_{\perp}-k_{\perp}k_z\frac{1}{\omega_{ci}}\frac{\partial v_{z0}}{\partial r}\frac{\omega_{pi}^{2}}{\omega_{ci}^{2}}\right)}{\left(1-\frac{\lambda k_{\perp}}{\omega_1\omega_{ci}}v_{ti}^{2}+\frac{k_{\perp}k_z}{\omega_1^{2}}\frac{1}{\omega_{ci}}\frac{\partial v_{z0}}{\partial r}v_{ti}^{2}-\frac{k_z^{2}v_{ti}^{2}}{\omega_1^{2}}\right)}-\frac{\omega_{pi}^{2}}{c_s^{2}\delta}\right]. \quad (4.30)$$

Here, ω_{pb}, ω_{pi}, and v_{te} are the ion beam, ion plasma frequencies and electron thermal velocity, respectively, $\beta = \frac{|I_{e0}|}{e}\left(\frac{n_{d0}}{n_{e0}}\right)$ and $\delta = \frac{n_{i0}}{n_{e0}}$.

If $n_{b0} \to 0$, i.e., $\omega_{pb} = 0$ (ion beam is absent), the solution of Bessel equation is given by:

$$\phi_1 = UJ_0(p_m r), \tag{4.31}$$

where U is a constant and the function, $J_o\left(p_m r\right)$ is called the zero-order Bessel functions of argument $\left(p_m r\right)$. At r = a_0, ϕ_1 must vanish, hence, $J_o(p_m a_0) = 0$, i.e., $p_m = \frac{x_m}{a_0}$ $(m = 1, 2, ...)$, where x_m are the zeros of the Bessel function $J_o(x)$.

The finite cylindrical boundaries lead to the effective wave number which is given by $k^2 = \left(\frac{x_m}{a_0}\right)^2 + k_z^2$, and $k_\perp{}^2 \cong p_m^2 = \left(\frac{x_m}{a_0}\right)^2$.

On the surface of cylindrical wave guide, $J_o(x) = 0$ then $x = 2.404$, and hence the effective radial wave number $p_m = 2.404/a_0$ is quantized. In the presence of beam, the solution of the wave function ϕ_1 can be given by a set of orthogonal wave functions:

$$\phi_1 = \Sigma_m A_m J_o\left(p_n r\right) \tag{4.32}$$

Using ϕ_1 in Eq. (4.29) and simplifying the Bessel equation (as discussed in previous chapter 2), we obtain

$$1 - \frac{\omega_{pb}{}^2 c_s^2 \delta\left(p_m^2 + k_z^2\right)}{\omega_{pi}^2\left(\omega_1 - k_z v_{b0}\right)^2} I - \frac{k_z{}^2}{\omega_1{}^2}\alpha_1^2 - \frac{\lambda p_m}{\omega_1 \omega_{ci}}\alpha_1^2 + \frac{p_m k_z}{\omega_1{}^2}\frac{1}{\omega_{ci}}\frac{\partial v_{z0}}{\partial r}\alpha_1^2$$

$$- \frac{i\beta}{(\omega + i\eta)}\left(\frac{k_z{}^2 c_s^2}{\omega_1{}^2} + \frac{\lambda p_m c_s^2}{\omega_1 \omega_{ci}} - \frac{p_m k_z c_s^2}{\omega_1{}^2}\frac{1}{\omega_{ci}}\frac{\partial v_{z0}}{\partial r}\right) = 0, \tag{4.33}$$

where $\alpha_1^2 = v_{ti}^2 + c_s^2\delta - \frac{\omega_{pb}^2}{\omega_{pi}^2}\frac{c_s^2 v_{ti}^2 \delta\left(p_m^2 + k_z^2\right)}{\left(\omega_1 - k_z v_{b0}\right)^2} I$ and $I = \frac{\int_0^{r_b} rJ_o(p_m r)J_o(p_n r)dr}{\int_0^{a_0} rJ_o(p_m r)J_o(p_n r)dr}$.

Equation (4.33) can be further rewritten as

$$\left(\omega_1^2 - \frac{\lambda k_\perp \alpha_2^2}{\omega_{ci}}\omega_1 - k_z{}^2\alpha_2^2 + \frac{k_y k_z}{\omega_{ci}}\frac{\partial v_{z0}}{\partial r}\alpha_2^2\right)\left(\omega_1 - k_z v_{b0}\right)^2 = \frac{\omega_{pb}{}^2 c_s^2 \delta\left(p_m^2 + k_z^2\right)\omega_1^2}{\omega_{pi}^2} I. \tag{4.34}$$

Here, $\alpha_2^2 = \alpha_1^2 + \frac{i\beta}{\omega + i\eta}c_s^2$.

When the beam is in Cerenkov resonance with the KHI mode, the two factors on the left-hand side of Eq. (4.34) are simultaneously zero in the absence of beam density i.e., $n_{b0} \to 0$, which yields the KHI mode and the beam mode as

$$\omega_1^2 - \frac{\lambda k_\perp \alpha_2^2}{\omega_{ci}}\omega_1 - k_z{}^2\alpha_2^2 + \frac{k_\perp k_z}{\omega_{ci}}\frac{\partial v_{z0}}{\partial r}\alpha_2^2 = 0, \tag{4.35}$$

and

$$\omega_1 \cong k_z v_{b0}, \tag{4.36}$$

respectively.

On solving equation (4.34) the dispersion relation for ion beam driven Kelvin Helmholtz instability in a plasma cylinder is obtained as

$$\Omega^2 - \frac{\beta_1 \Lambda}{q^0}\Omega - \frac{\gamma\left(\gamma - \beta_1 \mu_0\right)}{q^0} = 0, \tag{4.37}$$

Here, $\Omega = \omega_1/\omega_{ci}$, $\beta_1 = p_m \rho_i$, $\rho_i^2 = \frac{\alpha_2^2}{\omega_{ci}^2}$, $\Lambda = \lambda\rho_i$, $\gamma = k_z\rho_i$,

$q^0 = \left(1 - \frac{\omega_{pb}{}^2 c_s^2 \delta\left(p_m^2 + k_z^2\right)}{\omega_{pi}^2\left(\omega_1 - k_z v_{b0}\right)^2} I\right)$, and $\mu_0\left(= \frac{1}{\omega_{ci}}\frac{\partial v_{z0}}{\partial r}\right)$ is the shear parameter.

We also assume that $\beta_1^2 \le 1$ (i.e., $p_m^2\rho_i^2 \le 1$) and $\gamma^2 \le 1$ (i.e., $k_z^2\rho_i^2 \le 1$) i.e., ion

Larmor radius is smaller than the perpendicular wavelength and the parallel wavelength.

Let us write $\omega_1 = \omega_{1r} + i\omega_{1i}$ and assume that the wave is either weakly damped or growing (i.e., $\left|\omega_{1i}\right| << \omega_{1r}$). In the absence of beam (i.e., $\omega_{pb} \to 0$, q^0=1) and dust charge fluctuations (i.e., $\eta \to \infty$) for infinite geometry of plasma, the dispersion relations of Luo *et al.* [22] (cf. Eq.1) and D'Angelo & Song [17] (cf. Eq. 23) can be obtained.

From dispersion relation, Eq. (4.37) the maximized normalized growth rate $\Gamma\left(=\omega_{1i}/\omega_{ci}\right)$ can be found as

$$\Gamma = \left[\frac{1}{4}\beta_1^2\left(\frac{\mu_0^2}{q^0} - \frac{\Lambda^2}{\left(q^0\right)^2}\right)\right]^{1/2}. \qquad (4.38)$$

In the absence of beam and dust charge fluctuations for infinite geometry, Eq. (4.38) reduces to the expression for growth rate as given by Luo *et al.* [22] (cf. Eq. 2).

4.3.1 Results and Discussion (Non-Local Model)

To study the ion beam driven KHI for radially bounded systems, we have used the same plasma parameters as are used previously for local model (see Table-4.1) except the effective perpendicular wave number $k_\perp \approx p_m = 2.404/a_0 = 0.8\,\text{cm}^{-1}$ and the beam radius $r_b = 2$ cm i.e., less than the plasma radius a_0=3 cm.

The Radial Plasma density and potential profiles are plotted in Figs. 4.6 (a) & (b) which shows that the density as well as potential of the plasma decreases radially. The frequencies and the corresponding wave numbers of the KHI and beam modes are plotted using Eqs. (4.35 & 4.36) as shown in Fig. 4.7. The unstable wave frequencies and wave numbers are obtained by the point of intersections between the beam and plasma modes and are given in Table-4.3. From Table 4.3, we can say that the frequencies and axial wave vectors of KHI modes increase with the relative density of dust grains δ . This result is similar to the analytical results of Chow and Rosenberg

[36], where the wave becomes unstable because the axial wave vector k_z increases with relative density of dust grains δ. We have computed growth rate in presence of beam which is radially confined with the beam radius r_b = 2 cm < plasma radius a_0=3 cm.

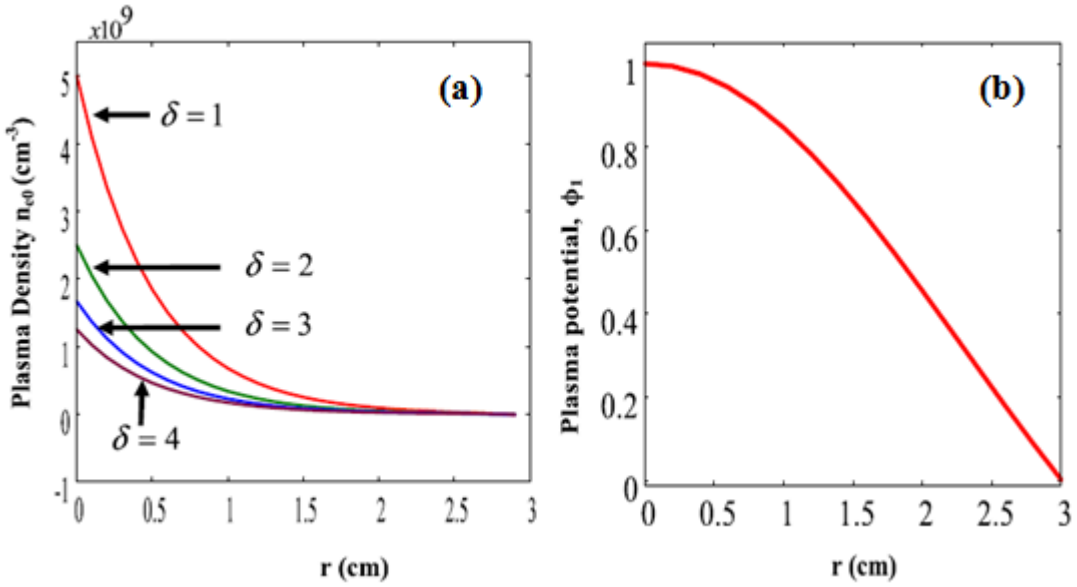

Fig. 4.6 (a) Radial profile of Plasma density at different relative densities of negatively charged dust grains, δ **(b)** Radial Plasma potential profile.

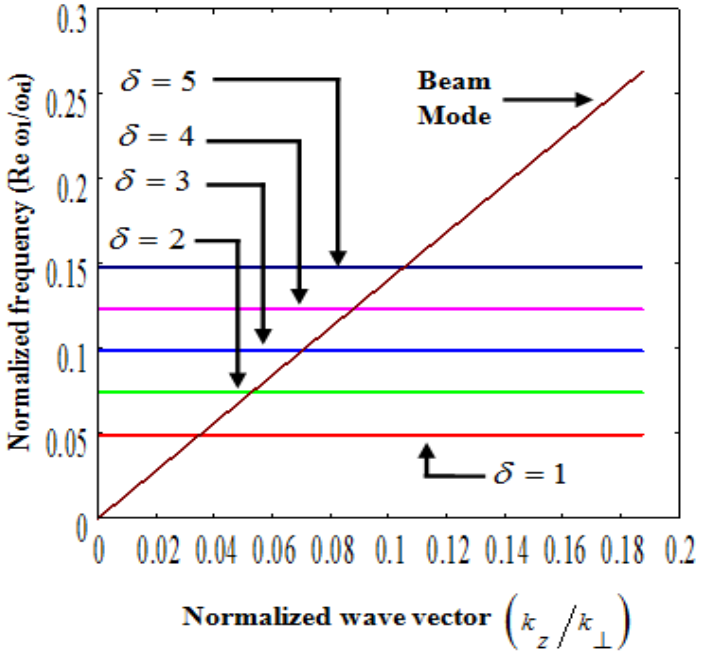

Fig. 4.7 Normalized real frequency $\Omega_r\left(=\omega_{1r}/\omega_{ci}\right)$ of the KHI as a function of normalized wave vector $\left(k_z/k_\perp\right)$ for different relative density of negatively charged dust grains $\delta\left(=1-5\right)$ and the beam mode.

Table-4.3 Unstable wave frequencies ω_{1r} (rad/s), normalized wave vectors $k_z/k_\perp$, axial wave vectors k_z (cm^{-1}) and wavelengths λ_z (cm) at different values of δ, for the cylindrical plasma waveguide.

δ	$k_z/k_\perp$	k_z (cm^{-1})	λ_z (cm)	ω_{1r} (rad/s) x10^4
1.0	0.0349	0.0279	224.91	1.7273
2.0	0.0531	0.0425	147.86	2.6015
3.0	0.0706	0.0565	111.23	3.4514
4.0	0.0876	0.0701	89.60	4.3019
5.0	0.1051	0.0841	74.69	5.1275

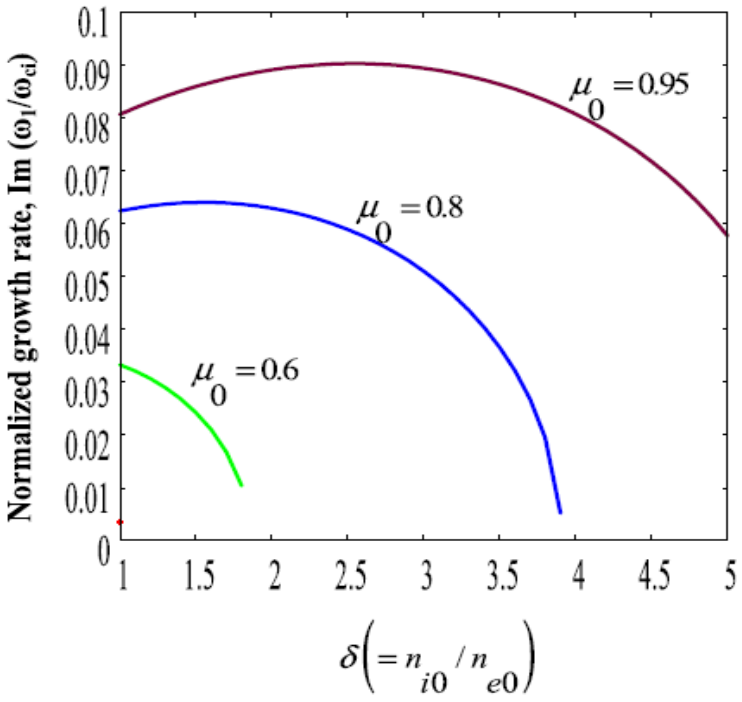

Fig. 4.8 Normalized growth rate $\Gamma\left(=\omega_{1i}/\omega_{ci}\right)$ of the KHI as a function of relative density of negatively charged dust grains $\delta\left(=n_{i0}/n_{e0}\right)$ for shear parameters $\mu_0 = 0.6, 0.8$ and 0.95.

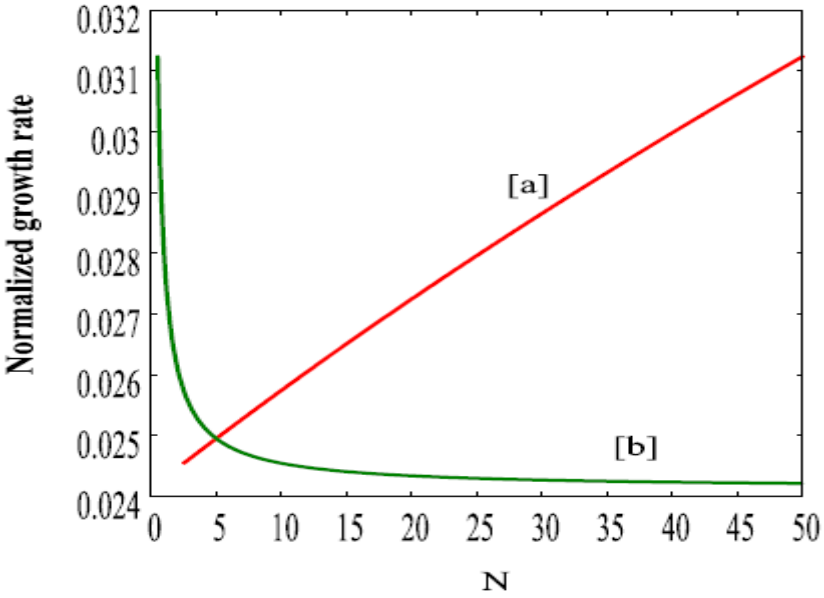

Fig. 4.9 Normalized growth rate $\Gamma\left(=\omega_{1i}/\omega_{ci}\right)$ of the KHI as a function of N, where N stands for case **[a]** - ion beam density $n_{b0}\times10^{7}$ (cm^{-3}) and in case **[b]** - beam energy, $N\times10$ eV, for relative density of negatively charged dust grains $\delta\left(=4.0\right)$ and shear parameter $\mu_0=0.8$.

The growth rate has been plotted using Eq. (4.38) in Fig. 4.8 which shows an increase with increasing shear parameter in the presence of beam and stabilized with increase in relative density of negatively charged dust grains δ . However, the growth rate of KHI is stabilized for low shear parameters as was observed by Luo *et al* [22] and D'Angelo and Song [17]. An increase of ion beam density from 0.5-5.0 x 10^8 cm^{-3} destabilizes the KHI modes {cf. Fig. 4.9 (a)} and beyond the beam density 5.0 x 10^8 cm^{-3} growth rate of KHI is declined. Moreover, in Fig. 4.9 (b), we have plotted the growth rate of KHI with beam energy that varies from 1-500eV. It is investigated that an increase in beam energy suppresses the instability. These results are in good agreement with the results given by Prabhuram et al [29] that sufficiently high frequency of pump power suppresses the drift waves in an ion beam plasma systems due to enhanced Landau damping of electrons.

In Fig. 4.10 & 4.11, we compared frequency and growth rate of ion beam driven KHI modes for finite and infinite boundary plasma (in absence of dust charge

fluctuations) and found that the growth rate is reduced for bounded plasmas, which may be due to reduction in interaction region of the waveguide.

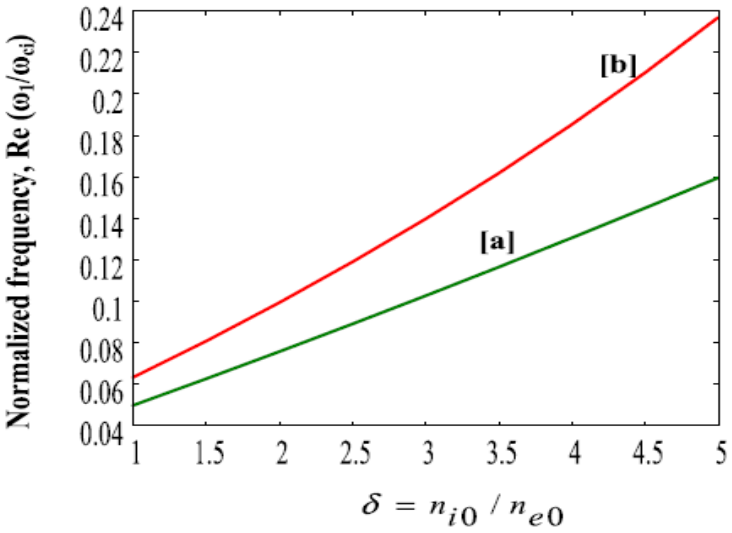

Fig. 4.10 Normalized frequency $\Omega_r \left(= \omega_{1r} / \omega_{ci}\right)$ of the KHI vs. the relative density of negatively charged dust grains $\delta\left(= n_{i0} / n_{e0}\right)$ in presence of beam [a]- for cylindrical waveguide [b]- for infinite geometry plasma waveguide for the shear parameter = 0.7.

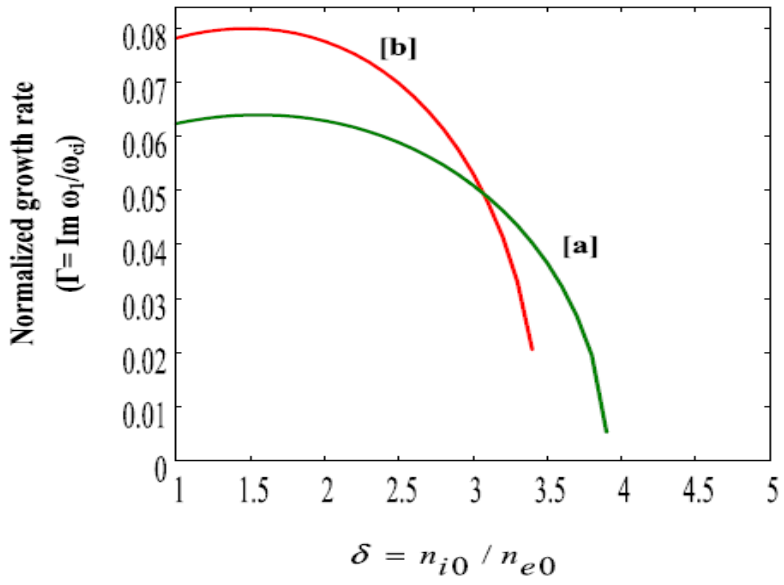

Fig. 4.11 Normalized growth rate $\Gamma\left(= \omega_{1i} / \omega_{ci}\right)$ of the KHI vs. the relative density of negatively charged dust grains $\delta\left(= n_{i0} / n_{e0}\right)$ in presence of beam [a]- for cylindrical waveguide [b]- for infinite geometry plasma waveguide for the shear parameter = 0.7.

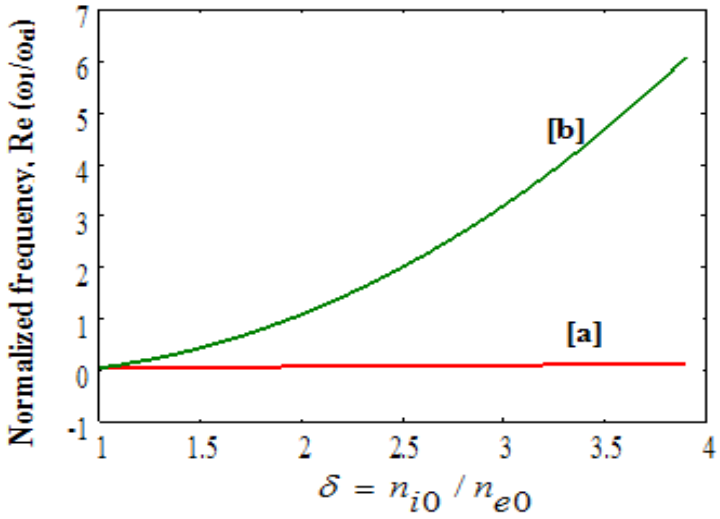

Fig. 4.12 Normalized frequency $\Omega_r \left(=\omega_{1r}/\omega_{ci}\right)$ of the KHI vs. the relative density of negatively charged dust grains $\delta\left(=n_{i0}/n_{e0}\right)$ in presence of beam for cylindrical waveguide **[a]** – in the absence of dust charge fluctuations **[b]** - in the presence of dust charge fluctuations for shear parameter $\mu_0 = 0.95$.

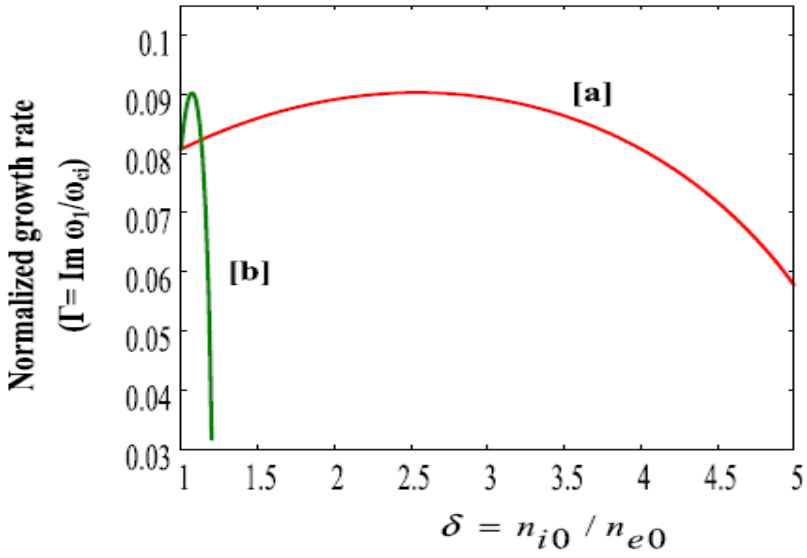

Fig. 4.13 Normalized growth rate $\Gamma\left(=\omega_{1i}/\omega_{ci}\right)$ of the KHI vs. the relative density of negatively charged dust grains $\delta\left(=n_{i0}/n_{e0}\right)$ in presence of beam for cylindrical waveguide **[a]** – in the absence of dust charge fluctuations **[b]** - in the presence of dust charge fluctuations for shear parameter $\mu_0 = 0.95$.

In Figs. 4.12 & 4.13, we have plotted frequency and the growth rate of KHI in the absence and presence of dust charge fluctuations for finite geometry cylindrical waveguide. We observed that the frequency of KHI significantly increases with relative density of dust grains in presence of dust charge fluctuations but the growth rate (amplitude) of KHI modes is stabilized with increase in relative density of dust grains δ. These results are in fine agreement with theoretical predictions of Singh et al. [20] which indicated that the presence of dust charge fluctuations yields a purely damped mode. Although, it is observed that the destabilizing effect of dust charge fluctuations on the KHI modes can be seen only for cylindrical plasma waveguide at large shear parameters i.e., above $\mu_0 = 0.9$ for relatively small density of dust grains. However, it is noticed that the effect of beam can be prominently seen on the growth rate of KHI only in the absence of dust charge fluctuations.

4.4 CONCLUSION

In conclusion we can say that an ion beam drives KHI via Cerenkov interaction in magnetized dusty unbounded and bounded cylindrical plasma. The frequency of ion beam driven KH Instability is increased with relative density of negatively charged dust grains δ. The KHI modes are destabilized at large shear parameters and stabilized with increase in relative density of negatively charged dust grains δ. Our theoretical results are well in agreement with the experimental results given by Luo *et al*. [22] and D'Angelo & Song [17].

It is observed that the ion beam energy and density play an important role in modifying the growth rate of KHI modes in the bounded plasmas. The prominent effect of dust charge fluctuations on the growth rate can be noticed for finite geometry of plasma. Moreover, for unbounded plasmas, the effect of beam on the growth rate of KHI mode can be prominently observed in the absence of dust charge fluctuations. The effect of radial boundaries is to provide a minimum effective wave number $k_\perp$ which in turn modifies the dispersion properties of KHI modes. Our results may be useful for the study of instabilities in laboratory plasmas and beam plasma systems.

REFERENCES

[1]. A. I. Ershkovich, "Kelvin–Helmholtz instability in type–1 comet tails and associated phenomena," *Space Sci. Rev.* **25**, No. 1, pp. 3–34, 1980.

[2]. S. I. Akasofu, *Space Sci. Rev.* **28**, 121 (1981).

[3]. Z. Y. Pu and M. G. Kivelson, *J. Geophys. Res.* **88**, 841 (1983).

[4]. M. G. Kivelson and Z. Y. Pu, *Planet Space Sci.* **32**, 1335 (1984).

[5]. A. Miura, *Geophys. Res. Lett.* **17**, 749 (1990).

[6]. A. Miura, *J. Geophys. Res.* **97**, 10655 (1992).

[7]. P. H.M. Galopeau, P. Zarka, and D. Le Queau, *J. Geophys. Res.* **100**, 26397 (1995).

[8]. T. Penz, N. V. Erakaev, H. K. Biernet, H. Lammer, U.V. Amerstorfer, H. Gunell, E. Kallio, S. Barabash, S. Orsini, A. Milillo, and W. Baumjohann, *Planet. Space Sci.* **52**, 1157 (2004).

[9]. M. F. El-Sayed and D. F. Hussein, *Prog. Appl. Math.* **3**, 1 (2012).

[10]. R. Keppens , G. T ´Oth , R. H. J. Westermann, and J.P. Goedbloed, *J. Plasma Phys.* **61**, 1 (1999).

[11]. H. Hasegawa, M. Fujimoto, T. D. Phan, H. Re `me, A. Balogh, M. W. Dunlop, C. Hashimoto, and R. T. Dokoro, *Nature* **430**, 755 (2004).

[12]. K. Nykyri, A. Otto, B. Lavraud, C. Mouikis, L. M. Kistler, A. Balogh and H. R`eme, *Ann. Geophys.* **24**, 2619 (2006).

[13]. G.V. Miloshevsky and A. Hassanein, *Nucl. Fusion* **50**, 115005 (2010).

[14]. S. Chandrasekhar, "*Hydrodynamic and Hydromagnetic Stability*", Oxford University Press, Oxford (1961), Chap. XI.

[15]. N. D'Angelo, *Phys. Fluids* **8**, 1748 (1966).

[16]. N. D'Angelo and S. Von Goeler, *Phys. Fluids* **9**, 309 (1966).

[17]. N. D' Angelo and B. Song, *Planet. Space Sci.* **38**, 1577 (1990).

[18]. N. D' Angelo and B. Song, *IEEE trans. Plasma Sci.* **19**, 42 (1991).

[19]. T. An, R. L. Merlino, and N. D'Angelo, *Phys. Lett. A* **14**, 47 (1996).

[20]. S.V. Singh, N.N. Rao and R. Bharuthram, *Phys. Plasmas* **5**, 7 (1998).

[21]. N. N. Rao, *Phys. Plasmas* **6**, 6 (1999).

[22]. Q. Z. Luo, N. D' Angelo and R. L. Merlino, *Phys. Plasmas* **8**, 31 (2001).

[23]. H. M. Wiechen, *Phys. Plasmas* **13**, 062104 (2006).

[24]. N. Kumar, V. Kumar and A. Kumar, *in Proceedings of 31st International Conference on Phenomenon in Ionized Gases*, Granada, Spain, 14 July 2013.

[25]. D. Bohm and E. P. Gross, *Phys. Review* **79**, 992 (1950).

[26]. P.K. Shukla and M. Rosenberg, *Phys. Plasmas* **6**, 1038 (1999).

[27]. S. Y. Udovichenko, *Tech. Phys.* **52**, 199 (2007).

[28]. S. Seiler, M. Yamada, and H. Ikezi, *Phys. Rev. Lett.* **37**, 700 (1976).

[29]. G. Praburam, H. Honda, and M. Sugawa, *J. Phys. Society* Japan **62**, 4262 (1993).

[30]. M. Sugawa, S. Iwamoto, T. Kondo, S. Utsunomiya, T. Maehara, and R. Sugaya, *in Proceedings of International Conference on Plasma Physics*, Nagoya, Japan, 1996.

[31]. E.C. Whipple, T.G. Northdrop and D.A. Mendis, *J. Geophys. Res.* **90**, 7405 (1985).

[32]. M. R. Jana, A. Sen and P. K. Kaw, *Phys. Rev. E* **48**, 3930 (1993).

[33]. R. K. Varma, P. K. Shukla and V. Krishan, *Phy. Rev. E* **47**, 3612 (1993).

[34]. M. S. Barnes, J. K. Keller, J. C. Forster, J. A.O'Neill and D. K.Coultas, *Phys. Rev. Lett.* **68**, 313 (1992).

[35]. S. C. Sharma and M. P. Srivastava, *Phys. Plasmas* **8,** 679 (2001).

[36]. V.W. Chow and M. Rosenberg, *Planet. Space Sci.* **43**, 613 (1995).

CHAPTER 5

Theoretical Modelling of an Ion Beam Driven Kelvin Helmholtz Instability in a Negative Ion Plasma

This chapter consists of theoretical model for an ion beam driven Kelvin Helmholtz instability (KHI) in a local and nonlocal cylindrical magnetized plasma containing two kind of ions-positive ions and negative ions. A comparison of mode frequency and the growth rate for both the positive ion and negative ion KHI modes have been done for finite and infinite geometries of the plasma. The chapter throws light on the effect of presence of beam and various parameters of beam on the growth rate of KHI for both the ion modes for both the geometries of plasmas. Moreover, the effect of relative mass of positive and negative ions has also been explicated.

5.1 INTRODUCTION

It has already been enlightened in chapter 4 that the study of KHI is of profound interest in various near Earth environmental and astrophysical situations [1] - [5]. Chandrasekhar [6] firstly described the KHI for heterogeneous fluids, later on, for the magnetized plasmas. It has been observed that a relative speed of the order of Alfven wave speed is sufficient to produce KHI in magnetized compressible fluids [7]. Later on, Q-machine experiments [8] confirmed these features. Moreover, the instability also gets stabilized under Landau damping [9]. Various authors have investigated theoretically or experimentally the destabilization of KHI in the presence of negative ions and negatively charged dust at low concentration of negative ions or negatively charged dust grains [10]-[13] and stabilization of KHI modes at a relatively large concentration of negative ions or negatively charged dust grains.

It has been observed that the presence of negative ions modify the dispersion properties of various ion wave modes [14]-[16]. Moreover, an ion beam propagating through the negative ion plasmas is found to have destabilizing effect on electrostatic ion cyclotron (EIC) waves and ion-acoustic waves [17]-[19]. The ion beams propagating through the ion beam plasma systems play a key role in the growth of waves & instabilities [20] - [21] in these systems. Various plasma instabilities with and without beam have been investigated in the negative ion plasmas.

Here, we attempt to investigate the effects of infinite and finite geometries on the dispersion properties of ion beam driven KHI modes in the negative ion plasma as the growth of waves and instabilities is found to be reduced for bounded plasmas [22]. Moreover, the negative ion plasmas are analogous to dusty plasmas (except the dust charge and size fluctuates) and have great significance in surface technologies such as plasma enhanced chemical vapor deposition (PECVD), ion implantation, microelectronic fabrication & etching, and creation of nano and macro particles [23]-[25] and Earth's ionosphere's instabilities [26].

5.2 ANALYTICAL MODEL

A multi-component collisionless plasma having electrons, positive ions K^+ (Potassium ions) and negative ions SF_6^- (Sulfur hexafluoride ions) having equilibrium densities of components as $n_{0j} = \overline{n_{0j}} e^{-\lambda x}$, where $j(=e,p,n)$ for electron, positive ion, and negative ions, respectively, $\overline{n_{0j}} (=\text{constant})$ and λ is the inverse e-folding length of the density gradient [13]. The static magnetic field B_0 is applied along positive z-direction. We choose SF_6^- negative ions as SF_6 has a large electron capture cross section for low-energy electrons [19].

The Equilibrium densities of electrons, positive ions and negative ions are represented as $n_{0e}\left(=(1-\varepsilon)n_0\right)$, $n_{0p} = n_0$, and $n_{0n} = \varepsilon n_0$, where n_0 is the plasma density and $\varepsilon\left(=n_{SF_6^-}\Big/ n_{K^+}\right)$ is the relative concentration of negative ions. The

equilibrium velocity of plasma constituents is given by $v_{0j} = (0,\ v_{0yj},\ v_{0zj}(x))$ with $v_{0yj}\,(=\text{constant})$. The charges, masses and temperatures of electrons, positive ions and negative ions are denoted by $(-e, m_e, T_e)$, (e, m_p, T_p) and $(-e, m_n, T_n)$, respectively. An ion beam of radius r_b, mass m_b, and density $n_{0b} \ll n_0,\ n_{0p}$ propagates through plasma with velocity $v_{0b} \parallel \hat{z}$ along the direction of magnetic field.

The system prior to perturbation is assumed to be quasi-neutral such that

$$en_{0e} - en_{0p} - en_{0b} + en_{0n} \approx 0 .$$

The electrostatic perturbation $\phi = \phi_0(r)e^{-i(\omega t - \vec{k}.\vec{r})}$ is applied to the potential, where the first order quantities vary as $e^{-i(\omega t - k_y y - k_z z)}$.

The electron, positive ion and negative ion perturbed densities obtained from

$$m_e \frac{d\vec{v}e}{dt} = -e\vec{E} - \frac{e}{c}\vec{v}e \times \overrightarrow{B_0} - \frac{\nabla(n_e T_e)}{n_e}. \tag{5.1}$$

and continuity equations are

$$n_{1e} = n_{0e}\frac{e\phi}{T_e}. \tag{5.2}$$

$$n_{1p} = \frac{n_{0p}e\phi}{m_p}\frac{\left(\frac{\nabla_\perp^2}{\left(\omega_{cp}^2-\Omega_p^2\right)}+\frac{k_z^2}{\Omega_p^2}+\frac{\lambda k_y\omega_{cp}}{\Omega_p\left(\omega_{cp}^2-\Omega_p^2\right)}-\frac{k_yk_z\omega_{cp}}{\Omega_p^2\left(\omega_{cp}^2-\Omega_p^2\right)}\frac{\partial v_{0zp}}{\partial x}\right)}{\left(1-\frac{\nabla_\perp^2 v_{tp}^2}{\left(\omega_{cp}^2-\Omega_p^2\right)}-\frac{k_z^2v_{tp}^2}{\Omega_p^2}-\frac{\lambda k_y v_{tp}^2\omega_{cp}}{\Omega_p\left(\omega_{cp}^2-\Omega_p^2\right)}+\frac{k_yk_zv_{tp}^2\omega_{cp}}{\Omega_p^2\left(\omega_{cp}^2-\Omega_p^2\right)}\frac{\partial v_{0zp}}{\partial x}\right)}. \tag{5.3}$$

and $n_{1n} = \frac{-n_{0n}e\phi}{m_n}\frac{\left(\frac{\nabla_\perp^2}{\left(\omega_{cn}^2-\Omega_n^2\right)}+\frac{k_z^2}{\Omega_n^2}-\frac{\lambda k_y\omega_{cn}}{\Omega_n\left(\omega_{cn}^2-\Omega_n^2\right)}+\frac{k_yk_z\omega_{cn}}{\Omega_n^2\left(\omega_{cn}^2-\Omega_n^2\right)}\frac{\partial v_{0zn}}{\partial x}\right)}{\left(1-\frac{\nabla_\perp^2 v_{tn}^2}{\left(\omega_{cn}^2-\Omega_n^2\right)}-\frac{k_z^2v_{tn}^2}{\Omega_n^2}+\frac{\lambda k_y v_{tn}^2\omega_{cn}}{\Omega_n\left(\omega_{cn}^2-\Omega_n^2\right)}-\frac{k_yk_zv_{tn}^2\omega_{cn}}{\Omega_n^2\left(\omega_{cn}^2-\Omega_n^2\right)}\frac{\partial v_{0zn}}{\partial x}\right)}$, (5.4)

where $v_{tp}\left[=\left(\frac{T_p}{m_p}\right)^{1/2}\right]$ is the positive ion thermal velocity, $v_{tn}\left[=\left(\frac{T_n}{m_n}\right)^{1/2}\right]$ is the thermal velocity of negative ions, $\omega_{cp}\left(=eB_0/m_pc\right)$ and $\omega_{cn}\left(=eB_0/m_nc\right)$ are the cyclotron frequencies of positive and negative ions, $\Omega_p\left[=\omega-k_yv_{0yp}-k_zv_{0zp}\right]$ and $\Omega_n\left[=\omega-k_yv_{0yn}-k_zv_{0zn}\right]$ are the shifted Doppler frequencies for positive and negative ions, respectively.

The density perturbations of the ion beam are given by [17]

$$n_{1b}=\frac{n_{0b}e(k_y^2+k_z^2)\phi}{m_b(\omega-k_zv_{0b})^2}, \tag{5.5}$$

where $\left(k_y^2+k_z^2\right)\approx k^2$.

5.2.1 Infinite Geometry Analysis

Using Eqs. (5.2) - (5.5) in the Poisson equation $\nabla^2\phi=4\pi(n_{1e}e-n_{1p}e-n_{1b}e+n_{1n}e)$, and simplifying we get,

$$1-\frac{c_p^2}{(1-\varepsilon)}\frac{A^2}{\left(\Omega_p^2-v_{tp}^2A^2\right)}-\frac{\varepsilon c_n^2}{(1-\varepsilon)}\frac{B^2}{\left(\Omega_n^2-v_{tn}^2B^2\right)}=\frac{\omega_{pb}^2(k_y^2+k_z^2)v_{te}^2}{\omega_{pe}^2\left(\omega-k_zv_{0b}\right)^2}, \tag{5.6}$$

where $c_p\left(=T_e/m_p\right)^{1/2}$, $c_n\left(=T_e/m_n\right)^{1/2}$, $\omega_{pb}\left[=\left(4\pi n_{0b}e^2/m_b\right)^{1/2}\right]$, $\omega_{pe}\left[=\left(4\pi n_{0e}e^2/m_e\right)^{1/2}\right]$ and $v_{te}\left[=\left(T_e/m_e\right)^{1/2}\right]$ are positive ion sound speed, negative ion sound speed, ion beam plasma frequency, electron plasma frequency and thermal velocity of electrons, respectively,

$$A^2 = \left(k_z^2 - \frac{k_y^2 \Omega_p^2}{\left(\omega_{cp}^2 - \Omega_p^2\right)} + \frac{\lambda k_y \omega_{cp} \Omega_p}{\left(\omega_{cp}^2 - \Omega_p^2\right)} - \frac{k_y k_z \omega_{cp}}{\left(\omega_{cp}^2 - \Omega_p^2\right)} \frac{\partial v_{0zp}}{\partial x} \right), \tag{5.7}$$

and

$$B^2 = \left(k_z^2 - \frac{k_y^2 \Omega_n^2}{\left(\omega_{cn}^2 - \Omega_n^2\right)} - \frac{\lambda k_y \omega_{cn} \Omega_n}{\left(\omega_{cn}^2 - \Omega_n^2\right)} + \frac{k_y k_z \omega_{cn}}{\left(\omega_{cn}^2 - \Omega_n^2\right)} \frac{\partial v_{0zn}}{\partial x} \right). \tag{5.8}$$

Equation (5.6) yields the dispersion relation of KHI driven by an ion beam in a negative ion plasma as

$$\left(\Omega_p^2 - P_p^2 A^2\right)\left(\Omega_n^2 - P_n^2 B^2\right) - \alpha A^2 B^2 = \frac{\omega_{pb}^2 (k_y^2 + k_z^2) k^2 v_{te}^2}{\omega_{pe}^2 \left(\omega - k_z v_{0b}\right)^2} \left(\Omega_p^2 - v_{tp}^2 A^2\right)\left(\Omega_n^2 - v_{tn}^2 B^2\right), \tag{5.9}$$

where $P_p^2 = v_{tp}^2 + \frac{c_p^2}{(1-\varepsilon)}$, $P_n^2 = v_{tn}^2 + \frac{\varepsilon c_n^2}{(1-\varepsilon)}$, and $\alpha = \frac{\varepsilon c_p^2 c_n^2}{(1-\varepsilon)^2}$.

When beam is absent, i.e., $n_{0b} \to 0$ or $\omega_{pb} = 0$, Eq. (5.9) reduces to

$$\left(\Omega_p^2 - P_p^2 A^2\right)\left(\Omega_n^2 - P_n^2 B^2\right) - \alpha A^2 B^2 = 0. \tag{5.10}$$

Equation (5.10) is similar to the dispersion relation of D'Angelo and Song [11] (see Eq. (26)). The proceeding sections describe the beam driven KHI modes for positive K^+ and negative ions SF_6^- using Eq. (5.6).

5.2.1.1 Interaction of Ion Beam with the Positive ions $\left(K^+\right)$

Eq. (5.6) can be simplified in the limit $\omega \sim \omega_{cp}$, for larger perpendicular wavelength of the positive ion mode than the Larmor radius of positive ion as

$$1 - \frac{c_p^2}{(1-\varepsilon)} \frac{A^2}{\left(\Omega_p^2 - v_{tp}^2 A^2\right)} = \frac{\omega_{pb}^2 (k_y^2 + k_z^2) v_{te}^2}{\omega_{pe}^2 \left(\omega - k_z v_{0b}\right)^2}. \tag{5.11}$$

Equation (5.11) can further be simplified as

$$\left(\Omega_p^2 - P_p^2 A^2\right) = \frac{\omega_{pb}^2 (k_y^2 + k_z^2) v_{te}^2}{\omega_{pe}^2 \left(\omega - k_z v_{0b}\right)^2} \left(\Omega_p^2 - v_{tp}^2 A^2\right). \qquad (5.12)$$

When beam is absent, i.e., $n_{0b} \to 0$ or $\omega_{pb} = 0$, the solutions of Eq. (5.12) can be obtained for the positive ion KHI mode in Cerenkov resonance with the ion beam applying the limit of low frequency approximations i.e., $\Omega_p^2 \ll \omega_{cp}^2$, and long perpendicular wavelength i.e., $k_y^2 \Omega_p^2 \ll \omega_{cp}^2$ as

$$\left(\Omega_p^2 - \frac{\lambda k_y P_p^2}{\omega_{cp}} \Omega_p - k_z^2 P_p^2 + \frac{k_y k_z P_p^2}{\omega_{cp}} \frac{\partial v_{0zp}}{\partial x} \right) = 0, \qquad (5.13a)$$

and

$$\omega \cong k_z v_{0b}. \qquad (5.13b)$$

Equation (5.13a) and (5.13b) represents the positive ion KHI mode and the beam mode, respectively.

Let us write $\Omega_p = \Omega_{rp} + i\Omega_{ip}$ and assume that (i.e., $\left|\Omega_{ip}\right| << \Omega_{rp}$). Equation (5.12) gives

$$\zeta_p^2 - \frac{\Lambda_1 \beta_1}{r} \zeta_p - \frac{\gamma_1}{r}\left(\gamma_1 - \beta_1 S_1\right) = 0, \qquad (5.14)$$

where, $\zeta_p \left(= \Omega_p / \omega_{cp}\right)$ (here $\zeta_p = \zeta_{rp} + i\Gamma_p$), $\rho_1^2 \left(= \rho_p^2 / \omega_{cp}^2\right)$ (here, $\rho_p^2 = \mathrm{P}_p^2 - \frac{\omega_{pb}^2 (k_y^2 + k_z^2) v_{tp}^2 v_{te}^2}{\omega_{pe}^2 \left(\omega - k_z v_{0b}\right)^2}$), $\lambda \rho_1 = \Lambda_1$, $k_y \rho_1 = \beta_1$, $k_z \rho_1 = \gamma_1$, $\frac{1}{\omega_{cp}} \frac{\partial v_{0zp}}{\partial x} = S_1$ and

$$r=\left(1-\frac{\omega_{pb}{}^{2}(k_y^2+k_z^2)v_{te}^2}{\omega_{pe}^2\left(\omega-k_z v_{0b}\right)^2}\right).$$

Equation (5.14) represents the dispersion relation for Positive ion KHI mode driven by an ion beam. Eq. (5.14) yields the dispersion relation of D'Angelo & Song [11] (see Eq. 23) in the limit $\varepsilon \to Z\varepsilon$ and $\omega_{pb} \to 0$, i.e., r =1, and for same electron and positive ion temperature, the dispersion relation of D'Angelo [7] (see Eq. 15) can be recovered.

The maximized normalized growth rate $\Gamma_p\left(=\Omega_{ip}/\omega_{cp}\right)$ can be found using Eq. (5.14) as

$$\Gamma_p=\left[\frac{1}{4}\beta_1^2\left(\frac{S_1^2}{r}-\frac{\Lambda_1^2}{r^2}\right)\right]^{1/2}. \tag{5.15}$$

For $\varepsilon \to Z\varepsilon$, and r=1, Eq. (5.15) is yields the expression for growth rate of Luo *et al.* [13] (see Eq. 2).

5.2.1.2 Interaction of Ion Beam with the Negative ions (SF_6^-)

In the limit of larger perpendicular wavelength of negative ion mode than the Larmor radius of negative ions and $\omega \sim \omega_{cn}$, Eq. (5.6) can be simplified as

$$1-\frac{\varepsilon c_n^2}{(1-\varepsilon)}\frac{B^2}{\left(\Omega_n^2-v_{tn}^2B^2\right)}=\frac{\omega_{pb}^2(k_y^2+k_z^2)v_{te}^2}{\omega_{pe}^2\left(\omega-k_z v_{0b}\right)^2}. \tag{5.16}$$

which can further be rewritten as

$$\left(\Omega_n^2-P_n^2B^2\right)=\frac{\omega_{pb}^2(k_y^2+k_z^2)v_{te}^2}{\omega_{pe}^2\left(\omega-k_z v_{0b}\right)^2}\left(\Omega_n^2-v_{tn}^2B^2\right). \tag{5.17}$$

In the limit of long perpendicular wavelength of negative ions i.e., $k_y^2\Omega_n^2 \ll \omega_{cn}^2$, low frequency i.e., $\Omega_n^2 \ll \omega_{cn}^2$, and absence of beam $\omega_{pb} = 0$, Eq. (5.17) gives

$$\left(\Omega_n^2 + \frac{\lambda k_y P_n^2}{\omega_{cn}} \Omega_n - k_z^2 P_n^2 - \frac{k_y k_z P_n^2}{\omega_{cn}} \frac{\partial v_{0zn}}{\partial x} \right) = 0, \tag{5.18a}$$

and

$$\omega \cong k_z v_{0b}. \tag{5.18b}$$

Equation (5.18a & b) represents the negative ion KHI mode and the beam mode, respectively. Let, $\Omega_n = \Omega_{rn} + i\Omega_{in}$ and $\left|\Omega_{in}\right| << \Omega_{rn}$). Eq. (5.17) gives the dispersion relation of negative ion KHI mode driven by ion beam as

$$\zeta_n^2 + \frac{\Lambda_2 \beta_2}{r} \zeta_n - \frac{\gamma_2}{r}\left(\gamma_2 + \beta_2 S_2\right) = 0, \tag{5.19}$$

where $\zeta_n \left(= \Omega_n / \omega_{cn}\right)$ (here, $\zeta_n = \zeta_{rn} + i\Gamma_n$), $\rho_2^2 \left(= \rho_n^2 / \omega_{cn}^2\right)$ (here, $\rho_n^2 = \mathrm{P}_n^2 + \frac{\omega_{pb}^2 k^2 v_{tn}^2 v_{te}^2}{\omega_{pe}^2 \left(\omega - k_z v_{0b}\right)^2}$), $\lambda\rho_2 = \Lambda_2$, $k_y\rho_2 = \beta_2$, $k_z\rho_2 = \gamma_2$, $\frac{1}{\omega_{cn}} \frac{\partial v_{0zn}}{\partial x} = S_2$,

and $r = \left(1 - \frac{\omega_{pb}^2 k^2 v_{te}^2}{\omega_{pe}^2 \left(\omega - k_z v_{0b}\right)^2} \right)$.

Eq. (5.19) gives the maximized normalized growth rate $\Gamma_n \left(= \Omega_{in} / \omega_{cn}\right)$ as

$$\Gamma_n = \left[\frac{1}{4} \beta_2^2 \left(\frac{S_2^2}{r} - \frac{\Lambda_2^2}{r^2} \right) \right]^{1/2}. \tag{5.20}$$

For $\varepsilon \to Z\varepsilon$, and neglecting ion beam, i.e., r=1, Eq. (5.20) yields the growth rate of Luo *et al.* [13] (see Eq. 2).

5.2.2 Finite Geometry Analysis

A cylindrical plasma of radius a having electrons, positive ions K^+ and negative ions SF_6^- is considered. The equilibrium densities, mass and temperatures of constituents are same as infinite geometry analysis. The magnetic field is along z-direction and equilibrium densities of constituents vary radially as $n_{0j} = \overline{n_{0j}} e^{-\lambda r}$. An ion beam with velocity $v_{0b} \| \hat{z}$, mass m_b, density $n_{0b} \ll n_{0p}$, and radius $r_b (\neq a)$ is propagating through cylindrical plasma waveguide.

For the bounded plasma cylinder, the Poisson equation can be expressed as a Bessel Equation in ϕ, which for azimuthally and axially symmetric case is

$$\frac{\partial^2 \phi}{\partial r^2} + \frac{1}{r}\frac{\partial \phi}{\partial r} + q^2 \phi = -\frac{\omega_{pb}^2 k^2 \phi}{(\omega - k_z v_{b0})^2}, \tag{5.21}$$

where

$$q^2 = -k_z^2 - \frac{\omega_{pe}^2}{v_{te}^2}\left[1 - \frac{c_p^2}{(1-\varepsilon)}\frac{A_1^2}{\left(\Omega_p^2 - v_{tp}^2 A_1^2\right)} - \frac{\varepsilon c_n^2}{(1-\varepsilon)}\frac{B_1^2}{\left(\Omega_n^2 - v_{tn}^2 B_1^2\right)}\right]. \tag{5.22}$$

Here,

$$A_1^2 = \left(k_z^2 - \frac{k_\perp^2 \Omega_p^2}{\left(\omega_{cp}^2 - \Omega_p^2\right)} + \frac{\lambda k_\perp \omega_{cp} \Omega_p}{\left(\omega_{cp}^2 - \Omega_p^2\right)} - \frac{k_\perp k_z \omega_{cp}}{\left(\omega_{cp}^2 - \Omega_p^2\right)}\frac{\partial v_{0zp}}{\partial r}\right) \tag{5.23}$$

and

$$B_1^2 = \left(k_z^2 - \frac{k_\perp^2 \Omega_n^2}{\left(\omega_{cn}^2 - \Omega_n^2\right)} - \frac{\lambda k_\perp \omega_{cn} \Omega_n}{\left(\omega_{cn}^2 - \Omega_n^2\right)} + \frac{k_\perp k_z \omega_{cn}}{\left(\omega_{cn}^2 - \Omega_n^2\right)}\frac{\partial v_{0zn}}{\partial r}\right). \tag{5.24}$$

If the beam is absent, i.e., $n_{0b} \to 0$ & $\omega_{pb} = 0$, the solution of Eq. (5.21) is given by

$$\phi = U J_0(q_m r), \tag{5.25}$$

where U is a constant, and the function $J_o\left(q_m r\right)$ is the zeroth-order Bessel function of the first kind. Here, $q_m\left(=x_n/a\right)$, and x_n be the zeros of the Bessel function $J_o(x_n)$. At cylinder's surface, the potential must vanish, hence, $J_o(q_m a)=0$ then x=2.404 be the first zero of Bessel function and $q_m = 2.404/a$. The solution of wave function ϕ can be expressed as a series of orthogonal wave functions, in the presence of beam:

$$\phi = \sum_m U_m J_o\ (q_m r). \tag{5.26}$$

Putting Eq. (5.26) in Eq. (5.21), and multiplying Eq. (5.21) by $rJ_o\ (q_n r)$ on both sides and integrating over r from 0 to a, the plasma radius, and simplifying only for the mode (m=n), we have

$$q^2 - q_m{}^2 = -\frac{\omega_{pb}^2 k^2 I}{(\omega - k_z v_{bo})^2}, \tag{5.27}$$

where $I = \dfrac{\int_0^{r_b} rJ_o(p_m r)J_0(p_n r)dr}{\int_0^{a} r\ J_o(p_m r)J_0(p_n r)dr}$ and $k^2 = q_m^2 + k_z^2$.

Using q^2 in Eq. (5.27), we get

$$1-\frac{c_p^2}{(1-\varepsilon)}\frac{A_1^2}{\left(\Omega_p^2 - v_{tp}^2 A_1^2\right)} - \frac{\varepsilon c_n^2}{(1-\varepsilon)}\frac{B_1^2}{\left(\Omega_n^2 - v_{tn}^2 B_1^2\right)} = \frac{\omega_{pb}^2\left(q_m^2 + k_z^2\right)v_{te}^2}{\omega_{pe}^2\left(\omega - k_z v_{0b}\right)^2}. \tag{5.28}$$

Now, From Eq. (5.28) we will discuss the interaction of ion beam with positive and negative ion KHI modes in the same manner as was done for infinite geometry analysis.

5.2.2.1 Interaction of Ion Beam with the Positive ions $\left(\mathrm{K}^+\right)$

Applying the similar limit as applied for a local plasmas boundary, Eq. (5.28) gives

$$1-\frac{c_p^2}{(1-\varepsilon)}\frac{A_1^2}{\left(\Omega_p^2-v_{tp}^2A_1^2\right)}=\frac{\omega_{pb}^2\left(q_m^2+k_z^2\right)v_{te}^2}{\omega_{pe}^2\left(\omega-k_zv_{0b}\right)^2}. \tag{5.29}$$

Equation (5.29) yields the positive ion KHI mode and beam mode, in the absence of beam for the same limits as applied for infinite geometry of plasma waveguide as

$$\left(\Omega_p^2-\frac{\lambda q_m P_p^2}{\omega_{cp}}\Omega_p-k_z^2P_p^2+\frac{q_mk_zP_p^2}{\omega_{cp}}\frac{\partial v_{0zp}}{\partial r}\right)=0, \tag{5.30a}$$

and

$$\omega\cong k_zv_{0b}. \tag{5.30b}$$

Equation (5.30a & b) represents the positive ion KHI mode and beam mode, respectively. Eq. (5.29) yields the dispersion relation of beam driven KHI positive ion modes for cylindrical wave guide as

$$\zeta_p^2-\frac{\Lambda_1'\beta_1'}{r_1}\zeta_p-\frac{\gamma_1'}{r_1}\left(\gamma_1'-\beta_1'S_1'\right)=0, \tag{5.31}$$

where $\zeta_+=\frac{\Omega_+}{\omega_{c+}}$, $\Lambda_1'=\lambda\rho_1'$, $\beta_1'=q_m\rho_1'$, $\gamma_1'=k_z\rho_1'$, $S_1'=\frac{1}{\omega_{cp}}\frac{\partial v_{0zp}}{\partial r}$, $\rho_1'^2=\frac{\rho_p'^2}{\omega_{cp}^2}$

(here, $\rho_p'^2=P_p^2-\frac{\omega_{pb}^2\left(q_m^2+k_z^2\right)v_{tp}^2v_{te}^2I}{\omega_{pe}^2\left(\omega-k_zv_{0b}\right)^2}$), $r_1=\left(1-\frac{\omega_{pb}^2\left(q_m^2+k_z^2\right)v_{te}^2I}{\omega_{pe}^2\left(\omega-k_zv_{0b}\right)^2}\right)$ and

$P_p^2=v_{tp}^2+\frac{c_p^2}{(1-\varepsilon)}$.

Eq. (5.31) gives the maximized normalized growth rate $\Gamma_p\left(=\Omega_{ip}/\omega_{cp}\right)$ as

$$\Gamma_p=\left[\frac{1}{4}\beta_1'^2\left(\frac{S_1'^2}{r_1}-\frac{\Lambda_1'^2}{r_1^2}\right)\right]^{1/2}. \tag{5.32}$$

5.2.2.2 Interaction of Ion Beam with the Negative ions (SF_6^-)

Similar to the infinite geometry case and in the same limits, Eq. (5.28) yields

$$1-\frac{\varepsilon c_n^2}{(1-\varepsilon)}\frac{B_1^2}{\left(\Omega_n^2-v_{tn}^2B_1^2\right)}=\frac{\omega_{pb}^2\left(p_m^2+k_z^2\right)v_{te}^2}{\omega_{pe}^2\left(\omega-k_zv_{0b}\right)^2}. \tag{5.33}$$

which gives the negative ion KHI mode as

$$\left(\Omega_n^2+\frac{\lambda q_m P_n^2}{\omega_{cn}}\Omega_n-k_z^2P_n^2-\frac{q_m k_z P_n^2}{\omega_{cn}}\frac{\partial v_{0zp}}{\partial r}\right)=0, \tag{5.34a}$$

and the beam modes as

$$\omega\cong k_zv_{0b}. \tag{5.34b}$$

In the presence of beam, Eq. (5.33) yields the dispersion relation of negative ion KHI mode as

$$\zeta_-^2+\frac{\Lambda_2'\beta_2'}{r_1}\zeta_--\frac{\gamma_2'}{r_1}\left(\gamma_2'+\beta_2'S_2'\right)=0, \tag{5.35}$$

where $\zeta_-=\frac{\Omega_-}{\omega_{c-}}\,(\zeta_-=\zeta_{r-}+i\Gamma_-)$, $\Lambda_2'=\lambda\rho_2'$, $\beta_2'=q_m\rho_2'$, $\gamma_2'=k_z\rho_2'$, $\rho_2'^2=\frac{\rho_-'^2}{\omega_{c-}^2}$

$\frac{1}{\omega_{cn}}\frac{\partial v_{0zn}}{\partial r}=S_2'$, $r_1=\left(1-\frac{\omega_{pb}{}^2\left(q_m^2+k_z^2\right)v_{te}^2I}{\omega_{pe}^2\left(\omega-k_zv_{0b}\right)^2}\right)$, $\rho_-'^2=P_-^2+\frac{\omega_{pb}{}^2\left(q_m^2+k_z^2\right)v_{t-te}^2I}{\omega_{pe}^2\left(\omega-k_zv_{0b}\right)^2}$ and

$P_n^2=v_{tn}^2+\frac{\varepsilon c_n^2}{(1-\varepsilon)}$.

From Eq. (5.38), the maximized normalized growth rate $\Gamma_n\left(=\Omega_{in}/\omega_{cn}\right)$ can be found as

$$\Gamma_n=\left[\frac{1}{4}\beta_2'^2\left(\frac{S_2'^2}{r_1}-\frac{\Lambda_2'^2}{r_1^2}\right)\right]^{1/2}. \tag{5.36}$$

5.3 RESULTS AND DISCUSSION

The slightly varied parameters of [12] are used in calculations as shown in Table-5.1.

Table- 5.1 The parameter of negative ion plasma used.

Parameters	Values
Plasma density n_0	1.0x 10^{11} cm^{-3}
Relative density of negative ions ε	0.0, 0.2, 0.4, 0.6, 0.8, 0.95
Electron Temperature T_e	0.2 eV
Positive Ion Temperature T_p	0.2 eV
Negative Ion Temperature T_n	0.2 T_e
Plasma radius a	3 cm
Beam radius r_b	3 cm
Perpendicular wave number k_y or $q_m = 2.404/a$, respectively	1.0 cm^{-1} or 0.8 cm^{-1}
Parallel wave number k_z	0.0- 0.7 cm^{-1}
Static magnetic field B_0	4x10^3 Gauss
Inverse density gradient length λ	2 cm^{-1}
Ion Beam energy E_b	0.5 eV
Ion beam density n_{0b}	2.5x10^8 cm^{-3}
Shear parameter μ	0.6-2.0

The normalized frequency of KHI modes for positive ion $\zeta_{rp}\left(=\Omega_{rp}/\omega_{cp}\right)$ using Eqs.(5.13a) & (5.30a) and negative ion $\zeta_{rp}\left(=\Omega_{rp}/\omega_{cp}\right)$ using Eq. (5.18a) & (5.34a) vs. normalized wave number $k_z/k_\perp$ at different negative ion concentrations ε and the beam mode have been plotted in Fig. 5.1 (a) & (b) and Fig. 5.2 (a) & (b), respectively, for infinite and finite geometries of plasma waveguide for above mentioned parameters in Table-5.1. The unstable mode frequencies and wave numbers can be obtained from the point of intersections of the beam mode and KHI modes for both kind of ions, for infinite and finite geometry of plasma waveguide and are given in Tables-5.2 – Table-5.5.

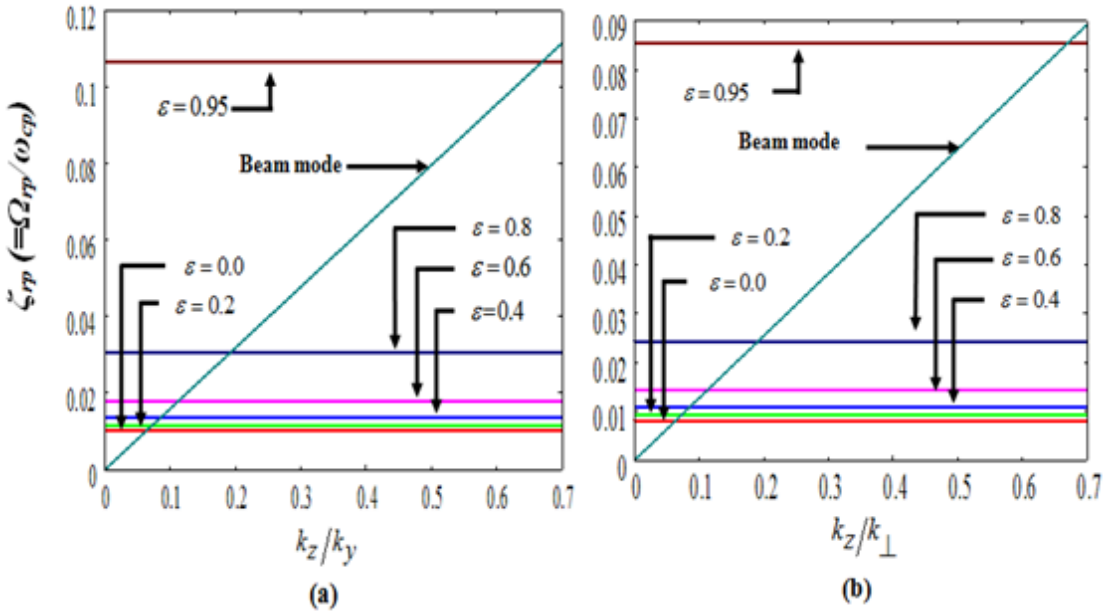

Fig. 5.1 Normalized frequency $\zeta_{rp}\left(=\Omega_{rp}/\omega_{cp}\right)$ of positive ion KHI mode vs. normalized wave number $k_z/k_\perp$ for different concentrations of negative ions ε for case **(a)** Infinite and **(b)** Finite geometry of plasma, where $k_\perp \approx k_y$ for infinite geometry. The parameters are given in Table-5.1.

Table-5.2 The ion beam driven positive ion KHI modes frequencies Ω_{rp} (rad/sec) obtained from normalized frequencies $\zeta_{rp}\left(=\Omega_{rp}/\omega_{cp}\right)$, normalized wave numbers k_y/k_z, axial wave number k_z (cm^{-1}) and wavelengths λ_z (cm) for different values of ε as obtained from Fig. 5.1 (a) for infinite geometry of plasma waveguide.

ε	Kz/ky	k_z (cm^{-1})	λ_z (cm)	Ω_{rp}/ω_{cp}	Ω_{rp} (rad/sec)
0.0	0.063378	0.063378	99.09	0.010078	9.897 x10^3
0.2	0.071544	0.071544	87.86	0.010357	10.171 x10^3
0.4	0.084618	0.084618	74.22	0.013432	13.190 x10^3
0.6	0.111554	0.111554	56.30	0.017895	17.572 x10^3
0.8	0.190716	0.190716	32.93	0.030739	30.186 x10^3
0.95	0.667368	0.667368	9.41	0.106673	104.753 x10^3

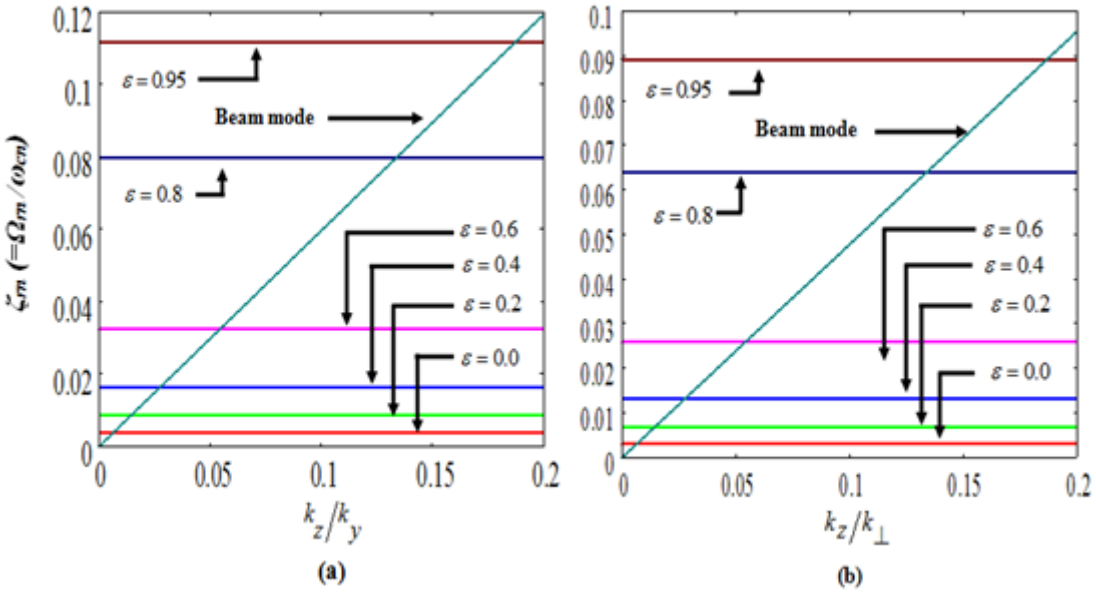

Fig. 5.2 Normalized frequency $\zeta_{rn}\left(=\Omega_{rn}/\omega_{cn}\right)$ of negative ion KHI mode vs. normalized wave number $k_z/k_\perp$ for different concentrations of negative ions ε for case **(a)** Infinite and **(b)** Finite geometry . The parameters are same as Fig. 5.1.

Table-5.3 The ion beam driven positive ion KHI mode frequencies Ω_{rp} (rad/sec) from normalized frequencies $\zeta_{rp}\left(=\Omega_{rp}/\omega_{cp}\right)$, normalized wave numbers $k_z/k_\perp$, axial wave numbers k_z (cm^{-1}) and wavelengths λ_z (cm) for different ε values as obtained from Fig. 5.1 (b) for finite geometry of plasma waveguide.

ε	$k_z/k_\perp$	k_z (cm^{-1})	λ_z (cm)	Ω_{rp}/ω_{cp}	Ω_{rp} (rad/sec)
0.0	0.064201	0.051361	122.38	0.008395	8.244 x10^3
0.2	0.070755	0.056604	110.95	0.009237	9.071 x10^3
0.4	0.083794	0.067035	93.77	0.010911	10.715 x10^3
0.6	0.112377	0.089902	69.92	0.014472	14.212 x10^3
0.8	0.190716	0.152573	41.16	0.024518	24.077 x10^3
0.95	0.669015	0.535212	11.74	0.085240	83.706 x10^3

Table-5.4 The ion beam driven negative ion KHI mode frequencies Ω_{rn} (rad/sec) from normalized frequencies $\zeta_{rn}\left(=\Omega_{rn}/\omega_{cn}\right)$, normalized wave numbers k_z/k_y, axial wave numbers k_z (cm^{-1}) and wavelengths λ_z (cm) for different ε values as obtained from Fig. 5.2 (a) for infinite geometry case.

ε	k_z/k_y	k_z (cm^{-1})	λ_z (cm)	Ω_{rn}/ω_{cn}	Ω_{rn} (rad/sec)
0.0	0.006216	0.006216	1011.23	0.003935	1.039×10^3
0.2	0.014382	0.014382	437.04	0.008683	2.292×10^3
0.4	0.027902	0.027902	225.07	0.016779	4.430×10^3
0.6	0.054029	0.054029	116.34	0.032412	8.557×10^3
0.8	0.133775	0.133775	46.94	0.079877	21.088×10^3
0.95	0.187176	0.187176	33.55	0.111142	29.342×10^3

From Table-5.2-5.5, it is observed that in the presence of beam the KHI mode frequencies for positive and negative ions increase with increase in the relative concentration of negative ions. The frequency of positive ions increases by a factor ~ 0.36, 1.24, and 2.47, respectively when ε varies from 0.0 to 0.4, 0.4 to 0.8 and 0.8 to 0.95, respectively, for infinite geometry of plasma while for finite geometry of waveguide, the frequency of positive ions increases by a factor ~0.30, 1.23, and 2.52 when ε changes from 0.0 to 0.4, 0.4 to 0.8, and 0.8 to 0.95, respectively. The frequency of negative ions is found to increase by a factor ~3.26, 3.76, and 0.39 when ε varies from 0.0 to 0.4, 0.4 to 0.8, and 0.8 to 0.95, respectively for infinite geometry and for finite geometry the frequency of negative ions is found to increase by a factor ~3.05, 3.84, and 0.39 when ε changes from 0.0 to 0.4, 0.4 to 0.8 and by 0.8 to 0.95, respectively. Tables-5.2 -5.5 shows that with increase in relative concentration of negative ions ε, the axial wave number k_z increases which matches the theoretical predictions of Chow and Rosenberg [27].

Table-5.5 The ion beam driven negative ion KHI mode frequencies Ω_{rn} (rad/sec) from normalized wave frequencies $\zeta_{rn}\left(=\Omega_{rn}/\omega_{cn}\right)$, normalized wave numbers $k_z/k_\perp$, axial wave numbers k_z (cm^{-1}) and wavelengths λ_z (cm) for different ε as obtained from Fig. 5.2 (b) for finite geometry case.

ε	$k_z/k_\perp$	k_z (cm^{-1})	λ_z (cm)	Ω_{rn}/ω_{cn}	Ω_{rn} (rad/sec)
0.0	0.006451	0.005161	1216.82	0.003279	0.866 x10^3
0.2	0.014618	0.011694	537.03	0.007004	1.849 x10^3
0.4	0.027441	0.021953	286.33	0.013285	3.507 x10^3
0.6	0.054255	0.043404	144.82	0.026080	6.885 x10^3
0.8	0.133775	0.107020	58.68	0.064001	16.896 x10^3
0.95	0.187176	0.149741	41.94	0.089359	23.591 x10^3

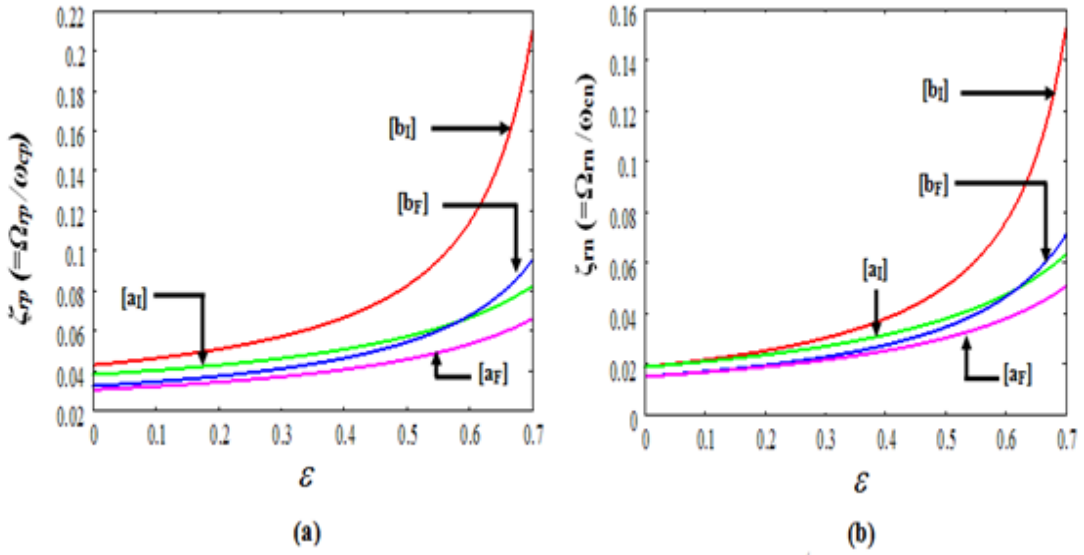

Fig. 5.3 Normalized frequency of **[a]** positive ion KHI modes, $\zeta_{rp}\left(=\Omega_{rp}/\omega_{cp}\right)$ and **[b]** negative ion KHI mode $\zeta_{rn}\left(=\Omega_{rn}/\omega_{cn}\right)$ vs. the relative negative ion concentration ε for cases: [a_I] - in the absence of beam, and [b_I]-in the presence of beam, for infinite geometry, [a_F]- in the absence of beam and [b_F]- in the presence of beam for finite geometry of plasma. The parameters are same as Fig.5.1 & 5.2.

We have plotted normalized frequencies for positive and negative ion KHI modes Fig. 5.3 (a) & (b) using Eqs. (5.14) & (5.31) and Eqs.(5.19) & (5.35), as a function of relative negative ion concentration ε for the same parameters as used for plotting Figs. 5.1(a) & (b) and Figs.5.2(a) & (b), respectively, for infinite and finite boundaries of plasma in the absence and presence of beam. Figs. 5.3 (a) & (b) shows that the KHI modes frequencies for both positive ion and negative ion modes increase with an increase in the relative negative ion concentration in infinite as well as finite geometries of plasma which is well in agreement with the experimental observations of (EIC) waves [28] (see Fig.3 p.1555) and (IAW) [19] (see Fig.1 p.285) in a negative ion plasma where the wave modes frequencies and the phase velocities increase with relative density of negative ions. The presence of beam slightly increases the KHI modes frequencies at large density of negative ions. The frequencies of KHI modes for infinite geometry of plasma waveguides are greater than for finite geometry of plasma which is line with the results of Prakash *et al.* [23] for bounded plasmas.

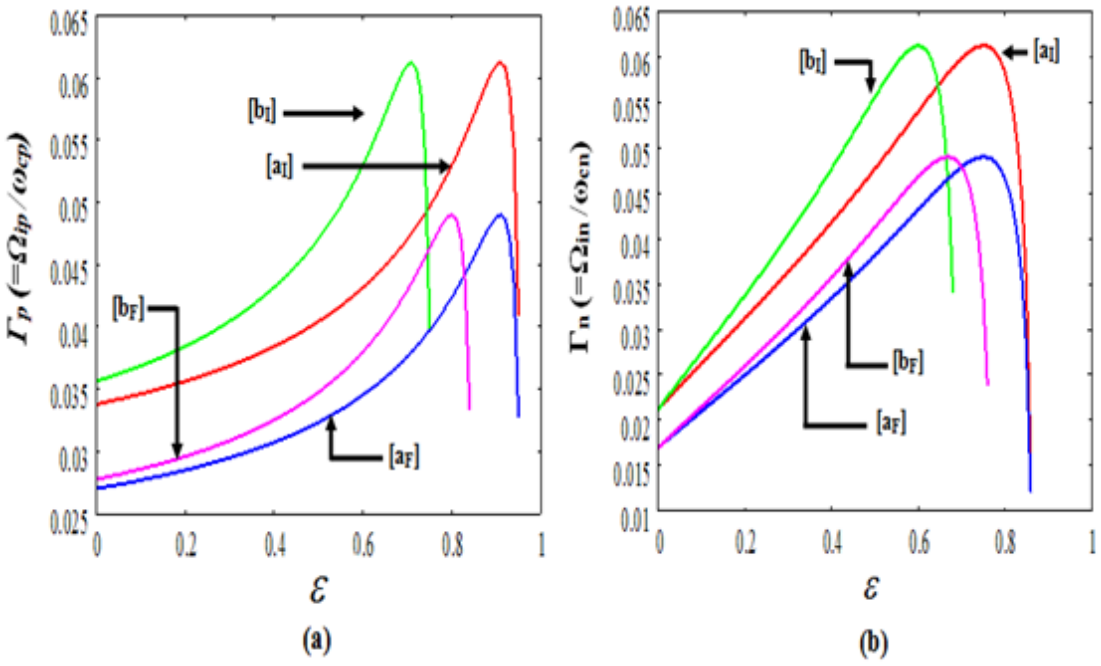

Fig. 5.4 Normalized growth rate of KHI for **[a]**-positive ions $\Gamma_p\left(=\Omega_{ip}/\omega_{cp}\right)$, and **[b]**- negative ions $\Gamma_n\left(=\Omega_{in}/\omega_{cn}\right)$ vs. the relative negative ion concentration ε for cases: [a_I] - in the absence of beam, and [b_I]-in the presence of beam, for infinite geometry, [a_F]- in the absence of beam and [b_F]- in the presence of beam for finite geometry of plasma. The parameters are same as Fig.5.3.

The normalized growth rates for positive ion KHI mode $\Gamma_p \left(= \Omega_{ip} / \omega_{cp} \right)$ and for negative ion KHI mode $\Gamma_n \left(= \Omega_{in} / \omega_{cn} \right)$ have been plotted as a function of relative negative ions concentration ε, in Figs. 5.4 (a) & (b) using Eqs.(5.15) & (5.32) & Eqs. (5.20) & (5.36), respectively in the absence and the presence of beam for infinite and finite geometries of plasma waveguides for the same parameters as used for plotting Fig. 5.3 (a) & (b) and the shear parameters (=0.7). It is observed that the growth rate of KHI for positive ion mode shoots up to 30% for infinite geometry of plasma waveguide and only upto 14% for cylindrical waveguide at a constant $\varepsilon = 0.7$ as the ion beam is turned on. The growth rate of KHI negative ion mode at $\varepsilon = 0.6$ in infinite geometry case shows an increase up to 13%, while for finite geometry case only upto 8% in the presence of beam.

We can say from Figs. 5.4 (a) & (b), that the growth rate of positive and negative ions KHI modes increases with increase in relative negative ion density for both infinite and finite geometries of plasma waveguides in the presence of beam. A large concentration of negative ions further stabilizes the KHI modes. These observations are in good agreement with the experimental results of An *et al.* [12] (see Figs.4 &5, p.50). The destabilizing effect of beam on the KHI modes can be prominently observed for large values of shear parameters and ε which is well in agreement with the predictions of D'Angelo and Song [11] (see Figs 1-5, p.44-45) i.e., KHI modes are highly destabilized at relatively high shear parameters and concentration of negative ions.

The normalized growth rate of positive and negative ions KHI modes have also been plotted in Figs. 5.5 & 5.6, respectively, for different relative negative ion masses $\left(m_n / m_p \right)$, as a function of relative negative ion concentration ε, in the presence of beam for the same parameters as in Figs. 5.4 (a) & (b), for infinite and finite boundaries of plasma waveguides. Figs. 5.5 and 5.6 show the stabilizing effect of increasing relative mass of negative ions on both the KHI modes. These results agree well with the theoretical results of D'Angelo and Song [11] (see Fig. 6, p.45). Moreover, finite boundary effects further lowers the growth rate of positive & negative ion KHI modes with increase in relative mass of the negative ions.

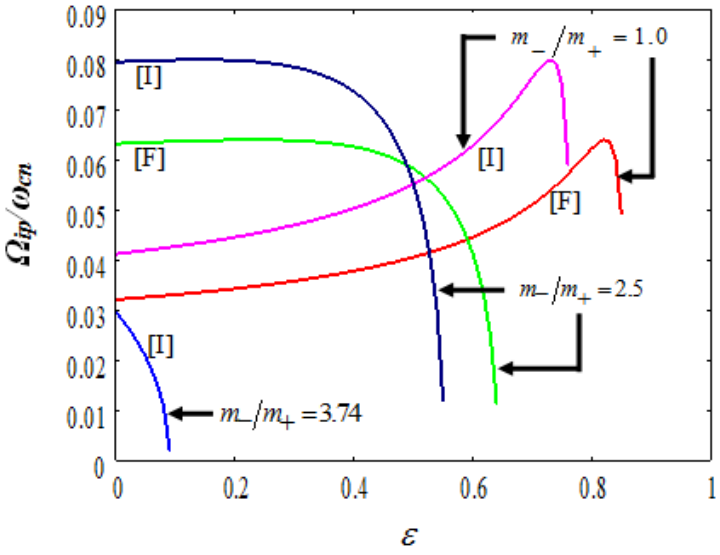

Fig. 5.5 Normalized growth rate Ω_{ip}/ω_{cn} of the ion beam driven positive ion KHI mode vs. relative concentration of negative ions ε for **[I]** - Infinite geometry and **[F]**- finite geometry of plasma at different relative negative ion masses $\left(m_n/m_p\right)$(=1.0, 2.5, 3.74) for the same parameters as Fig. 5.4 (a).

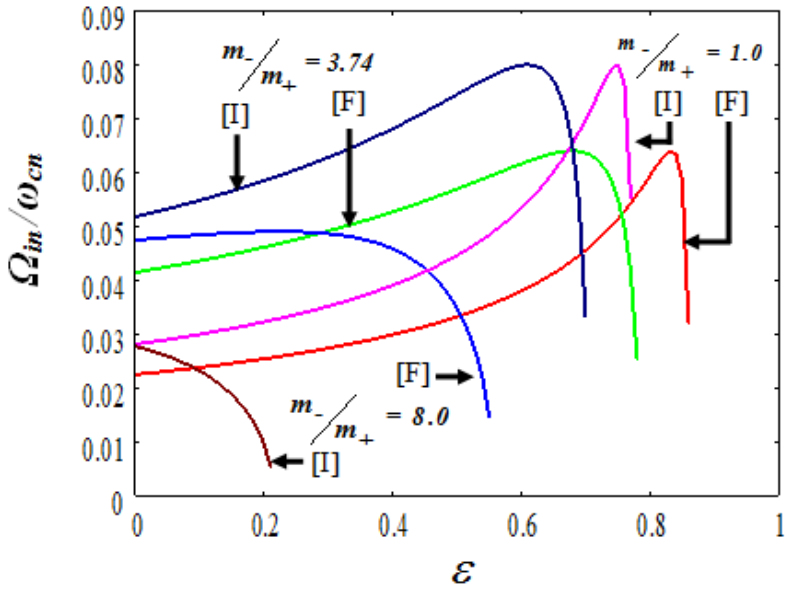

Fig. 5.6 Normalized growth rate Ω_{in}/ω_{cn} of the ion beam driven negative ion KHI mode vs. relative concentration of negative ions ε for **[I]** - infinite geometry and **[F]**- finite geometry of plasma at different relative negative ion masses $\left(m_n/m_p\right)$(=1.0, 3.74, 8.0) for the same parameters as Fig. 5.4 (b).

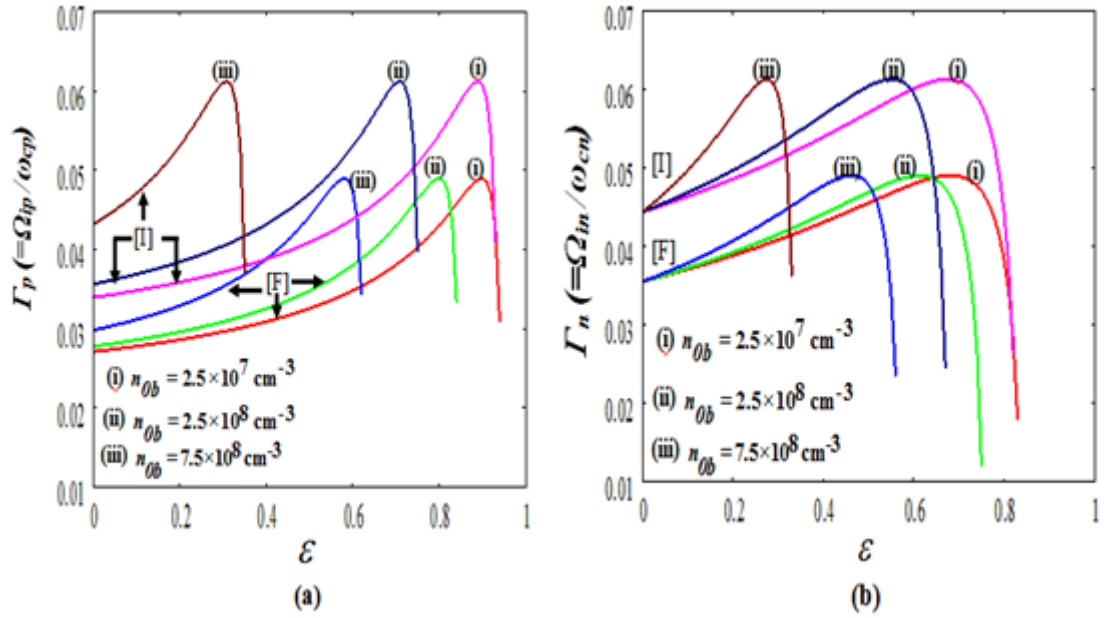

Fig. 5.7 Normalized growth rate of ion beam driven KHI for **[a]**-positive ions $\Gamma_p\left(=\Omega_{ip}/\omega_{cp}\right)$, and **[b]**- negative ions $\Gamma_n\left(=\Omega_{in}/\omega_{cn}\right)$ vs. the relative negative ion concentration ε, for [I]-infinite and [F]-finite geometries of plasma waveguides, for ion beam densities, n_{0b}(=2.5×10^7, 2.5×10^8, 7.5×10^8) cm^{-3}. The other parameters are same as Fig. 5.4 (a) & (b).

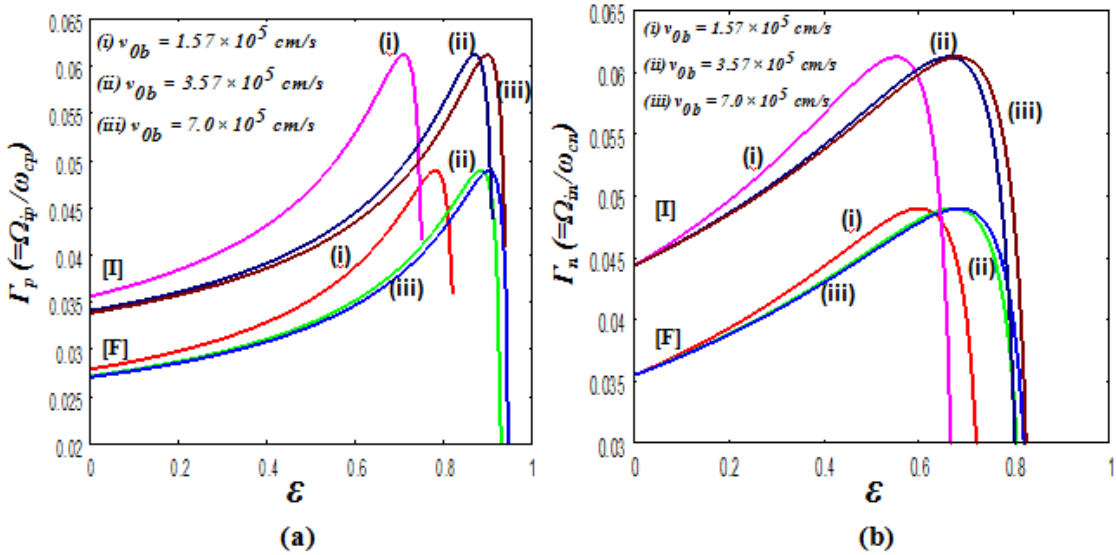

Fig. 5.8 Normalized growth rate of ion beam driven KHI for **[a]**-positive ions $\Gamma_p\left(=\Omega_{ip}/\omega_{cp}\right)$, and **[b]**- negative ions $\Gamma_n\left(=\Omega_{in}/\omega_{cn}\right)$ vs. the relative negative ion concentration ε, for [I]-infinite and [F]-finite geometries of plasma waveguides and ion beam velocities v_{0b}(=1.57×10^5, 3.57×10^5, 7.0×10^5) cm/s. The other parameters are same as Fig. 5.7.

The growth rates of beam driven positive ion and negative ion KHI modes have also been plotted as a function of relative negative ion concentration ε to investigate the effect of different ion beam densities n_{0b}(=2.5×10^{7}, 2.5×10^{8}, 7.5×10^{8}) cm^{-3} (see Figs. 5.7 (a) & (b)), and energies/velocities $v_{0b}\left[=\left(2E_b/m_b\right)^{1/2}\right]=1.57\times10^{5}$, 3.57×10^{5}, 7.0×10^{5} cm/s (see Figs. 5.8 (a) & (b)). The other parameters have been kept same as Figs. 5.4 (a) & (b). It is noticed that the beam density have a destabilizing effect on growth rate of KHI modes while the growth rate of KHI lowers down with increase in beam energies/velocities. An increase in ion beam density may increase the ions influx which in turn may support the critical shear responsible for enhancing the growth rate of the KHI modes while an increase in ion beam energy may disturb the relative motion of ions by increasing their velocity and Landau damping [29] thereby reducing the growth rate of KHI.

5.4 CONCLUSION

The Kelvin Helmholtz instability can be driven unstable by an ion beam via Cerenkov interaction in a magnetized negative ion plasma. Our theoretical investigations in the absence of beam yield the theoretical results of D'Angelo and Song [11] (see Figs. 1-5). It is also noticed that KHI modes gets destabilized upto $\varepsilon \le 0.7$ in presence of negative ions and then stabilized at relatively large negative ion concentrations. This is well in agreement with the experimental results of An *et al.* [12] (see Figs. 4 &5, p.50). The prominent beam effect on the growth rate of KHI is observed at relatively large negative ion concentration ε. Negative ion KHI modes get stabilized for even a small $\varepsilon \le 0.6$ in the presence of ion beam. It is also observed that the presence of heavier negative ions in the plasma stabilizes the KHI mode which is similar to as observed by D'Angelo and Song [11] (see Fig 6, p.45). A comparison of infinite and finite boundary effects explicates that cylindrical plasma waveguide have lesser values of frequencies and growth rates of KHI due to reduced interaction region [23]. An increase in KHI modes frequencies and growth rate well matches with the experimental results of Kim *et al.* [28] for EICWs and Song *et al.* [19] for IAWs in a

plasma having negative ions. The beam parameters like beam density and energy also modify the growth rate of K-H instability.

Our general results of KHI may be useful in understanding the negative ion plasmas instabilities occurring in surface plasma technologies [30] - [32], beam plasma systems [33], magneto-hydrodynamic fluids [34] and the near Earth environment [2] – [5], [26].

REFERENCES

[1]. N. D'Angelo, *J. Geophys. Res.* **78,** 1206 (1973).

[2]. A. I. Ershkovich, *Space Sci. Rev.* **25**, 3 **(**1980).

[3]. S. Migliuolo, *J. Geophys. Res.* **89**, 27 (1984).

[4]. A. Miura, *Geophys. Res. Lett.* **17**, 749 (1990).

[5]. H. Hasegawa, M. Fujimoto, T. D. Phan, H. Re `me, A. Balogh, M. W. Dunlop, C. Hashimoto, and R. T. Dokoro, *Nature* **430**, 755 (2004).

[6]. S. Chandrasekhar, "*Hydrodynamic and Hydromagnetic Stability*," Clarendon Press, Oxford (1961), Chap. XI, 481.

[7]. N. D'Angelo, *Phys. Fluids* **8**, 1748 (1965).

[8]. N. D'Angelo and S. V. Goeler, *Phys. Fluids* **9**, 309 (1966).

[9]. C. G. Smith, and S. V. Goeler, *Phys. Fluids* **11**, 2665 (1968).

[10]. N. D' Angelo and B. Song, *Planet. Space Sci.* **38**, 1577 (1990).

[11]. N. D' Angelo and B. Song, *IEEE Trans. Plasma Sci.* **19**, 42 (1991).

[12]. T. An, R. L. Merlino, and N. D'Angelo, *Phys. Lett. A* **14**, 47(1996).

[13]. Q. Z. Luo, N. D' Angelo and R. L. Merlino, *Phys. Plasmas* **8**, 31 (2001).

[14]. T. An, R. L. Merlino, and N. D' Angelo, *Phys. Fluids B* **5**, 1917 (1993).

[15]. N. D'Angelo and R. L. Merlino, *IEEE Trans. Plasma Sci.* **14**, 285 (1986).

[16]. M. Rosenberg, and R. L. Merlino, *Planet. Space Sci.* **55**, 1464 (2007).

[17]. S. C. Sharma, and M. P. Srivastava, *Phys. Plasmas* **8**, 679-686, 2001.

[18]. S. C. Sharma, and A. Gahlot, *Phys. Plasmas* **15,** 073705 (2008).

[19]. B. Song, N. D'Angelo, and R. L. Merlino, *Phys. Fluids B* **3**, 284 (1991).

[20]. K. Yatsui, and Y. Yamamoto, *Phys. Lett.* **30A**, 135 (1969).

[21]. R. P. Chang, *Phys. Rev. Lett.* **35**, 285 (1975).

[22]. V. Prakash, S. C. Sharma, Vijayshri, and R. Gupta, *Phys. Plasmas* **21**, 033701 (2014).

[23]. K. Ostrikov, *Vacuum* **83,** 4 (2008).

[24]. K. Ostrikov, S. Kumar, and H. Sugai, *Phys. Plasmas* **8,** 3490 (2001).

[25]. K. Ostrikov, *Rev. Mod. Phys.* **77**, 489 (2005).

[26]. T. W. Moore, K. Nykyri, and A. P. Dimmock, *Nat. Phys*. **12**, 1164 (2016).

[27]. V. W. Chow and M. Rosenberg, *Plasma Phys.* **3**, 1202 (1996).

[28]. S. H. Kim, J. R. Heinrich, and R. L. Merlino, *Planet. Space Sci.* **56**, 1552 (2008).

[29]. G. Praburam, H. Honda, and M. Sugawa, *J. Phys. Society* Japan **62**, 4262 (1993).

[30]. R. K. Tyagi, R. S. Pandey, and A. Kumar, *Theor. Found. Chem. Engg.* **46**, 508 (2012).

[31]. E. Stoffels, W. W. Stoffels and G. M. W. Kroesen, *Plasma Sources Sci. Tech.* **10**, 311 (2001).

[32]. V. P. Kuznetsova, S. Yu. Tarasov, and A. I. Dmitriev, *J. Mat. Proc. Tech.* **217**, 327 (2015).

[33]. M. Rosenberg and P. K. Shukla, *Phys. Plasmas* **5,** 3786 (1998).

[34]. C. Matsuoka, *Scholarpedia* **9**, 11821 (2014).

CHAPTER 6

Current Driven Low Frequency Modes in a Strongly Coupled Magnetized Collisional Dusty Plasma

This Chapter deals with the local and non-local theoretical model based on Generalized Hydrodynamic (GH) approach of one component plasma (OCP) to study the excitation of low frequency electrostatic wave modes in a magnetized collisional plasma having strongly coupled dust grains. The longitudinal and transverse modes have been studied under the effect of magnetic field aligned plasma currents in the hydrodynamic regime for a local dusty plasma and in the strong coupling regime (frequency much higher than the dust particle relaxation time) for a non-local cylindrical dusty plasma waveguide. The effect of strong correlation parameters, drift velocity of ions on the dispersion properties of longitudinal and transverse wave modes has been discussed. The dispersion properties are found to be modified under the effect of magnetic field aligned plasma drifts and collisions. Moreover, the finite boundaries and applied magnetic field tend to modify the dispersion properties of low frequency modes. The longitudinal mode observed is a dust ion hybrid like mode while the transverse mode is a peculiar elastic mode.

6.1 INTRODUCTION

It is well known that dust is found to be a detrimental component in various astrophysical and laboratory situations like Saturn rings, cometary tails, interstellar clouds, supernova shocks, Earth's ionosphere [1]–[7], vicinity of artificial satellites and

space stations, plasma technologies such as plasma deposition and etching, thin films & nanoparticles production, and thermonuclear fusion [8]-[9] etc. The variation in dust size and fluctuations of dust charge [10]-[15] not only modify the existing high frequency wave modes but also excites the low frequency dust wave modes [16]–[17]. Moreover, formation of crystal like structures [18]–[20] due to strong correlation among dust particles is a fascinating phenomenon shown by dusty plasmas. These strongly correlated dust systems are characterized by the Coulomb coupling parameter $\Gamma = \frac{Z_d^2 e^2}{a_d T_d} \exp\left(-\frac{a_d}{\lambda_D}\right)$ (as discussed in chapter 1 sec. 1.2.1.3). Here, e is the electronic charge, Z_d is the dust charge state ~10^3-10^4, T_d is the dust temperature, $a_d \left(= 3/4\pi n_{d0}\right)^{1/3}$ is the inter-grain distance, λ_D is the plasma Debye length and n_{d0} is the equilibrium dust density. In a strongly coupled system where $\Gamma \geq 1$ the dust plays an important role in dynamics of the plasma wave modes while for a weakly coupled systems, i.e., $\Gamma << 1$, the wave modes are not affected by particle correlations, except through collisional effects. The simplest case is the so-called one-component plasma (OCP). A system with $1 < \Gamma < 170$ is in the strongly coupled fluid state [21]. The dust particles undergo crystallization beyond $\Gamma \sim 170$ [21] but in a dusty plasma (DPX) experiment the authors have shown the evidence of dust fluid state upto $\Gamma \sim 300$ [22].

The study of waves and instabilities in strongly coupled dusty plasmas is of considerable interest because of their possible space and laboratory applications. Moreover, strongly coupled dusty plasmas can sustain novel kind of low frequency waves such as the dust acoustic waves (DAW) [23]–[30] and dust lattice waves (DLW) [31]–[34], which have no counterpart in conventional plasmas. Various researchers have studied low frequency electrostatic wave modes experimentally or theoretically in weakly or strongly coupled magnetized or unmagnetized dusty plasmas [35]-[38]. These low frequency electrostatic modes have been investigated experimentally and theoretically using different approaches like generalized hydrodynamic (GH) approach, Quasi Localized charge approximation, kinetic theory and Yukawa potential [39]–[45] etc. by many researchers in strongly coupled unmagnetized dusty plasmas.

Pieper and Goree [26] have supported the applicability of fluid model for dust acoustic waves in strongly coupled dusty plasmas. Praburam and Goree [39] experimentally observed the two low frequency microscopic wave modes in dusty plasma. Rosenberg and Kalman [27] have theoretically investigated the dispersion relation for dust acoustic instability using a quasi-localized charge approximation in a dusty plasma comprising of strongly coupled negatively charged dust grains, and weakly correlated classical ions and electrons. The dust grains were assumed to interact via a (screened Coulomb) Yukawa potential. Kaw and Sen [40] studied the effect of strong correlation parameter on the frequency and phase velocity of low frequency dust acoustic modes using the generalized hydrodynamic model in a dusty plasma. Nonumura *et al.* [41] investigated th*e* longitudinal and transverse waves in 2-D screened coulomb crystal experimentally. The longitudinal collective wave modes in strongly coupled plasmas were studied using multi-component kinetic theory by Murillo [42]. Kaw [43] has observed the collective modes in strongly coupled plasmas involving non-uniform charge number equilibrium and delayed charging effects. Xie *et al.* [44] also investigated the ion flow driven low frequency electrostatic dust instability in a strongly coupled plasma and showed the effect of dust charge relaxation and coupling parameter on the behaviour of instability. Xie and Chen [45] also studied the low frequency modes in strongly correlated magnetized plasma and found that a weakly damped hybrid like longitudinal mode exists in a direction perpendicular to the magnetic field and a transverse shear mode exists in a direction parallel to the magnetic field which is analogous to torsional vibration mode in a solid. A few decades ago, Shukla and Rosenberg [46] developed a theory for low frequency electrostatic waves in a bounded magneto-dusty plasma showing relevance to the laboratory plasmas and discussed the possibility of different coupled modes such as dust cyclotron and dust acoustic but have not accounted for the strong coupling among dust grains and neutral drag. Few members of broad dusty plasma research community have devised a magnetized dusty plasma experiment (MDPX) [47] to analyze magnetized dust modes in strongly coupled dusty plasma systems.

It is well known that the relative drifts produced by electric and magnetic fields, being free source of energy tends to excite the waves and instabilities in a collisional dusty plasma [48]-[54]. Hence, in this chapter, we tried to observe the

excitation of longitudinal and transverse electrostatic wave modes by the ion current drifts in a collisional magnetized local plasma having strongly correlated dust grains.

Moreover, as the dusty plasma devices are mostly bound hence we also develop a nonlocal theory employing generalized hydrodynamic (GH) equation to provide a simple picture of strongly correlated dust grains on excitation of longitudinal and transverse shear dust wave modes by magnetic field aligned ion and dust currents in a collisional magnetized dusty plasma cylinder. The cylindrical geometry is chosen so that it can find applications in discharge tubes, plasma waveguides, magnetrons for metal deposition, inertial confinement fusion devices and dust plasma devices [55]-[60]. Furthermore, the bounded plasma systems also render the large background pressure of neutrals which in turn support the strong correlations among dust grains [39].

Now, we discuss two different cases to study the low frequency longitudinal and transverse wave modes in a magnetized strongly coupled collisional dusty plasma: (i) Local analysis in hydrodynamic limit ($\omega\tau_m \ll 1$) and (ii) nonlocal analysis in strongly coupled kinetic regime ($\omega\tau_m \gg 1$).

6.2 Local Theory (Hydrodynamic regime, $\omega\tau_m \ll 1$)

A collisional magnetized dusty plasma having electrons, ions and dust grains is considered where magnetic field B is along positive z-direction. The equilibrium densities of electrons, ions, dust grains are given by n_{e0}, n_{i0} and n_{d0}. The charge, mass and temperature of the three species are denoted by $(-e, m_e, T_e)$, (e, m_i, T_i) and $(-Z_d e, m_d, T_d)$, respectively. The collisional frequencies of electrons and ions are given by ν_e and ν_i, respectively where the dust neutral collisions have been neglected to observe the effect of strong correlation on wave dynamics of current driven low frequency waves in presence of magnetic field. The drift velocities of electrons and ions produced by electric and magnetic fields nearly along z direction are v_{de} and v_{di}, respectively. The dust drifts have been neglected due to its large mass.

The electrostatic perturbations vary as $\sim e^{-i(\omega t - k_x x - k_z z)}$. Due to high charge on the dust particles, strong coupling parameter is, $\Gamma \geq 1$ and hence the plasma can be considered as a high effective viscosity fluid or a solid.

In the range, $1 < \Gamma < \Gamma_c$ i.e., strongly coupled fluid regime and may be even in super cooled regime above Γ_c as long as the plasma retain its fluid characteristics, the generalized hydrodynamic (GH) momentum equation may be used to describe dust motion [61]. The GH equation for motion of dust is given as

$$\left(1+\tau_m \frac{\partial}{\partial t}\right)\left[m_d n_{d0}\frac{\partial}{\partial t}\delta\vec{u}d+\nabla\delta P+Z_d e n_{d0}\delta\vec{E}+\frac{1}{c}Z_d e n_{d0}\delta\vec{u}d\times\vec{B}\right] = \eta\nabla.\nabla\delta\vec{u}d+\left(\zeta+\frac{\eta}{3}\right)\nabla\left(\nabla.\delta\vec{u}d\right), \quad (6.1)$$

where δu_d is the perturbed velocity of dust, δP is pressure, η is the shear viscosity coefficient, ζ is the coefficient of bulk viscosity, and τ_m is the relaxation time. The presence of large magnetic field may modify the values of transport coefficients η and ζ along or in perpendicular direction of applied magnetic field. Another important term that will be used is compressibility of dust fluid which is given as

$$\mu_d = \left(\partial_n P_d\right)_T \Big/ T_d = 1+\frac{1}{3}u(\Gamma)+\frac{1}{9}\frac{\partial u(\Gamma)}{\partial\Gamma}, \quad (6.2)$$

here $u(\Gamma)$ is a measure of excess internal energy which is different for weak and strong coupling in plasma. For strong coupling regime, $u(\Gamma)$ is obtained by Monte Carlo simulations or MD simulations [62] and is given by

$$u(\Gamma) \simeq -0.89\Gamma + 0.95\Gamma^{1/4} + 0.19\Gamma^{-1/4} - 0.82, \text{ for } 1 \leq \Gamma \leq 200 . \quad (6.3)$$

The typical approximate values of transport quantities are obtained by fitting expressions as

$$\eta^* = \frac{\left(\zeta+\frac{4}{3}\eta\right)}{m_d n_{d0}\omega_{pd}a_d^2} \sim 0.02\,\Gamma^{1/2} \quad (6.4)$$

and

$$\tau_m^* = \omega_{pd}\tau_m \approx 0.375\,\Gamma^{1/2}, \tag{6.5}$$

where $\tau_m = \left(\zeta + \frac{4}{3}\eta\right) \Big/ n_{d0}T_d\left(1-\gamma_d\mu_d + {}^{4u(\Gamma)}/_{15}\right)$, in limit $10 \le \Gamma \le 200$ [62]. We considered the regime, $\omega\tau_m \ll 1$ to study longitudinal as well as transverse wave modes so that the wave dynamics of laboratory dusty plasmas can well be explained through GH model in the limit of long wavelength $ka_d \le 1$.

A. ***Longitudinal Electrostatic Mode***

In this low frequency mode, the dust particles provide inertia and the shielding electrons and ions provide thermal effects. For simplicity we considered $\vec{k} \approx kx$ and $\delta\vec{E} \approx \delta E_x x$ such that $k^2 \approx k_x^2 \gg k_z^2$. Using equation of continuity,

$$\frac{\partial}{\partial t}\delta n_d + \nabla.\left(n_d\delta\vec{u}_d\right) = 0\ , \tag{6.6}$$

we have

$$\delta n_d = \frac{kn_{d0}}{\omega}\delta u_{dx} \tag{6.7}$$

and then using Eq. (6.7) in compressibility equation $\nabla\delta P = \left(\frac{\partial P}{\partial n}\right)_T \nabla\delta n_d$, we have

$$\nabla\delta P = i\gamma_d\mu_d T_d \frac{k^2 n_{d0}\delta u_{dx}}{\omega}. \tag{6.8}$$

Here γ_d is adiabatic index and μ_d is compressibility of fluid. Eq. (6.8) can be used in Eq. (6.1) to get perturbed dust speed,

$$\delta u_{dx} = \left(-Z_d e n_{d0}\delta E_x\phi\right)\times$$

$$\left[im_d n_{d0} \left(\frac{k^2 \gamma_d \mu_d T_d}{\omega m_d} - \omega \right) + \frac{k^2 \left(\zeta + \frac{4}{3}\eta \right)}{(1 - i\tau_m \omega)} + \frac{\omega_{cd}^2 m_d^2 n_{d0}^2}{\left(\frac{k^2}{(1 - i\tau_m \omega)} - i\omega m_d n_{d0} \right)} \right]^{-1}. \quad (6.9)$$

Now using perturbed dust speed in Eq. (6.7), we get perturbed dust density,

$$\delta n_d = \frac{k^2 \phi Z_d e n_{d0} / m_d}{\omega^2 \left[\left(\frac{k^2 \gamma_d \mu_d T_d}{\omega^2 m_d} - 1 \right) - \frac{ik^2 \left(\zeta + \frac{4}{3}\eta \right)}{(1 - i\tau_m \omega) \omega m_d n_{d0}} + \frac{\omega_{cd}^2}{\left(\frac{i\eta k^2 \omega}{(1 - i\tau_m \omega) m_d n_{d0}} + \omega^2 \right)} \right]}, \quad (6.10)$$

where $\omega_{cd} = \left[-\left(Z_d e \right) B / m_d c \right]$ is dust cyclotron frequency.

Similarly electron and ion perturbed densities are obtained from Eq. (6.10) by neglecting transport coefficients η, ζ, τ_m and putting $\gamma_d = 1$, $\mu_d = 1$. The perturbed electron and ion densities are given as

$$\delta n_e = \frac{k^2 \phi e n_{e0}}{m_e \left[k^2 v_{te}^2 - \omega_1^2 + \omega_{ce}^2 \right]} \quad (6.11)$$

and

$$\delta n_i = \frac{-k^2 \phi e n_{i0}}{m_i \left[k^2 v_{ti}^2 - \omega_2^2 + \omega_{ci}^2 \right]}, \quad (6.12)$$

where

$\omega_1 = \left(\omega - k_z v_{de} + i\nu_e \right)$, $\omega_2 = \left(\omega - k_z v_{di} + i\nu_i \right)$, $v_{te} = \left[T_e / m_e \right]^{1/2}$ and $v_{ti} = \left[T_i / m_i \right]^{1/2}$.

Also, $\omega_{ce} \left[= -eB / m_e c \right]$ and $\omega_{ci} \left[= eB / m_i c \right]$ are the electron cyclotron and ion cyclotron frequencies, respectively.

Now substituting the perturbed densities of dust, electrons and ions in Poisson equation,

$$-\nabla^2\phi = 4\pi\left(-e\delta n_e - Z_d e\delta n_d + e\delta n_i\right), \tag{6.13}$$

the dispersion relation for longitudinal mode can be obtained as,

$$1+\frac{\omega_{pe}^2}{\left(k^2v_{te}^2+\omega_{ce}^2-\omega_1^2\right)}+\frac{\omega_{pi}^2}{\left(k^2v_{ti}^2+\omega_{ci}^2-\omega_2^2\right)}-\frac{\omega_{pd}^2}{\left(\omega^2+i\eta_1\omega-k^2\gamma_d\mu_d v_{td}^2-\frac{\omega_{cd}^2}{\left(1+\eta_2\right)}\right)}=0, \tag{6.14}$$

where $\eta_1=\dfrac{k^2\left(\zeta+\frac{4}{3}\eta\right)}{\left(1-i\tau_m\omega\right)m_d n_{d0}}$ and $\eta_2=\dfrac{\eta k^2}{\left(1-i\tau_m\omega\right)\omega m_d n_{d0}}$.

In the absence of current drifts and collisional frequencies of ions and electrons, Eq. (6.14) is same as dispersion relation given by Xie and Chen [45] {cf. Eq. (9) p.3521}. It is observed that wave modes can exist only when η_1 and η_2 be small which is possible only if $\omega \gg \omega_{cd}$ i.e., unmagnetized dust. Under assumptions $\omega^2 \ll \omega_{ci}^2 \ll \omega_{ce}^2$ and $|\omega| \ll k_z v_{di}$, Eq. (6.14) can be simplified as

$$\omega^2+i\eta_1^{'}\omega-k^2v_{td}^2\gamma_d\mu_d-\frac{\omega_{cd}^2}{\left(1+\eta_2^{'}\right)}-\frac{\omega_{pd}^2}{\left(1+\frac{1}{\Omega_e^2}+\frac{\omega_{pi}^2}{\Omega_i^2\omega_{pi}^2-i2\upsilon_i\left(\omega-k_z v_{di}\right)}\right)}=0, \tag{6.15}$$

where $\eta_1^{'}=\dfrac{k^2\left(\zeta+\frac{4}{3}\eta\right)}{m_d n_{d0}}$, $\eta_2^{'}=\dfrac{\eta k^2}{\omega m_d n_{d0}}$,

$$\Omega_e^2=\frac{k^2v_{te}^2}{\omega_{pe}^2}-\frac{k_z^2v_{de}^2}{\omega_{pe}^2}+\frac{v_e^2}{\omega_{pe}^2}+\frac{\omega_{ce}^2}{\omega_{pe}^2}\approx k^2\lambda_{De}^2+V_{Ae}^2,$$

and $\Omega_i^2=\dfrac{k^2v_{ti}^2}{\omega_{pi}^2}-\dfrac{k_z^2v_{di}^2}{\omega_{pi}^2}+\dfrac{v_i^2}{\omega_{pi}^2}+\dfrac{\omega_{ci}^2}{\omega_{pi}^2}\approx k^2\lambda_{Di}^2+V_{Ai}^2-\dfrac{k_z^2v_{di}^2}{\omega_{pi}^2}+\dfrac{v_i^2}{\omega_{pi}^2}$.

Equation (6.15) can be simplified, as

$$1+\frac{1}{\Omega_e^2}+\frac{\omega_{pi}^2}{\Omega_i^2\omega_{pi}^2-i2\upsilon_i(\omega-k_z v_{di})}-\frac{\omega_{pd}^2}{\left(\omega^2+i\eta^* k^2a^2\omega_{pd}\omega-k^2v_{td}^2\gamma_d\mu_d-\omega_{cd}^2\right)}=0, \tag{6.16}$$

where $\eta^*=\dfrac{\left(\zeta+\frac{4}{3}\eta\right)}{m_d n_{d0}\omega_{pd}a^2}$.

Equation (6.16) is the dispersion relation for current driven longitudinal modes in strongly coupled dusty plasma which is similar to the dispersion relation given by Kaw and Sen [40] for ion streaming instabilities {cf. Eq. (28) p.3556} in the absence of magnetic field. Eq. (6.16) in the absence of strong coupling effects and magnetic field is also similar to the dispersion relations given for dust acoustic waves in the presence of streaming of ions and collisional effects for unmagnetized weakly coupled dusty plasmas {cf. Eqs. 5.2.15} [47].

Equation (6.16) can further be rewritten as

$$\omega^2+i\eta^* k^2a^2\omega_{pd}\omega-k^2v_{td}^2\gamma_d\mu_d-\omega_{cd}^2-\frac{\omega_{pd}^2}{\left(1+\frac{1}{\Omega_e^2}+\frac{\omega_{pi}^2}{\Omega_i^2\omega_{pi}^2-i2\upsilon_i(\omega-k_z v_{di})}\right)}=0, \tag{6.17}$$

In the absence of current drift, and plasma neutral collisions, the dispersion relation is similar to as given by Xie and Chen [45] {cf. Eq. (16) p.3521} and Kaw and Sen [40] {cf. Eq. (13) p.3554}. As $\Omega_e^2\approx k^2\lambda_{De}^2+V_{Ae}^2\gg 1$ and $1/\Omega_e^2\ll 1$, hence the contribution of electron term is neglected to observe low frequency perturbations.

Let $\omega=\omega_r+i\gamma$, where $\omega_r\gg\gamma$ is the real frequency and γ is the growth rate of longitudinal waves. Equation (6.17) can further be simplified to obtain real frequency and growth rate as

$$\omega_r = \omega_{pd}\left[\frac{P}{Q}+k^2a^2\gamma_d\mu_d+\omega_{cd}^2/\omega_{pd}^2-\left(\eta^*k^2a^2\right)^2\right]^{1/2}, \qquad (6.18)$$

where $P=\left[\left(\Omega_i^2\omega_{pi}^2\right)^2+4k_z^2\nu_{di}^2\nu_i^2\right]$ and $Q=\left[\left(\Omega_i^2\left(1+\Omega_i^2\right)\omega_{pi}^4\right)+4k_z^2\nu_{di}^2\nu_i^2\right]$.

The growth rate is given by

$$\gamma=\left[\frac{k_z\nu_{di}\nu_i\omega_{pi}^2}{P\omega_{pd}}\omega_r^3-\frac{\eta^*k^2a^2}{2}\right]. \qquad (6.19)$$

In the absence of current drift, and plasma neutral collisions, the above results are same as solutions given by Xie and Chen [45] {cf. Eqs.(17) & (18)}. It is observed that the viscosity plays an important role in damping of wave modes. Now critical drift speed of ions can be obtained from Eq. (6.19) which is given by

$$v_{di}^c \approx \frac{\eta^*k^2r_d^2\omega_{pd}^3}{2k_z\omega_{pd}\nu_i\omega_{pi}^2\omega_r^3}\left(k^2v_{ti}^2+\omega_{ci}^2+\nu_i^2\right)^2. \qquad (6.20)$$

Equation (6.20) shows that critical drift velocity of ions depends on the phase speed of longitudinal wave modes, collisional frequency of ions and strong coupling parameter in a collisional strongly coupled plasma. Longitudinal modes in general are ion dust hybrid kind of modes containing ion cyclotron and dust cyclotron motions.

B. Transverse Mode

The transverse mode arises as a result of rigidity provided by strong correlations to the transverse motion of waves. For simplicity we consider the propagation of wave nearly parallel to the direction of magnetic field. Hence, we can eliminate the longitudinal component by operating $\nabla\times$ on both sides of Eq. (6.1).

On simplifying, we get,

$$\left(\omega+i\eta_2\right)\vec{k}\times\delta\vec{u}_d+i\frac{Z_de}{m_d}\left(\vec{k}\times\delta\vec{E}\right)+i\frac{Z_de}{m_dc}\left(\vec{k}\bullet\vec{B}\right)\delta\vec{u}_d=0. \qquad (6.21)$$

If electric and magnetic fields are neglected, then Eq. (6.21) gives

$$\left(\left(1-i\tau_m\omega\right)i\omega m_d n_{d0}-\eta k^2\right)\vec{k}\times\delta\vec{u}_d=0. \tag{6.22}$$

Equation (6.22) is same as the dispersion relation for transverse shear waves given by Kaw and Sen [40] {cf. Eq. (20) p.3555}.

Now as we are interested for case when electric and magnetic both fields are present along with current drifts so Eq. (6.21) can be simplified to obtain perturbed velocities of dust along x and y direction as under

$$\delta u_{dx}=\frac{Z_d e/m_d\,\omega_{cd}\delta E_y-iZ_d e/m_d\delta E_x\left(\omega+i\eta_2\right)}{\left[\left(\omega+i\eta_2\right)^2-\omega_{cd}^2\right]}, \tag{6.23}$$

and

$$\delta u_{dy}=\frac{-Z_d e/m_d\,\omega_{cd}\delta E_x-iZ_d e/m_d\delta E_y\left(\omega+i\eta_2\right)}{\left[\left(\omega+i\eta_2\right)^2-\omega_{cd}^2\right]}. \tag{6.24}$$

Using Eqs. (6.23) & (6.24) in continuity equation for dust particle, we get perturbed density of dust as

$$\delta n_d=\frac{k_x^2 Z_d e n_{d0}/m_d\left(\omega+i\eta_2\right)}{\omega\left[\omega_{cd}^2-\left(\omega+i\eta_2\right)^2\right]}\phi. \tag{6.25}$$

The electron and ion densities can be obtained by neglecting transport parameters in Eq. (6.25)

$$\delta n_e=\frac{k_x^2 e n_{e0}/m_e}{\left[\omega_{ce}^2-\omega_1^2\right]}\phi \tag{6.26}$$

and

$$\delta n_i=\frac{-k_x^2 e n_{i0}/m_i}{\left[\omega_{ci}^2-\omega_2^2\right]}\phi. \tag{6.2}$$

Substituting the values of perturbed densities of dust, electrons and ions in Poisson equation, we get dispersion relation for transverse waves as

$$1+\frac{\omega_{pi}^2}{\left(\omega_{ci}^2-\omega_2^2\right)}+\frac{\omega_{pd}^2\left(\omega+i\eta_2^{'}\right)}{\omega\left[\omega_{cd}^2-\left(\omega+i\eta_2^{'}\right)^2\right]}=\frac{\omega_{pe}^2}{\left(\omega_1^2-\omega_{ce}^2\right)}, \tag{6.28}$$

where $\eta_2^{'}=\dfrac{\eta k^2}{\left(1-i\tau_m\omega\right)m_d n_{d0}}$.

Equation (6.28) is similar to the dispersion relation obtained by Xie and Chen [45] {cf. Eq. (33) p.3522} in the absence of current drifts and collisional frequencies of plasma constituents. Also, if magnetic field is absent then the above equation gives the same results as is given by Kaw and Sen [40] {cf. Eqs.(22) p.3556}.

Now Eq. (6.28) can be simplified in the regime, $\omega\tau_m \ll 1$ taking $\omega \ll \eta_2^{'} \ll \omega_{cd}$ and $\omega \ll \omega_{ci}$ as

$$\omega^2\left(\frac{\omega_{pi}^2}{\Omega_1^{'2}}+\frac{\omega_{pd}^2}{\omega_{cd}^2}-i\frac{2k_z\nu_{di}\nu_i\omega_{pi}^2}{\Omega_1^{'4}}\right)-i\frac{\eta_2^{''}\omega_{pd}^2}{\omega_{cd}^2}\omega-k^2c^2=0, \tag{6.29}$$

where $\eta_2^{''}=\dfrac{\eta k^2}{m_d n_{d0}}$ and $\Omega_1^{'2}=\left(\omega_{ci}^2-k_z^2\nu_{di}^2+\nu_i^2\right)$.

Equation (6.29) is the dispersion relation for transverse mode in regime $\omega\tau_m \ll 1$ which is similar to Eq. (34) of Xie and Chen [45] {see p.3523} if we neglect drift velocities and collisional frequencies of plasma constituents. Equation (6.29) can be simplified to give real frequency and the growth rate of transverse mode as

$$\omega_r = kc\left(\frac{\omega_{pi}^2}{\Omega_1^{'2}}+\frac{\omega_{pd}^2}{\omega_{cd}^2}\right)^{-1/2} \tag{6.30}$$

and

$$\gamma = \left(-\frac{\eta_2^{''}\omega_{pd}^2}{2\omega_{cd}^2} + \frac{k_z v_{di} \nu_i \omega_{pi}^2}{\Omega_1^{'4}} \omega_r \right) \times \left(\frac{\omega_{pi}^2}{\Omega_1^{'2}} + \frac{\omega_{pd}^2}{\omega_{cd}^2} \right)^{-1}, \qquad (6.31)$$

which (in the absence of magnetic fields) is similar to the results given by Kaw and Sen [40] for transverse mode and the special case of strong coupling for transverse mode as discussed by Xie and Chen [45] if drifting current and collisions of plasma constituents with neutrals are neglected. In general, it is a dust modified whistler ion wave. In the absence of current drift, plasma neutral collisions and magnetic field, Eq. (6.31) yields a purely damped mode similar to Kaw and Sen [40] {cf. Eq. (23) p.3556}.

Now the critical drift can be easily obtained from the growth rate of transverse mode {cf. Eq. (6.31)} as

$$v_{di}^{c} \approx \frac{\eta_2^{''}\omega_{pd}^2 \omega_{ci}^4}{2k_z \omega_{cd}^2 \nu_i \omega_{pi}^2 \omega_r}. \qquad (6.32)$$

Equation (6.32) shows that the critical drift velocity of ions depends on parallel wave vector, strong coupling parameter and phase velocity of transverse waves.

6.2.1 Results and Discussion

We studied the excitation of low frequency electrostatic modes in strongly coupled collisional magnetized dusty Argon plasma in the presence of current drift of plasma constituents. The laboratory parameters for strongly coupled collisional [63] plasma systems considered are as follows: density of ions, dust and electrons are given as $n_{d0}/n_{i0} \sim 5\times10^{-4}$, $n_{e0} \approx 0.5\, n_{i0}$, respectively, here $n_{i0} \approx 10^8 \mathrm{cm}^{-3}$ dust charge $-Z_d e \approx -10^3 \mathrm{e}$, electron temperature $T_e \simeq 1.0eV$, ion temperature=dust temperature $T_i \sim T_d = 0.3eV$, dust grain size a=5.0 x10^{-4} cm, a weak guide magnetic field B~ 400 Gauss, strong coupling parameter, $\Gamma \gg 1$, collisional frequency of ions, $\nu_i = 0.5\, \omega_{ci}$. The drift velocity of ions is $v_{di} \sim (0-3.0)\, v_{ti}$, where v_{ti} refers to ion's thermal speed. Our results follow the condition of strong coupling plasmas having parameter in the

range i.e., $\lambda_D > a_d \gg \lambda_{Dd}$, where λ_D is plasma Debye length $\sim \lambda_{Di}$ (ion's Debye length), a_d is intergrain spacing, and λ_{Dd} is dust Debye length. Moreover, we have considered the screening constant $\kappa = \frac{a_d}{\lambda_D} < 1$ so the OCP results for transport coefficient can be applied [62] but for $\kappa = \frac{a_d}{\lambda_D} \geq 1$, one must use the results of Yukawa fluid simulations [64].

Our dispersion relations {cf. Eqs. (6.16) and (6.28)} obtained for current driven electrostatic wave modes for regime, $\omega\tau_m \ll 1$ are well matched with the dispersion relations of longitudinal and transverse modes as given by Xie and Chen [45] in the absence of current drift and collisionality. Moreover, if electric and magnetic fields are absent our results are same as Kaw and Sen [40]. Longitudinal modes are like ion dust hybrid modes. Now, if coupling parameter is strong enough to make viscosity term larger than the current drift terms as given in Eq. (6.19), then longitudinal modes are purely damped as given by Xie and Chen [45] {cf. Eq. (18)}. Transverse modes are like dust modified ion cyclotron and whistler ion wave modes same as Xie and Chen [45] in a magnetized strongly coupled plasmas.

We have plotted the real frequency of longitudinal modes using Eq. (6.18) in Fig. 6.1. The plot of normalized frequencies of longitudinal modes $\left(\omega_r/\omega_{pd}\right)$ with normalized wave number $\left(ka_d\right)$, for different Coupling parameters $\Gamma = 10,\ 29,\ 65$ and 85 in the presence of small drift velocity of ions, $v_{di} = 0.2\ v_{ti}$ & $\nu_i = 0.5\ \omega_{ci}$ is as shown by Fig. 6.1. Here $k \approx k_x \gg k_z$.

It is observed that the normalized frequency of longitudinal waves increases with normalized wave number in the presence of drift in a magnetized plasma but decreases with increase in strong coupling parameter at higher wave number. The increase of mode frequency with wave number is in line with the results given by Chow and Rosenberg [36] for electrostatic ion cyclotron instability. For long wavelength regime

i.e., $ka_d \leq 1$, normalized frequency ~25 Hz is observed which shows the low frequency waves in presence of magnetic field and current drift of ions.

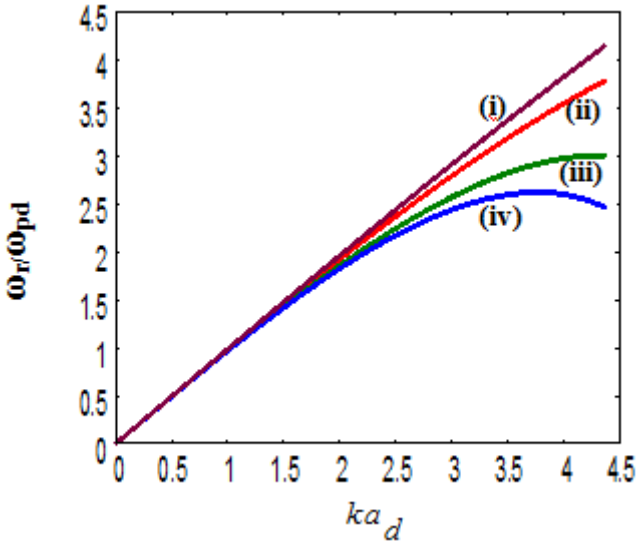

Fig. 6.1 Normalized frequency ω_r/ω_{pd} of longitudinal waves as a function of normalized wave number $\left(ka_d\right)$ for strong coupling parameters Γ(i, ii, iii, iv) = 10, 29, 65, 85, $v_i = 0.5\ \omega_{ci}$, $v_{di} = 0.2v_{ti}$ and $k_z = 2.0$ cm^{-1}.

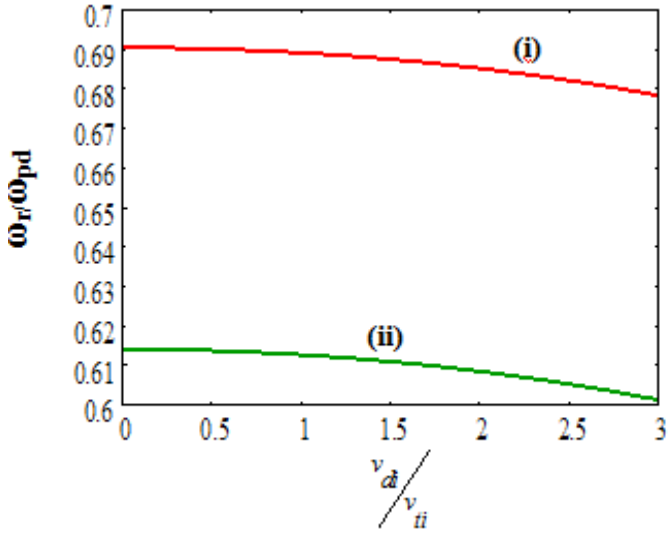

Fig. 6.2 Normalized frequency ω_r/ω_{pd} of longitudinal waves as a function of normalized drift velocity of ions v_{di}/v_{ti}, for strong coupling parameters Γ **(i)** Γ = **29** and **(ii)** Γ = **65.** Given: $v_i = 0.5\ \omega_{ci}$, $k = 20$ cm^{-1} and $k_z = 2.0$ cm^{-1}.

This result is similar to the low frequencies acoustic modes (~15 Hz) observed by Praburam and Goree [39] and Barkan *et al.* [25]. The effect of strong correlation parameter cannot be significantly observed in long wavelength regime but in short wavelength regime $ka_d \geq 1$ shows a reduction in mode frequency. Our dispersion results are in line with results obtained by Rosenberg and Kalman [27] {cf. Fig 1 p.7171}, Kaw and Sen [40] {cf. Fig. 1. p.3555} and Kaw [43].

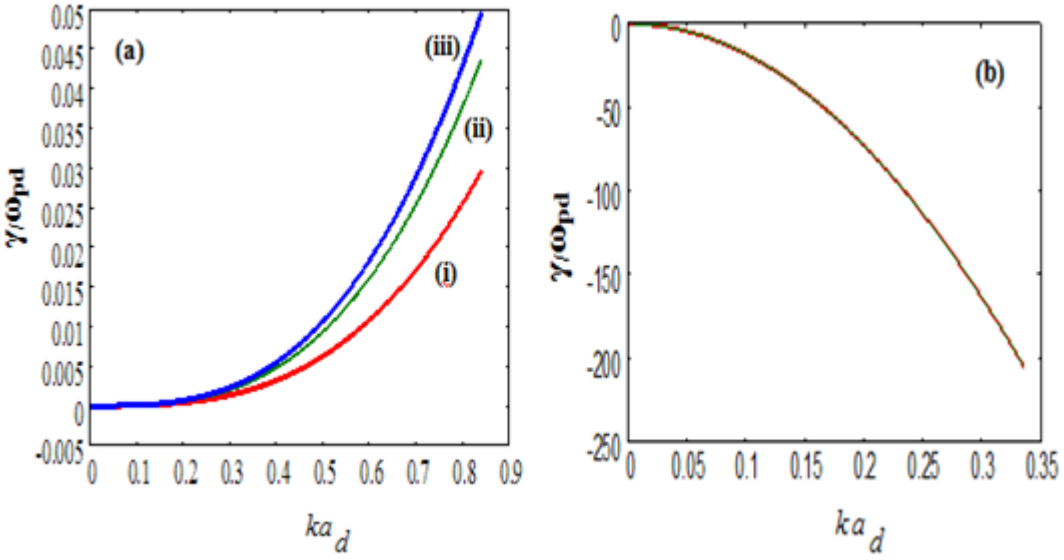

Fig. 6.3 Normalized growth rate γ/ω_{pd} of longitudinal waves as a function of normalized wave number $\left(ka_d\right)$ for strong coupling parameters, Γ(i, ii, iii = 29, 65, 85) [Note: all Γ values lie on the same line.] **(a)** for $\nu_i = 0.5\omega_{ci}$, $v_{di} = 0.2v_{ti}$ and $k_z = 2.0$ cm^{-1} **(b)** for $\nu_i = 0.0$, $v_{di} = 0.0$ and $k_z = 2.0$ cm^{-1}.

In Fig. 6.2 we have plotted the normalized frequency ω_r/ω_{pd} of longitudinal modes with normalized drift velocity of ions v_{di}/v_{ti} for different strong coupling parameter. The plot shows a slight decrease in the mode frequency with a large increase in drift velocity of ions from (0.0 -3.0) v_{ti}. For a small drift velocity of ions the frequency remains nearly the same. The behaviour of frequency with drift velocity depends on the parallel wave vector k_z which for longitudinal waves is considered small. For large k_z, the frequency shows an appreciable decrease with increasing v_{di} and beyond $v_{di} \geq v_{ti}$, it shows an increase which implies that a large drift velocity of

ions is required to enhance the frequency of longitudinal modes in a magnetized strongly coupled plasma.

In Fig. 6.3(a), we have plotted the normalized growth rate γ/ω_{pd} of longitudinal modes with normalized wave number ka_d for different strong correlation parameter $\Gamma = 29,\ 65$ and 85 using Eq. (6.19). It is observed that the growth rate of longitudinal waves increases with the normalized wave vector in the presence of drift and collisions of ions in a magnetized dusty plasmas.

Ion drifts overcome the damping effect of transport coefficients resulting in to an increase in growth rate of longitudinal waves. This result is similar to results of Merlino *et al.* [51] which showed an increase in growth rate of ion acoustic instability with the electric field that supports the current driven instability. It is also observed that at much larger k values~$10^3 cm^{-1}$, the growth rate shows a decrease. This shows that for very short wavelengths growth rate of longitudinal modes is reduced as the effect of viscous damping may overcome the increase due to drift. The growth rate of longitudinal modes is higher for large strong coupling parameters Γ than for small coupling parameters at a constant value of k.

In Fig. 6.3 (b), we have also plotted the normalized growth rate γ/ω_{pd} of longitudinal modes with normalized wave vector $\left(ka_d\right)$ for different strong correlation parameter $\Gamma = 29,\ 65$ and 85 using Eq. (6.19) in the absence of drift of ions and collisions, and observed a purely damped mode as was observed by Kaw and Sen [40] and Xie and Chen [45]. The effect of increase in strong correlation factor is not significantly observed.

We have plotted normalized ion drift velocity v_{di}/v_{ti} with normalized wave number k/k_z of longitudinal modes in Fig. 6.4, using Eq. (6.20). It is observed that the critical drift required for exciting the longitudinal modes decreases with increasing perpendicular wave number k. It is also observed that the value of critical drift at a particular k value increases with strong coupling parameter. The experimental verification of this fact for strongly coupled dusty plasmas is not present till now. But it

is foremost understood that the damping effects of strong coupling parameter needed a large drift velocity of ions to support the growth of longitudinal modes.

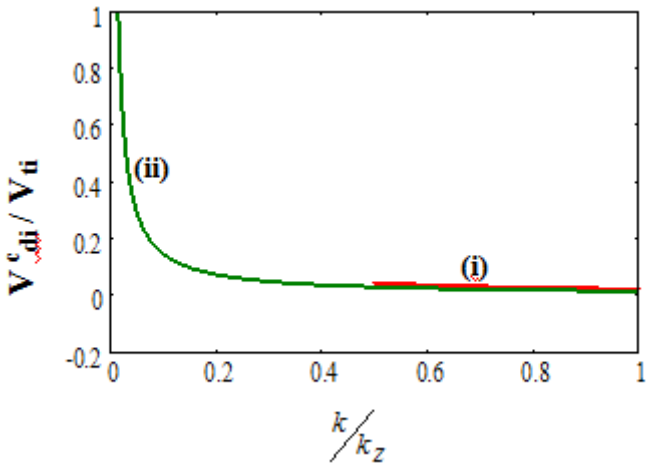

Fig. 6.4 Normalized critical drift speed of ions $\left(v_{di}^{c}/v_{ti}\right)$ of longitudinal waves as a function of normalized wave number k/k_z for strong coupling parameter, $\Gamma(i,\ ii) = 10,\ 29.$ (The parameters are same as Fig. 6.1.)

Now to investigate the behaviour of transverse waves in presence of drifting ion currents and ion neutral collisions, we have plotted in Fig. 6.5 using Eq. (6.30), the normalized frequency of transverse modes ω_r/ω_{pd} with normalized wave number k/k_z for different strong coupling parameters, $\Gamma(\text{i, ii, iii} = 29, 65, 85)$. It is observed that the frequency of transverse modes increases with increasing the wave number k. In this case $k \approx k_x \ll k_z$ .Our results of increase in frequency of transverse mode are in line with Kaw and Sen [40], Kaw [43], Murillo [42] and Nonumura et al. [41] {cf. Fig. 4 p.5143}.

It is observed that a small wave number k (in transverse direction) is required to study transverse modes in presence of magnetic field than the longitudinal modes. This characterizes the transverse modes as long wavelength modes as described by [27] & [40]-[42]. It is also investigated that the frequency for weakly collisional ($\nu_i = 0.05\ \omega_{ci}$

), and strongly collisional ($\nu_i = 0.5\ \omega_{ci}$) plasma are same but decreases with strong coupling parameter.

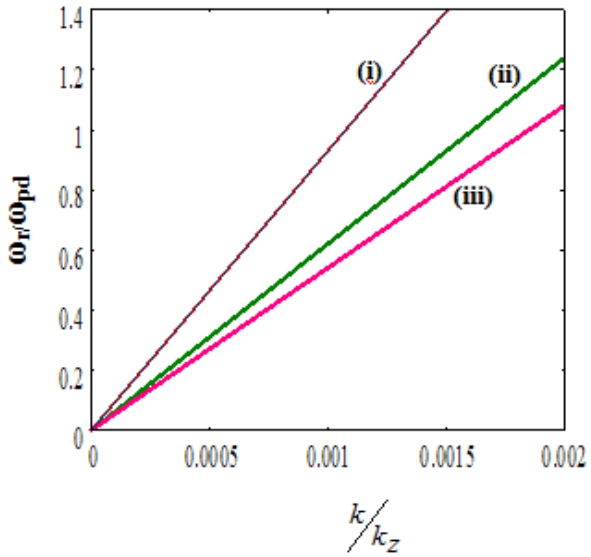

Fig. 6.5 Normalized frequency ω_r/ω_{pd} of transverse waves as a function of normalized wave number k/k_z, for strong coupling parameters Γ(i, ii, iii) = 29, 65, 85, Given: $\nu_i = 0.5\ \omega_{ci}$, $\nu_{di} = 0.2\ \nu_{ti}$ and $k_z = 0.07$ cm^{-1}.

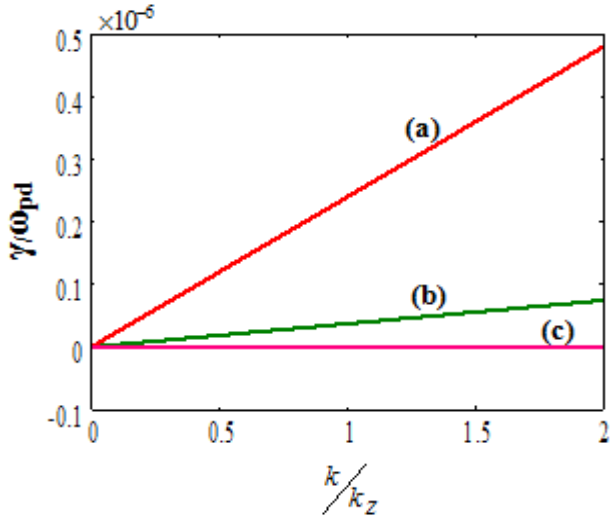

Fig. 6.6 Normalized growth rate, γ/ω_{pd} of transverse waves as a function of normalized wave number k/k_z for strong coupling parameters Γ(i, ii, iii= 29, 65, 85), **(a)** $\nu_i = 0.5\ \omega_{ci}$, $\nu_{di} = 0.2\ \nu_{ti}$ **(b)** $\nu_i = 0.05\ \omega_{ci}$, $\nu_{di} = 0.2\ \nu_{ti}$ **(c)** $\nu_i = 0.0$, $\nu_{di} = 0.0$ Given : $k_z = 0.07$ cm^{-1}. [Note: all Γ values lie on the same line.]

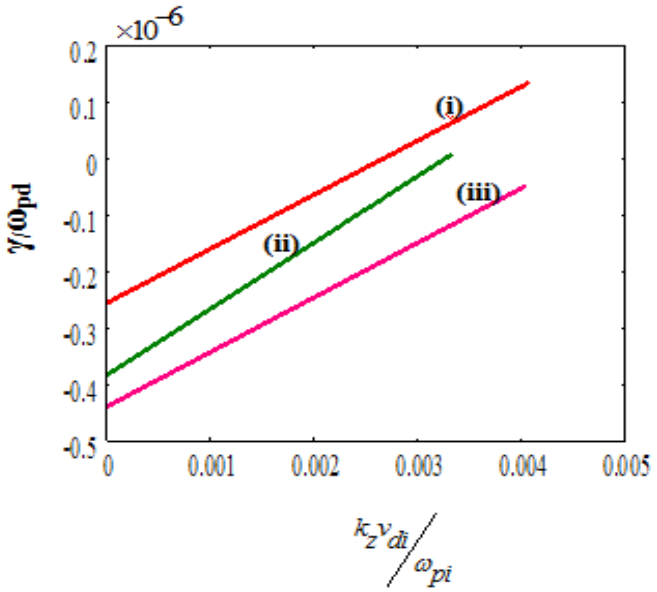

Fig. 6.7 Normalized growth rate, γ/ω_{pd} of transverse waves as a function of normalized ion's drift velocity $\left(k_z v_{di}/\omega_{pi}\right)$ for strong coupling parameters Γ(i, ii, iii= 29, 65, 85). Given: $\nu_i = 0.5\ \omega_{ci}$, $v_{di} = (0.0-1.0)v_{ti}$, $k_z = 0.1\ \text{cm}^{-1}$, $k = 0.01\ \text{cm}^{-1}$.

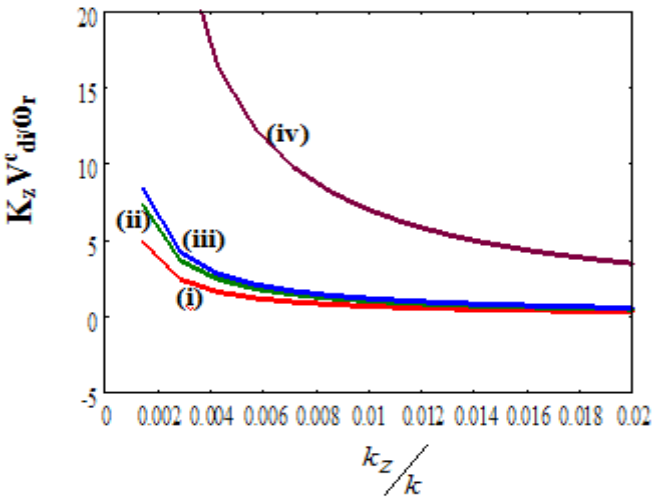

Fig. 6.8 Normalized critical drift speed of ions, $\left(k_z v^c_{di}/\omega_r\right)$ of transverse waves as a function of normalized wave number k_z/k for strong coupling parameters Γ(i, ii, iii, iv=10, 29, 65, 85). Given: $\nu_i = 0.5\ \omega_{ci}$, $k = 0.07\ \text{cm}^{-1}$.

The group velocity is proportional to wave number k similar to Wang *et al.* [65]. It is also observed that the drift of ions does not have a significant effect on frequency of transverse modes only shows a slight decrease. These results are in line with results given by Kaw [43] that the wavelength of transverse modes increases with electric field showing the long wavelength transverse oscillations.

The normalized growth rate γ/ω_{pd} of transverse modes is plotted with normalized wave number k/k_z using Eq. (6.31) as shown in Fig. 6.6. It is observed that the growth rate of transverse modes also increases with normalized wave number but its dependence on the strong coupling parameter is washed out. We have plotted the growth rate for different collisional frequencies of ions and observed that the growth of transverse modes is large in strongly collisional plasmas and in presence of drift velocity of ions {see Fig. 6.6}. These results are in line with the experimental results for transverse waves given by Nonumura *et al.* [41] which showed an increase of growth rate with wave number {cf. Fig 4(a) p.5143}. Now in the absence of drifts and ion neutral collisions our results well matched the dispersion curves for transverse shear modes as given by Kaw [43] {cf. Fig. 7 (b) p.1876, the uncoupled mode}.

In Fig. 6.7, we have plotted the normalized growth rate γ/ω_{pd} of transverse modes with normalized drift speed of ions $\left(k_z v_{di}/\omega_{pi}\right)$ and observed that the growth rate of transverse modes increases significantly in the presence of ion drifts. These results are similar to Merlino *et al.* [51] for unmagnetized plasma in presence of electric field drifts that the growth of ion acoustic instability increases with electric field and hence field drifts. In Fig. 6.8 we have plotted the normalized critical drift speed of ions $k_z v_{di}^c/\omega_r$ with normalized wave number k_z/k and found that the critical drift speed of ions decreases with normalized wave number and increases with the strong coupling among dust grains.

6.2.2 Conclusion

We have investigated the excitation of low frequency electrostatic waves by current drifts in a collisional strongly coupled magnetized dusty plasma for the case,

$\omega\tau_m \ll 1$, as the typical system parameters support this regime. It is found that the current drift plays a significant role in exciting longitudinal waves and transverse waves. Our frequencies for the longitudinal modes well matched with frequencies observed by Chu *et al.* [19], Barkan *et al.* [25] and Praburam and Goree [39]. The current drifts of ions do not have a significant effect on wave frequencies for both the modes. But for large magnetic field aligned currents, the frequency and growth rate of modes are significantly modified. Our results are in line with result given by Pandey *et al.* [54]. As we observed the magnetized plasma so effect of strong coupling parameter is overpowered by cyclotron frequencies of electron and ions in transverse modes. The collisionality enhances the growth of transverse modes. Our results are in line with the results of Xie and Chen [45] and Kaw and Sen [40] & [43] under specific conditions and may be useful for study of laboratory magnetized dusty plasmas in strong coupling regime. Our results mainly focus on the laboratory plasmas but may also be useful for near earth space environments, ionosphere and cometary physics [66] as it contains a substantial amount of dust, neutral gases and source of current drifts.

6.3 Nonlocal Theory (Strongly Coupled Kinetic regime $\omega\tau_m \gg 1$)

We consider a collisional strongly coupled dusty plasma cylinder of radius r_0 having electrons, ions and dust grains. An axial magnetic field B is applied along z direction. The equilibrium densities, charge, mass and temperature of electrons, ions, and dust grains are similar to as mentioned previously in local plasma analysis (see sec. 6.2). The neutral collisional frequencies of electrons, ions and dust grains are given by ν_e , ν_i and ν_d , respectively. The magnetic field aligned drift velocities of electrons, ions and dust grains are given by v_{de}, v_{di} and v_{dd}, respectively. The electrostatic perturbations $\sim e^{-i(\omega t-\vec{k}\bullet\vec{r})}$ are applied. The GH momentum equation used to describe dust motion [61] in the fluid regime with $\Gamma < 170$, is given as

$$\left(1+\tau_m\frac{\partial}{\partial t}\right)\left[m_d n_{d0}\frac{\partial}{\partial t}\delta\vec{u}d+\nabla\delta P+Z_d e n_{d0}\delta\vec{E}+\frac{1}{c}Z_d e n_{d0}\delta\vec{u}d\times\vec{B}\right.$$

$$+m_d n_{d0} \nu_d \delta\vec{u}d \Big] = \eta \nabla.\nabla \delta\vec{u}d + \left(\zeta + \frac{\eta}{3}\right) \nabla\left(\nabla.\delta\vec{u}d\right). \quad (6.33)$$

The terminologies used are same as the previous local analysis sec 6.2. The compressibility of dust fluid μ_d, and functional relations for transport coefficients η^* and τ_m^* are given by Eqs.(6.2), (6.4) & (6.5), respectively. Now we will discuss the longitudinal and transverse modes for the bounded cylindrical plasma in the strongly coupled kinetic regime $\omega\tau_m \gg 1$.

A Longitudinal Mode

These modes propagate nearly perpendicular to magnetic field with a finite k_z so that the electrons and ions remain nearly in Boltzmann equilibrium [67] and the dust provides inertia. Using equation of continuity {see Eq. (6.6)} and compressibility equation {see Eq. (6.2)} in Eq. (6.33), we get perturbed velocity of dust grains as

$$\delta u_d = \frac{\left(-Z_d e n_{d0} \delta E\right)}{\mathrm{A}}, \quad (6.34)$$

where $A = \Bigg[im_d n_{d0} \left(\frac{k^2 \gamma_d \mu_d T_d}{\left(\omega - k_z v_{dd}\right) m_d} - \left(\omega - k_z v_{dd} + i\nu_d\right) \right) + \frac{k^2 \left(\zeta + \frac{4}{3}\eta\right)}{\left(1 - i\tau_m \omega\right)}$

$$+ \frac{\omega_{cd}^2 m_d^2 n_{d0}^2}{\left(\frac{\eta k^2}{\left(1 - i\tau_m \omega\right)} - i\left(\omega - k_z v_{dd} + i\nu_d\right) m_d n_{d0} \right)} \Bigg]. \quad (6.35)$$

Here $\omega_{cd} = \left[-\left(Z_d e\right) B \Big/ m_d c \right]$ is dust cyclotron frequency. Now the perturbed dust density is given by

$$\delta n_d = \frac{ik^2 \phi Z_d e n_{d0}^2}{(\omega - k_z v_{dd}) A}, \quad (6.36)$$

where A is same as Eq.(6.35). The perturbed electron and ion densities can be simply

obtained by neglecting transport coefficients η, ζ, τ_m and using $\gamma_d = 1$, $\mu_d = 1$ in Eq.(6.36) as

$$\delta n_j = \pm \frac{e n_{j0} k^2 \phi}{m_j \left[k^2 v_{tj}^2 + \omega_{cj}^2 - \left(\omega - k_z v_{dj} + i\nu_j\right)\left(\omega - k_z v_{dj}\right) \right]} \tag{6.37}$$

where $j = e$ or i, $v_{tj} = \left[T_j / m_j\right]^{1/2}$ be the thermal velocities of electrons or ions and $\omega_{cj}\left[= \mp eB / m_j c \right]$ be the cyclotron frequencies of electrons or ions, respectively. Substituting the perturbed densities of dust, electrons and ions in Poisson equation $-\nabla^2\phi = 4\pi\left(-e\delta n_e - Z_d e\delta n_d + e\delta n_i\right)$ and rewriting it for axially and azimuthally symmetric cylindrical case as a second order differential equation in ϕ, we get

$$\frac{\partial^2 \phi}{\partial r^2} + \frac{1}{r}\frac{\partial \phi}{\partial r} + q^2 \phi = -\frac{\omega_{pd}^2 k_z^2 \phi}{(\omega - k_z v_{dd}) A}, \tag{6.38}$$

where

$$q^2 = -k_z^2 - k^2 \left[\frac{\omega_{pe}^2}{\left[k^2 v_{te}^2 + \omega_{ce}^2 - \left(\omega - k_z v_{de} + i\nu_e\right)\left(\omega - k_z v_{de}\right) \right]} + \frac{\omega_{pi}^2}{\left[k^2 v_{ti}^2 + \omega_{ci}^2 - (\omega - k_z v_{di} + i\nu_i)(\omega - k_z v_{di}) \right]} + \frac{\omega_{pd}^2 k_\perp^2 \phi}{k^2 (\omega - k_z v_{dd}) A} \right]. \tag{6.39}$$

In the absence of dust dynamics i.e., $\omega_{pd} = 0$. The solution of Bessel equation is given by:

$$\phi = U J_0(q_m r), \tag{6.40}$$

where U is a constant and the function, $J_o\left(q_m r\right)$ is called the zero-order Bessel functions of argument $\left(q_m r\right)$. At plasma boundary $r = r_0$, potential ϕ must vanish so

the solution of Eq. (6.38) is given by $J_o\left(q_m r_0\right)=0$, i.e., $q_m = x_m/r_0$. Here $(m = 1,2,....)$, and x_m are the zeros of the Bessel function $J_o(x)$. The finite cylindrical boundaries led to an effective perpendicular wave number which is given by $k_\perp{}^2 \cong q_m^2 = \left(\frac{x_m}{r_0}\right)^2$ such that $k^2 \approx q_m^2 + k_z^2$. We also consider, $k^2\left(=k_\perp^2+k_z^2\right)$ $\approx q_m^2 \gg k_z^2$.

On the surface of cylindrical waveguide, $J_o(x) = 0$ then $x = 2.404$, and hence the effective radial wave number is given by $q_m = 2.404/r_0$. In the presence of dust dynamics, the solution of the wave function ϕ can be given by a set of orthogonal wave functions:

$$\phi = \sum_m A_m J_0(q_n r). \tag{6.41}$$

Using the value of ϕ from Eq. (6.41) in Eq. (6.38) and multiplying both sides of Eq. (6.38) by $rJ_0(q_n r)$ and integrating over r from 0 to r_0 (where r_0 is the plasma radius), retaining only the dominant mode (m=n), we get

$$q^2 - q_m^2 = -\frac{\omega_{pd}^2 k_z^2 I}{(\omega - k_z v_{dd})A}, \tag{6.42}$$

where $I = \dfrac{\int_0^r rJ_o\left(q_m r\right)J_o\left(q_n r\right)dr}{\int_0^{r_0} rJ_o\left(q_m r\right)J_o\left(q_n r\right)dr}$.

Using the value of q^2 from Eq. (6.39) in Eq. (6.42) and simplifying in the limit, $\omega \ll k_z v_{de}, \nu_e \ll k v_{te} < \omega_{ce}$, we obtain the dispersion relation for longitudinal mode

$$1+\frac{1}{\Omega_e^2}+\frac{\omega_{pi}^2}{\left[\Omega_i^2\omega_{pi}^2 - i\nu_i\left(\omega - k_z v_{di}\right)\right]}-\frac{\omega_{pd}^2 I}{\left(\omega - k_z v_{dd}\right)A}=0, \tag{6.43}$$

where, $\Omega_e^2 = q_m^2\lambda_{De}^2 + V_{Ae}^2$, $\Omega_i^2 = \left(q_m^2\lambda_{Di}^2 + V_{Ai}^2 - \left(k_z^2 v_{di}^2/\omega_{pi}^2\right)\right)$ and A is given by Eq. (6.35). Here $\lambda_{De}\left(=v_{te}/\omega_{pe}\right)$, $\lambda_{Di}\left(=v_{ti}/\omega_{pi}\right)$, $V_{Ae}\left(=\omega_{ce}/\omega_{pe}\right)$ and $V_{Ai}\left(=\omega_{ci}/\omega_{pi}\right)$. In the absence of dust drifts and magnetic field, Eq. (6.43) is similar to dispersion relation for longitudinal dust acoustic perturbations in presence of ion streaming effects given by Kaw and Sen [40, Eq. (28), p. 3556]. In the absence of strong coupling effects, magnetic field, and dust drift Eq. (6.43) will yield similar results as the dispersion relations given for dust acoustic waves in the presence of streaming of ions and collisional effects for unmagnetized weakly coupled dusty plasmas [47, Eq. (5.2.15) , p.141].

In the limit $\omega\tau_m \gg 1$, Eq. (6.43) yields the dispersion relation for longitudinal dust modes as

$$\left(\omega - k_z v_{dd}\right)^2 + iv_d\left(\omega - k_z v_{dd}\right) - q_m^2\gamma_d\mu_d v_{td}^2 - q_m^2 a_d^2\omega_{pd}^2\frac{\eta_2^*}{\tau_m^*} - \frac{\omega_{cd}^2}{\left(\frac{\left(\omega - k_z v_{di} + iv_d\right)}{\omega} - \frac{\eta_1^*}{\tau_m^*}\frac{q_m^2 a_d^2\omega_{pd}^2}{\omega^2}\right)}$$

$$= \frac{\omega_{pd}^2 I}{\left(1 + \frac{1}{\Omega_e^2} + \frac{\omega_{pi}^2}{\left[\Omega_i^2\omega_{pi}^2 - iv_i\left(\omega - k_z v_{di}\right)\right]}\right)}, \qquad (6.44)$$

Here $\eta_1^* = \dfrac{\eta}{\omega_{pd} m_d n_{d0} a_d^2}$ and $\eta_2^* = \dfrac{\left(\zeta + \frac{4}{3}\eta\right)}{m_d n_{d0}\omega_{pd} a_d^2}$.

Equation (6.44) is the dispersion relation for current driven longitudinal dust modes in a magnetized strongly coupled collisional dusty plasma cylinder. In the absence of current drifts and collisions, Eq. (6.44) is similar to the dispersion relation given by Xie and Chen [45, Eq. (19), p.3522]. Under assumptions $\omega^2 \ll \omega_{ci}^2 \ll \omega_{ce}^2$,

$k_z v_{dd} \ll |\omega| \ll k_z v_{di}$, $1/\Omega_e^2 \ll 1$ and $\omega^2 \gg \eta_1^* q_m^2 a_d^2 \omega_{pd}^2 / \tau_m^*$, Eq. (6.44) can be simplified to obtain longitudinal mode frequency as

$$\omega_r^l = k_z v_{dd} + \omega_{pd} \left[\frac{P}{Q} I + q_m^2 \lambda_d^2 \gamma_d \mu_d + \frac{\eta_1^*}{\tau_m^*} q_m^2 a_d^2 + \frac{\omega_{cd}^2}{\omega_{pd}^2} \right]^{1/2}, \tag{6.45}$$

where $P = \left[\left(\Omega_i^2 \omega_{pi}^2 \right)^2 + k_z^2 v_{di}^2 \nu_i^2 \right]$ and $Q = \left[\left(1+\Omega_i^2 \right)^2 \omega_{pi}^4 + k_z^2 v_{di}^2 \nu_i^2 \right]$.

The growth rate is given by

$$\gamma^l = \left[-\frac{\nu_d}{2} + \frac{k_z v_{di} \nu_i \omega_{pi}^2 \omega_{pd}^2}{2P(\omega_r - k_z v_{dd})} I + \frac{\nu_d}{2} \frac{\omega_{cd}^2}{\omega_{pd}(\omega_r - k_z v_{dd})} \right]. \tag{6.46}$$

Equation (6.46) shows that the longitudinal modes are ion dust hybrid like mode but in most of the experimental situations the dust remains unmagnetized and it is hard to observe the dust ion hybrid modes unless a large magnetic field is applied and the strong coupling among dust grains remain small. One can obtain critical drift of ions for the longitudinal dust modes from the condition of marginal stability $\left(\gamma^l = 0 \right)$ as given below

$$v_{di}^l \approx \frac{\nu_d \left(1+\Omega_i^2 \right)^2 \omega_{pi}^2}{2 k_z \nu_i \omega_{pd}^2 I} \left(\omega_r - k_z v_{dd} \right). \tag{6.47}$$

Equation (6.47) shows that critical drift velocity of ions depends on the phase speed of the waves, ion and dust neutral collisional frequencies, strong correlation parameter and finite geometry parameter I.

B. Transverse Shear Mode

The transverse shear mode is a mechanical disturbance which arises as a result of rigidity provided by strong correlations among dust grains. One can eliminate the longitudinal component by operating $\nabla \times$ on both side of Eq. (6.33). On simplifying Eq. (6.33), we get

$$\left(\omega + i\nu_d + i\eta_1\right)\vec{k}\times\vec{u}_d + i\frac{Z_d e}{m_d}\left(\vec{k}\times\delta\vec{E}\right) + i\frac{Z_d e}{m_d c}\left(\vec{k}\bullet\vec{B}\right)\delta\vec{u}_d = 0, \qquad (6.48)$$

where $\eta_1 = \frac{\eta k^2}{m_d n_{d0}\left(1 - i\tau_m\omega\right)}$.

In the absence of dust collisions, electric and magnetic fields Eq. (6.48) gives same dispersion relation as given by Kaw and Sen [40, Eq. (20) p.3555]. When electric and magnetic both fields are present along with ion and dust drifts, Eq. (6.48) can be simplified to obtain perturbed velocity of dust transverse to magnetic field as

$$\delta u_{d\perp} = \frac{\left(\omega + i\nu_d + i\eta_1\right)^2}{\left[\left(\omega + i\nu_d + i\eta_1\right)^2 - \omega_{cd}^2\right]}\left[\frac{k_\perp v_{dd}}{k_z} - \frac{i\frac{Z_d e}{m_d}\delta E_\perp}{\left(\omega + i\eta_1 + i\nu_d\right)}\right]. \qquad (6.49)$$

Using Eq. (6.49) in continuity equation, we get perturbed dust density as

$$\delta n_d = \frac{k_\perp^2\left(\omega + i\eta_1 + i\nu_d\right)Z_d e n_{d0}/m_d}{\left(\omega - k_z v_{dd}\right)\left[\omega_{cd}^2 - \left(\omega + i\eta_1 + i\nu_d\right)^2\right]}\phi. \qquad (6.50)$$

Similar to longitudinal case, electron and ion densities can be obtained by neglecting transport parameters as

$$\delta n_j = \pm\frac{k_\perp^2\left(\omega + i\nu_j\right)en_{j0}/m_e}{\left(\omega - k_z v_{dj}\right)\left[\omega_{cj}^2 - \left(\omega + i\nu_j\right)^2\right]}\phi, \qquad (6.51)$$

where j = e or i.

Substituting the values of perturbed densities of dust, electrons and ions in Poisson equation and simplifying it for axially and azimuthally symmetric case, we get

$$\frac{\partial^2\phi}{\partial r^2} + \frac{1}{r}\frac{\partial\phi}{\partial r} + p^2\phi = -\frac{\omega_{pd}^2 k_z^2\phi\left(\omega + i\nu_d + i\eta_1\right)}{\left(\omega - k_z v_{dd}\right)\left(\left[\omega_{cd}^2 - \left(\omega + i\nu_d + i\eta_1\right)^2\right]\right)}, \qquad (6.52)$$

where

$$p^2 = -k_z^2 + k_\perp^2 \left[\frac{\omega_{pe}^2 (\omega + i\nu_e)}{\left(\omega - k_z v_{de}\right)\left(\omega_{ce}^2 - (\omega + i\nu_e)^2\right)} - \frac{\omega_{pi}^2 \left(\omega + i\nu_i\right)}{\left(\omega - k_z v_{di}\right)\left(\omega_{ci}^2 - \left(\omega + i\nu_i\right)^2\right)} \right.$$

$$\left. + \frac{\omega_{pd}^2 k_\perp^2 \phi \left(\omega + i\nu_d + i\eta_1\right)}{\left(\omega - k_z v_{dd}\right)\left(\left[\omega_{cd}^2 - \left(\omega + i\nu_d + i\eta_1\right)^2\right]\right)} \right]. \qquad (6.53)$$

Now, simplifying the Bessel Eq. (6.52) in the similar way as is discussed earlier for the longitudinal mode, we get

$$1 + \frac{p_m^2}{k^2} \frac{\omega_{pi}^2 \left(\omega + i\nu_i\right)}{\left(\omega - k_z v_{di}\right)\left(\omega_{ci}^2 - \left(\omega + i\nu_i\right)^2\right)} + \frac{p_m^2}{k^2} \frac{\omega_{pd}^2 \left(\omega + i\nu_d + i\eta_1\right) I}{\left(\omega - k_z v_{dd}\right)\left(\omega_{cd}^2 - \left(\omega + i\nu_d + i\eta_1\right)^2\right)}$$

$$= \frac{p_m^2}{k^2} \frac{\omega_{pe}^2 (\omega + i\nu_e)}{\left(\omega - k_z v_{de}\right)\left((\omega + i\nu_e)^2 - \omega_{ce}^2\right)}, \qquad (6.54)$$

where $p_m = 2.404/r_0 \cong k_\perp$.

Equation (6.54) gives the dispersion for transverse shear dust wave mode in a bounded magnetized collisional plasma having strongly coupled dust grains in the presence of ion-dust drifts. In the absence of drifts, collisions, magnetic field and finite geometry (cylindrical), Eq. (6.54) yields the dispersion relation as given by Kaw and Sen for transverse mode [40, Eq. (22), p.3556]. Also, if only magnetic field is there, it becomes similar to [45, Eq. (33), p.3522].

Further Eq. (6.54) can be simplified in the limit, $\omega\tau_m \gg 1$ to obtain the low frequency dust wave modes, under assumptions $\omega \ll \omega_{ci}$, ν_i & ω_{ce}, ν_e and $\omega \ll \eta_1 \ll \omega_{cd}$ as

$$1-\frac{p_m^2}{k^2}\frac{i\nu_i\omega_{pi}^2}{k_z\nu_{di}\left(\omega_{ci}^2+\nu_i^2\right)}-\frac{p_m^2\omega_{pd}^2 I}{k^2\left(\omega-k_z\nu_{dd}\right)\left(\omega+i\nu_d-\frac{\eta k^2}{m_d n_{d0}\tau_m\omega}\right)}=0. \qquad (6.55)$$

Equation (6.55) can further be simplified as $\varepsilon_r(\omega,k)+i\varepsilon_i(\omega,k)=0$, to obtain the mode frequency and growth rate of transverse waves as follows

$$\omega_r^t=\omega_{pd}\left[\frac{k_z\nu_{dd}}{2\omega_{pd}}\pm\left(\frac{\left(k_z\nu_{dd}\right)^2}{4\omega_{pd}^2}+\frac{\eta k^2}{m_d n_{d0}\tau_m\omega_{pd}^2}+\frac{p_m^2 I}{\left[k^2+\frac{p_m^2\nu_i\omega_{pi}^2}{k_z\nu_{di}\left(\omega_{ci}^2+\nu_i^2\right)}\right]}\right)^{1/2}\right] \qquad (6.56)$$

and

$$\gamma_t=-\frac{\nu_d}{\omega_r}\left(\omega_r-k_z\nu_{dd}\right)+\frac{\nu_i\omega_{pi}^2\omega_{pd}^2}{\omega_r\left(k_z\nu_{di}\left(\omega_{ci}^2+\nu_i^2\right)\frac{k^4}{p_m^4}+\frac{k^2}{p_m^2}\nu_i\omega_{pi}^2\right)}I. \qquad (6.57)$$

In the absence of magnetic field & plasma drifts, the unmagnetized collisionless plasma of infinite geometry gives the mode frequency as $\omega_t=\omega_{pd}\left[\eta k^2/\left(m_d n_{d0}\tau_m\omega_{pd}^2\right)\right]^{1/2}$, which is same as frequency of transverse mode given by Kaw and Sen [40, Eq.(24) p. 3556)]. Eq. (6.56) shows a propagating elastic wave for transverse mode as discussed by Xie and Chen [45, p. 3523, eq. (41)] in the absence of ion-dust drifts and ion-dust neutral collisions.

The critical drift velocity of ions can be readily obtained from the growth rate Eq. (6.57) of transverse mode as

$$\nu_{di}^t\approx\frac{p_m^2\omega_{pi}^2\nu_i}{k_z\left(\omega_{ci}^2+\nu_i^2\right)}\left[\frac{\omega_{pi}^2 I}{k^2\left(\omega_r-k_z\nu_{dd}\right)\nu_d}-1\right]. \qquad (6.58)$$

Equation (6.58) shows the dependence of critical drift on the wave number, strong

correlation parameter, collisional frequencies of ions & dust, and the phase velocity of transverse waves.

6.3.1 Results and Discussion

We studied the low frequency modes in strongly coupled collisional magnetized dusty plasma cylinder of radius $r_0 = 3.0\,\text{cm}$ in the presence of magnetic field aligned drifts of ions and dust grains in the kinetic regime $\omega\tau_m \gg 1$. Slightly modified parameters for strongly coupled magnetized dusty plasma systems [46] considered are as follows: density of dust, ions and electrons are given as $n_{d0}/n_{i0} \sim 5\times10^{-4}$, $n_{e0} \approx 0.5\, n_{i0}$, here $n_{i0} \approx 10^8 \text{cm}^{-3}$, dust charge $-Z_d e \approx -10^3 \text{e}$, electron temperature $T_e \simeq 1.0eV$, ion temperature T_i =dust temperature $T_d \sim 0.3eV$, dust grain size a=0.5 x10^{-4} cm, dust mass ~ 10^{12} mass of proton, guide magnetic field B ~400 - 40000 Gauss, collisional frequency of ions and dust is $\nu_i \approx 0.5\,\omega_{ci}$ and $\nu_d \approx 0.002 - 0.2\,\omega_{pd}$, respectively. The drift velocity of ions is $v_{di} \sim (0 - 10.0)\, v_{ti}$, the ion's thermal velocity, and drift velocity of dust is $v_{dd} \sim (0 - 2.0)\, v_{td}$, the thermal speed of dust. The effective radial wave number on the cylindrical plasma surface is $k_\perp \approx p_m \approx q_m = \frac{2.404}{r_0} = 0.8$ cm^{-1}.

The parameters satisfy the conditions for strongly coupled OCP system i.e., $\lambda_D > a_d \gg \lambda_{Dd}$, where λ_D is plasma Debye length $\sim \lambda_{Di}$ (ion's Debye length) , a_d is intergrain spacing, and λ_{Dd} is dust Debye length and the screening constant $\kappa\left(=a_d/\lambda_D\right) < 1$. The Yukawa potential results must be applied for $\kappa\left(=a_d/\lambda_D\right) \geq 1$ [64]. Before going into detail, one must address the experimental criterion [68] to observe the magnetized dust modes in bounded plasma devices. For dust to be fully magnetized, the dust gyro radius $\rho_d \left[= \frac{v_{td}}{\omega_{cd}}\right]$ should be much less than the plasma size $2r_0$ and dust

cyclotron frequency ω_{cd} should be much greater than the dust collisional frequency ν_d. Both the criterion requires a strong magnetic field ~4 T, a very small dust size of few micron and low dust temperature ~0.025 eV. However, in the situations where dust charge on a small grain of micrometer size is still high like in most astrophysical dusty plasmas, the dust can be magnetized. But at this low dust temperature, the strong coupling among dust grains increases and hence a transition from liquid to crystalline state may takes place where addressing the screened coulomb potential is a must. The temperature we considered is to retain the fluid characteristics of dust grains and to maintain an agreement between theory and experimental results [29].

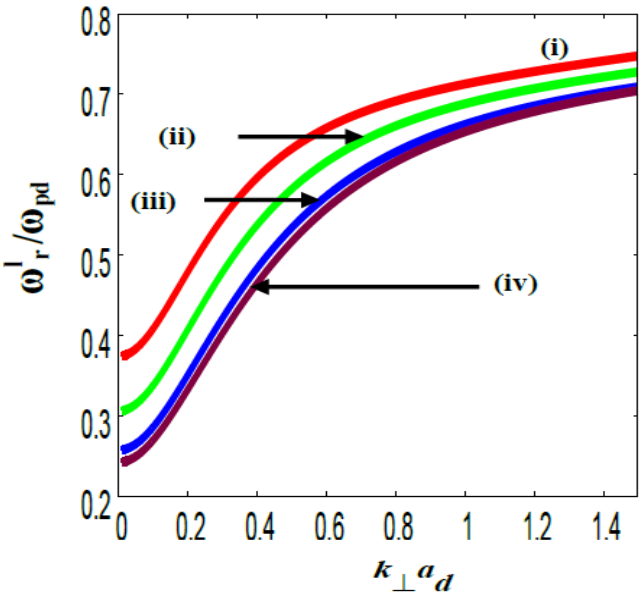

Fig. 6.9 Normalized frequency $\left(\omega_r^l/\omega_{pd}\right)$ of longitudinal waves as a function of normalized wave number $\left(k_\perp a_d\right)$ for strong correlation parameters **(i) Γ = 10, (ii)** Γ = **29**, **(iii)** Γ = **65, (iv)** Γ = **85**, $\nu_i = 0.5\,\omega_{ci}$, $\nu_{di} = 0.5\,\nu_{ti}$, $\nu_{dd} = 2.0\,\nu_{td}$, $k_z = 0.2$ cm^{-1} and B = 4000 Gauss.

We have plotted the normalized frequencies $\left(\omega_r^l/\omega_{pd}\right)$ of longitudinal modes using Eq. (6.45) with normalized perpendicular wave number $\left(k_\perp a_d\right)$ in Fig.6.9, for different Coupling parameters $\Gamma = 10, 29, 65$ and 85 followed by a comparison between finite and infinite boundaries of plasma waveguide at $\Gamma = 10$ in Fig. 6.10. From Fig.

6.9, it is observed that the normalized frequency of current driven longitudinal modes increases with normalized wave number in a magnetized dusty plasma cylinder but decreases with increase in strong coupling parameter. The increase in mode frequency is greater for infinite boundaries than for finite boundaries due to reduction in interaction region for bounded plasmas (see Fig. 6.10).

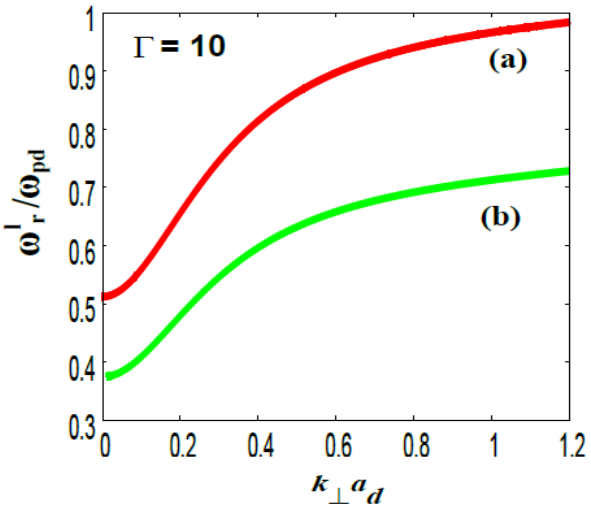

Fig. 6.10 Normalized frequency $\left(\omega_r^l/\omega_{pd}\right)$ of longitudinal waves as a function of normalized wave number $\left(k_\perp a_d\right)$ for strong correlation parameter, Γ **= 10, (a)** for infinite geometry of plasma waveguide **(b)** for finite cylindrical geometry, $\nu_i = 0.5\ \omega_{ci}$, $v_{di} = 0.5\ v_{ti}$, $v_{dd} = 2.0\ v_{td}$, $k_z = 0.2$ cm^{-1} and B = 4000 Gauss.

The longitudinal mode observed is theoretically a hybrid between dust ion cyclotron modes and dust acoustic modes. These dust ion hybrid modes can be observed only for small values of strong correlation parameters $\Gamma < 5$ for large magnetic fields upto 4T until the condition for strong coupling regime ($\omega\tau_m \gg 1$) is fulfilled. These results of increase in frequency with the wave number for hybrid longitudinal modes are similar to numerical simulation results for dust acoustic waves shown by Winske *et al.* [28, Figs. 1 & 2]. These results are also similar to the experimental observations of Kim et al. [69, Fig. 8, p.1110] for low frequency electrostatic waves in a magnetized heavy negative ion plasma and collisional instabilities in a dusty plasma with ion drifts effects by Kaw and Singh [70, Fig.1, p.

425]. In the long wavelength regime i.e., $k_\perp a_d \leq 1$, normalized frequency ~ 30-50 Hz is observed which is nearly twice above the low frequency dust acoustic modes (~10-25 Hz) observed by Thomas Jr. and Merlino [29] in the unmagnetized Dusty plasma experiment (DPX). It is also slightly above the frequencies observed by Praburam and Goree [39] and Barkan *et al.* [25] for DAWs. An increase in frequency is as a result of the magnetization of dusty plasma which also shows the dust acoustic modes modified due to dust ion cyclotron motions as a result of the coupling between the dusty modes and the magnetic field. This is in good agreement with the conclusion of theory developed by Shukla and Mamun [47] low frequency electrostatic modes for a bounded magneto-plasma. The mode frequency shows a decrease with strong coupling parameters which are in line with results obtained by Rosenberg and Kalman [27, p.7172, Fig. 3], Kaw and Sen [40, p. 3555, Fig. 1], Kaw [47] and Winske et al. [28].

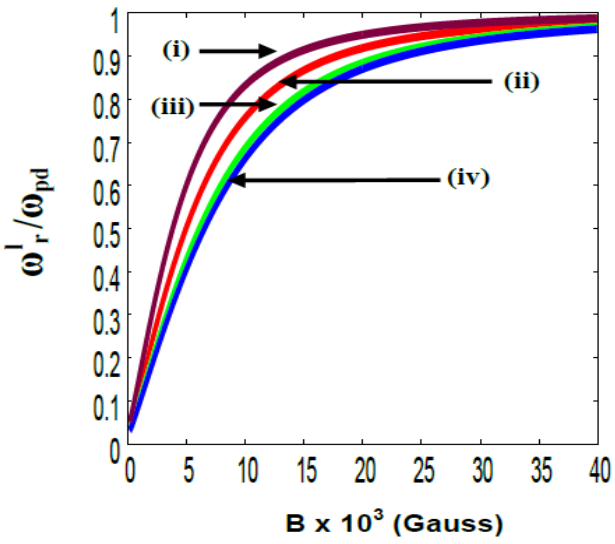

Fig. 6.11 Normalized frequency $\left(\omega_r^l/\omega_{pd}\right)$ of longitudinal wave modes as a function of magnetic field $B\times10^3$ Gauss, for strong correlation parameters **(i)** Γ = **10, (ii)** Γ = **29**, **(iii)** Γ = **65, (iv)** Γ = **85**, Given: $v_i = 0.5\ \omega_{ci}, v_d = 0.02\ \omega_{pd}$, $v_{di} = 0.8\ v_{ti}$, $v_{dd} = 1.0\ v_{td}$, $k_\perp = 0.8$ cm^{-1}, $k_z = 0.2$ cm^{-1}.

In Fig. 6.11 we have plotted the normalized frequency $\left(\omega_r^l/\omega_{pd}\right)$ of longitudinal modes in the plasma cylinder with magnetic field B to observe the effect of increasing magnetic field. The plot shows an increase in mode frequency with increasing magnetic field which is in close agreement with the increase in mode frequency of low frequency electrostatic waves with magnetic field as given by Kim *et al.* [69, p. 1109, Fig. 6]. It is

observed that beyond a magnetic field of 20000 Gauss the mode frequency nearly saturates. Fig. 6.12 shows the normalized frequency $\left(\omega_r^l/\omega_{pd}\right)$ of longitudinal modes as a function of normalized drift speed of ions $\left(v_{di}/v_{ti}\right)$ for different strong coupling parameter. The plot shows a slight decrease in the mode frequency with an increase in drift velocity of ions. The mode frequency shows a weak dependence on the drift velocity of ions but dust drift tend to increase the mode frequency.

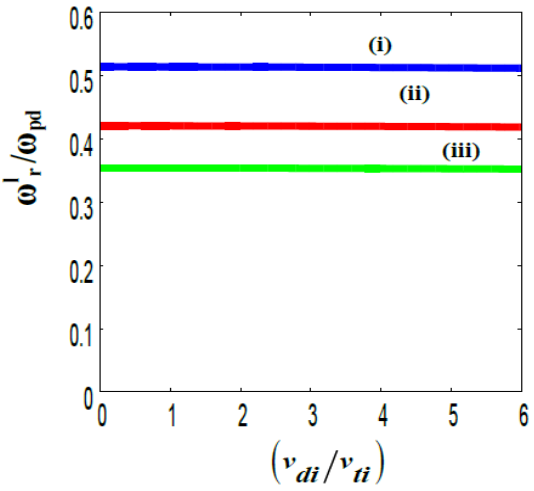

Fig. 6.12 Normalized frequency $\left(\omega_r^l/\omega_{pd}\right)$ of longitudinal waves as a function of normalized drift velocity of ions $\left(v_{di}/v_{ti}\right)$ for strong coupling parameters Γ **(i)** Γ = **10, (ii)** Γ = **29,** and **(iii)** Γ =**65**. Given: $\nu_i = 0.5\ \omega_{ci}$, $\nu_d = 0.02\ \omega_{pd}$, $v_{di} = 0.8\ v_{ti}$, $v_{dd} = 1.0\ v_{td}$, $k_\perp = 0.8$ cm^{-1}, $k_z = 0.2$ cm^{-1} and B = 4000 Gauss.

In Fig. 6.13 (a), we have plotted the normalized growth rate $\left(\gamma_l/\omega_{pd}\right)$ of longitudinal modes as a function of normalized perpendicular wave number $\left(k_\perp a_d\right)$ for different strong correlation parameter $\Gamma = 10,\ 29,\ 65$ and 85 using (6.46). It is observed that the growth rate of current driven longitudinal dust waves is declined with the normalized perpendicular wave number in a magnetized dusty plasmas cylinder in the regime $\omega\tau_m \gg 1$. The reduction in growth rate of longitudinal dust modes with increasing perpendicular wave number matches well with numerical simulation results of dust acoustic waves given by Winske et al. [28, Fig.2, p.2266], Kaw and Singh [70,

Fig. 1, p. 425], and Xie and Yu [71, Fig.5 p.8505]. It is observed that at small magnetic fields below 10000 Gauss the modes with large strong coupling parameters are damped. We stress on the possibility of observing these small amplitude hybrid like modes in the long wavelength regime in the magneto-dusty plasma experiments.

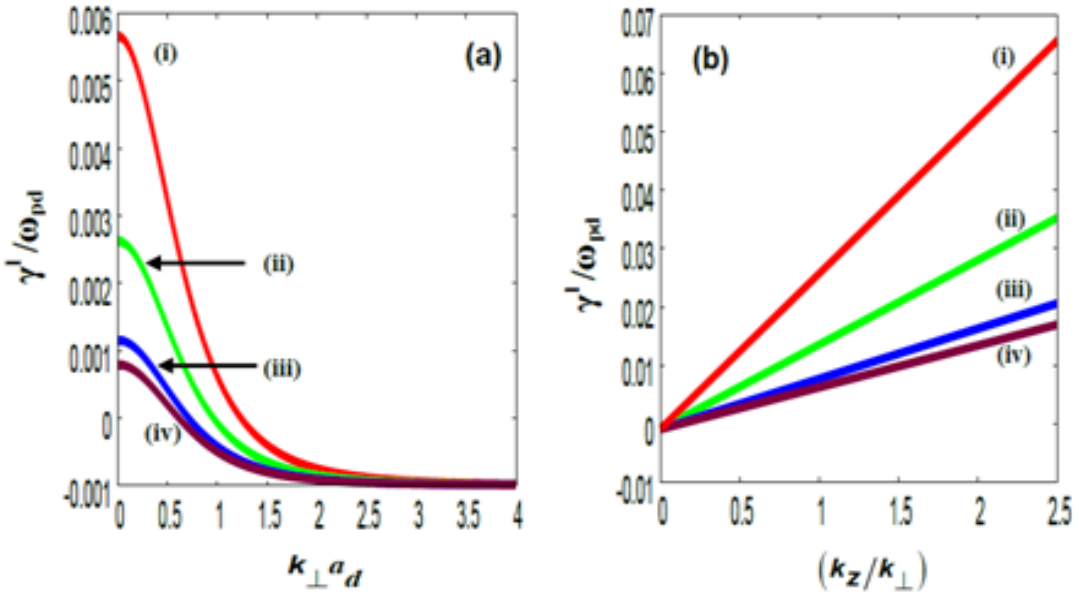

Fig. 6.13 Normalized growth rate $\left(\gamma l/\omega_{pd}\right)$ of longitudinal waves as a function of normalized wave number **(a)** $\left(k_\perp a_d\right)$ **(b)** $\left(k_z/k_\perp\right)$, for strong coupling parameters, **(i)** Γ **= 10, (ii)** Γ = **29, (iii)** Γ = **65, and (iv)** Γ = **85** . Given: $\nu_i = 0.5\ \omega_{ci}$, $\nu_d = 0.002\ \omega_{pd}$, $\nu_{di} = 0.5\ \nu_{ti}$, $\nu_{dd} = \nu_{td}$, and B = 20000 Gauss.

The normalized growth rate $\left(\gamma^l/\omega_{pd}\right)$ is also plotted as a function of normalized wave number $\left(k_z/k_\perp\right)$ in Fig. 6.13 (b), where $k_\perp$ is fixed but k_z increases. It is observed that an increase in parallel wave number k_z, enhances the growth rate of longitudinal modes but as $k_z \ll k_\perp$ so the modes for small magnetic fields below 10000 Gauss and large strong coupling parameter are damped in long wavelength regime where $k_z/k_\perp \ll 1$.

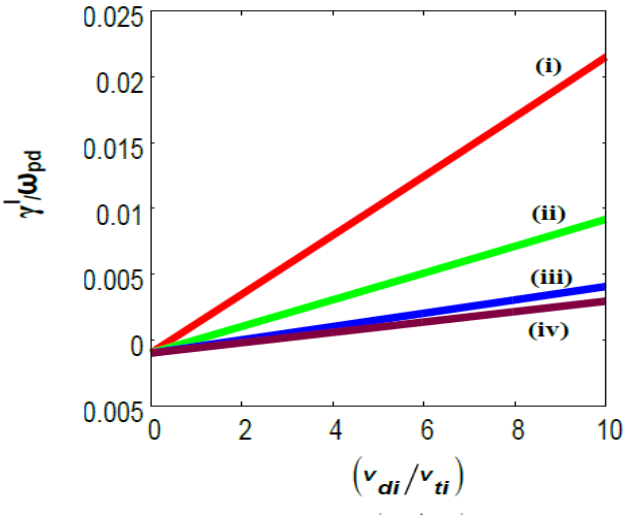

Fig. 6.14 (a): Normalized growth rate $\left(\gamma l/\omega_{pd}\right)$ of longitudinal waves as a function of normalized drift velocity of ions $\left(v_{di}/v_{ti}\right)$ for strong coupling parameters, **(i)** Γ **= 10, (ii)** Γ = **29, (iii)** Γ = **65, and (iv)** Γ = **85**. Given: $v_i = 0.5\ \omega_{ci}$, $v_d = 0.02\ \omega_{pd}$, $v_{dd} = 1.0\ v_{td}$, $k_\perp$ =0.8 cm^{-1}, $k_z = 0.2$ cm^{-1}, and B = 10000 Gauss.

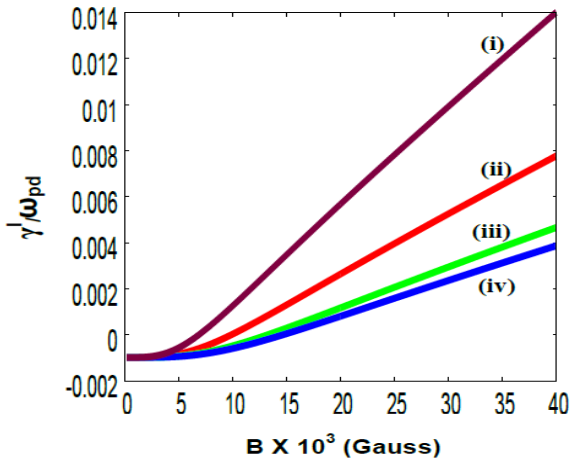

Fig. 6.14 (b) Normalized growth rate $\left(\gamma l/\omega_{pd}\right)$ of longitudinal waves as a function of magnetic field **B** for different strong coupling parameters, **(i)** Γ **= 10, (ii)** Γ = **29, (iii)** Γ = **65**, and **(iv)** Γ = **85**. Given: $v_i = 0.5\ \omega_{ci}$, $v_d = 0.02\ \omega_{pd}$, $v_{di} = v_{ti}$, $v_{dd} = v_{td}$, $k_\perp = 0.8$ cm^{-1}, and $k_z = 0.2$ cm^{-1}.

The growth rate of longitudinal dust modes is found to be decreased with an increase in strong coupling parameter Γ as well due to increase in viscosity of the dust fluid. In actual, the observed longitudinal modes for the radially bounded magnetized

dusty plasma are the damped modes for $\Gamma > 10$ for small magnetic fields until the dust remain unmagnetized. These results of damped mode are similar to dust acoustic wave modes as analyzed by Kaw and Sen [40], and Xie and Chen [45].

In Fig. 6.14 (a), we have plotted the normalized growth rate $\left(\gamma^{l}/\omega_{pd}\right)$ of longitudinal modes with normalized ion drift $\left(v_{di}/v_{ti}\right)$ for different strong correlation parameter Γ and observed an increase in growth rate of longitudinal modes with drift velocity of ions which well matches the experimental results of DAW driven by ion dust streaming instability in laboratory discharge dusty plasmas given by Merlino [72] which supports the excitation of dust acoustic modes due to ion dust drifts. It is found that a relatively large drift velocity of ions, above six times the ion thermal speed is required to destabilize the growth of longitudinal wave modes in a bounded magnetized plasma. Moreover, the modes with large strong correlations among dust grains with $\Gamma > 10$ are found to be still damped at large ion drifts for small magnetic fields.

In Fig 6.14 (b), normalized growth rate of longitudinal modes have been plotted with magnetic field and found to be destabilized. It is found that upto the magnetic field of 1T the modes having strong coupling parameter $\Gamma > 10$ remain damped but beyond this value of magnetic field the modes starts to grow which shows a large magnetic field is required to excite the longitudinal dust modes as investigated experimentally [46]. However, the modes with strong coupling parameter $\Gamma < 5$ are destabilized for magnetic fields upto 10000 Gauss. The magnetic field strength required to destabilize the growth of longitudinal dust modes increases with increase in strong coupling parameter Γ.

We have plotted the normalized critical drift velocity of ions v_{di}^{l}/v_{ti} with normalized perpendicular wave number $k_{\perp}a_{d}$, and magnetic field B for longitudinal modes in Fig. 6.15 (a) & (b), respectively using Eq. (6.47). It is observed that the critical drift required for exciting the longitudinal modes increases with increase in perpendicular wave number $k_{\perp}$ and strong coupling parameter Γ but decreases with increase in magnetic field. It has already been observed that the oscillations are damped under the effect of increase in strong coupling parameter and perpendicular wave number (see Fig. 6.13 (a) & (b) so to support them a large drift would be

required. Moreover, it is observed that the drift velocity of ions required to excite longitudinal modes in local plasma is slightly less than the drift required for a bounded plasma. The above discussed results for the longitudinal modes are found to have a great similarity with the drift instability discussed by Rosenberg and Merlino [73] in a positive –negative ion plasma.

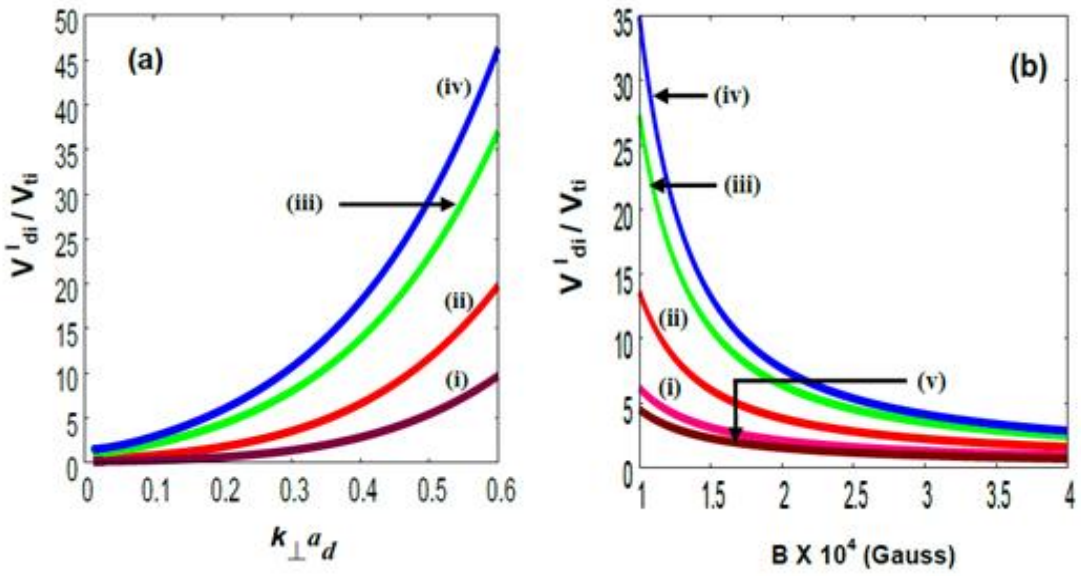

Fig. 6.15 Normalized critical drift speed of ions $\left(v^{l}_{di}/v_{ti}\right)$ of longitudinal waves as a function of **(a)** normalized wave number $k_{\perp} a_d$ **(b)** magnetic field **B x 10^4** Gauss, for strong coupling parameters, **(i)** Γ **= 10 (ii)** Γ = **29** and **(iii)** Γ = **65 (iv)** Γ = **85** for cylindrical case and **(v)** at Γ **= 10** for infinite geometry of plasma at a fixed $k_{\perp} = 0.8$ cm^{-1} Given: $\nu_i = 0.5\ \omega_{ci}$, $\nu_d = 0.002\ \omega_{pd}$, $\nu_{di} = 0.5\ \nu_{ti}$, $\nu_{dd} = \nu_{td}$, and B = 10000 Gauss.

Now to investigate the behaviour of transverse wave modes in presence of magnetic field aligned currents & collisions for a bounded plasma, we have plotted Fig. 6.16 (a) using Eq. (6.56), that shows the variation of the normalized frequency of transverse modes $\left(\omega^{t}_{r}/\omega_{pd}\right)$ with normalized wave number ka_d for different strong coupling parameters, Γ(i, ii, iii, iv = 10, 29, 65, 85). It is observed that the frequency of transverse modes in the regime $\omega\tau_m \gg 1$, shows a cut-off at very long wavelength and then increases linearly with increasing normalized wave number ka_d. This result is analogous to results of Kaw [43]. In the long wavelength range the transverse modes observed are of very low frequency but in short wavelength range the mode frequency

increases linearly which are similar to results for dust lattice waves by Nonumura et al. [41]. It has been analyzed that the frequency of transverse modes is not affected by increase in magnetic field but decreases with increase in strong coupling parameter Γ. This increase in frequency of transverse mode is in fine agreement with the results of transverse waves in absence of magnetic field given by Kaw and Sen [40], Nonumura *et al.* [41, p. 5143, Fig. 4], Murillo [42], and Kaw [43]. This linear increase of frequency with wave number confirms the behaviour of transverse modes as non-dispersive elastic waves similar to the experimental results of Nonumura et al. [41, p.5143] for a two dimensional screened coulomb systems.

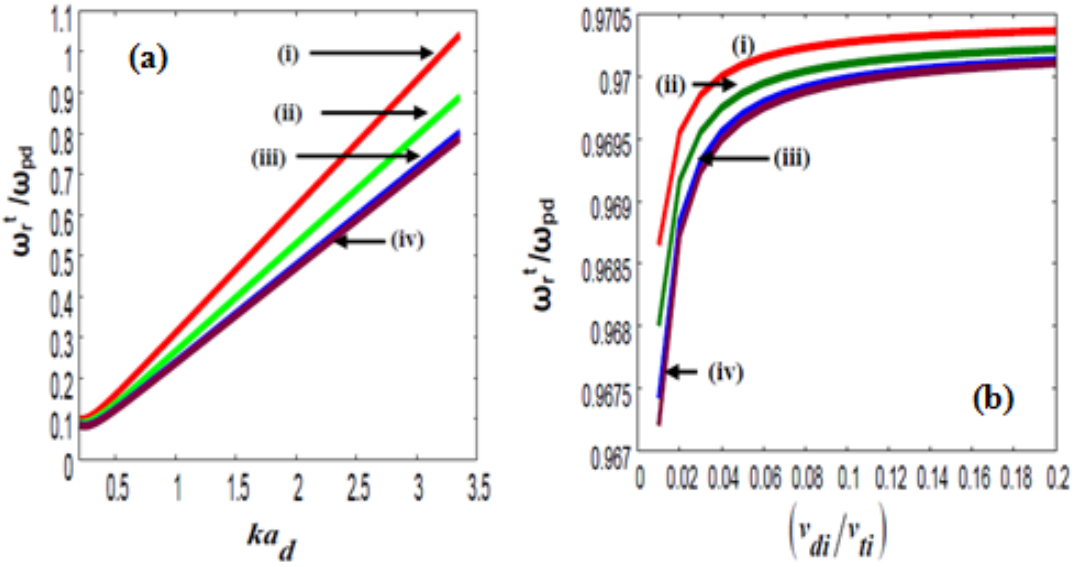

Fig. 6.16 Normalized frequency $\left(\omega_r^t/\omega_{pd}\right)$ of transverse waves as a function of **(a)** normalized wave number ka_d and **(b)** normalized drift velocity of ions $\left(v_{di}/v_{ti}\right)$**,** for strong coupling parameters, **(i)** Γ **= 10, (ii)** Γ = **29, (iii)** Γ = 65, and **(iv)** Γ = **85.** Given: $v_i = 0.5\omega_{ci}$, $v_{di} = 0.5\, v_{ti}$, $v_{dd} = v_{td}$, $k_\perp = 0.8$ cm^{-1}, $k_z = 0.001 - 200.0$ cm^{-1} and B = 4000 Gauss. Here $k\left(=\sqrt{k_\perp^2 + k_z^2}\right)$.

It is observed that the frequency of transverse wave modes show a small increment with a small increase in drift velocity of ions then saturates for large ion drifts (see Fig. 6.16 (b)) while an appreciable increment is observed with increasing drift velocity of dust grains (see Fig. 6.17 (a)) which suggests the transverse modes to be basically dust driven modes. Fig. 6.17(b) shows a comparison of dispersion curve

for finite and infinite geometry of plasma waveguide for strong coupling parameter Γ=10.

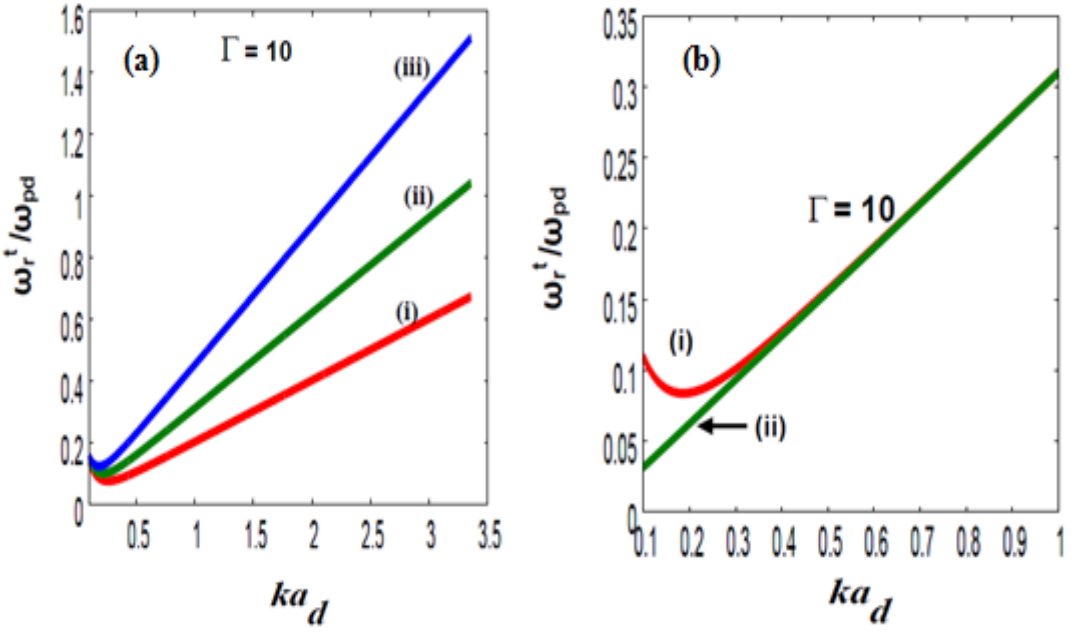

Fig. 6.17 Normalized frequency $\left(\omega_r^t/\omega_{pd}\right)$ of transverse waves as a function of normalized wave number ka_d, for Case **(a)** for Γ = **10** at different dust drift speeds **(i)** $v_{dd} = 0.0001\, v_{td}$ **(ii)** $v_{dd} = 1.0\, v_{td}$ **(iii)** $v_{dd} = 2.0\, v_{td}$, and Case **(b)** at Γ = **10** **(i)** finite geometry **(ii)** infinite geometry $\left(k_\perp = 0.2\ \text{cm}^{-1}\right)$. **Given:** $\nu_i = 0.5\omega_{ci}$, $\nu_{di} = 0.5\, \nu_{ti}$, $\nu_{dd} = \nu_{td}$, $k_\perp = 0.8\ \text{cm}^{-1}$, $k_z = 0.001 - 200.0\ \text{cm}^{-1}$ and B = 4000 Gauss.

It is observed that the wave modes in a bounded plasma have the frequency slightly greater than the unbounded plasma in long wavelength regime $ka_d \leq 1$ while in short wavelength region $ka_d > 1$, the frequency is independent of the choice of geometry of the plasma. The dispersion curve for transverse shear wave modes has also been plotted {see Fig. 6.18} by varying the perpendicular wave number at different plasma radius and it is observed that the mode frequency shows a decrease with decrease in perpendicular wave number $k_\perp = \frac{2.404}{r_0}$ in the long wavelength regime $ka_d \leq 1$ then becomes independent of perpendicular wave number in the short wavelength region. This stresses the fact that the transverse mode frequency is

independent of bounded or unbounded nature of a plasma in the short wavelength range $ka_d > 1$.The transverse modes require a large parallel wave number which characterizes the transverse modes as short wavelength modes as described by [40]-[43], [45].

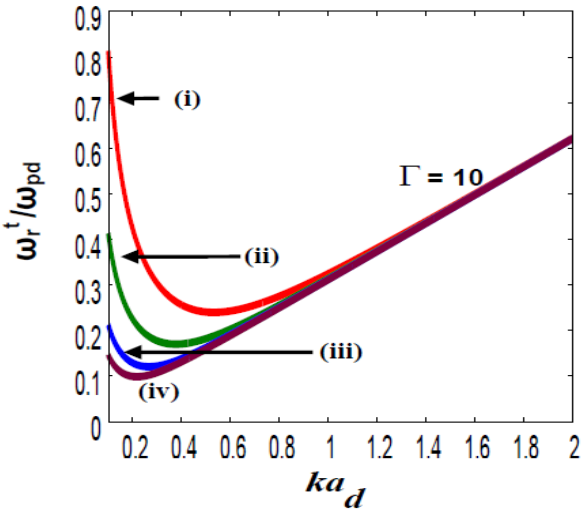

Fig. 6.18 Normalized frequency $\left(\omega_r^t/\omega_{pd}\right)$ of transverse waves as a function of normalized wave number ka_d, for Γ **= 10** at different values of perpendicular wave number $k_\perp = 2.404/r$ obtained by varying plasma radius **(i) r=0.5, (ii) r= 1.0, (iii) r=2.0, and (iv) r = 3.0.** [Note: Rest of the parameters is same as Fig. 6.17].

Our results of transverse waves driven by magnetic field aligned ion and dust drifts are also similar to the results of dissipative instability driven by relative drift between ions and dust observed by Kaw and Singh [70]. Fig.6.19 (a) have been plotted using Eq. (6.57) and shows the normalized growth rate $\left(\gamma^t/\omega_{pd}\right)$ of transverse wave modes as a function of normalized wave number ka_d at different values of Γ and found that the growth rate is stabilized with increasing wave number. The negative growth rate shows that the wave modes are damped modes as shown by Kaw [43, p.1876, Fig.7.(b)]. These results also found similarity with the recombination driven collisional instabilities in dusty plasma by Kaw and Singh [70, p.425, Fig.1]. A positive growth rate is observed in long wavelength regime $ka_d \ll 1 \sim 0.05$ but above it the modes are damped which shows a fine agreement with the experiments of Nonumura et al. [41] and Kaw [43] which shows the transverse oscillations of very low frequency in a long

wavelength regime. The dependence on the strong coupling parameter in long wavelength region is not significant but a small decrease with strong coupling parameter Γ is observed in the short wavelength regime. It is also observed from Fig. 6.19(b) that the growth rate for a finite geometry of plasmas is more than for infinite geometry in long wavelength regime but in short wavelength regime the growth rate for infinite geometry is slightly above the finite geometry of plasma waveguide but the modes are still damped.

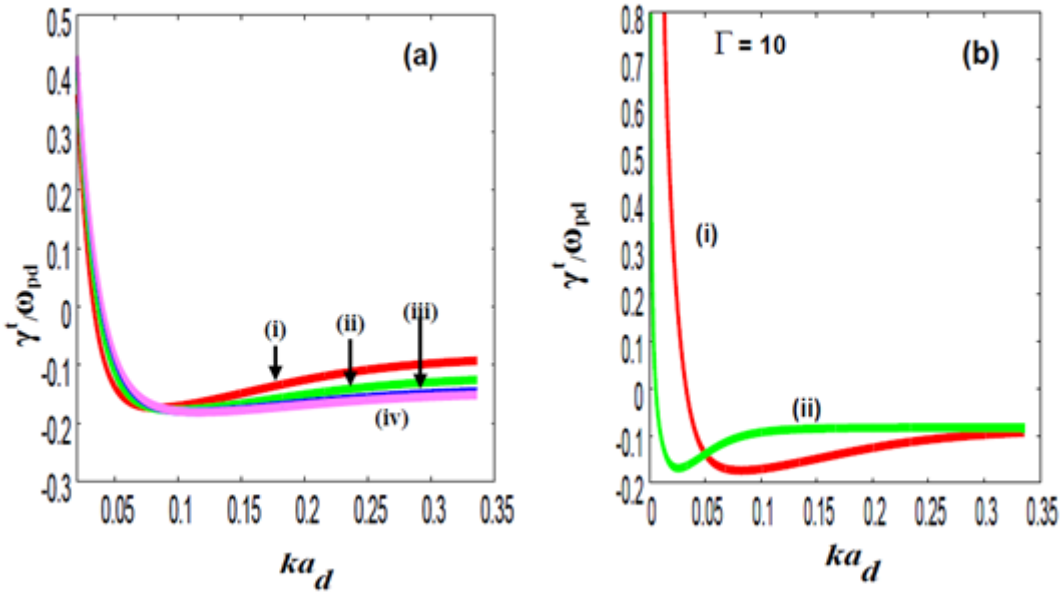

Fig. 6.19 Normalized growth rate $\left(\gamma^t/\omega_{pd}\right)$ of transverse waves as a function of normalized wave number $\left(ka_d\right)$ for two cases, Case: **(a)** for strong coupling parameters, **(i)** Γ = **10, (ii)** Γ = **29, (iii)** Γ = **65,** & **(iv)** Γ = **85** and Case **(b)** at Γ = **10 (i)** for bounded plasma cylinder **(ii)** for unbounded plasma $\left(k_\perp\text{=}0.07\ \text{cm}^{-1}\right)$. The other parameters are $v_d = 0.2\ \omega_{pd}$, $v_{di} = 0.5\ v_{ti}$, $v_{dd} = 1.0\ v_{td}$, $k_\perp = 0.8\ \text{cm}^{-1}$, $k_z = 0.001\ –20.0\ \text{cm}^{-1}$ and B = 4000 Gauss.

Fig.6.20 shows the growth rate $\left(\gamma^t/\omega_{pd}\right)$ of transverse mode as a function of normalized drift velocity of ions $\left(v_{di}/v_{ti}\right)$ at different dust drifts. The results show a decrease in growth rate of transverse modes with increasing drift speed of ions but an increase with increasing drift speed of dust grains. Fig. 6.21 has been plotted using (6.58) and shows the normalized critical drift velocity of ions $\left(k_z v_{di}^t/\omega_r\right)$ as a

function of normalized wave number ka_d. It is observed that the critical drift required for exciting the transverse wave modes decreases with increase in wave number k which justify the increase in growth rate of transverse wave modes at large wave numbers i.e., in short wavelength regime.

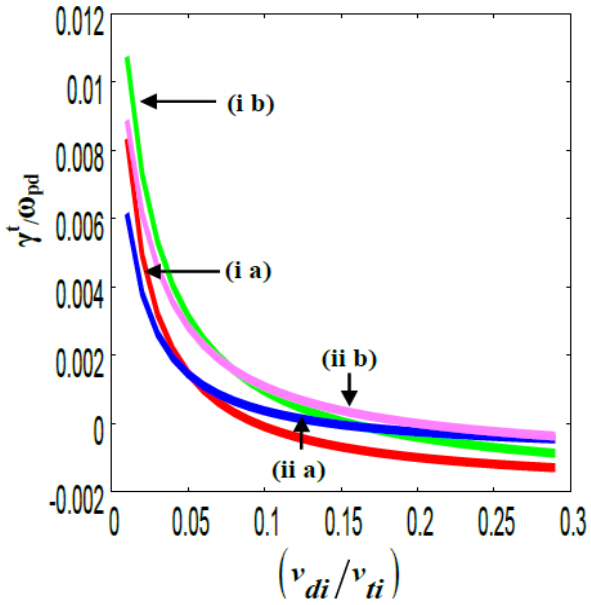

Fig. 6.20 Normalized growth rate, $\left(\gamma^t/\omega_{pd}\right)$ of transverse waves as a function of normalized ion's drift velocity $\left(v_{di}/v_{ti}\right)$ for strong coupling parameters, **(i)** Γ =**10, (ii)** Γ =**29** for **(a)** $v_{dd} = 0.01\, v_{td}$, **(b)** $v_{dd} = 1.0\, v_{td}$. Given: $\nu_i = 0.5\, \omega_{ci}$, $\nu_d = 0.02\, \omega_{pd}$, $v_{di} = 0.5\, v_{ti}$, $k_\perp = 0.8$ cm^{-1}, $k_z = 20.0$ cm^{-1}, and B = 4000 Gauss.

It is found that the critical drift velocity of ions required to excite the transverse wave modes is independent of the extent of strong coupling among the dust grains in a magnetized collisional bounded dusty plasma which supports the rigidity of the dust system for transverse shear modes. The local theory developed for hydrodynamic regime $\omega\tau_m \ll 1$, have shown that longitudinal modes and transverse modes can be excited in the presence of plasma current drifts at even fields upto 400 Gauss. Moreover, both the modes were destabilized with normalized wave number. The present model, in the kinetic regime, $\omega\tau_m \gg 1$ shows that a large magnetic field above

10000 Gauss is required for current driven longitudinal modes to grow in bounded magneto dusty plasma while the transverse modes are still damped.

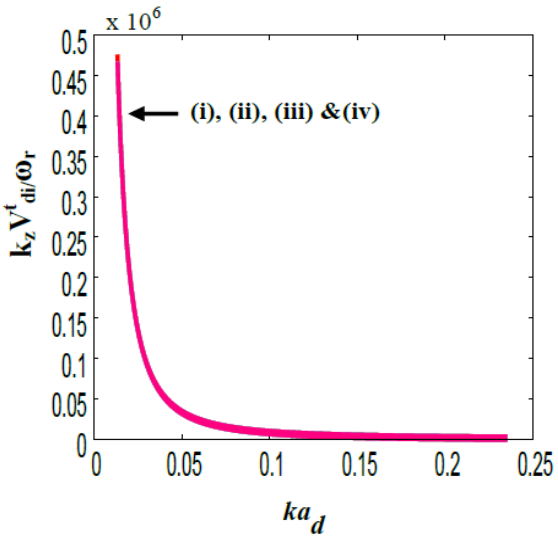

FIG. 6.21: Normalized critical drift speed of ions, $\left(k_z v_{di}^t / \omega_r\right)$ of transverse waves as a function of normalized wave number $\left(ka_d\right)$ for strong coupling parameters **(i)** Γ **= 10 (ii)** Γ = **29,** and **(iii)** Γ = **65 (iv)** Γ = **85** for. [Note: All Γ values lie on the same line]. The parameters are same as Fig. 6.20.

6.3.2 Conclusion

To summarize, we have investigated the excitation of low frequency wave modes by magnetic field aligned ion and dust drifts in a magnetized strongly coupled collisional dusty plasma having a cylindrical geometry in the kinetic regime $\omega\tau_m \gg 1$, using a nonlocal theory of generalized hydrodynamic model. It is found that the magnetic field aligned current drifts play a crucial role in exciting the low frequency dust wave modes in a magnetized dusty plasma cylinder having neutral background. The longitudinal mode observed is a result of coupling between dust ion cyclotron hybrid modes and dust acoustic modes, and transverse shear mode shows are the elastic wave modes. It is observed that the excitation of longitudinal dust ion hybrid modes requires a large magnetic field and low collisional regime in the presence of strong correlations among dust grains while the transverse shear modes are hard to observe in

a collisional dust fluid (liquid) having strong correlations in a magnetized dusty plasmas. Our frequencies for the magnetized longitudinal modes lies close to the frequencies observed experimentally by Thomas et al. [29], Chu et al. [19], Barkan *et al.* [25] and Praburam and Goree [39] thereby justifying the modes as the low frequency dust wave modes. It is observed that the presence of radial boundaries modify the dispersion properties of both the modes. Our theoretical results are in good agreement with the theoretical results of Xie and Chen [45], Kaw and Sen [40] & Kaw [43] and experimental results of Nonumura et al. [41] for transverse shear waves.

The results obtained may be useful in laboratory strongly coupled magnetized dusty plasma like in inertial confinement fusion devices and magnetized dusty plasma experiments [46] for study of waves and instabilities in magneto dusty plasmas. Though the theory applies to the bounded plasmas but a comparison of bounded and unbounded plasmas may also be applicable for study of cosmic and near earth environments. Finally, we would like to remark that there is a need to entail dependence of viscosity coefficients on the magnetic field to elucidate the behaviour of the strongly coupled viscoelastic magnetized dust modes more effectively.

REFERENCES

[1]. P. K. Shukla, and A.A. Mamun, *"Introduction to dusty plasma physics"* IOP publishing LTD. (2002), Chapter I.

[2]. T. G. Northdrop, *Phys. Scripta* **45**, 475 (1992).

[3]. A. Bouchoule, *"Technological impacts of dusty plasmas. In Dusty plasmas: Physics, chemistry and technological impacts in plasma processing",* Bouchoule, A. (ed.): Wiley, Chichester, (1999).

[4]. E. C. Whipple, *Rep. Prog. Phys.* **44,** 1197 (1981).

[5]. P.A. Robinson, P. Coakley, *IEEE Trans. Electr. Insul.* **27**, 944 (1992).

[6]. V. E. Fortov, G.E. Morfill, *"Complex and Dusty Plasmas- from Laboratory to space,"* Series in Plasma Physics; 25 (2010), CRC Press: Taylor & Francis Group, New York.

[7]. M. Bocchio, A. P. Jones, and J. D. Slavin, *Astronomy and Astrophys.* **570**, A 32 (2014).

[8]. J. Winter, G. J. Gebauer, *J. Nucl. Mater.* **266-269**, 228 (1999).

[9]. J. Winter, *Phys. Plasmas* **7**, 3862 (2000).

[10]. E.C. Whipple, T.G. Northdrop, and D.A. Mendis**,** *J. Geophys. Res.* **90**, 7405 (1985).

[11]. M. R. Jana, A. Sen and P.K. Kaw, *Phys. Rev. E* **48**, 3930 (1993).

[12]. C. Cui and J. Goree, *IEEE Trans. Plasma Sci.* **22**, 151 (1994).

[13]. W. Xu, B. Song, R. L. Merlino, and N. D'Angelo, *Rev. Sci. Instrum.* **63**, 5266 (1992).

[14]. W. Xu, N. D'Angelo, and R. L. Merlino, *J. Geophys. Res*. **98**, 7843 (1993).

[15]. A. Barkan, N. D'Angelo, and R. L. Merlino, *Phys. Rev. Lett.* **73,** 3093 (1994).

[16]. P. K. Shukla, *Astrophys. Space Sci.* **264**, 235 (1999).

[17]. M. K. Islam, Y. Nakashima, K. Yatsu, and M. Salimullah, *Phys. Plasmas* **10**, 591 (2003).

[18]. H. Ikezi, *Phys. Fluids* **29**, 1764 (1986).

[19]. J. H. Chu, J. B. Du, and I. Lin, *J. Phys. D: Appl. Phys.* **27**, 296 (1994).

[20]. N. D'Angelo, *J. Phys. D: Appl. Phys.* **28**, 1009 (1995).

[21]. S. Ichimaru, *Rev. Mod. Phys.* **54**, 1017 (1982).

[22]. E. Thomas Jr., R. Fisher, and R.L. Merlino, *Phys Plasmas* **14**, 123701 (2007).

[23]. N. N. Rao, P. K. Shukla, and M. Y. Yu, *Planet. Space Sci.* **38**, 543 (1990).

[24]. F. Melandsø, T. K. Aslaksen, and O. Havnes, *J. Geophys. Res.* **98**, 13315 (1993).

[25]. A. Barkan, R. L. Merlino, and N. D'Angelo, *Phys. Plasmas* **2,** 3563 (1995).

[26]. J. B. Pieper and J. Goree, *Phys. Rev. Lett.* **77**, 3137 (1996).

[27]. M. Rosenberg and G. Kalman, *Phys. Rev. E* **56,** 7166 (1997).

[28]. D. Winske and M. S. Murillo, *Phys. Rev. E* **59**, 2263 (1999).

[29]. E. Thomas Jr. and R. L. Merlino, *IEEE Trans. Plasma Sci.* **29**, 152 (2001).

[30]. R. L. Merlino, *J. Plasma Phys.*, 1 (2014) (doi: 10.1017/S0022377814000312).

[31]. G. Morfill, A. V. Ivlev, and J. R. Jokipii, *Phys. Rev. Lett.* **83**, 971 (1999).

[32]. B. Farouki, P. K. Shukla, N. L. Tsintsadze, and D. D. Tskhakaya, *Phys Lett. A* **264**, 318(1999); *Phys. Plasmas* **7**, 814 (2000).

[33]. P. Bandyopadhyay, G. Prasad, A. Sen, and P. K. Kaw, *Phys. Lett. A* **372**, 5467 (2008).

[34]. N. F. Otani, A. Bhattacharjee, and X. Wang, *Phys. Plasma* **6**, 409 (1999).

[35]. N. D'Angelo, *Planet. Space Sci.* **38**, 1143 (1990).

[36]. V. W. Chow, and M. Rosenberg, *Planet Space Sci.* **43**, 613 (1995).

[37]. P.K. Shukla, and H. U. Rahman, *Planet Space Sci.* **46**, 541 (1998).

[38]. A. Sabeen, W. Masood, M. N. S. Qureshi, and H. A. Shah, *Phys. Plasmas* **24**, 073704 (2017).

[39]. G. Praburam and J. Goree, *Phys. Plasmas* **3,** 1212 (1996).

[40]. P. K. Kaw and A. Sen, *Phys. Plasmas **5**,* 3552 (1998).

[41]. S. Nonumura, D. Samsonov, and J. Goree, *Phys. Rev. E* **65**, 066402 (2000a); *Phys. Rev. Lett.* **84**, 5141 (2000).

[42]. M. S. Murillo, *Phys. Plasmas* **7,** 33 (2000); *Phys. Rev. Lett.* **85,** 2514 (2000).

[43]. P. K. Kaw, *Phys. Plasmas* **8**, 1870 (2001).

[44]. B. S. Xie, Y. P. Chen and M. Y. Yu, *IEEE Trans. Plasma Sci.* **29**, 226 (2001).

[45]. B. S. Xie and Y. P. Chen, *Phys. Plasmas* **11**, 3519 (2004).

[46]. E. Thomas Jr., U. Konopka, D. Artis, B. Lynch, S. Leblane, S. Adams, R. L. Merlino, and M. Rosenberg, *J. Plasma Phys.* **81**, 345810206 (2015).

[47]. P. K. Shukla and A. A. Mamun, *J. Plasma Phys.* **65**, 97 (2001).

[48]. K. Arshad, M. Lazar, S. Mahmood, A. U. Rehman, and S. Peodts, *Phys. Plasmas* **24**, 033701 (2017).

[49]. K. Arshad, Z. Ahsan, S. A. Khan, and S. Mahmood, *Phys. Plasmas* **21**, 023704 2014.

[50]. N. D'Angelo and R. L. Merlino, *Planet. Space Sci.* **44**, 1593 (1996).

[51]. R. L. Merlino, *IEEE Trans. plasma sci.* **25,** 60 (1997).

[52]. M. K. Islam, Y. Nakashima, K. Yatsu, and M. Salimullah, *Phys. Plasmas* **10**, 591 (2003).

[53]. S. C. Sharma, M. Sugawa, and V. K. Jain, *Phys. Plasmas* **7,** 457 (2000).

[54]. B.P. Pandey, S. V. Vladimirov, and A. Samaria, *Phys. Plasmas* **16**, 113708 (2009).

[55]. C. D. Rapozo, P.H. Sakanaka, and H. Torres, *Revista Brasileira de Fisica* **17**, 222 (1987).

[56]. G R Tynan, C Holland, J H Yu, A James, D Nishijima, M Shimada and N Taheri, *Plasma Phys. Control. Fusion* **48**, S51 (2006).

[57]. M. Amberg, J. Geerk, M. Keller, and A. Fischer, *Plasma Devices and Operations* **12**, 175 (2004).

[58]. N. Buzarbaruah, N. J. Dutta, D. Borgohain, S. R. Mohanty, and H. Bailung, *Phys. Lett. A* **381**, 2391 (2017).

[59]. J. Badzaik et al., *Phys. Plasmas* **16**, 114506 (2009).

[60]. T. Windisch, O. Grulke, V. Naulin, and T. Klinger, *Plasma Phys. Control. Fusion* **53**, 085001 (2011).

[61]. S. Ichimaru, H. Iyetomi, and S. Tanaka, *Phys. Rep.* **149**, 91 (1987).

[62]. W. L. Slattery, G. D. Doolen, and H. E. DeWitt , *Phys. Rev. A* **21**, 2087 (1980); *Phys. Rev. A* **26**, 2255 (1982).

[63]. D. M. Suszcynsky, S. L. Cartier, R. L. Merlino, and N. D'Angelo, *J. Geophys. Res.* **91**, 13729 (1986).

[64]. S. Hamaguchi, and R. T. Farouki, *J. Chem. Phys.* **101**, 9876 (1994); S. Hamaguchi, R. T. Farouki, and D. H. E. Dubin, *J. Chem. Phys.* **105**, 7641 (1996).

[65]. X. Wang, A. Bhattacharjee, and S. Hu, *Phys. Rev. Lett.* **86**, 2569 (2001).

[66]. M. J. Kurian, S. Jyothi, S. K. Leju, M. Isaac, C. Venugopal and G. Renuka, *PRAMANA J. Phys.* **73**, 1111 (2009).

[67]. R. L. Merlino, A. Barkan, C. Thompson, and N. D'Angelo, *Phys. Plasmas* **5**, 1607 (1998).

[68]. E. Thomas Jr., R. L. Merlino, and M. Rosenberg, *Plasma Phys. Control Fusion* **54**, 124034 (2012).

[69]. S. H. Kim, R.L. Merlino, J. K. Meyer, and M. Rosenberg, *J. Plasma Phys.* **79**, 1107 (2013).

[70]. P.K. Kaw and R. Singh, *Phys. Rev. Lett.* **79**, 423 (1997).

[71]. B. S. Xie and M. Y. Yu, *Phys. Rev. E* **62**, 8501 (2000).

[72]. R. L. Merlino, *Phys. Plasmas* **12**, 124501 (2009).

[73]. M. Rosenberg and R. L. Merlino, *J. Plasma Phys.* **79**, 949 (2013).

CHAPTER 7

Conclusion and Future Prospective

In this chapter, the conclusions drawn from the present research work are summarized and future directions are enlightened.

7.1 CONCLUSION

It has already been observed in the previous chapters that the ubiquitously found ingredient called "DUST" plays a vital role in exciting the new collective phenomenon or in modifying the existing wave phenomenon in a plasma due to their variable size and charge. Presence of an external ion beam or free sources of energies in the plasma tend to excite various waves and instabilities in the dusty plasma. The finite plasma boundaries and the strong coupling among dust grains also modify the dispersion properties of the collective modes as well. In the present thesis work, the role of dust dynamics and charge fluctuations as well as the parameters of external ion beam source, magnetic field, and finite geometry has been theoretically investigated in excitation of various plasma wave modes and instabilities. The results obtained from theoretical fluid models are found to be in good agreement with the experimental observations and theoretical predictions of various authors and may found applications for astrophysical and fusion plasmas. The conclusions drawn from the research work done in the present thesis have been summarized as follows:

- ♠ Electrostatic ion-acoustic waves are driven to instability in a magnetized dusty plasma cylinder by an ion beam via Cerenkov interaction. The frequency of

unstable mode as well as the phase velocity is found to be increased with the relative density of negatively charged dust grains δ. The increase in phase velocity results in a decrease in the collisionless Landau damping of ion acoustic waves in the presence of negatively charged dust grains. The decrease in Landau damping with increase in relative density of negatively charged dust grains δ in turn results in an increase in the growth rate of IAWs. Moreover, the beam parameters such as density and energy play significant role in enhancing the real frequency and the growth rate of the unstable mode. The results may found implications in study of waves in ion beam plasma systems, laboratory plasmas.

♠ Current-driven EIC waves in a collisional magnetized dusty plasma in the presence and absence of dust charge fluctuations in addition to dust dynamics have been examined. The dust charge fluctuations play an important role in suppression of current driven electrostatic ion cyclotron waves. Moreover, the wave frequency remains unchanged with an increase in electron-neutral collisional frequency while the growth rate of current driven EIC waves increases with electron-neutral collisional frequency. It is observed that the dust dynamics effect does not contribute significantly because of dust grain mass. The theory of EIC instability having dust grains may be applied to magnetized plasma systems, astrophysical plasmas, Earth's ionosphere.

♠ Kelvin Helmholtz instability in a magnetized dusty plasma can be driven by an ion beam via Cerenkov interaction. Unstable KHI mode frequencies and axial wave vectors increase with the relative density of negatively charged dust grains δ in the presence of beam. The KHI mode frequency is enhanced in the presence of dust charge fluctuations while dust charge fluctuations play a significant role in damping of the KH- instability modes which may be due to the decrease in velocity shear required to sustain K-H instability. The amplitude of the KHI is stabilized for low shear parameters and destabilized for large shear parameters. The instability growth rate of the KHI is more affected by beam at large shear parameter and for large value of δ (relative density of dust grains). The normalized growth rate of KHI modes for a cylindrical plasma waveguide is enhanced with increasing density of ion beam while the increase in beam energy

suppresses the growth of KHI modes. This may be attributed to the fact that an increase in beam density may increase the influx and parallel flow of ions along the magnetic field thereby supporting the critical shear and hence the KHI modes. Moreover, an increase in beam energy may provide energy to the ions in relative motion thereby disturbing their shear flows and enhancing Landau damping which results in stabilizing the KHI modes. A comparison of frequency and the growth rate for finite and infinite geometry of plasma waveguide shows a reduction in both frequency and the growth rate for finite geometry which can be due to the reduction in interaction region. Moreover, the radial boundaries provide an effective perpendicular wave number which in turn modifies the dispersion properties of the KHI modes. The theory of stabilization of growth rate of ion beam driven KHI modes with density of dust grains can be applied to the earth's ionosphere, magneto-hydrodynamic systems, stellar interiors and bounded systems like inertial confinement devices, surface technologies etc.

♠ The Kelvin Helmholtz instability in a magnetized plasma having negative ions is driven by an ion beam via a Cerenkov interaction. Unstable wave frequencies and axial wave vectors of the both positive ion and negative ion KHI modes increase with the relative density of negative ions ε in the presence of beam. The frequency of negative ion KHI mode shows an increase ~ 8 times while ~ 3 times for the positive ion KHI mode with relative concentration of negative ions ε. The growth rates of the both the positive and negative ion KHI modes are declined for low shear parameters and enhanced for large shear parameters similar to the case of negatively charged dust grains. Normalized growth rate of positive ions shows a detrimental increase from 18-30% in presence of beam on moving from finite to infinite geometry while for negative ions 10-15% in the presence of beam which shows the stabilizing effect of negative ions. The relative increase in mass of negative ions shows the stabilizing effect on both the KHI modes. The normalized growth rate of both the KHI modes is enhanced with increasing density of ion beam while the increase in beam velocity/energy suppresses the growth of KHI modes as a sufficiently large pump power suppress the waves in an ion beam plasma system. A comparison of frequency and the growth rate for finite and infinite geometry of plasma wave guide shows

a reduction in both frequency and the growth rate for finite geometry. This may be due to the reduction in region of interaction which in turn may support the collisional damping of the modes. Hence, we can say that the presence of negative ions destabilizes the KHI modes which can found applications in surface plasma technologies and near Earth environment.

♠ Low frequency longitudinal and transverse modes can be excited by magnetic field current drifts in hydrodynamic regime, $\omega\tau_m \ll 1$ in a strongly coupled collisional magnetized dusty plasma. Longitudinal modes contain ion dust hybrid modes while transverse mode is similar to a whistler ion wave. A low frequency longitudinal mode of ~ 25 Hz is observed which well matches the experimental frequencies obtained for dust acoustic modes. An increase in longitudinal mode frequency with wave number shows the modes are similar to low frequency dust acoustic modes. The growth rate of longitudinal modes enhances in presence of drift of ions which supports the current driven cyclotron modes while in absence of ion drifts a purely damped mode is obtained. Transverse mode frequency and the growth rate increases with normalized wave number similar to dust lattice modes. The critical drift required for exciting the longitudinal and transverse modes decreases with increasing wave number. The strong correlation parameter has a stabilizing effect on current driven longitudinal modes due to increase in viscous damping while for transverse modes the effect of viscous damping is weak due to restoring force provided by elastic effects.

♠ The excitation of low frequency wave modes by magnetic field aligned ion and dust drifts in a magnetized strongly coupled collisional dusty plasma having a cylindrical geometry in the kinetic regime $\omega\tau_m \gg 1$, using a non-local theory of generalized hydrodynamic model. It is found that the magnetic field aligned current drifts play a crucial role in exciting the low frequency dust wave modes in a magnetized dusty plasma cylinder having neutral background. The longitudinal mode observed is a result of coupling between dust ion cyclotron hybrid modes and dust acoustic modes and transverse shear mode are the elastic wave modes. It is observed that the excitation of longitudinal dust ion hybrid modes requires a large magnetic field and low collisional regime in the presence

of strong correlations among dust grains while the transverse shear modes are hard to observe in a collisional dust fluid (liquid) having strong correlations in a magnetized dusty plasmas. Our frequencies for the magnetized longitudinal modes lie close to the frequencies observed experimentally by various authors thereby justifying the modes as the low frequency dust wave modes. It is observed that the presence of radial boundaries modify the dispersion properties of both the modes. The results obtained may be useful in laboratory strongly coupled magnetized dusty plasma like in inertial confinement fusion devices and magnetized dusty plasma experiments for study of waves and instabilities in magneto-bounded dusty plasmas. Though the theory applies to the bounded plasmas but a comparison of bounded and unbounded plasmas may also be applicable for study of cosmic and near earth environments.

7.2 FUTURE PROSPECTIVE

A few aspects out of the present research work that may be discussed in future are enlightened below.

- We have neglected the dust size & shape effects and $\vec{E}\times\vec{B}$ flows in the magnetized plasmas which can be considered in future discussions.
- The theoretical investigations can be extended to study nonlinear behaviour of different waves and instabilities.
- The investigations can be extended for the astrophysical plasma parameters as well as the theories of bounded plasmas can be extended for the fusion devices parameters.
- The theory of EIAWs can be extended to study ion beam plasma systems, and plasma waveguides for transmission of radio waves.
- The theory of EIC instability having dust grains can be investigated for bounded plasmas that can find implications in the fusion plasma devices.
- The theory of ion beam driven KHI modes can be extended after considering the $\vec{E}\times\vec{B}$ flows and axial boundaries as well.

- The theory of current driven low frequency modes in unbounded as well as bounded plasmas can be extended for the parameters of nuclear fusion devices and quark gluon plasmas. We would like to remark that there is a need to incorporate the dependence of viscosity coefficients on the magnetic field to elucidate the behaviour of the strongly coupled viscoelastic magnetized dust modes more effectively.
- Dusty plasma systems can be used to study "nano-dynamic" behavior of systems at the kinetic level, e.g., physics of liquids, phase transitions, etc.
- Moreover, many more low frequency waves and instabilities having dust particle gravitational effects are yet to be analysed for the similar plasma conditions.